Synthesis and Characterisation of Full-Interpenetrating Polymer Network Hydrogels for Environmental and Biomedical Applications

Submitted by

Zarah Alzahrani

Master of Chemical Sciences

2015 La Trobe University

A thesis submitted in total fulfilment

of the requirements for the degree of

Doctor of Philosophy

Department of Chemistry and Physics

School of Molecular Sciences

College of Science, Health and Engineering

La Trobe University

Victoria, Australia

May 2020

Table of Contents

List of Figures

List of Tables

List of Schemes

Abstract

Hydrogels are three-dimensional, hydrophilic polymeric networks that can absorb large amounts of water because of the presence of hydrophilic groups, such as carboxylic acids, hydroxyls, amides, sulfonic acids, and amines, attached to the polymer backbone. Due to their useful properties, such as biocompatibility, permeability, surface properties, and mechanical attributes, hydrogels can be used for different environmental and biomedical applications. Recently, hydrogels prepared as interpenetrating polymer networks (IPNs) have generated considerable interest because of their enhanced mechanical stability and chemical responsiveness.

Full-interpenetrating polymer network (full-IPN) hydrogels based on poly(vinyl alcohol) (PVA) as a base polymer with different monomers including 2-hydroxyethyl methacrylate (HEMA), 4-hydroxybutyl acrylate (HBA), acrylic acid (AA), itaconic acid (IA), and methyl methacrylate (MMA) were investigated. The preparation of PVA/PHEMA, PVA/P(HBA-co-AA), and PVA/P(MMA-co-IA) as full-IPN hydrogels by free radical polymerization in the presence of ethylene glycol dimethacrylate as crosslinker and azobisisobutyronitrile as an initiator was achieved. The full-IPN hydrogels were prepared as a series with 10, 20 or 30 wt% glutaraldehyde as crosslinking agent for the PVA network, and with HBA to AA ratios of 14:20, 20:14 & 27:7, and MMA to AA ratios of 10:24, 17:17 & 24:10 for the hydrophobic network. The effect of amounts of GA, HBA and MMA on gel content, chemical structure, swelling and water retention was studied. The results indicated that full-IPN PVA/PHEMA gel with 10 wt% GA displayed good hydrogel properties and stability for applications of solute delivery and recovery. A series of novel full-IPN hydrogels incorporating Acorga P50 or Cu (II)-Acorga P50 complex, or Aliquat 336 as carrier were prepared and investigated as adsorbents for Cu (II) ions and naproxen from aqueous solutions, respectively. Finally, the chemical structure, surface morphology and thermal properties of the full-IPN PVA/PHEMA, PVA/P(HBA-co-AA) and PVA/P(MMA-co-IA) hydrogels with and without carrier were investigated by FTIR and ToF-SIMS, SEM and TGA.

Statement of Authorship

Except where reference is made in the text of the thesis, this thesis contains no material published elsewhere or extracted in whole or in part from a thesis accepted for the award of any other degree or diploma. No other person's work has been used without acknowledgment in the main text of the thesis. This thesis has not been submitted for the award of any degree or diploma in any other tertiary institution.

Acknowledgements

This is a great opportunity to express my sincere gratitude to my supervisor Dr Ian Potter for his help, support, and encouragement during my PhD journey. Although there were many difficulties that I have faced during my project, his kind words always reduced my stress, fear and made me more motivated and confident. One important thing that I have learned is the more challenges you face, the more success you will experience. I would also like to thank him for his enthusiasm and support throughout the writing of my thesis.

I would like to express my deep appreciation to Drs Robert Jones and Peter Lock for their training and support for the analysis using ToF-SIMS and SEM, respectively.

I am thankful for my loving family, my husband Fahad and my brave boy Yazeed, who have supported and stood by my side during my study. We faced a lot of challenges as a family during this journey, but both of you were always my source of inspiration to be strong.

My dad, my mum and siblings, without your support and kind words, I could not have reached my goal to achieve a PhD one day.

Finally, I take this opportunity to thank my lab friends. We spent a great time in the lab trying to solve our research problems and encourage each other to be more productive. Your friendship is one of the best things that I have gained on my PhD journey.

List of Abbreviations

A	Exposed surface area of gel disc
AA	Acrylic acid
Acorga P50	5-nonyl salicylaldoxime, salicylaldoxime
Acorga P50-imprinted-full-IPN PVA/P(HBA-co-AA)	Salicylaldoxime -imprinted- poly(vinyl alcohol)/poly(4-hydroxbutyl acrylate-co-acrylic acid)
Acorga P50-imprinted-full-IPN PVA/P(HMMA-co-IA)	Salicylaldoxime -imprinted- poly(vinyl alcohol)/poly(methyl methacrylate-co-itaconic acid)
Acorga P50-imprinted-PVA/GA	Salicylaldoxime -imprinted- poly(vinyl alcohol)/glutaraldehyde
Acorga P50-imprinted-PVA/PHEMA	Salicylaldoxime -imprinted- poly(vinyl alcohol)/poly(2-hydroxyethyl methacrylate)
AIBN	Azobisisobutyronitrile
Aliquat 336-PVA/GA	Aliquat 336-poly(vinyl alcohol)/glutaraldehyde
Aliquat 336-PVA/P(HBA-co-AA)	Aliquat 336-poly(vinyl alcohol)/poly(4-hydroxbutyl acrylate-co-acrylic acid)
Aliquat 336-PVA/P(MMA-co-IA)	Aliquat 336-poly(vinyl alcohol)/poly(methyl methacrylate-co-itaconic acid)
Aliquat 336-PVA/PHEMA	Aliquat 336-poly(vinyl alcohol)/poly(2-hydroxyethyl methacrylate)
APS	Ammonium persulfate
BEx (%)	Back-extraction, percent
BLM	Bulk liquid membranes
$C_{f,0}$	Initial concentration in the feed phase
CMC	Carboxymethyl chitosan
CS	Chitosan,
C_t	Copper concentration in feed phase at interval time
CTA	Cellulose triacetate
Cu (II)-Acorga P50 complex-imprinted-PVA/GA	Copper(II)-salicylaldoxime complex-imprinted poly(vinyl alcohol)/glutaraldehyde

Cu (II)-Acorga P50 complex-imprinted-PVA/P(HBA-co-AA)	Copper(II)-salicylaldoxime complex-imprinted poly(vinyl alcohol)/ poly(4-hydroxbutyl acrylate-co-acrylic acid)
Cu (II)-Acorga P50 complex-imprinted-PVA/P(MMA-co-IA)	Copper(II)-salicylaldoxime complex-imprinted poly(vinyl alcohol)/ poly(methyl methacrylate-co-itaconic acid)
Cu (II)-Acorga P50 complex-imprinted-PVA/PHEMA	Copper(II)-salicylaldoxime complex-imprinted poly(vinyl alcohol)/ poly(2-hydroxyethyl methacrylate)
DEA	N,N-diethylacrylamide
DMSO	Dimethylsulfoxide
DSC	Differential scanning calorimetry
DVE-3	Triethylene glycol divinyl ether
Ex (%)	Extraction, percent
EGDMA	Ethylene glycol dimethacrylate
ELM	Emulsion liquid membrane
FTIR	Fourier transform infrared
Full/IPN PVA/(P(MMA-co-IA)	Full-interpenetrating network (poly(vinyl alcohol) /poly(methyl methacrylate -co-itaconic acid)
Full-IPN PVA/P(HBA-co-AA)	Full-interpenetrating network (poly(vinyl alcohol) /poly(4-hydroxy butyl acrylate-co-acrylic acid)
Full-IPN PVA/PAA	Full-interpenetrating network (poly(vinyl alcohol) /poly acrylic acid
Full-IPN PVA/PHBA	Full-interpenetrating network (poly(vinyl alcohol) /poly(4-hydroxy butyl acrylate
Full-IPN PVA/PHEMA	Full-interpenetrating network poly (vinyl alcohol)/2-hydroxyethyl methacrylate)
Full-IPN PVA/PIA	Full-interpenetrating network (poly(vinyl alcohol) /poly itaconic acid
Full-IPN PVA/PMMA	Full-interpenetrating network (poly(vinyl alcohol) /poly methyl methacrylate
Full-IPN	Full-Interpenetrating Polymer Network
ΔG	Gibbs free energy, Change in

GA	Glutaraldehyde
ΔH	Enthalpy, Change in
HBA	4-hydroxybutyl acrylate
HEMA	2-hydroxyethyl methacrylate
H-NMR	Proton nuclear magnetic resonance
IA	Itaconic acid
IBF	Ibuprofen
IIP	Ion-imprinted polymer
k	Rate constant
LC	Liquid chromatography
LCST	Low critical solution temperature
ln ($Cu_{f,0}/Cu_{f,t}$)	Initial concentration of copper in feed phase/copper concentration in feed phase at interval time
ln $[nap]_{f,0}/[nap]_{f,t}$	Initial concentration of naproxen in feed phase/ naproxen concentration in feed phase at interval time
MI	Molecular imprinting
MIPs	Molecular imprinted polymers
MMA	Methyl methacrylate
P	Permeability coefficient
P(AA-co-AAm-co-BMA)	Poly(acrylic acid-co-acrylamide-co-butyl methacrylate)
P(AA-co-MA)	Poly(acrylic acid-co-methacrylamide)
P(AAm-co-BMA),	Poly(acrylamide-co-butyl methacrylate)
P(AAm-co-HEMA)	Poly(acrylamide-co-2-hydroxyethyl methacrylate)
P(HEMA-co-MAA)	Poly(2-hydroxyethylmethacrylate-co-methylmethacrylate)
P(PNIPAAm-co-AA)	Poly(n-isopropyl acrylamide-co-acrylic acid)
PAA	Poly(acrylic acid)
PAAm	Poly(acrylamide)
PBA	Poly(butylacrylic acid)
PBS	Phosphate buffer solution (
PEA	Poly(ethylacrylic acid)

PEDAAm	Poly(N,N-diethylacrylamide)
PEG	Poly(ethylene glycol)
PEMA	Poly(2-hydroxyethyl methacrylate)
PIA/PHEMA	Poly(itaconic acid/2-hydroxyethyl methacrylate)
PIMs	Polymer inclusion membranes
PMMA	Poly(methyl methacrylate)
PNIPAAm	Poly(N-isopropyl acrylamide)
PVA	Poly(vinyl alcohol)
PVA/CS	Polyvinyl alcohol/chitosan
PVA/CS/GO	Polyvinyl alcohol/chitosan/ graphene oxide
PVA/GA	Poly(vinyl alcohol)/glutaraldehyde
PVA/P(DEA-co-IA)	Poly(vinyl alcohol)/poly(N,N-diethylacrylamide-co-itaconic acid)
PVAc	Poly(vinyl acetate)
PVA-g-AA)/SA	Poly(vinyl alcohol)-graft-acrylic acid)/sodium alginate
PVC	Polyvinyl chloride
PVP	Poly(vinyl pyrrolidone)
PVP/PAA	Polyvinyl pyrrolidone/polyacrylic acid
RF (%)	Recovery Factor, percent
ΔS	Entropy, Change in
SEM	Scanning electron microscopy
Semi-IPN (PVA/PAA)	Semi-interpenetrating network poly(vinyl alcohol)/poly acrylic acid)
Semi-IPN	Semi-interpenetrating network
SLM	Supported liquid membranes
SPE	Solid phase extraction
T_g	Glass transition temperature
TGA	Thermal gravimetric analysis
ToF-SIMS	Time-of-Flight Secondary Ion Mass Spectrometry
UCST	Upper Critical Solution Temperature
V	Volume of the feed solution
VA	Vinyl acetate

XRD	X-ray diffraction

Chapter 1: Literature review

1.1. General overview

Hydrogels are a special class of polymers that have been of great interest to scientists in recent years due to their unique and versatile properties[1-2]. Hydrogels exhibit physical properties like those of living tissues due to their high-water content. They have a rubbery and soft consistency, and exhibit a low interfacial tension with water[3] or biological fluids[1-2, 4-7]. These physical properties make hydrogels useful for different biomedical applications such as tissue engineering, wound dressing, artificial skin applications, drug delivery systems, biosensors and hemostasis bandages[1, 4-5, 8-17].

Hydrogels are hydrophilic polymer networks that have the ability to hold large amounts of water in spaces available in the network [9, 18-28]. Hydrogels can absorb water because of the presence of hydrophilic groups, such as carboxylic acid, hydroxyl, amide, sulfonic acid, and amine groups[29], attached to the polymeric backbone, and osmotic pressure and capillary effect [30-34]. Their resistance to dissolution in water and organic solvents is due to cross-links among the network polymer chains[28, 35].

The water content of a hydrogel can range from 10 - 1000%, or more, of its dry weight. Dried hydrogels that do not contain water are referred to as xerogels. Cross-linking density and number of hydrophilic groups of the polymer have a significant effect on water content of a hydrogel. A polymer with significant hydrophilic groups will have a better water-holding capacity. In contrast, a high extent of cross-linking involving hydrophilic groups results in a consequent increase in hydrophobicity and reduced water uptake[36]. This also results in reduced elasticity of the polymer network[36], which could be beneficial as a means to improve the mechanical properties of hydrogels used in tissue engineering and skin substitutes[7].

1.2. Classification of hydrogels

1.2.1. Classification based on source

Polymers regularly used for the synthesis of hydrogels for biomedical applications are mostly from natural or synthetic origins, or a combination of both [8, 37,] Hydrogels derived

from natural polymers (collagen, chitosan, gelatin and heparin) exhibit interesting properties, such as biocompatibility, low toxicity[9, 32, 38], cell signaling, biodegradability, and physicochemical properties. This indicates their usefulness for drug delivery applications. However, they show some limitations, such as significant chemical degradation, poor mechanical properties and possible immunogenicity[9, 39].

Alternatively, hydrogels prepared from synthetic polymers, such as poly(vinyl alcohol) (PVA), polyacrylamide (PAAm), poly(ethylene glycol) (PEG) and poly (2-hydroxyethyl methacrylate) (PHEMA), have a defined microstructure, controllable degradation, and good mechanical properties[38], but lack useful biological moieties[39-40].

Natural and synthetic polymers each have their own advantages and disadvantages. A combination of the benefits from both polymer types could be beneficial in preparing hydrogels for biological and biomedical applications[41].

1.2.2. **Classification according to composition**

Significant classes of hydrogels can be prepared by synthesis as follows.

(a) Homopolymeric hydrogels are prepared from a single hydrophilic monomer that forms the basic structural unit of the polymer network[2, 4, 32, 37, 42].

(b) Copolymeric hydrogels are formed from two or more monomers. One or more of the monomers is hydrophilic and the resulting polymer has an alternating or random block configuration along the polymer chains throughout the network[2, 4, 32, 37, 42].

(c) A significant class of hydrogels are known as interpenetrating polymer networks (IPNs) that contain a combination of two different polymers. One of them is synthesised or crosslinked inside the other, without any covalent bonds linking the separated different polymers[4, 37, 43-45]. The interpenetrating polymers can only be separated if chemical bonds of the polymer chains are broken. They are classified into two categories: full-IPNs and semi-IPNs. A full-IPN contains two crosslinked networks, whereas a semi-IPN contains a linear polymer that penetrates within a crosslinked network[46-49].

Moreover, IPN hydrogels can be further classified into categories based on preparation methods (Figure 1.1)[48]. A simultaneous IPN is obtained by mixing the precursors of both networks; the two networks are prepared at the same time by independent routes, including stepwise and chain polymerisation[48].

A sequential IPN results from swelling of a single-network hydrogel in a mixed solution of initiator, monomer, and activator, with or without a crosslinker. In the absence of a crosslinker, a semi-IPN network results, whereas a full-IPN network is generated in the presence of a crosslinker[48].

A semi-IPN hydrogel is formed by inserting a biopolymer or synthetic linear polymer into a matrix. After that, the full-IPN gel can be obtained through selective crosslinking of the linear polymer chains[48].

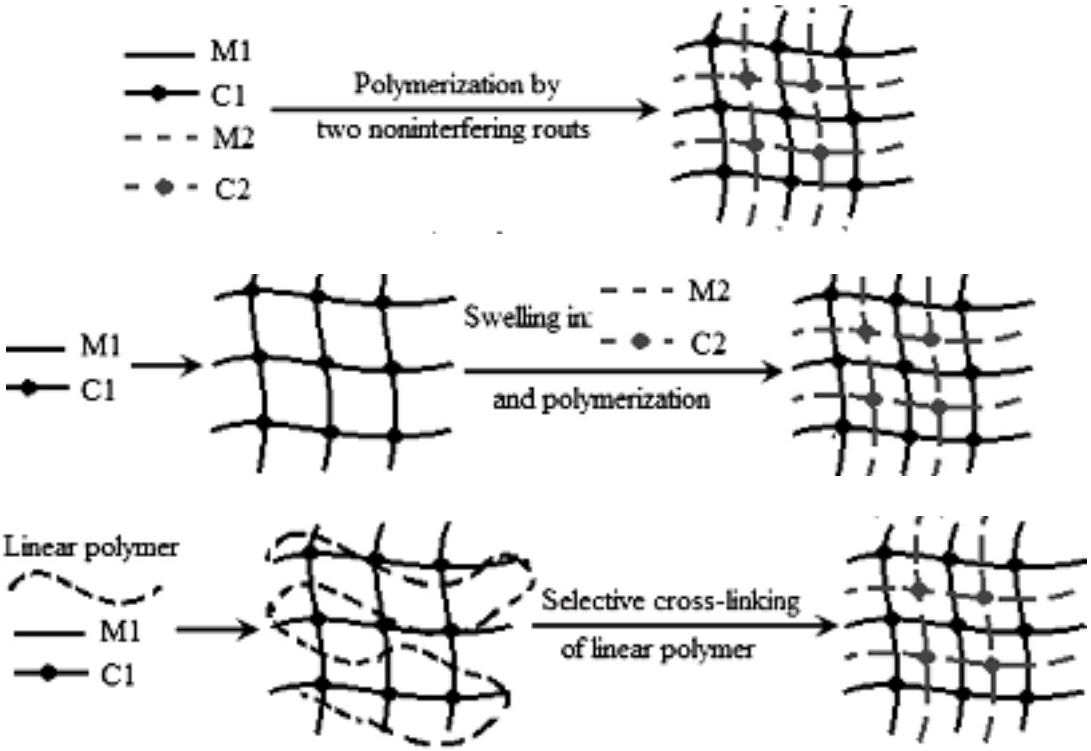

Figure 1.1. Methods to prepare simultaneous (a), sequential (b) and semi (c) full hydrogels. Where M1 & M2 are monomers 1 & 2, respectively, and C1 & C2 are cross-linking reagents 1 & 2, respectively.

Depending on their structure, IPN hydrogels are classified as: (i) homo-IPNs are exceptional cases in which independent networks with the same structure are formed from two polymers; (ii) IPNs designed by two networks, preferably juxtaposed, with many physical interactions and entanglements between them; or (iii) semi- or pseudo-IPNs result when one component forms a linear rather than a network structure[48]. Hydrogels obtained as IPNs produce materials with relatively dense matrices, which have

controllable physical properties, stiffer and better mechanical attributes, and more effective drug loading comparative to hydrogels of a single network[48].

1.2.3. **Classification based on cross-linking type**

Hydrogels are classified into two main groups depending on the physical or chemical nature of the cross-linking junctions[1, 37-38]. Physical networks have non-covalent junctions from ionic or hydrophobic interactions, and hydrogen bonds, whereas chemically cross-linked networks possess permanent junctions[37]. Hydrogels containing a combination of physical and chemical cross-linking offer unique "self-healing" properties that have been explored for applications including tissue engineering[50]

Examples of chemical hydrogels include PHEMA and poly(methyl methacrylate) (PMA), whereas physical hydrogels include gelatin gels, poly(vinyl alcohol-glycine), and agar-agar gels. When cross-linkers are added, the chemical and physical network properties of the polymer are affected, such as changed elastic modulus, solubility, glass transition temperature (Tg), and mechanical properties of strength and toughness[51]. A higher degree of cross-linking leads to reduced mesh size of the network, and decrease of diffusion rate and increase of mechanical strength[52].

Mesh size (**ξ**) is used to describe the diffusional space available for the transfer of particles or molecules throughout the matrix of a hydrogel[52]. (Figure 1.2)

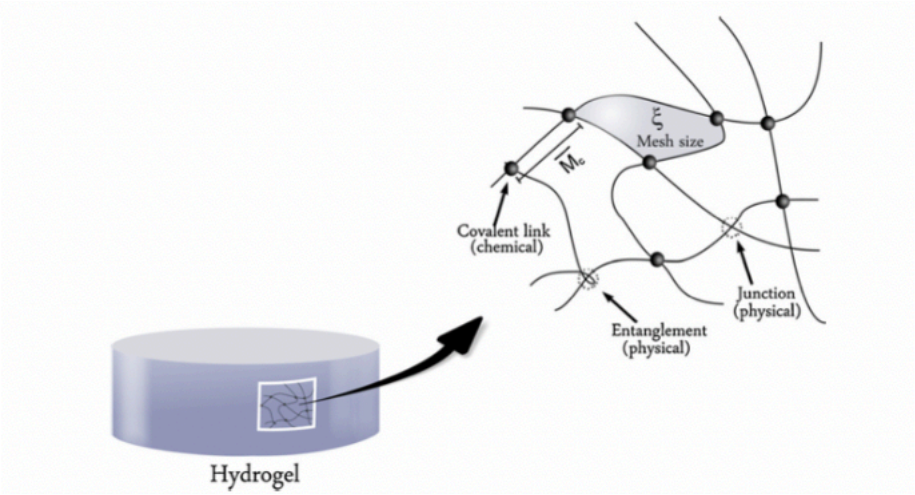

Figure 1.2. Structure of a physically and chemically cross-linked-hydrogel with defined mesh size [4, 52].

1.2.4. **Sensitivity of hydrogels toward environmental stimuli**

Hydrogels can be engineered with manageable chemical or physical responses to expand or shrink with variations in external environmental conditions. They can exhibit significant volume changes in response to types of chemical and physical stimuli. The chemical stimuli involve solvent composition, molecular species, ionic strength[53], and pH[54-57], whereas the physical stimuli include pressure, light[58], temperature[59-60], electric or magnetic field[61], and sound[40, 62] (Figure 1.3).

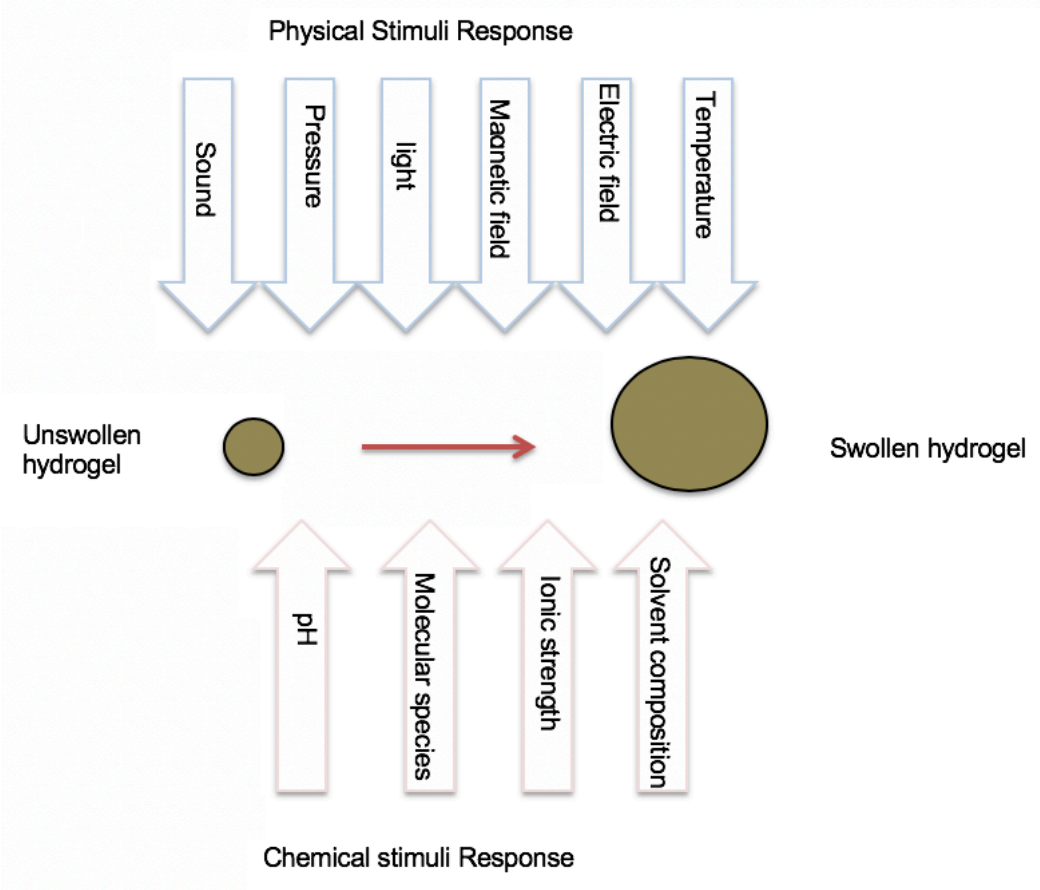

Figure 1.3. Chemical and Physical stimuli (Modified from reference 1)[1].

1.2.5. **pH-sensitive hydrogels**

Hydrogels show pH-dependent swelling in an aqueous solution of suitable pH and ionic strength owing to the formation of ionic networks due to the presence and nature of pendant polar groups that are readily ionized. The fixed charges that result along the polymer chains generate electrostatic repulsive forces throughout the network. This

affects the free volume that is responsible for pH-dependent swelling or deswelling of the hydrogel[63]. These pH-sensitive hydrogels are further divided into anionic and cationic hydrogels depending on the chemical nature of the polar groups.

Anionic hydrogels are defined as a swollen network with acidic pendant groups, such as sulfonic acid and carboxylic acid, showing a sudden or gradual variation in dynamic and equilibrium swelling behaviour as a consequence of altering the external pH. These hydrogels undergo significant ionization when the pH of the surrounding environment exceeds the pK_a of any acidic functional groups. As the pH of the system is increased, the extent of ionization also increases and this results in more fixed-charge sites, causing enhanced electrostatic repulsion among the polymer chains. Consequently, this increases the hydrophilicity of the polymer network and results in increased swelling. Examples of some polymers that exhibit anionic pH-sensitivity are shown in Figure 1.4.

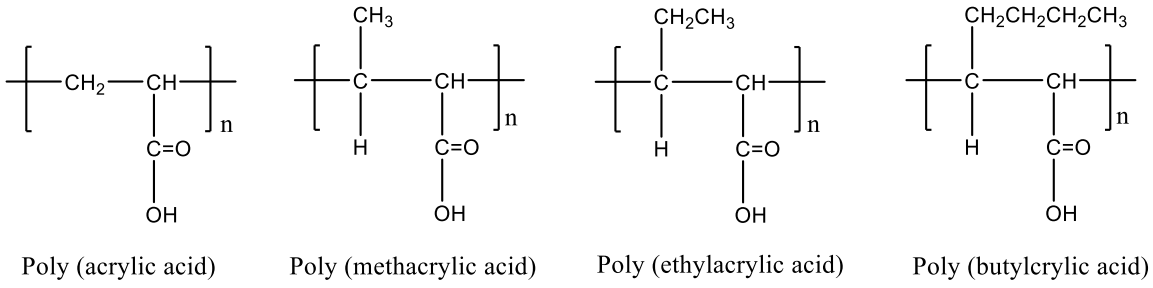

Figure 1.4. Structure of some pH-sensitive polymers with acidic functional groups.

In contrast, cationic materials include polymer chains with basic pendant functional groups, such as $-NH_2$, that can be ionized in environments that have a pH lower than the pK_b. Thus, for cationic hydrogels the ionization increases at low pH, resulting in significant electrostatic repulsion between polymer chains[63]. The resulting hydrogel becomes very hydrophilic and exhibits an increased swelling capacity[2, 5, 37-38, 64].

The swelling behaviour of anionic and cationic hydrogels in response to external pH stimuli is shown in Figure 1.5. There are examples of pH-sensitive polymers in the literature[65].

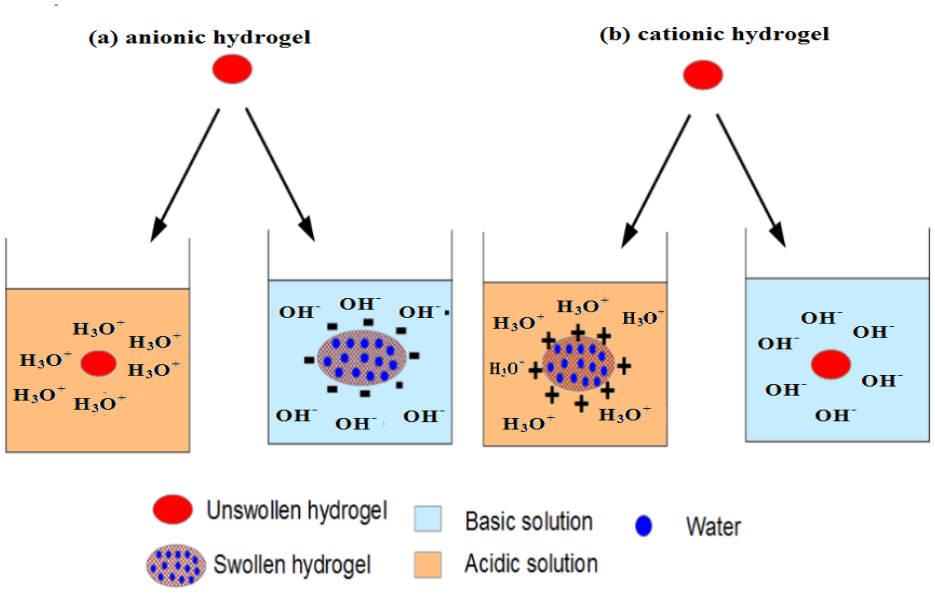

Figure 1.5. The pH-responsive swelling behaviour of (a) anionic and (b) cationic hydrogels in acidic (H_3O^+) and basic (OH^-) environments. Counter ions, such as Cl^- or Na^+, to maintain charge balance are not shown in this simplistic representation. (Modified from reference 64).

1.2.6. **Temperature-sensitive hydrogels**

Temperature-sensitive hydrogels are a focus of considerable attention in the pharmaceutical sector because they can be made to swell or deswell by altering the temperature of the surrounding fluid[2]. These hydrogels can be applied as biosensors, for on-off drug release mechanisms, and as intelligent cell culture dishes[7, 37, 64, 66].

Temperature-sensitive (also referred to as thermosensitive) hydrogels are categorised as negative or positive systems depending on the ability to swell or deswell as the temperature is lowered or raised. These properties are described more fully in the next two sections 1.2.6.1 & 1.2.6.2.

1.2.6.1. *Negative temperature-sensitive hydrogels*

A negative temperature-sensitive hydrogel has a low critical solution temperature (LCST) and contracts or deswells after being heated to a temperature above the LCST[37-38, 62, 64].

The LCST can be affected by several factors, including changing the solvent composition or mixing a small quantity of ionic copolymer in the hydrogels. The LCST of

polymers containing a lot of hydrophobic groups, generally, moves to lower temperatures. By varying the amount of hydrophobic to hydrophilic content of the hydrogel, the LCST can be altered. The general structure of negative thermosensitive hydrogels is composed of a hydrophobic part (-R-) and a hydrophilic segment (-CONH-)[67]. Polymers and copolymer with a LCST are indicated in Figure 1.6.

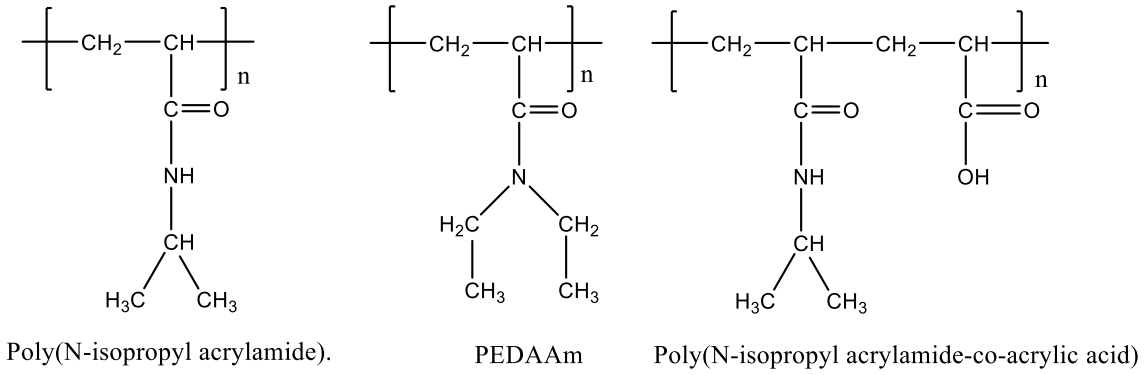

Figure 1.6. Negative-sensitive temperature polymers and copolymers.

When the temperature is below the LCST, fluid and water interact with the hydrophilic groups and form hydrogen bonds. Swelling and dissolution are enhanced as a result of the hydrogen bonding. Whereas, at temperatures above the LCST, hydrophobic interactions are stronger between hydrophobic groups. Consequently, hydrogen bonding is weakened and the hydrogel shrinks due to inter-polymer chain associations[65].

A good example of a negative temperature-sensitive hydrogel is poly(N-isopropyl acrylamide) (PNIPAAm). Hitotsu et al. examined crosslinked PNIPAA hydrogels and determined a LCST of 34.3 ^{o}C. An increased LCST was obtained by adding small amounts of ionic copolymers[32, 68].

1.2.6.2. *Positive temperature-sensitive hydrogels*

Conversely, a positive temperature-sensitive hydrogel possesses an upper critical solution temperature (UCST). These hydrogels contract when cooled to temperatures below the UCST because of significant hydrogen bonding within the network[35, 37-38, 62, 64]. At high temperatures, this structure dissociates because of the disruption to the hydrogen bonding and results in maximum swelling of the hydrogel. Examples of copolymers that

indicate positive temperature behaviour are poly(acrylamide-co-butyl methacrylate) (poly(AAm-co-BMA)) and poly(AA-co-AAm-co-BMA)[65].

Specific hydrogels produced as IPNs illustrate positive thermosensitivity, such as shrinking at low temperatures and swelling at high temperatures. A positive temperature effect on swelling is observed for IPNs of polyacrylamide (PAAm) and poly(acrylic acid) (PAA) or poly(AAm-co-BMA) where increased amounts of BMA shifts the UCST to a higher temperature. The swelling of these hydrogels is reversible and responds to stepwise temperature alterations. This feature has been demonstrated by different rates of uptake and release of ketoprofen (as a model drug) from a monolithic device[62].

1.2.6.3. *Thermo-reversible hydrogels*

Thermo-reversible hydrogels contain similar content and structure as positive and negative sensitive hydrogels, however, they differ by the type of transition process. In this class, the polymer chains are not covalently crosslinked, and the hydrogels undergo a sol-gel phase transformation instead of a swelling-shrinking transition. For example, the concentration of glucose in surrounding media can promote glucose responsive cross-linking that affects the sol-gel phase transition and initiates reversible sol-gel behaviour.

Pluronic and tetronic polymers, referred to as pluronics and tetronics, respectively, are common examples of hydrogels with thermo-reversible behaviour. A pluronic is a linear block co-polymer containing hydrophilic and hydrophobic segments, such as poly(ethylene oxide-co-propylene oxide) (PEO-PPO). Whereas, a tetronic polymer has a X-shape structure containing four blocks of PEO-PPO linked through a central ethylenediamine group, $(PEO\text{-}PPO)_2NCH_2CH_2(PEO\text{-}PPO)_2$. The structure of a pluronic and tetronic are shown in Figure 1.7[65].

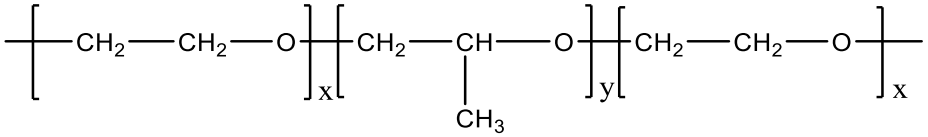

Pluronic

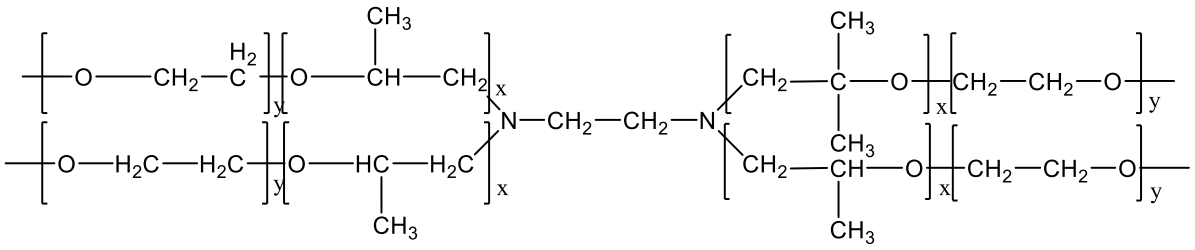

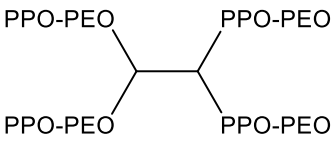

Tetronic

Figure 1.7. Structure of pluronic and tetronic polymers.

1.2.7. **Synthesis of hydrogels**

Hydrogels are routinely prepared by several methods to achieve chemical and physical crosslinking as shown in Figure 1.8[69].

1.2.7.1. *Physical cross-linking*

Physical hydrogels have attracted increased interest because of their comparatively easy production and added benefit of not needing to use a cross-linking agent, making them appropriate for cell and sensitive molecules.

The residual agents influence the integrity of substances, such as proteins and cells, to be entrapped and must be removed before application. They are reversible gels because the networks are maintained by molecular entanglement or secondary forces involving hydrogen-bonding, ionic[70-71], or hydrophobic interaction, and van der Waals forces[32, 38, 41, 72-73]. Moreover, the physical gels can be dissolved by changes to certain environmental conditions, such as pH, ionic strength of solution or temperature[74].

1.2.7.2. *Chemical cross-linking*

Chemical cross-linking involves using cross-linking agents to connect two polymer chains or the grafting of monomers to the backbone of a polymer. The cross-linking of synthetic and natural polymers is achieved by reactions involving functional groups, such as -COOH, -NH_2 and -OH, with cross-linking agents such as an aldehyde. For example, the reaction of adipic acid dihydrazide with glutaraldehyde. In addition, the resulting polymers are permanent gels because of the covalently- cross-linked networks[32, 38, 41, 72, 75].

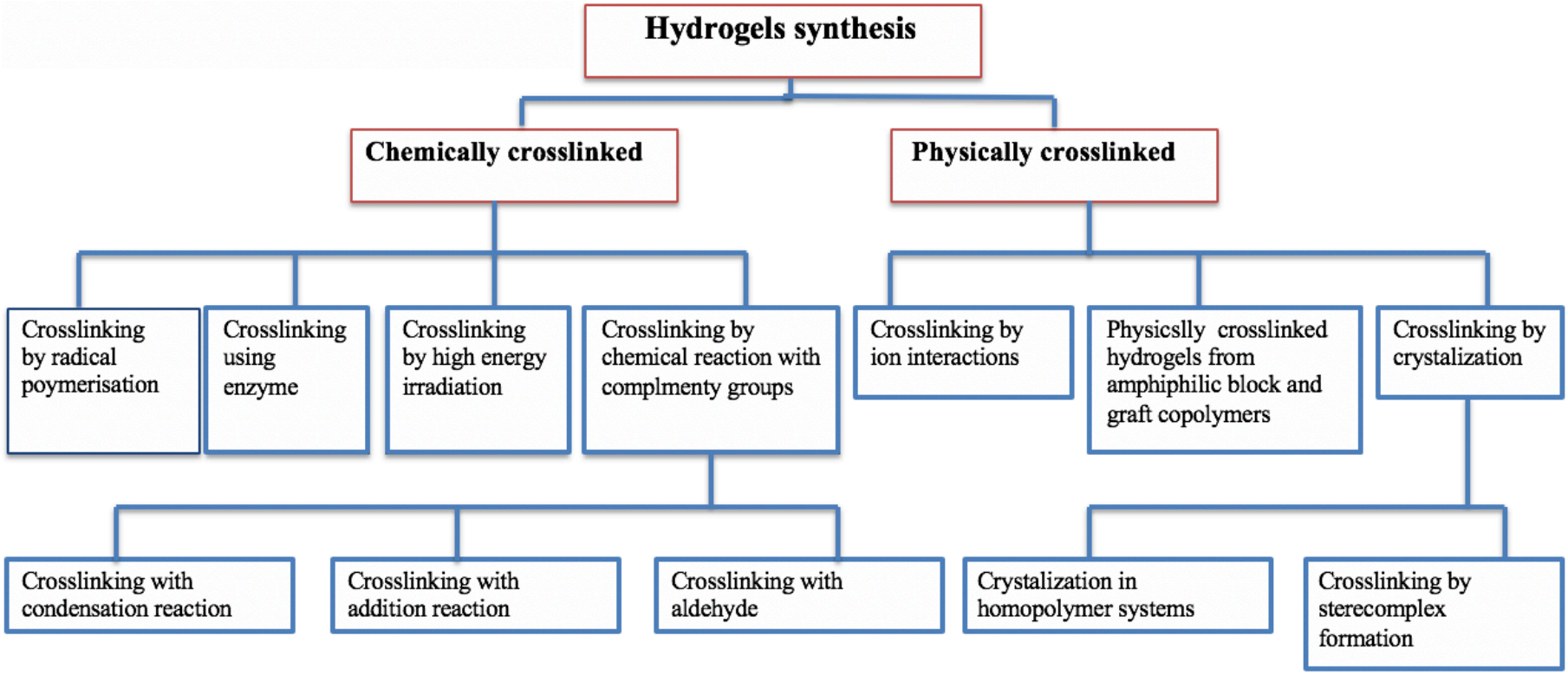

Figure 1.8. Crosslinking methods used to prepare hydrogels (Modified from reference 36).

1.2.8. **The theory of equilibrium swelling**

The Flory-Rehner theory[2,4] can be used to investigate the structure of non-polar hydrogels. According to this thermodynamic theory, the two opposing processes of thermodynamic force of mixing and retractive force of polymer chains determine the extent of equilibrium swelling of a cross-linked polymer gel when immersed in a liquid. Equilibrium swelling is reached when these processes are equalised. The Gibbs free energy change (ΔG_{total}) related with the process of solvent absorption by a hydrogel is described by the following equation

$$\Delta G_{total} = \Delta G_{elastic} + \Delta G_{mixing} \quad (1)$$

Where, $\Delta G_{elastic}$ is due to the elastic retractive forces that develop inside the hydrogel, and ΔG_{mixing} is the impact from the spontaneous mixing of polymer chains with fluid molecules. The compatibility of polymer with fluid molecules is indicated by ΔG_{mixing}, typically reported as the polymer-solvent interaction parameter (χ_1).

Equation 2 is derived by differentiation of equation 1 with respect to the moles of solvent, while the temperature and pressure are held constant.

$$\mu_1 - \mu_{1,}^{o} = \Delta\mu_{elastic} + \Delta\mu_{mixing} \quad (2)$$

In equation 2, $\Delta\mu$ indicates the compatibility of the penetrating solvent, μ_1 represents the chemical potential of the solvent in the polymer gel, and $\mu_{1,}^{o}$ is the chemical potential of the pure solvent. Equilibrium is achieved when there is zero difference between the chemical potential of the solvent inside and outside the gel. Consequently, a change to the overall chemical potential caused by mixing must be counter-balanced by the elastic forces if equilibrium is to be maintained.

The theory of rubber elasticity can be applied to determine the chemical potential change caused by the elastic retractive forces of polymer chains. When these two contributions are combined, the expression below is useful to indicate the molecular weight between two adjacent crosslinks of a neutral hydrogel in the absence of solvent, M_c.

$$\frac{1}{\bar{M}_c} = \frac{2}{\bar{M}_n} - \frac{\left(\bar{v}/V_1\right)\left[\ln\left(1-v_{2,s}\right)+v_{2,s}+\chi_1 v_{2,s}^2\right]}{v_{2,s}^{\frac{1}{3}} - \frac{v_{2,s}}{2}} \quad (3)$$

In equation 3, M_n is the molecular weight of similar polymer chains that are not crosslinked, V_1 is the molar volume of water, $\bar{v}$ is the exact volume of the polymer, $v_{2,s}$ is

the volume fraction of polymer in the swollen state, and (χ_1) is the polymer-solvent interaction parameter.

The original Flory-Rehner theory was modified by Peppas and Merrill[76] to give an expression for polar hydrogels that are prepared in a water-solvent mixture. It accounts for the change to chemical potential caused by the elastic forces within the hydrogel. Equation 4 is used to predict the molecular weight of polymer chains between crosslinking agents in a neutral hydrogel that has been prepared in an aqueous environment.

$$\frac{1}{\bar{M}_c} = \frac{2}{\bar{M}_n} - \frac{\left(\bar{v}/_{V_1}\right)\left[\ln\left(1-v_{2,s}\right)+v_{2,s}+\chi_1 v_{2,s}^2\right]}{v_{2,r}\left[\left(\frac{v_{2,s}}{v_{2,r}}\right)^{\frac{1}{3}}-\left(\frac{v_{2,s}}{2v_{2,r}}\right)\right]} \quad (4)$$

Where, $v_{2,r}$ represents the polymer volume fraction immediately after crosslinking.

The presence of ionic groups in the hydrogel further complicates the theoretical treatment of swelling. In addition to ΔG_{mixing} and $\Delta G_{elastic}$ in equation 1, the free energy associated with the ionic nature (ΔG_{ionic}) of the polymer network also contributes to the overall change in Gibbs free energy, resulting in equation 5.

$$\Delta G_{total} = \Delta G_{elastic} + \Delta G_{mixing} + \Delta G_{ionic} \quad (5)$$

The derivative of equation 5 with respect to the amount of solvent at constant pressure and temperature now yields equation 6, which is a similar expression to equation 2 in terms of chemical potential.

$$\mu_1 - \mu_{1,o} = \Delta\mu_{elastic} + \Delta\mu_{mixing} + \Delta\mu_{ionic} \quad (6)$$

Where $\Delta\mu_{ionic}$ in equation 6 represents the change in chemical potential caused by the ionic nature of the hydrogel.

Expressions have been created to demonstrate the ionic contribution to the chemical potential. These expressions reflect a significant contribution from the ionic strength of the encompassing fluid environment and the ionic characteristic of the solvent. Swelling derivative expressions for cationic and anionic hydrogels, respectively, in the presence of solvent are indicated by Equations 7 and 8.

$$\frac{V_1}{4\,I}\left(\frac{v_{2,s}^2}{\bar{v}}\right)\left(\frac{K_a}{10^{-pH}-K_a}\right)^2 = \left[\ln\left(1-v_{2,s}\right)+v_{2,s}+\chi_1 v_{2,s}^2\right]+$$

$$\left(\frac{V_1}{\bar{v}\,\bar{M}_c}\right)\left(1-\frac{2\bar{M}_c}{\bar{M}_n}\right)v_{2,r}\left[\left(\frac{v_{2,s}}{v_{2,s}}\right)^{1/3}-\left(\frac{v_{2,s}}{2v_{2,s}}\right)\right]\frac{V_1}{4I}\left(\frac{v_{2,s}^2}{\bar{\bar{v}}}\right)\left(\frac{K_b}{10^{pH-14}-K_b}\right)^2 \quad (7)$$

$$\frac{V_1}{4\,I}\left(\frac{v_{2,s}^2}{\bar{v}}\right)\left(\frac{K_a}{10^{-pH}-K_a}\right)^2=\left[\ln(1-v_{2,s})+v_{2,s}+\chi_1 v_{2,s}^2\right]+$$

$$\left(\frac{V_1}{\bar{v}\,\bar{M}_c}\right)\left(1-\frac{2\bar{M}_c}{\bar{M}_n}\right)v_{2,r}\left[\left(\frac{v_{2,s}}{v_{2,s}}\right)^{1/3}-\left(\frac{v_{2,s}}{2v_{2,s}}\right)\right] \quad (8)$$

Where, K_b and K_a in expressions 7 & 8 are the dissociation constants for the base and acid, respectively, and *I* is the ionic strength[2, 77].

1.2.9. **Rubber elasticity theory**

Hydrogels are similar to natural rubber because they have elastic properties making them flexible under external pressure. They have the capacity to quickly regain their original shape and size, especially when the deformation is less than 20%.

The original theory of rubber elasticity was improved by Flory and Treloar and provides a profound explanation of the elastic behaviour of hydrogels. Nevertheless, the theory is not applicable, specifically, to hydrogels that can only be made in the presence of a solvent. Silliman[78] made improvements to the original expressions, after which, Merrill and Peppas[75] made further changes to provide an expression for applied stress (τ) and information about the structure of the hydrogels that are prepared in a solvent environment.

$$\tau=\frac{\rho RT}{\bar{M}_c}\left(1-\frac{2\bar{M}_c}{\bar{M}_n}\right)\left(\propto-\frac{1}{\propto^2}\right)\left(\frac{v_{2,s}}{v_{2,r}}\right)^{1/3} \quad (9)$$

Where, in equation 9, ρ is the density of the polymer, τ is the stress applied to the hydrogel, R represents the universal gas constant, $\bar{M}_c$ is the polymer molecular weight between polymer crosslinks, and T is the experimental temperature (K).

A tensile testing system is used to conduct experiments to provide information and apply equation 9 to determine important information about the hydrogel structure using the theory of rubber elasticity. This theory has been applied to analyse hydrogels

with physical and chemical crosslinks, and also hydrogels with temporary crosslinks from hydrogen-bonding[2].

1.2.10. **Dynamics of swelling**

The swelling of hydrogels can be grouped into two mechanisms: diffusion-controlled, commonly known as Fickian, and relaxation-controlled swelling, usually referred to as non-Fickian. Diffusion-controlled swelling occurs when the diffusion rate of water into the hydrogel network is greater than the relaxation of polymer chains. Peppas and Colombo have mathematically analysed the dynamics of swelling[2, 8].

1.2.11. **Poly(vinyl alcohol) (PVA)**

Poly(vinyl alcohol) (PVA) is a linear polymer and has a simple chemical structure with pendant hydroxyl groups (Figure 1.9).

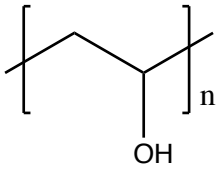

poly(vinyl alcohol)

Figure 1.9. Chemical structure of PVA.

PVA cannot be directly prepared by the polymerisation of vinyl alcohol monomer because it is unstable and cannot be isolated. Vinyl alcohols as monomers do not exist in a stable form. An indirect method to prepare PVA involves, firstly, the polymerisation of vinyl acetate to poly(vinyl acetate) (PVAc) and then hydrolysis of PVAc to PVA (Figure 1.10)[79-80].

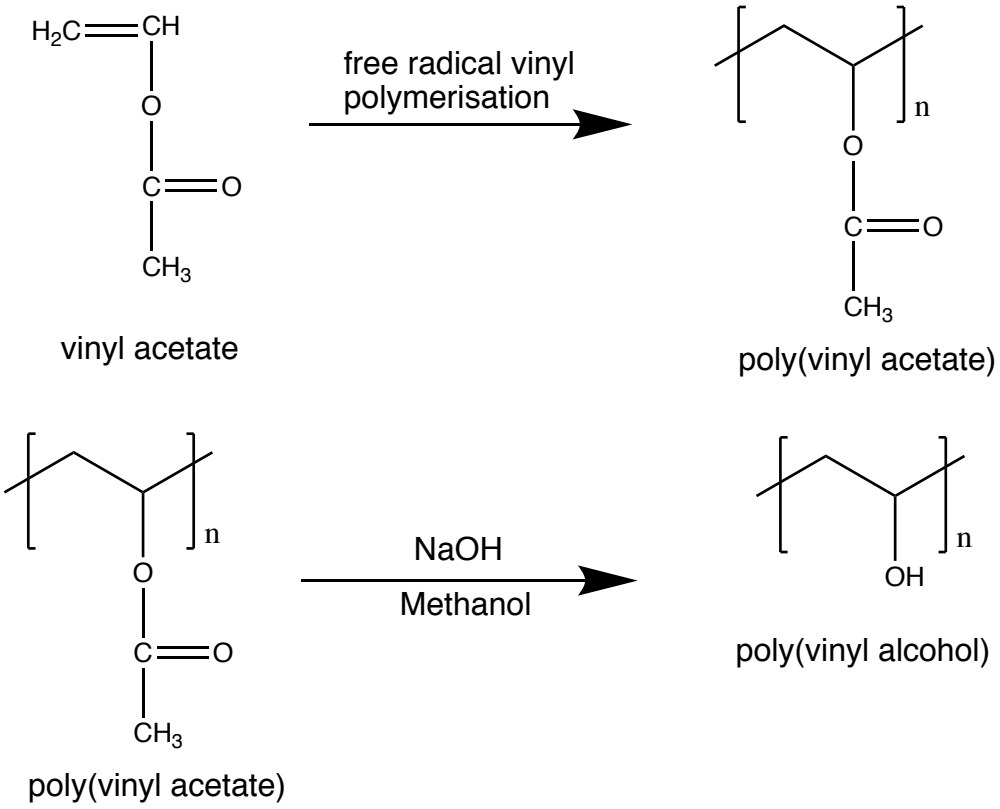

Figure 1.10. Synthetic routes for preparation of PVA.

PVA is always a copolymer with PVAc due to incomplete hydrolysis of the starting material[81]. In 1924, the first PVA solution was discovered by saponifying poly(vinyl ester) with caustic soda solution[82].

Commercial PVA grades are available with high degrees of hydrolysis - above 98.5%. The crystallizability and solubility of PVA is affected by the extent of remaining acetate groups as indicated by the degree of hydrolysis[81]. PVA cannot be readily dissolved in common organic solvents, such as methanol, ethanol, or chloroform; it is only soluble in DMSO and water[83]. The polymerisation and degree of hydrolysis affects the solubility of PVA in water; lower solubility results at an increased degree of hydrolysis. In addition, the hydroxyl pendant groups on PVA chains can interact to form internal intra- or intermolecular hydrogen bonding, which hinders its dissolution in water[84].

Based on the degree of hydrolysis, PVA is divided into two groups: partially hydrolysed and fully hydrolysed (Figure 1.11)[82]. Partially hydrolysed PVA has weakened internal hydrogen bonding interactions due to the presence of residual hydrophobic acetate groups, leading to increased external hydrogen bonding and water solubility. PVA

of this type can be dissolved in water at room temperature and is widely used in the food industry[82]. Nevertheless, the solubility of almost fully hydrolysed PVA in water needs a temperature higher than 80 ^{o}C in order to overcome hydrogen bonding interactions[84].

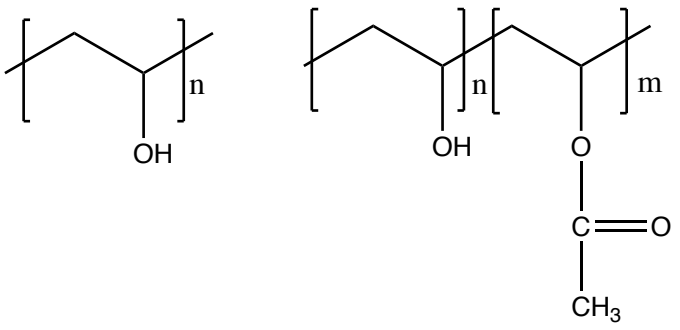

(A) (B)

Figure 1.11. Chemical structure of PVA: fully hydrolysed (A) and partially hydrolysed (B).

Free radical polymerisation is used to prepare PVA and subsequent hydrolysis results in a wide distribution of molecular weight. This is considered a significant feature of PVA because it influences its attributes, such as mechanical strength, diffusivity, crystallizabillity, and adhesion[81]. The effect of the degree of hydrolysis and molecular weight on the properties of PVA is indicated in Figure 1.12 [84].

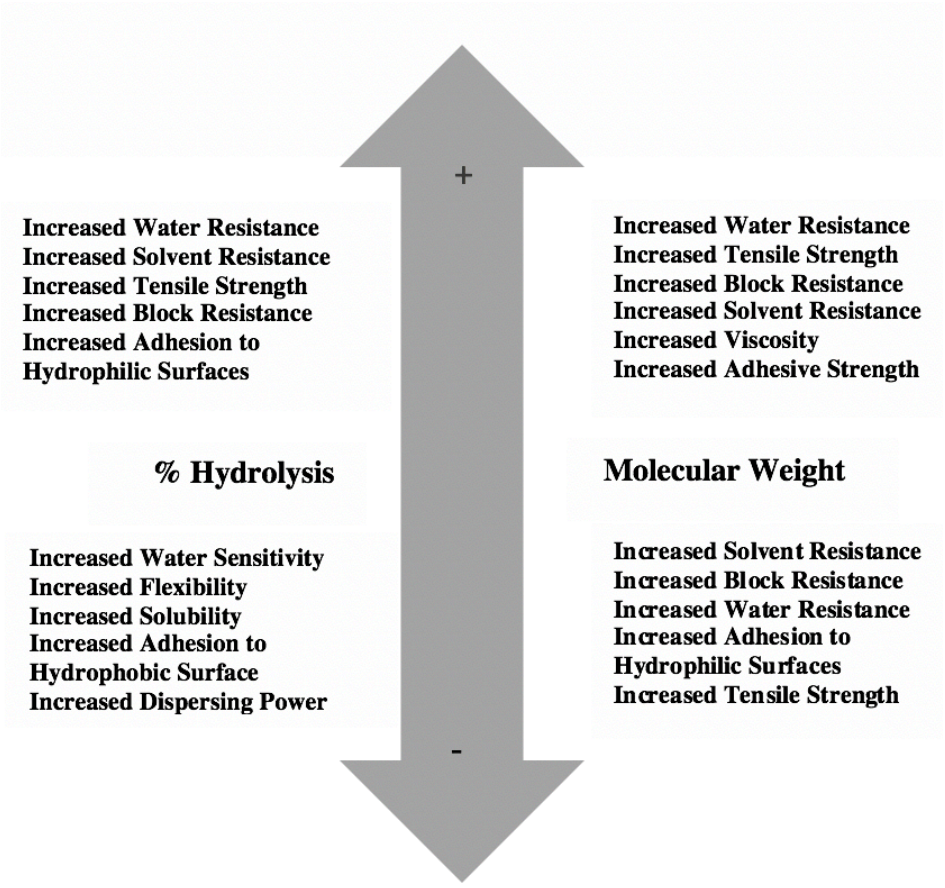

Figure 1.12. Characteristics of PVA[84].

1.2.12. **Preparation and properties of poly(vinyl alcohol) hydrogel**

Some of the interesting features of PVA include that it is biocompatible[85-89], hydrophilic[90], biodegradable[91], water-soluble, noncarcinogenic, nontoxic[92-90], and inexpensive. It can serve as a gas barrier and has good chemical resistance[93], processability, transparency[94] and good film-forming ability[95]. PVA can also form hydrogels using physical and chemical approaches to preparation. These unique features play a critical role in the design of biomedical and pharmaceutical devices, such as wound dressings[93], contact lenses, drug delivery devices, protein adsorption, artificial organs, and antibacterial and skin treatment systems[96].

Hydrogels of PVA can be easily ionised in buffer solutions due to the presence of hydroxyl groups. Factors such as pH and ionic strength weaken the hydrogen bonding and

other molecular interactions in the PVA network, which has a dramatic effect on swelling ability[97].

An aqueous solution of PVA can form a hydrogel with low mechanical properties when the solution is exposed to long storage times at room temperature**.** However, this does not result in a useful material for a broad range of applications because of the poor mechanical properties; considered the most important of hydrogel properties[94].

There have been numerous attempts to crosslink PVA using a freeze–thaw method, whereby a semi-crystalline network results as the solution of PVA is exposed to repeated cycles of freezing and thawing. The freeze–thaw method is preferred because it avoids contamination from toxic crosslinking agents used to prepare physically crosslinked hydrogels. The mechanical feature of physically crosslinked PVA can also be regulated by the number of freeze–thaw cycles, and the concentration and molecular weight of PVA. To meet some biomedical demands, PVA has been blended with other polymers to develop a hydrogel for particular applications, including wound dressing, drug delivery system, and tissue engineering. Examples of PVA compatible polymers include PVP, poly(N-isopropylacrylamide), chitosan, carboxymethyl chitosan, and dextran[94].

Hydrogels can also be produced by cooling semi-diluted PVA solutions at a low temperature. Pines et al. investigated the preparation of PVA hydrogels by both liquid–liquid phase separation and crystallization of PVA chains[98], whereby crosslinking sites are formed in the crystalline domains throughout the PVA network[99]. Consequently, PVA hydrogels can be produced without using crosslinking agents to make biomedical, biocompatible, and nontoxic devices[96, 100]. revise

Several studies have investigated the features and conditions of cryostructuring to prepare PVA cryogels[101-102]. Lozinsky et al. found that an increase in temperature from 295 K to 350–390 K significantly altered the mechanical properties of PVA gels[103]. Desirable properties of high water content, good clarity, and excellent mechanical characteristics resulted from cryostructuring to induce crystallization at low temperatures[104]. A further study prepared PVA hydrogels with higher water uptake, good adhesion properties, and elasticity features below 0 ^{o}C. In addition, hydrogels were used as a biomaterial for skin treatment systems by crystallization of domains in PVA at low temperatures[105]. A freeze–thaw cycle method was used to prepare semi-crystalline PVA hydrogels with PAA and poly(ethylene glycol) for drug delivery applications[106-107].

In addition, hydrogels, including those prepared from PVA, can be physically crosslinked by phase separation from theta-solutions or through crystallites that are formed during annealing and dehydration, and freeze–thaw cycling[108]. Hydrogels of PVA prepared by a repeated freezing and thawing approach indicate high water content and elastic mechanical features[109].

Thermosensitive hydrogels composed of PVA and N-tertiary butyl acrylamide (NTBA) were prepared using the free radical polymerisation method[110].

Graft copolymerisation of NTBA on PVA was used to prepare a PVA-g-PNTBA copolymer. Incorporation of NTBA on the surface of PVA was investigated using elemental analysis, H-NMR and infrared spectroscopy. Factors including hydrophobic content, annealing temperature, and temperature of the external medium had a great effect on the swelling behaviour. Results obtained by XRD, DSC, and DMA indicated that there was an increase in the crystallinity of the resulting copolymer as a function of annealing. A permeability study used a variety of solutes, such as vitamin B12, theophylline, and lysozyme. The results indicated that permeability of solutes was dependent on the solution temperature, hydrophobicity of the membrane, and the solute size[110].

Chemically crosslinked PVA hydrogels can be prepared using difunctional crosslinking agents, such as glutaraldehyde, acetaldehyde, formaldehyde, and other monoaldehydes. These crosslinking agents are initiated by acetic acid, sulfuric acid, or methanol, and result in formation of acetal rings and ether linkages between hydroxyl groups of PVA and aldehyde groups of the crosslinker. Peppa et al. prepared crosslinked PVA by electron beam irradiation methods in the presence of sodium borate and boric acid as crosslinking agents[109].

Hydrogels based on PVA and polyethylene glycol (PEG) were prepared using glutaraldehyde as a crosslinker. The resulting hydrogels were used to investigate the delivery of anti-inflammatory drugs, including ibuprofen. Solid inclusion complexes of ibuprofen in β–cyclodextrin (β–CD) were prepared by microwave irradiation and inserted in the hydrogel network to regulate the drug delivery. Hydrogels containing the inclusion complexes indicated controlled release of the drug in comparison to hydrogels that included free ibuprofen. Analysis of preliminary kinetics emphasised the important role of β–CD that affected the rate of polymer relaxation, contributing to a slower rate of drug release[111].

1.2.13. **Molecular imprinted polymers (MIPs)**

Molecular imprinting is a technique that can generate selective recognition sites throughout a synthetic material. Molecular imprinted polymers (MIPs) are crosslinked polymers that include particular bending sites with a pre-determined selectivity for a solute template[84]. The process of molecular imprinting to prepare a MIP is indicated in Scheme 1.1.

The template is inserted into the rigid matrix by interaction with functional monomers to form complexes during polymerisation[84]. Monomer-template complexes are formed by either weak non-covalent interactions (e.g. hydrogen and ionic bonding, hydrophobic interactions) or covalent bonds. The first method is commonly used because it offers simplicity of preparation. Template and monomer are mixed to form a complex and polymerisation in a suitable solvent is initiated in the presence of a crosslinking monomer. The template is removed from the polymerised matrix by, typically, liquid-liquid extraction.

However, there are difficulties associated with this method, including the proper selection of solvents and monomers. A low ratio of monomer-to-template leads to a low number of bonding sites, whereas a polymeric matrix with too high a ratio of monomer-to-template produces a material with non-specific recognition[112].

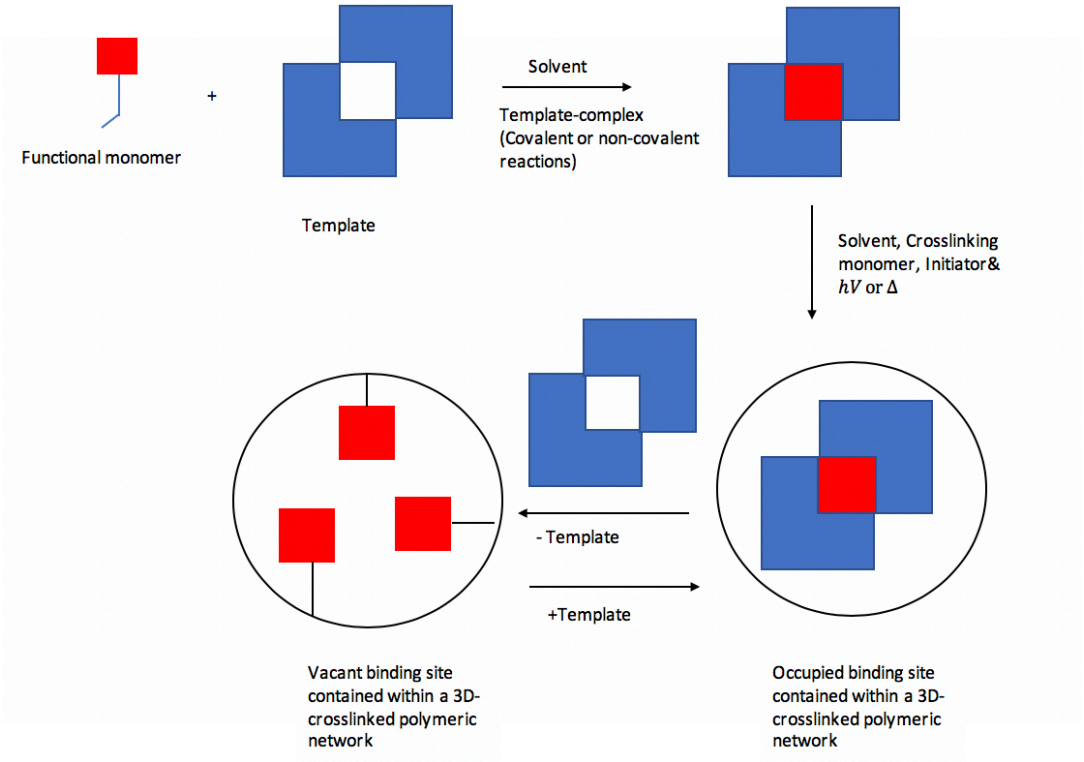

Scheme 1.1. Synthetic routes for preparation of MIPs.

A three-dimensional imprinted structure, consistent with the size and shape of the template molecule, is imposed throughout the polymer. Vacant recognition sites with high affinity for the target molecule result from the removal of the solute template. The selective recognition sites are able to respond to external environmental stimuli such as solvent composition[113], pH[114], temperature and electric field[115].

Some useful advantages of MIPs compared to simple polymers used for adsorption are resistance to pressure and higher temperatures, good mechanical strength, low cost of preparation, physical toughness, and inertness to many organic solvents, bases, acids, and metal ions. Due to their beneficial features, MIPs are useful for a variety of applications, such as sensors, drug delivery systems, catalysis, solid phase extraction (SPE), and liquid chromatography[84, 116].

1.3. Research Aim

Hydrogels are materials that display many useful properties that make them ideal candidates for solute extraction and delivery in aqueous environments. Compared to hydrogels prepared by other techniques, such as copolymerization methods, hydrogels prepared as interpenetrating polymer networks (IPNs) have generated much interest because they offer enhanced thermal stability, chemical responsiveness, and structural rigidity[47,133].

The preparation and investigation of physiochemical properties of a series of full-IPN PVA/PHEMA, full-IPN PVA/P(HBA-co-AA), and full-IPN PVA/P(MMA-co-IA) hydrogels is investigated. The use of extractants in an IPN could be a useful method to prepare a novel generation of adsorbent hydrogels with enhanced properties, including capacity for reuse and specific metal ion adsorption. Hydrogels as a system for delivery of drugs has been investigated, however, extraction of organic solutes by hydrogels used as adsorbents has yet to be reported.

The major aim of this research is to develop full-IPNs for the selective extraction of copper ions and removal of naproxen from an aqueous environment. The series of full-IPN hydrogels will be prepared incorporating Acorga P50 and Aliquat 336 as carriers for copper and naproxen, respectively, and the hydrogel properties and extraction performance will be evaluated.

1.4. Thesis outline

The first chapter presents a literature review associated with a general overview of hydrogels. The different methods to prepare hydrogels and their ability to respond to some external stimuli that make them ideal useful materials for different application is discussed.

Chapter 2 reports the preparation of hydrogels consisting of PVA with different monomers, such as 2-hydroxyethyl methacrylate (HEMA), acrylic acid (AA), 4-hydroxybutyl acrylate (HBA), methyl methacrylate (MMA), and itaconic acid (IA). Two different crosslinking agents were used, ethylene glycol dimethacrylate (EGDMA) for hydrophobic monomers and glutaraldehyde (GA) for PVA. The resulting hydrogels designed as full-IPN PVA/PHEMA, full-IPN PVA/P(HBA-co-AA), and full-IPN PVA/P(MMA-co-IA) were prepared by a free radical polymerisation using AIBN as an initiator. In particular, the effect of GA, HBA, and MMA amounts on the composition and properties, such as swelling behaviour, and thermal and morphological properties, of the hydrogels are investigated. The resulting hydrogels are characterised using Fourier transform infrared (FTIR) spectroscopy, ToF-SIMS, scanning electron microscopy (SEM), and thermal gravimetric analysis (TGA).

In chapter 3, the use of Acorga P50 as a copper carrier to prepare reagent imprinted and complex imprinted full-IPN hydrogels is reported. The full-IPNs imprinted with Acorga P50 or Cu (II)-Acorga P50 complex were used in extraction investigations of Cu (II) from an aqueous feed solution of 50 mg/L at pH 2. Copper was removed from the hydrogels using 2 M H_2SO_4. The physicochemical properties of the hydrogels were characterised by FTIR, SEM, and TGA. The kinetics and extraction performance were evaluated at different pH and initial Cu (II) concentrations. The current study also investigated the application of full-IPN hydrogels as artificial adsorbents for Cu (II) removal.

The objective of preparing novel-full-IPN hydrogels based on PVA containing Aliquat 336 as a basic carrier for anions is reported in chapter 4. The hydrogels (abbreviated as Aliquat 336-PVA/GA, Aliquat 336-full-IPN PVA/PHEMA, Aliquat 336-full-IPN PVA/P(HBA-co-AA), and Aliquat 336-full-IPN PVA/P(MMA-co-IA)) were used as adsorbents for the extraction of Naproxen as a model drug. Extraction and back-extraction experiments were performed using a feed solution of 125 mg/L at pH 7 and a stripping

solution of 1 M NaCl at pH 9, respectively. Naproxen extraction kinetics using the hydrogels was evaluated. The presence of Aliquat 336 in the hydrogel matrix was investigated using FTIR, SEM, and TGA

The final chapter presents a brief conclusion about all investigations and outcomes from this research, and reports on future work that builds on the already established positive attributes of full-IPNs and promising results reported in this thesis. Specifically, investigations using Acorga P50 and Aliquat loaded full-IPN hydrogels applied to real environmental samples to assess the interference of other chemicals, such as iron and zinc, on copper extraction, and other deprotonated organic and inorganic anions are needed.

Chapter 2: Preparation of full-IPN hydrogels

2.1. Introduction

Among the many significant hydrogels, poly(2-hydroxyethyl methacrylate) (PHEMA) was first synthesized in 1960 by Whichterle and Lim. Subsequently, it was cross-linked with ethylene glycol dimethacrylate (EGDMA) and used for the production of contact lenses[36, 51, 63, 117]. The most positive aspect of this novel biomaterial is its stability under a broad range of temperatures and pH, and its high hydrophilicity and excellent mechanical properties[41]. In the following two decades, research on hydrogels concentrated on producing chemically cross-linked networks of polymers for applications, principally, in drug delivery and ophthalmic research[39]**.** In addition, scientist have found that hydrogels based on PHEMA can be employed for other applications, such as implants for surgical reconstruction, artificial corneas, nasal cartilages, and surgery dressings to control wound infections[77].

Hydrogels containing methacrylic acid (MAA) and 2-hydroxyethyl methacrylate (HEMA) (Figure 2.1) exhibit sharp sensitivity to external pH. The pH-dependent swelling behaviour of poly(HEMA-co-MAA) hydrogels show extensive swelling in high pH media due to ionisation of the pendant COOH groups. The extent of the equilibrium swelling depends on the MAA composition and pH of the swelling medium. Alternatively, these hydrogels are maintained in a neutral state if the media is kept below pH 3.5, because poly(MAA) has a pK_a of 5.5. Thus, under these conditions these hydrogels will be in a comparatively shrunken state[118].

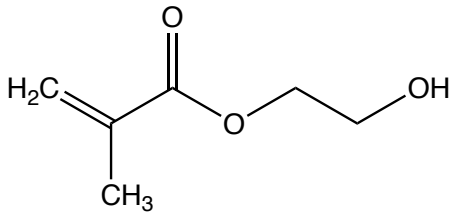

2-hydroxyethyl methacrylate (HEMA)

Figure 2.1. Chemical structure of 2-hydroxyethyl methacrylate (HEMA).

However, the mechanical properties of hydrogels based on PHEMA are poor in a swollen state[77] due to absorbed water which changes the distribution of and interaction between polymer chains to that in dried gels[119]. Hence, considerable effort has been made to improve the strength of hydrogels by using different approaches, such as bulk copolymerization, forming interpenetrating networks with natural biopolymers like collagen, and grafting to a natural or synthetic polymer. Although these modified compounds are more robust than pure compounds, their poor mechanical properties remain a problem[77].

In the most recent decade, research has tended to use other types of polymers with unique properties to prepare hydrogels for advanced biomedical applications[94]. In particular, poly(vinyl alcohol) (PVA) is frequently used as a synthetic polymer to produce hydrogels for purposes of wound dressing[119], drug delivery systems[94], artificial organs[120], and as an adsorbent for removal of heavy metal ions[121]. The widespread use of PVA is due to its unique properties, such as good biocompatibility, excellent transparency, non-toxicity, bioadhesive features, film-forming ability[24], and excellent hydrophilicity[90, 92, 95, 97, 122-133]. PVA crosslinked with formaldehyde was the first hydrogel, reported in 1949, for use as a biomedical implant[30].

PVA in an aqueous solution can be easy cross-linked to form hydrogels by using a range of techniques. The obtained hydrogels have desirable physicochemical features, such as a high degree of swelling and an elastic nature. Nonetheless, PVA has some drawbacks, including a resultant stiff membrane with insufficient elasticity, and lower mechanical strength due to an increased hydrophilic nature[43]. Incorporating PVA with HEMA into an interpenetrating polymer network (IPN) is a good way to increase the swelling features of the hydrogel[134].

Acrylic acid (AA) (Figure 2.2) is a non-toxic, hydrophilic monomer that can respond to changes produced by external stimuli such as pH[135]. Poly(acrylic acid) (PAA) has been largely utilized as a pH and electrical-sensitive material. Specifically, the pH-responsive nature of PAA results from the presence of carboxylic acid groups along the polymer chains[136].

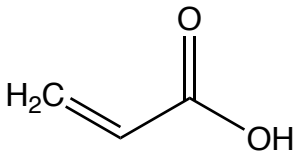

Acrylic acid (AA)

Figure 2.2. Chemical structure of Acrylic acid (AA).

Hydrogels containing PVA and stimuli-responsive monomers, especially AA, have attracted significant attention in polymer science for biomedical applications due to their unique features, including non-toxicity, biocompatibility, and high hydrophilicity. Hydrogels of PVA/AA were used as a drug delivery system for diclofenac, and indicated a higher rate of release, due to the hydrophilic group (-COOH) of PAA, than a simple PVA gel[46].

Hydrogels based on PAA and poly(acrylamide) (PAAm) (PAA/PAAm) exhibit temperature responsive sensitivity because of hydrogen bonding between COOH and NH_2 groups on neighbouring polymer chains. At temperatures below the upper critical solution temperature (UCST), the polymer network collapses because of extensive hydrogen bonding between the polar groups of each polymer. Conversely, at temperatures above the UCST, the hydrogen bonds are disrupted and the swelling ability of the hydrogels is increased[47].

Hydrogels containing many ionisable groups are defined as poly electrolytes and can be classified into two categories, cationic or anionic. Their capability to undergo changes in volume capacity as they respond to external stimuli, such as ionic strength, pH, and temperature, is an important feature. Poly(acrylamide-maleic acid), poly(acrylamide-co-itaconic acid), and poly(acrylamide-co-acrylic acid) are examples of polyelectrolyte hydrogels.

Itaconic acid (IA) (Figure 2.3) is an 'anionic' monomer that has been widely studied to enhance the biocompatibility, and pH-sensitive behaviour of PHEMA based hydrogels[42]. The two carboxylic groups on the side-chain of poly(itaconic acid) (PIA) have different pK_a (pK_{a1} 3.85, pK_{a2} 5.45) [137-138] that influence the hydrophilic character of the

hydrogel[139] and significantly increase its ability to absorb water. When 5 wt% of PIA is incorporated with PHEMA, the equilibrium degree of swelling of the resulting P(HEMA/IA) hydrogel in pH 7.4 buffer solution at 37 ^{o}C increases by more than 200%. Furthermore, increasing the IA content resulted in improved swelling ability of the hydrogel because of additional electrostatic repulsions of ionised acid groups in the gel[140]. Other studies have indicated a similar improvement in the swelling degree of poly(acrylamide) hydrogels incorporating PIA[141].

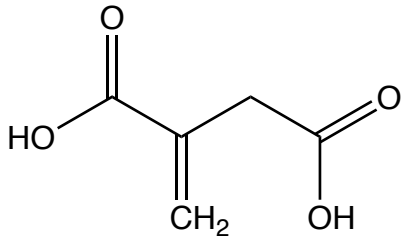

Itaconic acid (IA)

Figure 2.3. Chemical structure of itaconic acid (IA).

A combination of PVA and PIA in one matrix seems like a reasonable proposition to produce new materials with improved properties, including hydrophilicity, mechanical strength[91, 142], and pH-sensitive behaviour. Due to its unique attributes, such as high water absorption ability, chemical resistance and film forming ability, biodegradability and non-toxicity, PVA is a good candidate for extensive use to fabricate hydrogels[90, 92, 95, 97, 122-133]. PVA-based hydrogels show high water absorption capability and good mechanical strength[124-125, 143-144].

A pH-sensitive hydrogel composed of PVA, chitosan, vinyl acetate, and IA has been prepared using a freeze thaw method[162]. The hydrogels indicated a high degree of swelling at low pH (1.4) because of ionisation of the primary amino groups (-NH_3^+) on the surface of chitosan. The results from an x-ray diffraction (XRD) study showed a reduction in crystallinity of hydrogel films because of the presence of chitosan. A morphological study indicated that hydrogel pores were uniformly arranged with sizes from 20 - 100 μm, with larger pores at higher amounts of chitosan[145].

Most pH-thermo-sensitive hydrogels obtained by conventional preparation methods (e.g., copolymerisation) have some disadvantages, such as low rates of swelling and deswelling. These drawbacks limit their use for some applications, such as drug delivery systems, artificial organs, and separation science. There have been many attempts to enhance the water activity of hydrogels, including inserting grafted chains into the hydrogel matrices, employing high temperature preparation methods, and forming macroporous structures[146].

Recently, hydrogels prepared as interpenetrating polymer networks (IPNs) have generated much interest because they offer enhanced mechanical stability, chemical responsiveness, and structural rigidity compared to hydrogels prepared by other techniques, such as copolymerization methods[48, 147]. IPNs are described as an entangled combination of polymers in which one polymer is prepared or crosslinked inside the other, without any covalent bonds between them. An IPN is classified as either a semi-IPN or full-IPN depending on the preparation strategy. Hydrogels with dense matrices and tough mechanical properties can be produced using IPN methods[48, 147-148].

Semi-IPN hydrogels composed of PVA, acrylamide (AAm), and HEMA have been prepared by a microwave irradiation technique. The preparation of semi-IPN PVA/P(AAm-co-HEMA) involved a one-pot, two-step polymerisation method. A copolymer of P(AAm-co-HEMA) was prepared in an aqueous solution of PVA using ammonium persulfate (APS) as an initiator, followed by addition of glutaraldehyde (GA) as a crosslinker to form the semi-IPN. The outcomes revealed that the hydrogel obtained by the two-step polymerisation technique had a lower swelling ratio compared to the hydrogel prepared by the one-pot polymerization method. However, one-pot polymerisation was found to be a more useful technique, in terms of shorter preparation time, for preparing semi-IPN hydrogels [149].

Full- and semi-IPN hydrogels composed of PVA, HEMA, and acrylic acid (AA) were prepared and investigated. The full-IPN hydrogels had a higher crosslink density and smaller mesh size compared to semi-IPN hydrogels, whereas dye adsorption and swelling characteristics of semi-IPN hydrogels were higher than those of full-IPN hydrogels[125].

Hydrogels produced as IPNs of PAA and poly(acrylamide-co-butyl methacrylate) P(AAm-co-BMA) have used as a drug delivery system for ketoprofen. The IPN hydrogels

exhibited a better swelling degree when observed at temperatures above their UCST, leading to improved release of loaded ketoprofen[150].

Further studies have investigated IPN-hydrogels based on PVA and PAA. Specifically, equilibrium swelling studies to determine mesh size, crosslinking density, and average molecular weight were investigated. Swelling studies were performed in a series of pH buffer solutions (3, 6, & 8) and indicted improved equilibrium swelling degree as the pH increased from 3 to 6[151].

To prepare naturally derived, polymer-based hydrogels with specific properties, including controlled drug delivery and high mechanical strength, semi-IPN hydrogels composed of chemically crosslinked poly((vinyl alcohol)-graft-acrylic acid)/sodium alginate) (PVA-g-AA)/SA) were prepared and investigated. The resulting semi-IPN hydrogels exhibited optimum swelling, drug loading, and drug release at pH 7.4[124].

Hydrogels have been prepared from PVA, AA, and HEMA using IPN methods. The full-IPN and semi-IPN hydrogels were prepared via a free radical polymerization of HEMA and AA, using azobisisobutyronitrile (AIBN) as initiator, crosslinked with EGDMA in a PVA network. The full-IPN hydrogels exhibited higher crosslinking density and smaller mesh size compared to semi-IPN hydrogels[125].

Thermo and pH-sensitive semi-IPN PVA-based hydrogels were prepared with N,N-diethylacrylamide (DEA) and IA by free radical polymerisation, resulting in an interconnected porous structure. The resulting hydrogels showed a reduced equilibrium degree of swelling due to the formation of crystals at increased amounts of PVA. A fast deswelling rate was observed for semi-IPN PVA/P(DEA-co-IA) hydrogels because the linear polymer chains act as channels to release water molecules as shrinking occurs. Parameters such as pH, temperature, and PVA content had an effect on the oscillating deswelling/swelling behaviour[146].

A semi-IPN hydrogel containing poly(vinylpyrrolidone) (PVP), HEMA and IA was prepared by free radical crosslinking copolymerisation. The resulting hydrogels indicated pH-temperature sensitive behaviour, with a maximum degree of swelling observed at pH 6 and 41 ^{o}C[152].

However, due to weak mechanical strength, poor reswelling behaviour, and the high water loss from PVA hydrogels, it is necessary to identify ways to enhance these properties to satisfy the necessary requirements for effective hydrogels based on PVA[153].

Recently, the use of IPNs for the preparation of hydrogels has garnered interest. These polymer materials offer improved mechanical properties through better stability of the internal[153] and overall network structure[48, 134].

IPN-hydrogels prepared from PVA and PAA have been widely investigated[151, 154-155]. However, the preparation of full-IPN hydrogels containing PVA, AA, 4-hydroxybutyl acrylate (HBA), methyl methacrylate (MMA), IA, and HEMA have not yet been reported.

The main objective of the present work is to create novel pH-sensitive full-IPN hydrogels by utilising the ionisable groups of PVA, HEMA, HBA, MMA, IA and AA. The strategy is to prepare full-IPN hydrogels via insertion of a cross-linked copolymer of P(-HBA-co-AA), P(MMA-co-IA) or PHEMA into PVA. Hydrogels will be prepared by free radical polymerization using EGDMA as a crosslinking agent and AIBN as an initiator.

The first network of each full-IPN hydrogel will consist of PVA crosslinked with GA to form PVA/GA. Due to its unique features, including hydrophilic characteristics and film forming ability, PVA is used as the main polymer network to provide the resulting full-IPN hydrogels with improved swelling properties and ability to form films. The second network will utilise HEMA, HBA, MMA, AA and IA as hydrophobic, and hydrophilic components. Full-IPN PVA/PHEMA will be prepared by polymerisation of HEMA within the PVA network. Both HBA and MMA will be used as base monomers, to provide mechanical strength to the full-IPN, and copolymerised with AA and IA, respectively, to prepare P(HBA-co-AA) and P(MMA-co-IA).

The effect of amounts of GA, HBA and MMA on gel content, chemical structure, swelling and water retention will be studied. The chemical nature of the series of full-IPN hydrogels will be characterised by FTIR and ToF-SIMS. A pH-sensitivity study to probe water adsorption will be performed in a series of pH buffer solutions (3.4, 6.2, 7.2, and 8.2) at 37 ^{o}C. Water retention ratio study will be investigated at 30 ^{o}C. Finally, the surface morphology and thermal properties will be investigated by SEM and TGA, respectively, of the series of full-IPN PVA/PHEMA, PVA/P(HBA-co-AA) and PVA/P(MMA-co-IA) hydrogels.

2.2. Experimental

2.2.1. Materials

2-hydroxyethyl methacrylate (HEMA) (Aldrich), poly(vinyl alcohol) (PVA) (89 000-98 000, 99+% hydrolysed) (Aldrich), ethylene glycol dimethylacrylate (EGDMA) (Aldrich), glutaraldehyde (GA) (Aldrich), 4-hydroxybutyl acrylate (HBA), acrylic acid (AA), itaconic acid (IA), and methyl methacrylate (MMA) were used as reactants for preparation of hydrogels. HEMA, HBA, AA were purified using an activated alumina column and verified by ^{1}H-NMR. PVA, EGDMA and GA were used as received. 2,2'-Azobisisobutyronitrile (AIBN) was purified by recrystallization from ethanol[156]. Sodium dihydrogenphosphate dihydrate ($NaH_2PO_4.2H_2O$) (Aldrich) and disodium hydrogenphosphate heptahydrate ($Na_2HPO_4.7H_2O$) (Aldrich) were used as received. All other chemicals including dimethyl sulfoxide (DMSO), phosphoric acid (H_3PO_4) and sulfuric acid (H_2SO_4) were reagent grade and used as received. Deionised water was used to prepare all aqueous solutions.

2.2.2. Preparation of full-IPN hydrogels

Full-IPN PVA/PHEMA hydrogels were prepared by free radical polymerization using AIBN as initiator and EGDMA as a cross-linker. The procedure used to prepare the hydrogels is briefly described as follows. First, a weighed amount of PVA was dissolved in 15 mL DMSO in a three-neck round bottom flask, a water condenser attached, and the solution stirred using a magnetic stirrer bar. The solution was heated to 80 ^{o}C with continuous stirring at 800 rpm until a transparent solution was obtained. The solution was cooled to room temperature with continuous stirring at slow speed and dissolved oxygen purged by nitrogen gas (solution A). Different amounts of GA (10, 20, 30, 40 wt%) and 0.1 mL of sulfuric acid were added to solution A and stirred for 10 minutes. Secondly, solution B was prepared by addition of amounts of HEMA as monomer and EGDMA (0.1 g) as cross-linker to a small amount of DMSO (5 mL). Solution B was added to solution A. Finally, AIBN (0.1 g) as initiator was added to the mixed solution and stirred for 30 mins while maintaining a nitrogen atmosphere. Then, the solution was carefully transferred to glass reaction tubes (150 mm length, 16 mm i.d.), the tubes sealed under nitrogen, and immersed in a water bath at 60 ^{o}C for 7 h to continue polymerization. At the end of the polymerization, the tubes were carefully broken, and the gels cut into appropriate size (1 mm thick and 5 mm in diameter) pieces. The preparation of full-IPN PVA/P(HBA-co-AA)

and full-IPN PVA/P(MMA-co-IA) hydrogels was similar. The feed composition for each component used to prepare the different hydrogels is shown in Table 2.1.

2.2.3. **Determination of gel content**

The gels were dried in an oven at 30 ^{o}C for 24 h and the weight noted as W_0. Next, the gels were immersed in deionized water, and the water replaced everyday over a week to wash and remove any unreacted initiator and monomers. Subsequently, the gels were dried under vacuum at 30 ^{o}C to attain a xerogel of mass (W_1).

The gel content, percent (Gel%) of the hydrogel was determined using the following expression.

$$Gel\% = [W_1/W_0] \times 100$$

Where W_1 is the weight of dry gel after washing in deionised water and W_0 is the initial weight of dry gel[157].

2.2.4. **Buffer solutions**

Phosphate buffer solutions of 0.1 M ionic strength were used to induce swelling in the hydrogels. A solution of pH 3.4 was made from KH_2PO_4, and H_3PO_4, whereas pH 6.1, 7.2, and 8.2 solutions were prepared from $NaH_2PO_4.2H_2O$ and $Na_2HPO_4.7H_2O$. All solutions were prepared using deionised water. The pH of the prepared buffer solutions was measured using a pH meter (Seven Easy Model, China) calibrated with standard buffer solutions.

2.2.5. **Water uptake measurements**

The xerogel discs were left to swell in deionised water at 37 ^{o}C for 24 h. At different intervals, the swollen gels were removed and gently dried by resting on filter paper. After achieving a constant weight, the samples were returned to the swelling medium. The swelling measurements were continued until equilibrium swelling was reached for each sample. The swelling measurements indicate the extent of water absorption by the hydrogels.

Water uptake, percent (WU%) was calculated as follows:

Water uptake (WU%) = [$W_S - W_0$] / $W_0 \times 100$

Where W_0 and W_S are the weights of dry and wet discs, respectively. All swelling experiments using deionised water were performed in triplicate.

2.2.6. **pH- sensitivity study**

The pH-sensitivity behaviour of full-IPN hydrogels was studied in phosphate buffer solution (PBS) at various pH values. The xerogel discs were left to swell in buffer solutions of pH 3.2, 6.1, 7.2, or 8.2 with ionic strength of 0.1 M and at a temperature of 37°C. At different intervals, the swollen gels were removed and dried by resting on filter paper. After drying to constant weight, the samples were returned to the buffer solution. The swelling measurements were continued until equilibrium swelling was reached for each sample[6].

The equilibrium degree of swelling, percent (q_e%) was evaluated using the following expression:

$q_e\% = [W_S - W_0]/ W_0 \times 100$

where W_S is weight of wet sample at equilibrium , and W_0 is weight of dry sample[158]. All swelling experiments in buffer solution at different pH were performed in triplicate**.**

2.2.7. **Water retention measurements**

The dried full-IPN PVA/PHEMA, full-IPN PVA/P(HBA-co-AA), and full-IPN PVA/P(MMA-co-IA) gels, as a function of GA, HBA to AA, and MMA to IA ratios, respectively, were first soaked in water at room temperature until reaching an equilibrium weight (W_{eq}). The equilibrium swollen full-IPN gels were then transferred to an oven at 30°C. The gels were removed at predetermined times and the weight recorded; measurement continued until an equilibrium weight (W_t) of the dried gel was achieved The water retention, percent (WR%) was expressed by the following equation.

(WR%) = W_t/W_{eq} *100

Where, W_{eq} is the weight of the equilibrium swollen hydrogel, and W_t is the weight of dry gel[159].

2.3. Instrumental Analysis

2.3.1. Infrared Spectroscopy

The FTIR spectra of resulting PVA/GA, and full-IPN hydrogels were obtained using an Agilent Cary 600 series spectrometer. The dried gels were mixed with KBr prior to recording the spectra over the range 600 - 4000 cm^{-1} using a resolution of 4 cm^{-1}.

2.3.2. Time-of-Flight Secondary Ion Mass Spectrometry (TOF-SIMS)

Analyses were conducted using a TOF-SIMS IV instrument manufactured by ION-TOF GmbH (Münster, Germany). The hydrogel discs were loaded (fixed) on a substrate plate using double-sided tape. A pulsed primary ion source (bismuth beam, 30 keV, 0.501 pA) was bombarded over a sample area of 100 x 100 μm^2. Mass spectra (positive and negative polarity) were acquired for 100 s with an impact 9.41 x 10^{12} ions/cm^2 to guarantee static states. An argon-cluster source was used as the sputter/etch tool with 20 KeV sputter ion energy; the argon beam current was 9.224 nA. Analyses of the spectra of the full-IPN hydrogels were carried out using Surface Lab v5, IONTOF GmbH.

2.3.3. Scanning electron microscopy (SEM)

The surface morphology of prepared gels was studied by SEM using a HITACHI TM3030 Plus. The swollen hydrogels were dried using a freeze dryer (LABCONCO) at -80 ^oC for 24 h. The freeze-dried xerogels were loaded on the surface of an aluminium SEM specimen holder and sputter coated with gold for 2 minutes (Polaron sc7640 sputter coating) under vacuum prior to observation[160]. A magnification range of 100 - 10.000 was used in this study.

2.3.4. Thermogravimetric Analysis (TGA)

The thermal properties of full-IPN PVA/PHEMA, full-IPN PVA/P(HBA-co-AA) and full-IPN PVA/P(MMA-co-AA) hydrogels were investigated by TGA (TGA/DSC 1 STAR^e System (METTLER TOLEDO). Hydrogels with a mass of 8.5 mg under a purged nitrogen atmosphere were analysed over the temperature range of 50 – 500 ^oC at a heating rate of 10 ^oC/min.

2.4. Results and discussion

2.4.1. Preparation of full-IPN hydrogels

In a full-IPN hydrogel, both constituent polymers are cross-linked. In this study, the first full-IPN hydrogel consisted of poly(vinyl alcohol) (PVA) and poly(2-hydroxyethyl methacrylate (PHEMA). The full-IPN hydrogels were prepared by free radical polymerisation of 2-hydroxyethyl methacrylate (HEMA), with ethylene glycol dimethacrylate (EGDMA) in a matrix of poly(vinyl alcohol) (PVA) cross-linked with glutaraldehyde (GA).

A robust thin hydrogel film cannot be prepared from only copolymerization of HBA and AA, or MMA and IA because the resulting polymer lacks sufficient hydrophilic properties. Instead, poly(HBA-co-AA) and poly(MMA-co-IA) must be formulated in a polymer blend with a highly hydrophilic monomer or polymer, such as PVA, to have the ability to form hydrogel films.

The second full-IPN PVA/P(HBA-co-AA), and third full-IPN PVA/P(MMA-co-IA) hydrogels were prepared by free radical copolymerization of the acrylate monomers (HBA, AA, MMA and IA) to prepare a hydrophobic polymer within a network of hydrophilic PVA. The general synthetic route for preparation of the full-IPN PVA/PHEMA, PVA/P(HBA-co-AA) and PVA/P(MMA-co-IA) hydrogels, respectively, is indicated in Scheme 2.1.

The full-IPN hydrogels were prepared in dimethyl sulfoxide (DMSO) at 60℃ for 7 h for the first gel and 3 h for the second and third gels. DMSO is a good solvent for poly(vinyl alcohol), cross-linkers, monomers, and initiator. Azobisisobutyronitrile (AIBN) was used as the free-radical initiator for polymerisation in this study because it is known to polymerise monomers cross-linked with EGDMA.

The cross-linking reaction of PVA with GA was done by adding 0.1 mL of 10% H_2SO_4 as a catalyst. Due to the cross-linking process being adversely affected by the presence of oxygen in solution, which scavenges the free radicals responsible for initiating and propagating the polymerisation (as oxygen is a potent inhibitor[2])[125], the reaction mixture was purged with N_2 gas before polymerisation. Compared to other crosslinking regents, GA has lower cytotoxicity, and the resulting materials usually display good mechanical features in addition to being non-thrombogenic and biocompatible[161].

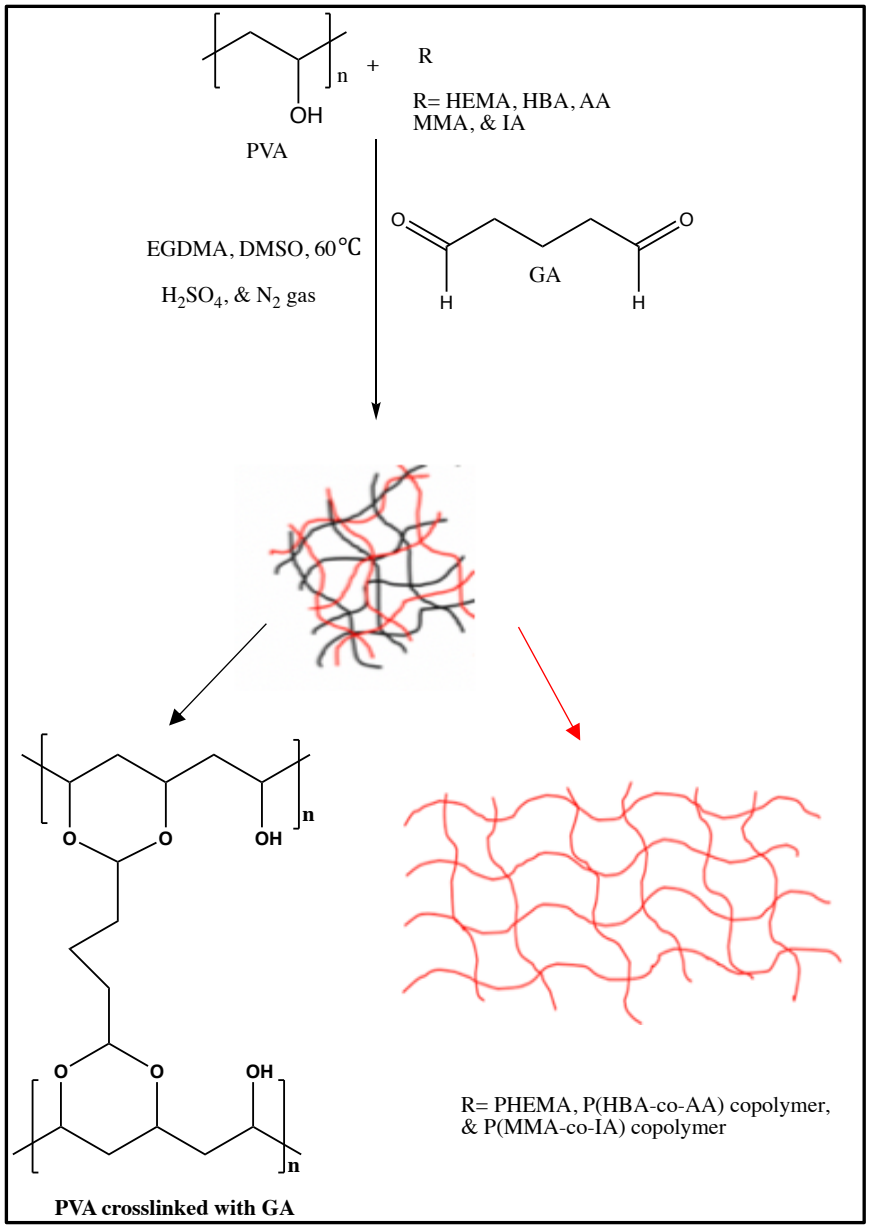

Scheme 2.1. Preparation of full-IPN hydrogels.

The full-IPN PVA/PHEMA hydrogel with a higher GA ratio (40 wt%) was revealed as hard and transparent discs, whereas gels with low GA ratio produced transparent discs with reduced hardness. The full-IPN PVA/(HBA-co-AA) and PVA/P(MMA-co-IA) hydrogels indicated harder and more rigid films as the amount of HBA and MMA were increased.

The amount of each monomer and reagent used to prepare the hydrogels is given in Table 2.1. The physical appearance of the prepared hydrogels after preparation, washing

with water, and drying is shown in Table 2.2. The high gel content of series 2 & 3 hydrogels is indicated by the retained swollen state after drying to remove free water.

Table 2.1. Composition (wt%) and gel content (%) of full-IPN hydrogels.

Hydrogel	PVA	GA	HEMA	HBA	AA	MMA	IA	EGDMA	Gel (%)
Series 1									
PVA/PHEMA1	40	10	40	-	-	-	-	10	45
PVA/PHEMA2	40	20	30	-	-	-	-	10	69
PVA/PHEMA3	40	30	20	-	-	-	-	10	92
PVA/PHEMA4	40	40	10	-	-	-	-	10	98
PVA/GA	60	40	-	-	-	-	-	-	97
PHEMA	-	-	90	-	-	-	-	10	96
Series 2									
PVA/(4-HBA-co-AA)1	33	27	-	14	20	-	-	6	96
PVA/(4-HBA-co-AA)2	33	27	-	20	14	-	-	6	97
PVA/(4-HBA-co-AA)3	33	27	-	27	7	-	-	6	98
PVA/PAA	36	29	-	-	29	-	-	6	98
PVA/P4-HBA	36	29	-	29	-	-	-	6	92
Series 3									
PVA/P(MMA-co-IA)1	33	27	-	-	-	10	24	6	94
PVA/P(MMA-co-IA)2	33	27	-	-	-	17	17	6	96
PVA/P(MMA-co-IA)3	33	27	-	-	-	24	10	6	98
PVA/PMMA	36	29	-	-	-	29	-	6	98
PVA/PIA	36	29	-	-	-	-	29	6	97

Table 2.2. Images of the physical appearance of full-IPN PVA/PHEMA (series 1), PVA/P(HBA-co-AA) (series 2), and PVA/P(MMA-co-IA) (series 3) hydrogels after preparation, washing with water, and after drying.

Hydrogel	After preparation	After washing	After drying
Full-IPN PVA/PHEMA (series 1)			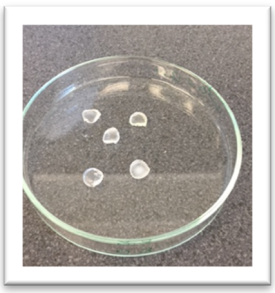
Full-IPN PVA/P(HBA-co-AA) (series 2)	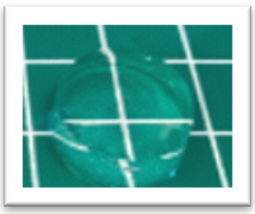		
Full-IPN PVA/P(MMA-co-IA) (series 3)			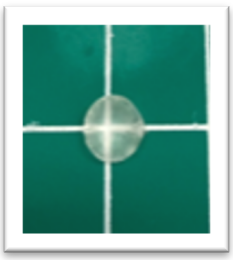

2.4.2. **Gel content**

A series (referred to as series 1) of full-IPN PVA/PHEMA hydrogels containing a hydrophilic content of PHEMA crosslinked with EGDMA were prepared. The series 1 hydrogels varied the amount of GA used to crosslink PVA to examine changes to the hydrophilic character. The gel content of the series 1 full-IPN PVA/PHEMA hydrogels as a function of GA, PVA/GA hydrogel and PHEMA are reported in Table 2.1. The gel content

increased substantially from 45 to 98% as the GA increased from 10 to 40 wt%, respectively. This is consistent with decreased separation of PVA as the amount crosslinking is increased. The effect of IPNs on gel content is emphasised by the regular PVA/GA and PHEMA polymers that both have a similarly high gel content. In particular, PVA/GA and IPN-PHEMA2, both with 20 wt% GA, had very different gel content of 97 and 69%, respectively, indicating the significant effect of reduced gel content from the interpenetrating polymer chains of PHEMA.

The gel content of all series 2 full-IPN hydrogels prepared from PVA, HBA and AA, that is, PVA/P(HBA-co-AA) with various amounts of HAB and AA, full-IPN PVA/PAA, and full-IPN PVA/PHBA, are indicated in Table 2.1. The PVA content in all hydrogels was kept at 33 wt% to maintain the same hydrophilicity and enable a ready investigation of the effect of varying the amounts of HBA and AA on the hydrophobic nature. A small increase in gel content of the full-IPN PVA/P(HBA-co-AA) hydrogels was noted as the ratio of HBA-to-AA increased. Also, AA made a more significant contribution to the gel content than HBA as indicated by the data for the full-IPN PVA/PAA and PVA/PHBA polymers. This is expected because AA is a smaller monomer than HBA and should be able to more readily penetrate PVA during polymerisation resulting in a more compact and entangled polymer network. PHBA is more regularly used as "backbone material" for secondary polymer networks[162].

A similar series of experiments were performed to investigate the effect of varying amounts of MMA and IA on gel content in series 3 full-IPN PVA/P(MMA-co-IA) hydrogels. A small increase in gel content was noted as the amount of MMA relative to IA increased in the hydrogel. However, neither MMA or IA had a significant outcome on gel content because both full-IPN PVA/PMMA and full-IPN PVA/PIA, containing same amounts of hydrophilic and hydrophobic components, had very similar gel content. This is somewhat unexpected because the additional -CH_2- and carboxylic group of IA would seemingly confer a larger size than the methyl groups of MMA to the respective acrylate monomers. However, the space-filling ability of the terminal methyl groups of MMA likely compensate for the slightly longer sidechains of IA. Both monomers must have a similar ability to penetrate PVA during polymerisation resulting in similar gel content of full-IPN PVA/PMMA and full-IPN PVA/PIA.

2.4.3. **Characterisation by Infrared Spectroscopy**

2.4.3.1. *Full-IPN PVA/PHEMA hydrogels*

Infrared spectroscopy was used to examine the chemical composition and nature of bond formation in the gel materials. The FTIR spectra of full-IPN PVA/PHEMA hydrogel, PVA/GA gel and PHEMA are presented in Figure 2.4. The broad bands between 3577 - 3202 cm^{-1} are linked to O-H stretching of hydroxyl groups in the crosslinked PVA hydrogel.

The FTIR spectra of PVA, cross-linked with GA gel, reveals an important band at 2755 cm^{-1} related to C–H stretching of aldehydes. The vibrational bands observed at 2940 and 2917 cm^{-1}, refers to C–H stretching of CH_2. The broad absorption peaks between 1094 – 958 cm^{-1} are related to C-O-C and C-O groups, due to formation of acetal or semi-acetal after crosslinking[129-130, 163].

Additionally, the FTIR spectrum of PHEMA indicates characteristic bands of the carbonyl and methyl groups at 1723 and 2886 cm^{-1}, respectively. The bands observed at 1452, and 1391 cm^{-1} have been attributed to the bending CH_2 and CH_3 deformation, and bending, C-O-H and bending CH_3 deformation, respectively. The bands between 2948 and 2886 cm^{-1} are assigned to C-H stretching of methyl groups ($-CH_3$) and methylene ($-CH_2$) of PHEMA in the gel[164-166].

Characteristic ethylene peaks (C=C) at 1636 and 1637 cm^{-1} for the HEMA monomer and EGDMA crosslinker, respectively, are not observed in the copolymer. This indicates high monomer conversion during polymerisation with negligible monomer residues. All characteristic peaks of crosslinked PVA and PHEMA polymers were present in the full-IPN hydrogel with a slight shift in wavenumber of characteristic bands at 3577 - 3202, 2940- 2917,2755, 1094-958, 1723, 1391 cm^{-1} towards 3563 - 3248, 2944- 2865, 2745, 1139 - 1020, 1725, 1384 cm^{-1}, respectively. The presence of a peak at 1725 cm^{-1} in the full-IPN spectrum is attributed to nonconjugated aldehyde in the crosslinked PVA[129]. From these results, the expected structure of the full-IPN hydrogels is indicated.

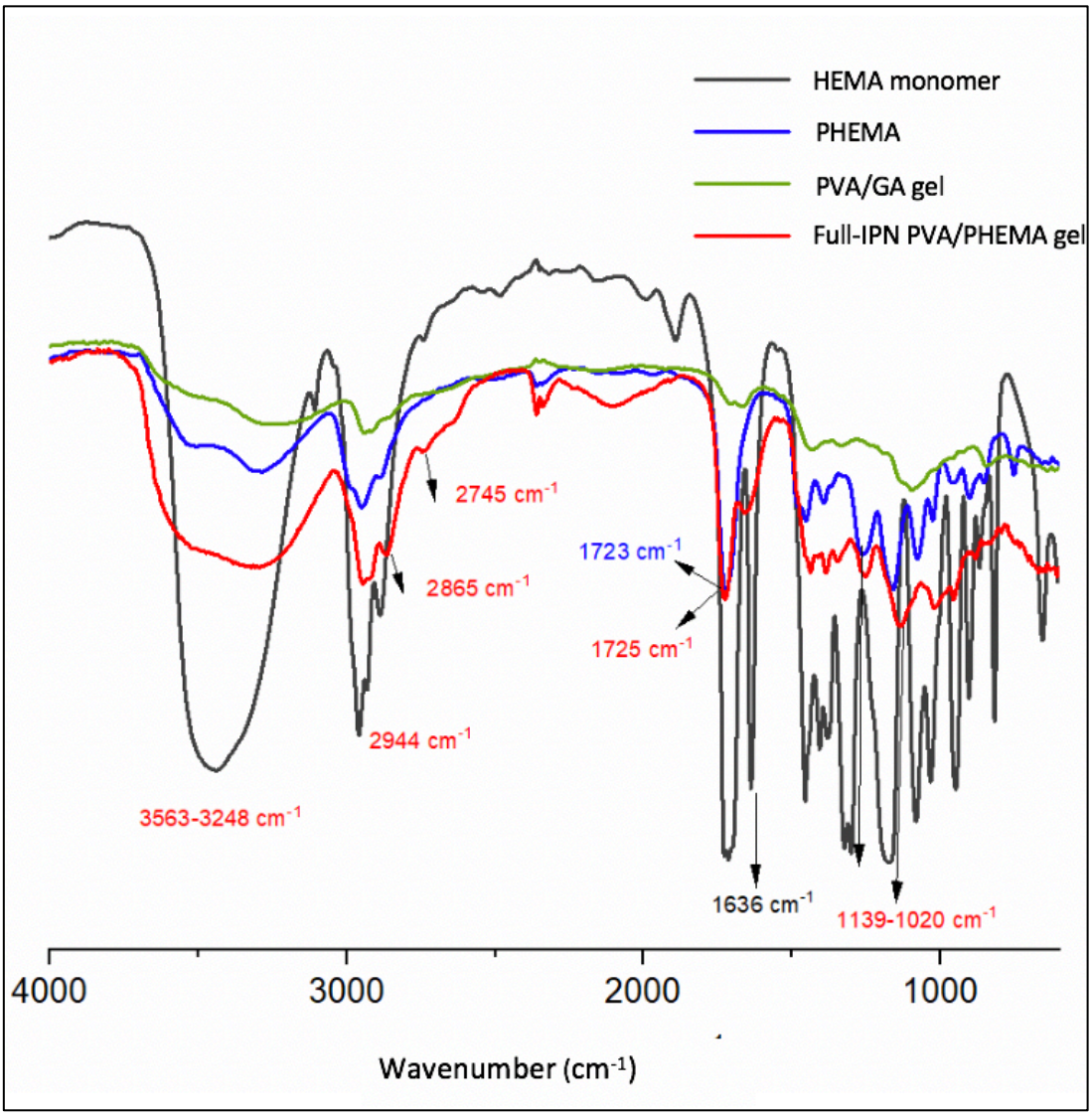

Figure 2.4. FTIR spectra of full-IPN PVA/PHEMA, PVA/GA, PHEMA hydrogels, and HEMA monomer.

2.4.3.2. *Full-IPN PVA/P(HBA-co-AA) hydrogels*

In the case of the full-IPN PVA/PAA hydrogel (Figure 2.5), the absorption peaks at 1725[148], 1434-1382, and 1236[167] cm^{-1}, are related to stretching and bending vibrations of C=O, C-H, and O-H groups, respectively, and are characteristic of PAA. The peak due to C=O stretching of PAA has been reported at 1714 cm^{-1} [168] and 1723 cm^{-1} [169]. Similarly, for the simple full-IPN PVA/PHBA hydrogel, peaks at 2944-2863, 1729, and 1218 -1165 cm^{-1} indicate the stretching and bending vibrations of C–H, C=O, and C-O-C, respectively, of the alkyl, carbonyl, and ester groups, respectively, that are characteristic of the -$OOCH_2$ group

in PHBA. Another characteristic peak of PHBA at 1023 cm^{-1} is assigned to C-O stretching associated with the terminal hydroxyl group.

The spectra of the co-polymer hydrogels show the expected characteristic peaks, although with a slight shift in frequency, to those observed in the full-IPN hydrogels, PVA/PHBA and PVA/PAA. For instance, signals at 1433-1382, 1728, and 1246 cm^{-1} corresponding to the O-H , C=O, C-H groups in PAA, and at 2940-2876, 1728, and 1164-1124 cm^{-1}, related to stretching vibrations of C-H, C=O, and C-O-C in PHBA, respectively. The observation of the characteristic bands indicates that all the expected groups of PVA, PHBA, and PAA have been incorporated in the full-IPN PVA/P(HBA-co-AA) hydrogel.

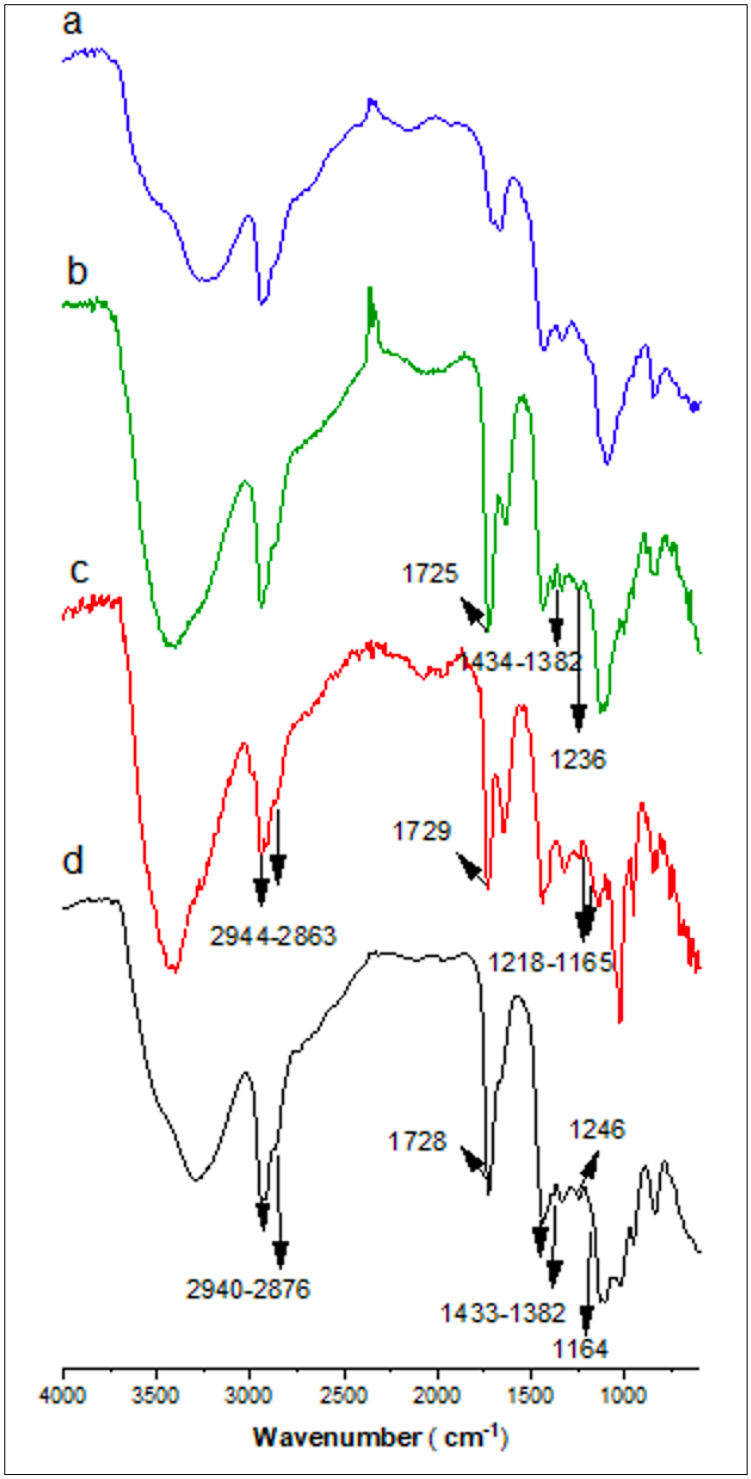

Figure 2.5. FTIR spectra of PVA/GA (a), full-IPN PVA/PAA (b), full-IPN PVA/PHBA (c), and full-IPN PVA/P(HBA-co-AA) (d) hydrogels.

2.4.3.3. *Full-IPN PVA/P(MMA-co-IA) hydrogels*

The FTIR spectra of full-IPN PVA hydrogels prepared with other components, including PIA and PMMA are indicated in Figure 2.6. In the FTIR spectra of full-IPN PVA/PMMA, characteristic absorption peaks of P(MMA) at 1730, 1458, and 1243 cm^{-1} are assigned to acrylate carbonyl group C=O stretching, bending vibration of C-H of methyl groups, and C–O stretching, respectively. Additionally, peaks at 2943 cm^{-1} and 2986 cm^{-1} are consistent with C-H stretching of CH_2 and -CH_3, respectively. Other observed peaks at 991, 1062 and 874 cm^{-1} are distinctive for PMMA[170-172]. For full-IPN PVA/IA, the peak at 1722 cm^{-1} is a characteristic band of the ester carbonyl group of PIA[173]. Broad peaks between 3145 – 3531 cm^{-1} are attributed to intermolecular hydrogen bonding of the hydroxy groups of IA. Other characteristic bands of PIA are observed at 1458 and 1426 cm^{-1} and attributed to vibrational stretching associated with C-O-H and CH_2 groups, respectively[139 174]. Assignment of infrared bands observed for full-IPN PVA/PMMA or PVA/PIA are indicated in Table 2.3. All characteristic peaks of PMMA and PIA are present in the spectrum of full-IPN PVA/P(MMA-co-IA), with only a slight shift in the frequency of bands at 2943-2986, 991, 1243, 1458, and 1722 cm^{-1} towards 2994, 2942, 999, 1247 1455, and 1730 cm^{-1}, respectively. All characteristic peaks of PVA, PMMA, and PIA are apparent in the FTIR spectrum of the full-IPN PVA/P(MMA-co-IA) hydrogel, indicating successful incorporation of all components in the polymer network.

Table 2.3. Assignment of characteristic bands observed in FTIR spectra of full-IPN PVA/PMMA and PVA/PIA hydrogels.

Band position (cm^{-1})	**Band assignment**
PVA/PMMA	
1475	δ (CH_2) (scissoring)
1448	δ_{as} (CH_3) of C-CH_3 (umbrella)
1388	δ_{sy} (CH_3) of C-CH_3 (umbrella)
1187, 1147	v_{as} (C-O-C)
1062	Skeletal *v* (C-C)
991	O-CH_3 rocking coupled with *v* (C-O-C)
874	CH_2 rocking
748	Skeletal *v* (C-C)
PVA/PIA	
3145 -3531	*v* O-H
1722	*v* C=O
1425	*v* C-O-H
1186	C-O
1458	CH_2

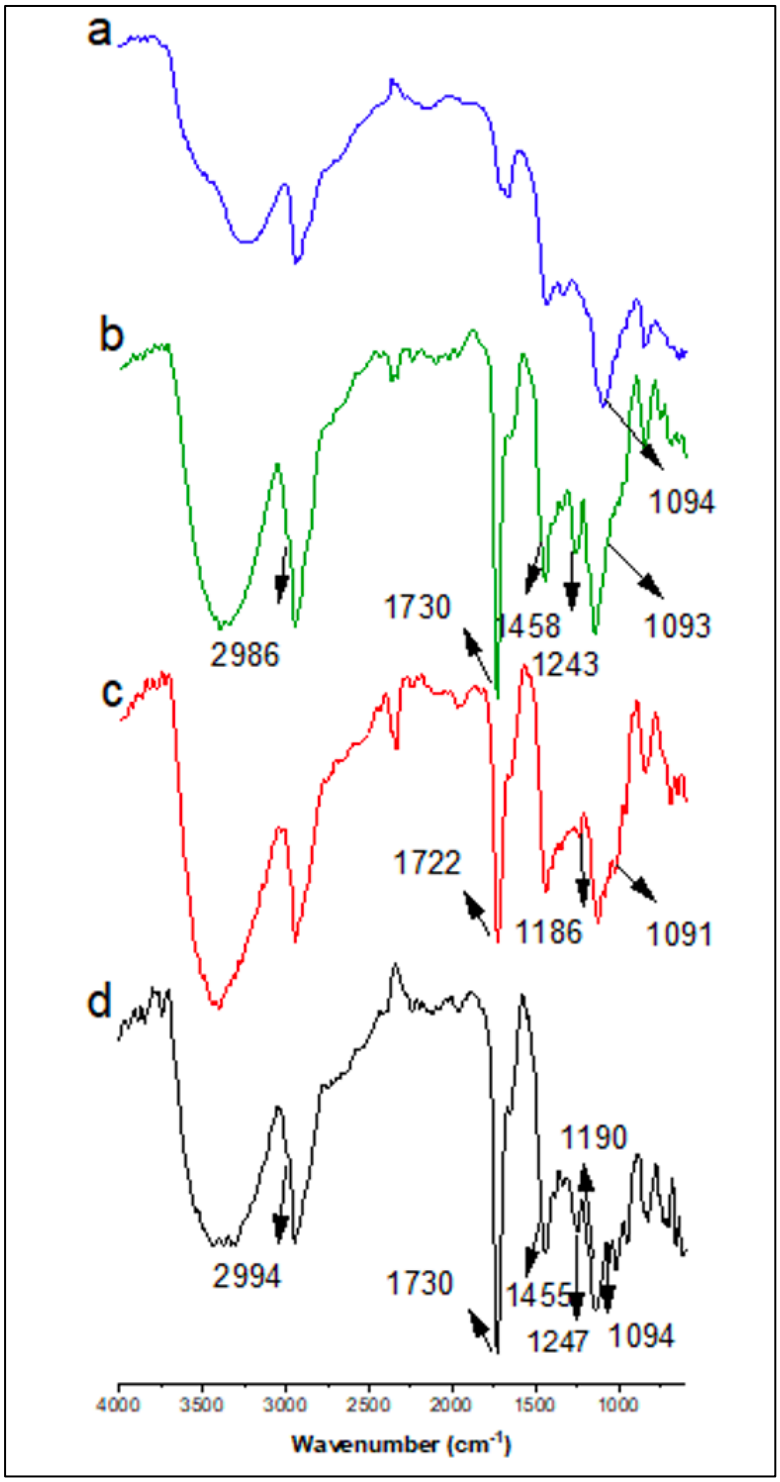

Figure 2.6. FTIR spectra of PVA/GA (a), full-IPN PVA/PMMA (b), full-IPN PVA/PIA (c), and full-IPN PVA/P(MMA-co-IA) (d) hydrogels.

2.4.4. **Characterisation by ToF-SIMS**

2.4.4.1. *Full-IPN PVA/PHEMA hydrogels*

The chemical composition of the resulting full-IPN PVA/PHEMA, PVA/P(HBA-co-AA) and PVA/P(MMA-co-IA) hydrogels was analysed by ToF-SIMS. Routine analysis by regular MS and ^{1}H-NMR techniques was prevented by the inherent insolubility of the hydrogels in organic solvents. The secondary ion spectra in both positive- and negative-mode polarities were acquired from the surface of full-IPN PVA/PHEMA and typical spectra are presented in Figure 2.7. The positive spectrum is dominated by secondary ion clusters at *m/z* 41, 45, 69 & 71 that are characteristic of PHEMA; chemical formulae are assigned in Table 2.4. The high relative intensity of signals at *m/z* 17, 25, 59, and 85 corresponding to OH^-, C_2H^-, $C_2H_3O_2^-$, and $C_4H_5O^-$, respectively, were chosen as characteristic cluster signals of PHEMA in the negative mode. Likely fragmentation patterns of PHEMA and cross-linked PVA to indicate the observed signals are shown in Figure 2.8.

Preliminary experiments indicated that observed signals of PVA/GA gel were more intense when acquired in the negative mode than the positive spectrum. Assigned signals of cross-linked PVA are presented in Table 2.4. The signals at *m/z* 183 and 239 were selected as characteristic of clusters of PVA/GA. The current study only indicates ToF-SIMS data of PVA/GA acquired in negative mode.

The results from the ToF-SIMS analysis of PVA crosslinked with GA and PHEMA hydrogels is consistent with outcomes reported in the literature[175-177], the data for PVA/GA hydrogel is reported in positive mode in previous studies. The current ToF-SIMS results provide evidence to support FTIR analysis that PHEMA has been incorporated into the network of cross-linked PVA.

Table 2.4. Assignment of positive and negative secondary ion signals of full-IPN PVA/PHEMA hydrogel.

	Ion structure (*m/z*)			
Hydrogel	**Cation (obs)**	**Cation (lit)[175-177]**	**Anion (obs)**	**Anion (lit)[177]**
PVA/GA	-	-	OH^- (17)	No reference found for negative data for the PVA/GA gel
		-	$C_2H_3^-$ (27)	
		-	$C_2H_4O^-$ (44)	
		$C_{12}H_{21}O_4^+$ (113)	$C_{12}H_{21}O_4^-$ (113)	
		$C_9H_{14}O_3^+$ (170)	**$C_9H_{14}O_3^-$ (170)**	
		$C_{10}H_{15}O_3^+$ (183)	**$C_{10}H_{15}O_3^-$ (183)**	
		$C_{12}H_{19}O_3^+$ (211)	$C_{12}H_{19}O_3^-$ (211)	
		$C_{12}H_{19}O_4^+$ (227)	$C_{12}H_{19}O_4^-$ (227)	
		$C_{12}H_{21}O_4^+$ (229)	$C_{12}H_{21}O_4^-$ (229)	
		$C_{13}H_{19}O_4^+$ (239)	**$C_{13}H_{19}O_4^-$ (239)**	
		$C_{13}H_{22}O_5^+$ (258)	$C_{13}H_{22}O_5^-$ (258)	
		$C_{18}H_{28}O_6^+$ (340)	$C_{18}H_{28}O_6^-$ (340)	
PHEMA	CH_3^+ (15)	-	**OH^- (17)**	-
	$C_2H_4^+$ (28)	-	**C_2H^- (25)**	-
	$C_2H_5^+$ (29)	-	$C_3H_5^-$ (41)	-
	$C_3H_3^+$ (39)	$C_3H_3^+$ (39)	**$C_2H_3O_2^-$ (59)**	$C_2H_3O_2^-$ (59)
	$C_3H_4^+$ (40)	$C_3H_5^+$ (41)	$C_4H_5O^-$ (69)	-
	$C_3H_5^+$ (41)	$C_2H_3O^+$ (43)	$C_3H_3O_2^-$ (71)	-
	$C_2H_3O^+$ (43)	$C_2H_5O^+$ (45)	$C_5H_5O^-$ (81)	-
	$C_2H_5O^+$ (45)	$C_4H_5O^+$ (69)	**$C_4H_5O^-$ (85)**	$C_4H_5O^-$ (85)
	$C_4H_5^+$ (53)	$C_6H_9O_2^+$ (113)		
	$C_3H_3O^+$ (55)			
	$C_3H_5O^+$ (57)			
	$C_4H_5O^+$ (69)			
	$C_3H_3O_2^+$ (71)			
	$C_5H_5O^+$ (81)			
	$C_5H_7O^+$ (83)			
	$C_7H_7^+$ (91)			
	$C_5H_7O_2^+$ (99)			
	$C_6H_9O_2^+$ (113)			

Note: characteristic signals indicated in **bold**. Where obs is observed and lit is literature.

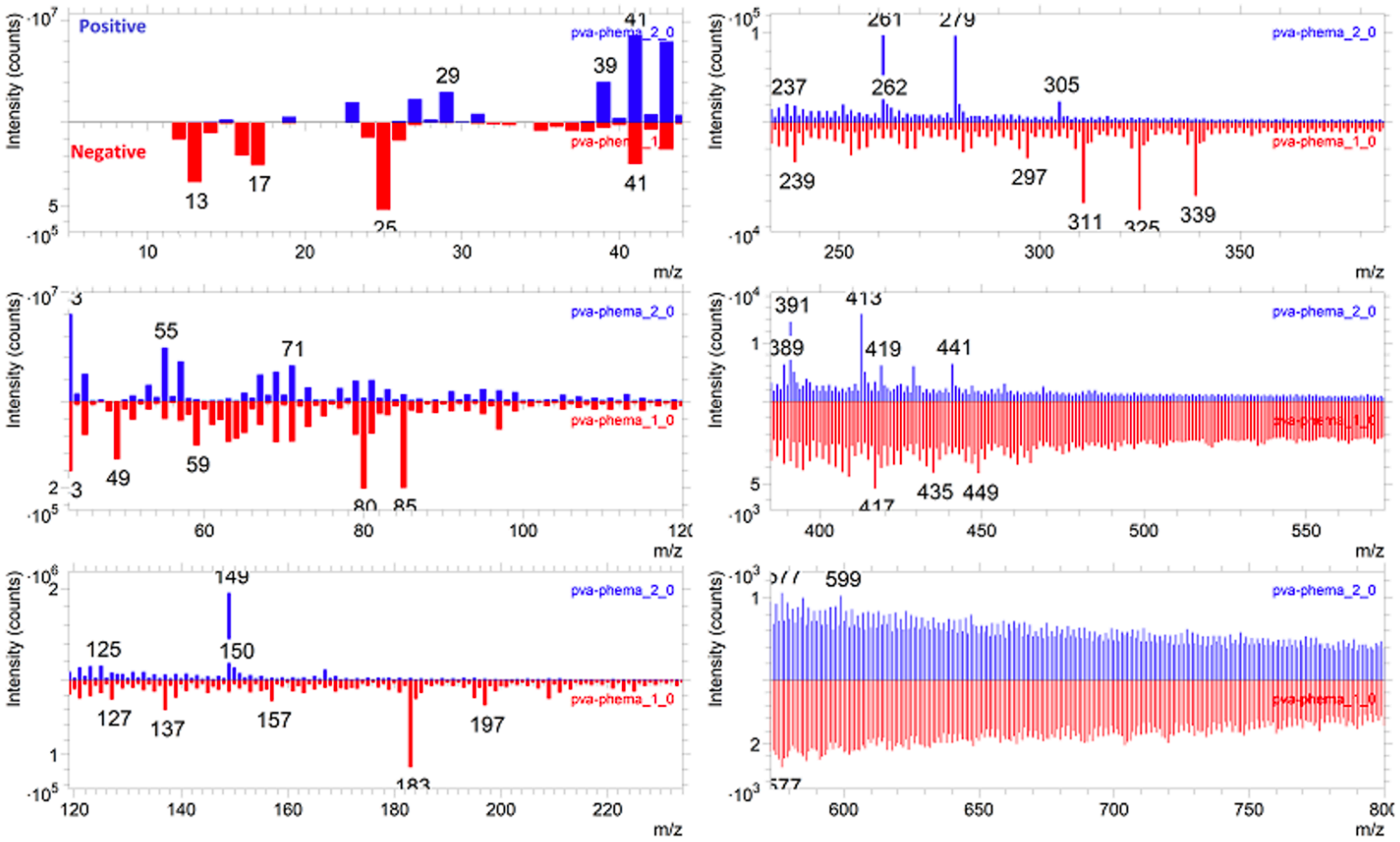

Figure 2.7. Positive (blue) and negative (red) secondary ion spectra of full-IPN PVA/PHEMA hydrogel.

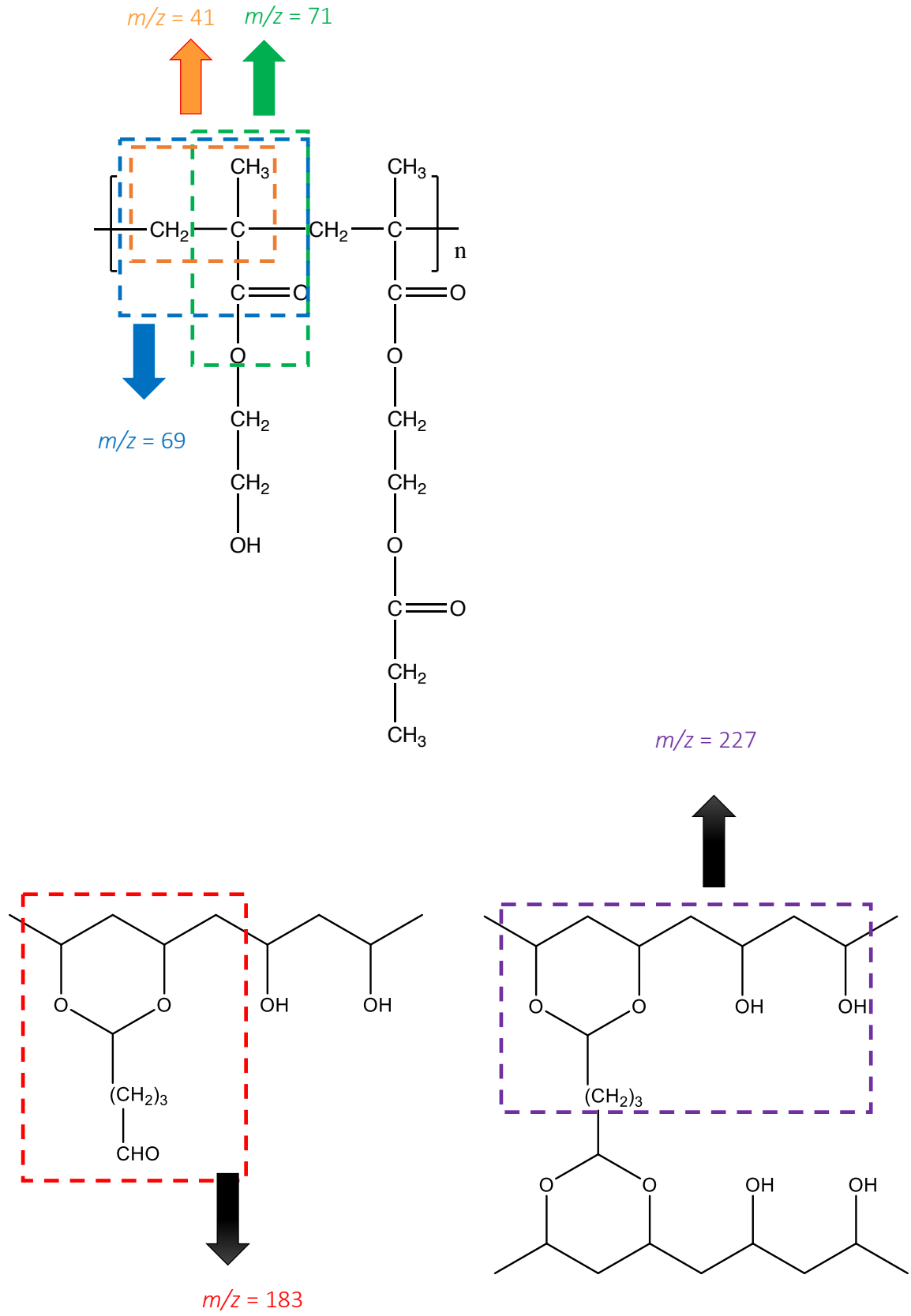

Figure 2.8. Positive and negative fragmentation patterns of PHEMA (upper) and crosslinked PVA/GA (lower).

2.4.4.2. *Full-IPN PVA/P(HBA-co-AA) hydrogels*

Characteristic peaks of the secondary ions of PHBA in the positive acquisition mode exhibited similar trends to those observed in the negative ion mode (Figure 2.9). Cations with a higher relative intensity that are characteristic of PHBA are observed at *m/z* 27, 41,43, 55, 57, and 58, corresponding to $C_2H_3^+$, $C_3H_5^+$, $C_3H_7^+$, $C_4H_7^+$, $C_3H_5O^+$, and $C_3H_6O^+$, respectively. Characteristic anion signals of PAA with a higher relative intensity are observed at *m/z* 16, 17, 41, 59 and 71, and duly assigned to O^-, OH^-, C_2HO^-, $C_2H_3O_2^-$, and $C_3H_3O_2^-$, respectively (Table 2.5). These assignments are consistent with previous reports of ToF-SIMS secondary ion spectra of PAA[178]. Characteristic secondary ion peaks of PHBA and PAA are reported in Table 2.5. Likely fragmentation patterns to support the assignment of characteristic signals of P(HBA-co-AA) are indicated in Figure 2.10.

Table 2.5. Assignment of secondary ion in positive and negative mode spectra of full-IPN PVA/(P(HBA-co-AA) hydrogel.

Hydrogel	**Ion (*m/z*)**		
Component	**Cation (obs)**	**Anion (obs)**	**Anion (lit)[178]**
PHBA	**$C_2H_3^+$ (27)**	O^- (16)	Not reported
	CH_3O^+ (31)	OH^- (17)	
	$C_3H_3^+$ (39)	$C_2H_3^-$ (27)	
	$C_3H_4^+$ (40)	$C_3H_5^-$ (41)	
	$C_3H_5^+$ (41)	$C_2H_3O^-$ (43)	
	$C_2H_3O^+$ (43)	$C_3H_3O^-$ (55)	
	$C_4H_5^+$ (53)	$C_3H_5O^-$ (57)	
	$C_3H_3O^+$ (55)	$C_3H_6O^-$ (58)	
	$C_3H_5O^+$ (57)	$C_4H_5O^-$ (69)	
	$C_3H_6O^+$ (58)	$C_3H_3O_2^-$ (71)	
	$C_4H_5O^+$ (69)	$C_5H_5O^-$ (81)	
	$C_3H_3O_2^+$ (71)	$C_4H_5O^-$ (85)	
	$C_6H_7^+$ (79)		
	$C_5H_5O^+$ (81)		
PAA	C_2HO^+ (41)	**O^- (16)**	O^- (16)
	CHO_2^+ (45)	**OH^- (17)**	OH^- (17)
		C_2HO^- (41)	C_2HO^- (41)
		$C_2H_3O_2^-$ (59)	$C_2H_3O_2^-$ (59)
		$C_3H_3O_2^-$ (71)	$C_3H_3O_2^-$ (71)

Characteristic signals indicated in **bold**. Where obs is observed and lit is literature.

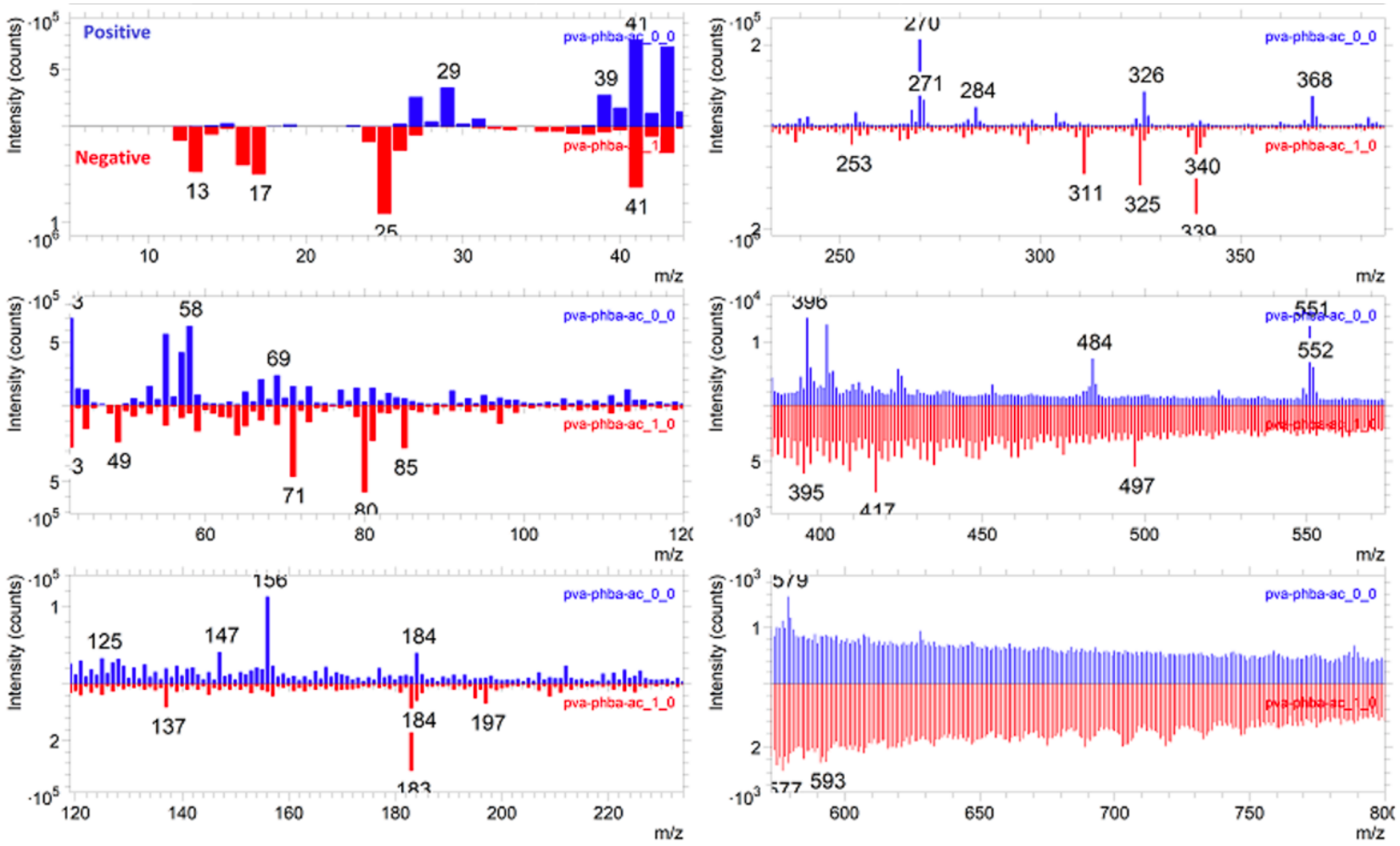

Figure 2.9. Positive (blue) and negative (red) secondary ion spectra of full-IPN PVA/P(HBA-co-AA) hydrogel.

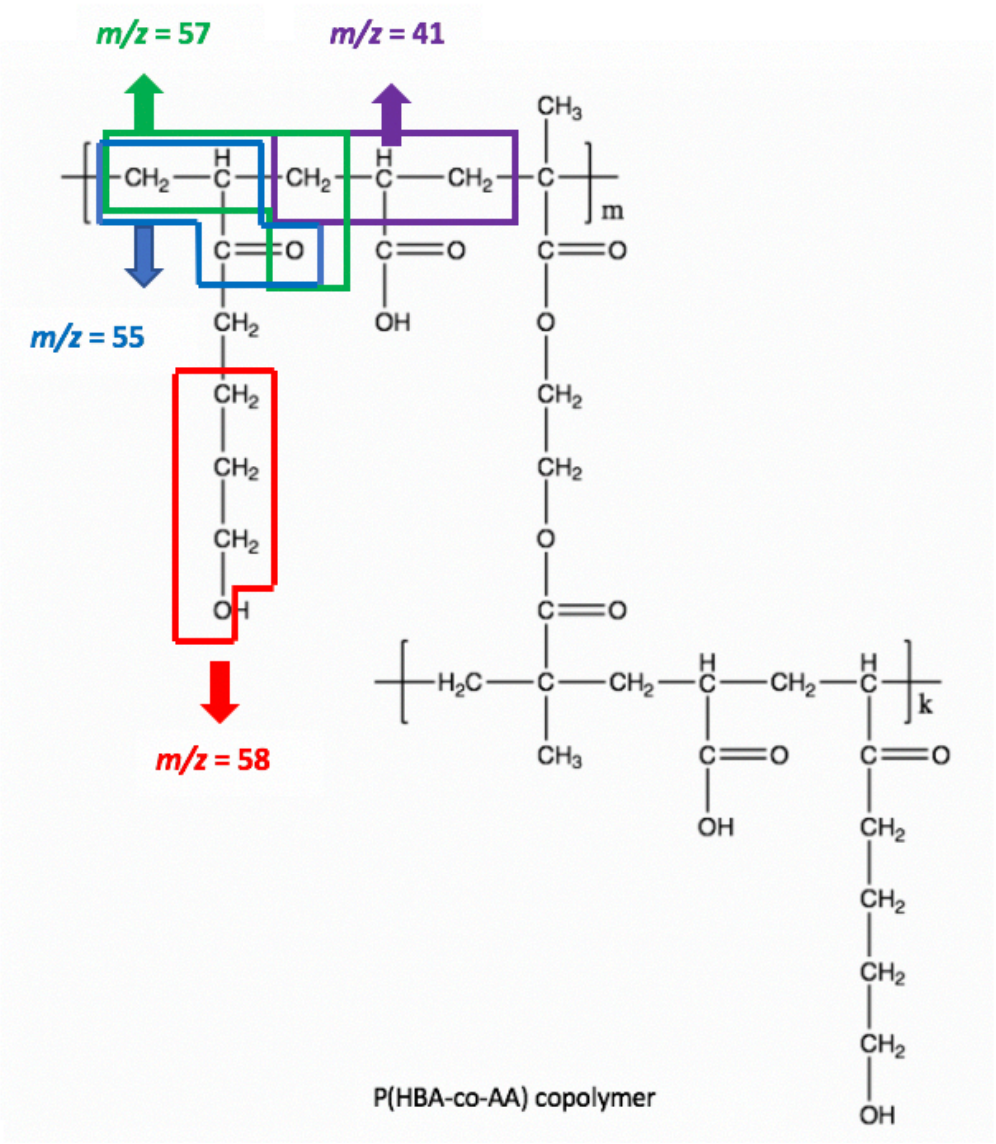

Figure 2.10. Likely fragmentation patterns of P(HBA-co-AA) copolymer.

2.4.4.3. *Full-IPN PVA/P(MMA-co-IA) hydrogels*

ToF-SIMS was used to indicate the chemical structure of full-IPN PVA/P(MMA-co-IA) hydrogels. The positive and negative polarity secondary ion spectra obtained from the surface of the hydrogel of PVA, PIA and PMMA are indicated in Figure 2.11. Signals at *m/z* 29, 39, and 43 were selected as characteristic secondary ion peaks of the polymer backbone and pendant group of PMMA in the positive mode. However, in the negative acquisition mode, anion signals of the polymer chain and pendant group of PMMA were observed at *m/z* 25, 41, 43, 55, 69 and 141. The corresponding formula for each characteristic peak is indicated in Table 2.6. The results from the positive and negative mode spectra for PMMA agree with previous investigations[179-180]. Diagnostic peaks of PIA were chosen in the positive mode at *m/z* 41, 43, 45 & 57, and at *m/z* 17 (OH^-) and *m/z* 43 ($C_3H_5^-$) n the negative mode spectra. Some likely fragmentation patterns associated with observed anions of P(MMA-co-IA) are indicated in Figure 2.12.

The results from ToF-SIMS clearly provides evidence of P(MMA-co-IA) and PVA/GA and supports the previous FTIR analysis, indicating the successful formation of a full-IPN PVA/P(MMA-co-IA) hydrogel.

Table 2.6. Assignment of secondary ion signals of full-IPN PVA/P(MMA-co-IA) hydrogel in positive and negative secondary mode ToF-SIMS spectra.

Hydrogel	**Ion (*m/z*)**			
Component	**Cation (obs)**	**Cation (lit)[179]**	**Anion (obs)**	**Anion (lit)[180]**
PMMA	CH_3^+ (15)	CH_3^+ (15)	CH^- (13)	CH_3O^- (31)
	$C_2H_5^+$ (29)	$C_2H_3O_2^-$ (59)	O^- (16)	$C_2H_3O^-$ (43)
	CH_3O^+ (31)		**C_2H^- (25)**	$C_3H_3O^-$ (55)
	$C_3H_3^+$ (39)		CH_3O^- (31)	$C_3H_3O_2^-$ (71)
	$C_3H_4^+$ (40)		**$C_3H_5^-$ (41)**	$C_8H_3O_2^-$ (141)
	$C_3H_5^+$ (41)		**$C_2H_3O^-$ (43)**	$C_4H_5O^-$ (85)
	$C_2H_3O^+$ (43)		$C_2H_5O^-$ (45)	
	$C_2H_5O^+$ (45)		**$C_3H_3O^-$ (55)**	
	$C_4H_5^+$ (53)		$C_3H_5O^-$ (57)	
	$C_3H_3O^+$ (55)		$C_2H_3O_2^-$ (59)	
	$C_3H_5O^+$ (57)		**$C_4H_5O^-$ (69)**	
	$C_2H_3O_2^-$ (59)		$C_3H_3O_2^-$ (71)	
	$C_4H_5O^+$ (69)		$C_4H_5O^-$ (85)	
	$C_3H_3O_2^+$ (71)		**$C_8H_3O_2^-$ (141)**	
	$C_5H_5O^+$(81)			
	$C_6H_9O_2^+$ (113)			
PIA	$C_3H_3^+$ (39)		O^- (16)	
	$C_3H_4^+$ (40)		**OH^- (17)**	
	$C_3H_5^+$ (41)		C_2H^- (25)	
	$C_2H_3O^+$ (43)		**$C_3H_5^-$ (41)**	
	$C_2H_5O^+$ (45)		$C_2H_2O^-$ (42)	
	$C_3H_3O^+$ (55)		$C_3H_5O^-$ (57)	
	$C_3H_5O^+$ (57)		$C_2H_2O_2^-$ (58)	
	$C_4H_4O^+$ (68)		$C_4H_4O^-$ (68)	
	$C_3H_3O_2^+$ (71)		$C_3H_3O_2^-$ (71)	
	$C_4H_5O^+$ (85)		$C_5H_5O^-$ (81)	
			$C_4H_5O^-$ (85)	

Note: characteristic signals indicated in **bold**. Where obs is observed and lit is literature.

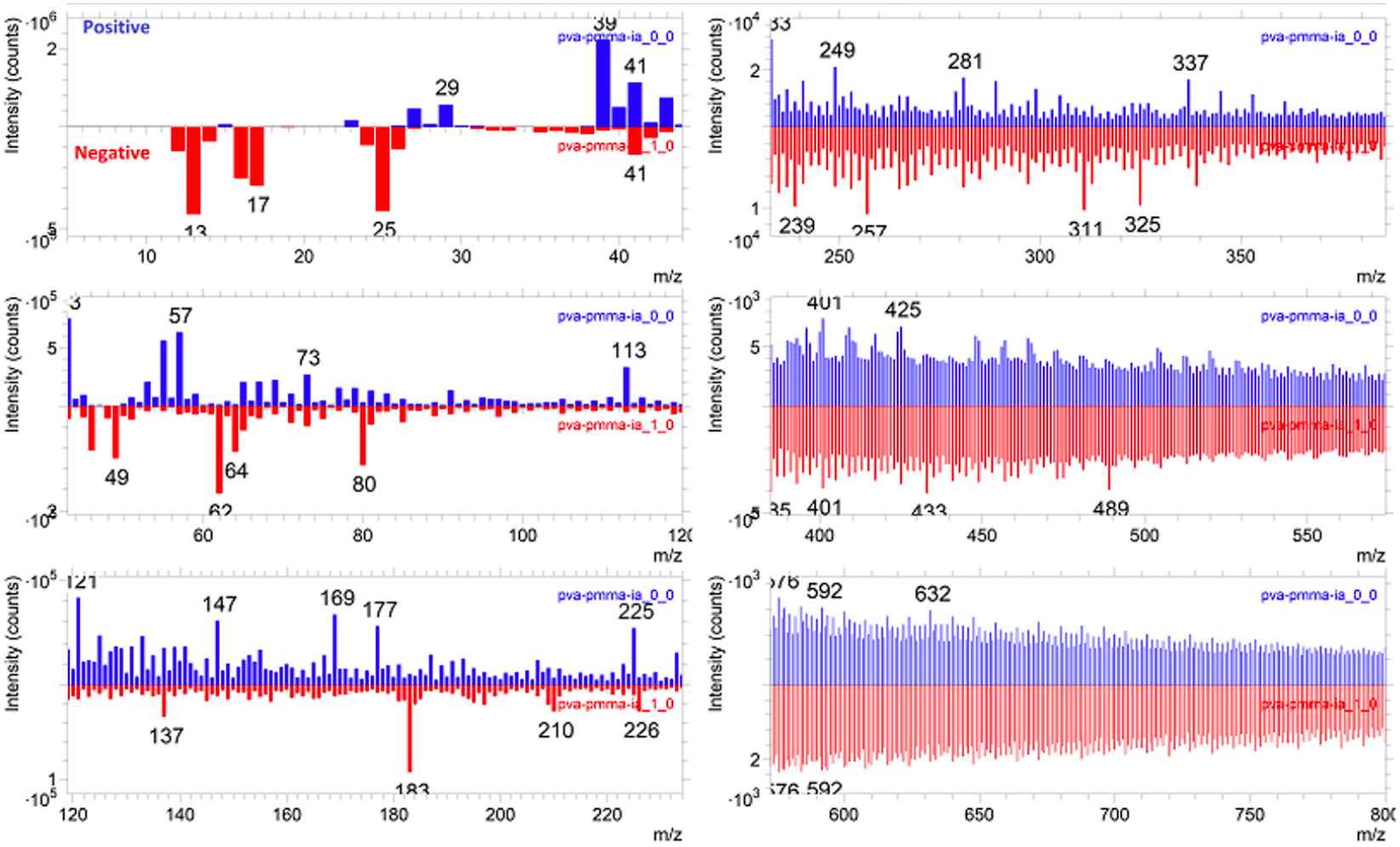

Figure 2.11. Positive (blue) and negative (red) secondary ion spectra of full-IPN PVA/P(MMA-co-IA) hydrogel.

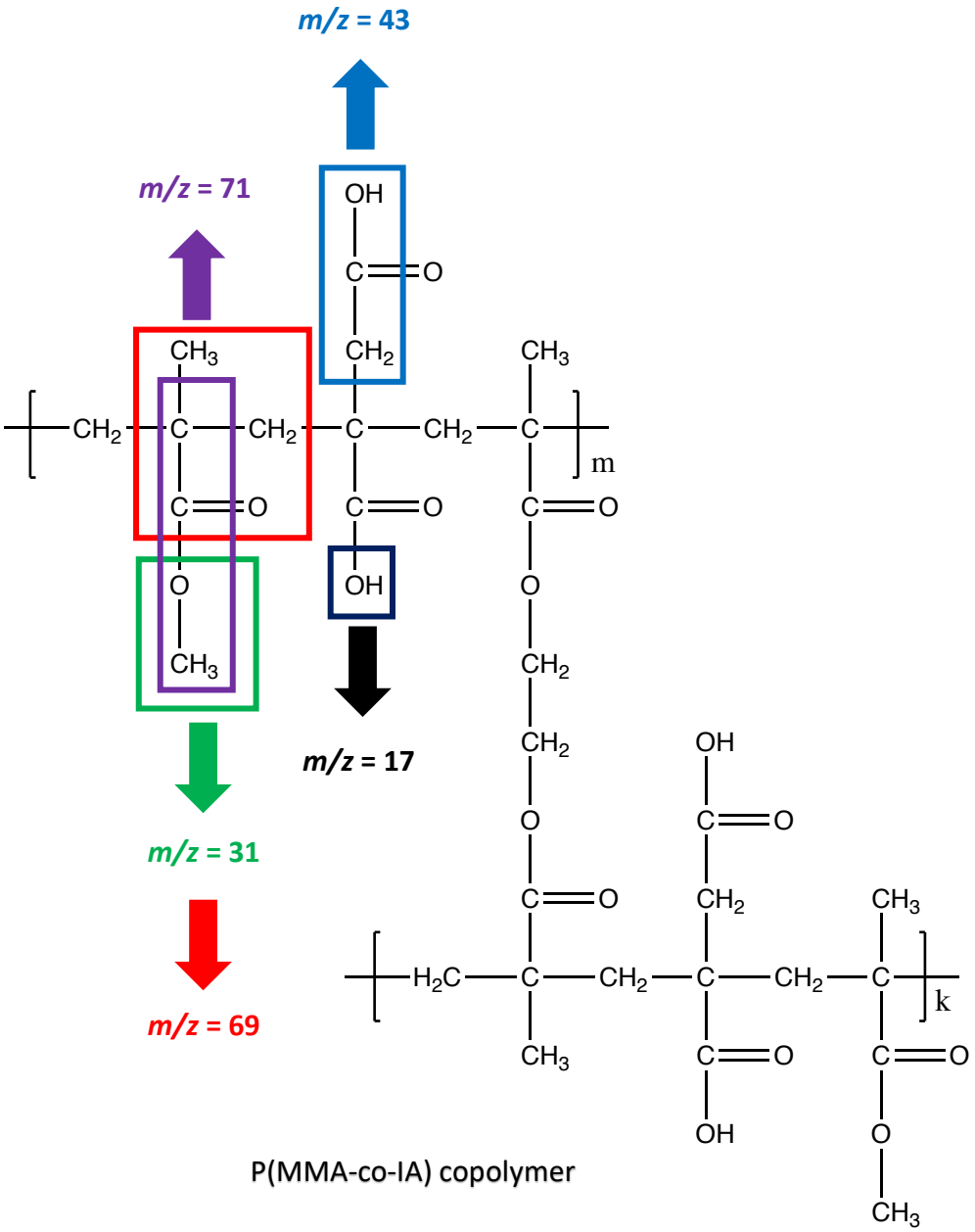

Figure 2.12. Negative ion fragmentation patterns of P(MMA-co-IA) copolymer.

2.4.5. **Effect of GA, HBA and MMA amounts on chemical structure of full-IPN hydrogels.**

2.4.5.1. *Full-IPN PVA/PHEMA hydrogels*

The chemical composition, that is choice of polymer components and extent of crosslinking, can affect pore size, solute interaction and other physiochemical properties of a hydrogel. The effect of different amounts of GA, HBA and MMA on the hydrophilic and hydrophobic properties was studied by investigating the swelling ability and pH sensitivity of the various full-IPN hydrogels.

Infrared spectroscopy was used to study the effect of GA at 10, 20, 30 & 40 wt% as a crosslinker of PVA in full-IPN PVA/PHEMA hydrogels, and the spectra are shown in Figure 2.13. Three groups of signals that exhibit significant stronger intensity as the amount of GA is increased are observed, these are:

(i) characteristic aldehyde peaks at 2755 and 2938 cm^{-1}.

(ii) peak at 1725 cm^{-1} at 40 wt% GA; indicative of carbonyl from unreacted GA[130].

(iii) peaks between 1020 - 1139 cm^{-1}; indicative of formation of acetal ring and ether linkage from cross-linking of GA to PVA.

Observation of free GA at 40 wt% indicates the upper limit of crosslinking has been reached. Free GA is removed during washing of the hydrogel. The observed changes in FTIR spectra, as the GA ratio is increased, also indicate a reduction in the relative intensity of the broad signal at about 3300 cm^{-1} due to hydroxyl groups of PVA. This consistent with the loss of hydrogen bonding associated with hydroxyl groups that are consumed as more ether linkages and acetal rings are formed during cross-linking. The observations in the study agree with results in the literature[130]. The relative reduced intensity of the band at about 840 cm^{-1} at high amounts of GA is a likely result of reduced vibrations of crosslinked carbon chains of PVA in PVA/GA.

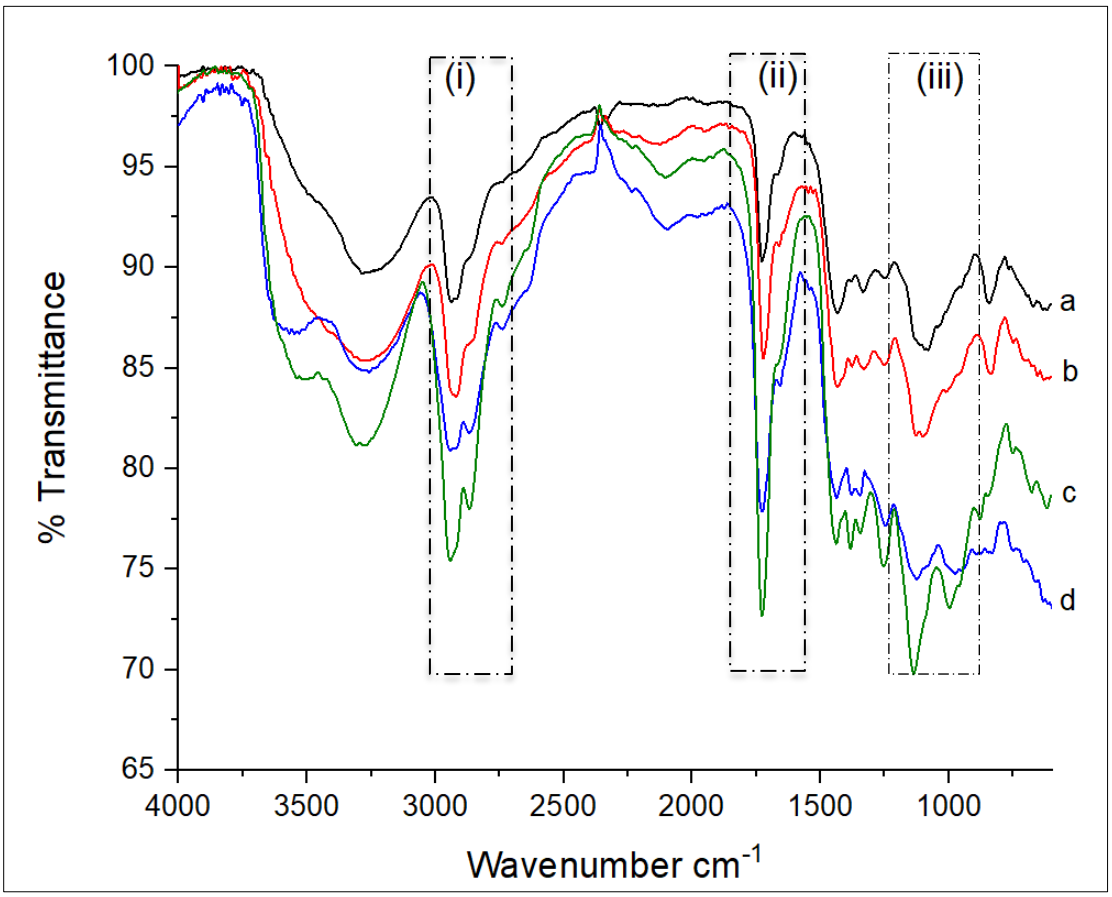

Figure 2.13. FTIR spectra of full-IPN PVA/PHEMA hydrogels showing regions (i, ii & iii) of change as a function of GA; 10 wt% (a), 20 wt% (b), 30 wt% (c), and 40 wt% (d).

2.4.5.2. *Full-IPN PVA/P(HBA-co-AA) hydrogels*

Changes to the chemical composition of full-IPN PVA/P(HBA-co-AA) hydrogels by varying the ratio of HBA-to-AA in the hydrophobic component of the polymer network was investigated. Typical infrared spectra are shown in Figure 2.14.

A reduction in the relative intensity of the C=O peak at 1729 cm^{-1} is noted as the wt% ratio of HBA-to-AA is increased from 14:20 to 27:7 This indicates more intensive hydrogen bonding between carbonyl groups of PAA and hydroxyl groups in PHBA or PVA. This assertion is supported by the change in shape of the broad peak indicative of hydrogen bonding at 3100 – 3600 cm^{-1}. At 14 wt% HBA, the peak maxima in this region occurs at 3280 cm^{-1}, and the peak shoulder at 3500 cm^{-1} indicates the presence of an underlying peak. However, at 27 wt% HBA, the contributions at these wavenumbers to the overall peak shape are reversed. This region is now dominated by an intense peak

with a maximum at 3457 cm^{-1}, and a peak shoulder at 3250 cm^{-1}, indicative of more free hydroxyl groups not involved in hydrogen bonding within the network.

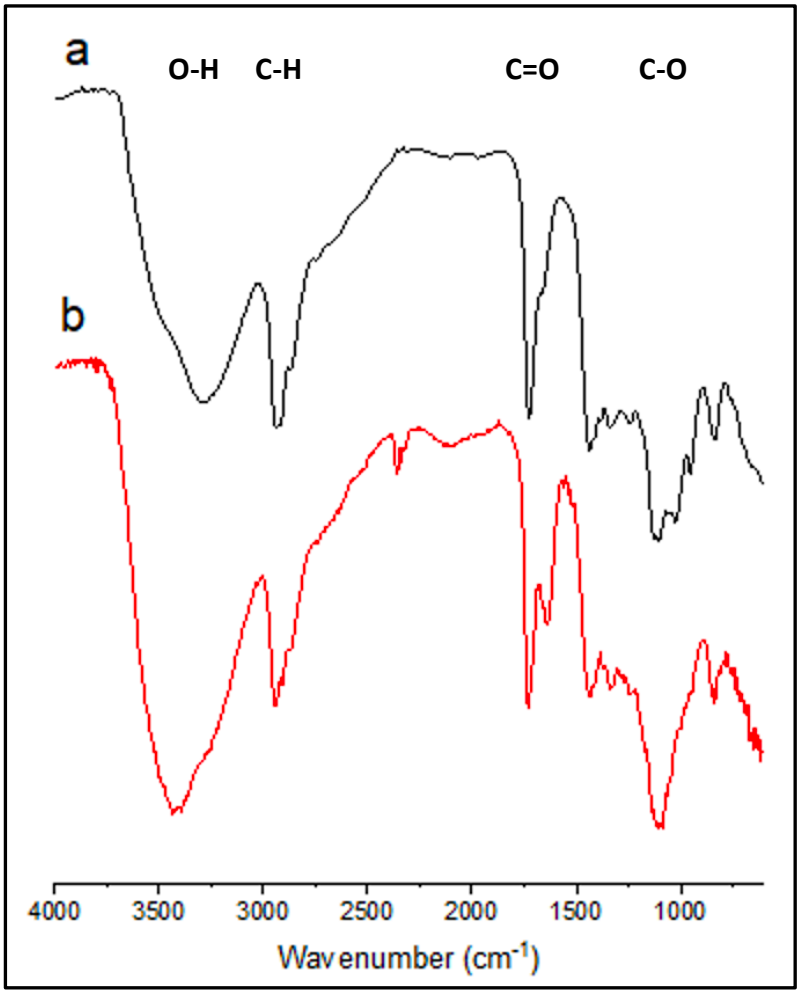

Figure 2.14. FTIR spectra of full-IPN PVA/P(HBA-co-AA) hydrogels as a function of HBA to AA wt% ratio: 14:20 (a), and 27:7 (b).

Moreover, with an increase in the amount of HBA in the full-IPN hydrogel, new or a shift in peaks assigned to carbonyl groups is observed at 1682 cm^{-1}. Also, the C-H stretching bands of PHBA at about 2944-2876 cm^{-1} are shifted to 2940-2872 cm^{-1}, which is related to more CH_2 groups of the copolymer. Additionally, the stretching band at 1099 cm^{-1} is shifted to 1091 cm^{-1} as the amount of HBA is increased, an indication of more esterification between hydroxyl groups in PVA and carboxyl groups in PAA.

2.4.5.3. *Full-IPN PVA/P(MMA-co-IA) hydrogels*

The influence of changing the ratio of MMA-to-IA on the chemical nature of full-IPN PVA/P(MMA-co-IA) hydrogels was investigated using infrared spectroscopy, and the resulting spectra are shown in Figure 2.15.

A significant increase in intensity of the characteristic peaks due to C=O, C-H, and C-O groups of PMMA in the co-polymer is apparent, in particular the acrylate carbonyl group C=O, as the amount of MMA is increased. This somewhat unusual because itaconic acid contains two carbonyl groups, consequently, such a significant increase of the carbonyl signal is unexpected. The unusual result reflects that carbonyl stretching of MMA occurs at a slightly higher wavenumber of 1730 cm^{-1} compared to 1710 cm^{-1} for IA, and that the absorption band of MMA is known to have higher intensity relative to IA, which is overlapped at high amounts of MMA. Furthermore, at the increased ratio of MMA-to-IA, there was a relative increase in intensity of the peak due to ν(C-O) at 1247 cm^{-1}. Other observations were associated with the intensity and location of peaks associated with stretching and bending vibrations of C-H. A significant signal from ν(C-H) at 2981 cm^{-1} and the appearance of a sharp peak due to δ(C-H) at 1455 cm^{-1} is further evidence of increased amounts of MMA in the copolymer configuration. The infrared evidence indicates that the extent of hydrophobic aggregates in the hydrogel network can be successfully varied by changes to the ratio of monomers used during preparation.

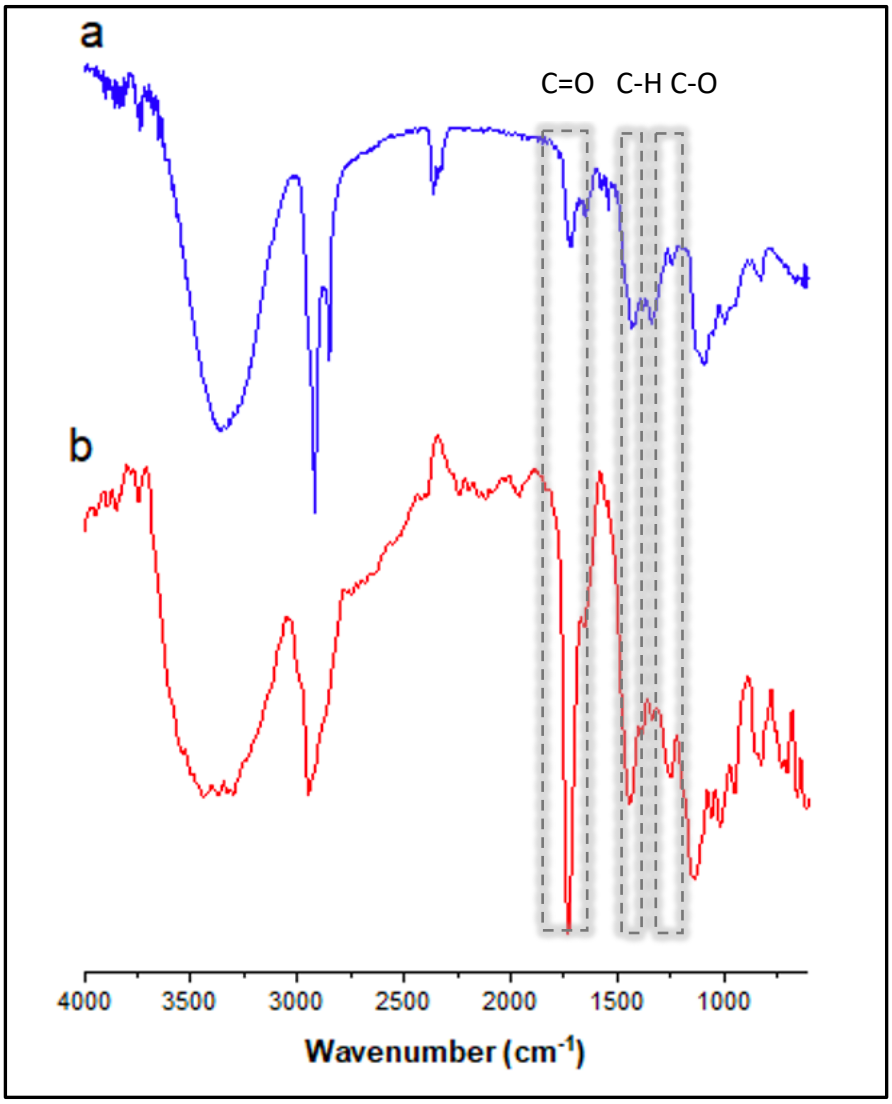

Figure 2.15. FTIR spectra of full-IPN PVA/P(MMA-co-IA) hydrogels as a function of MMA-to-IA wt% ratio 10:24 (a), and 24:10 (b).

2.4.6. **Water uptake measurements**

2.4.6.1. *Full-IPN PVA/PHEMA hydrogels*

The full-IPN PVA/PHEMA hydrogels in this study indicate good water uptake because PVA and PHEMA are hydrophilic polymers. The effect of glutaraldehyde ratio at 10, 20, 30, and 40 wt% on the swelling behaviour was studied while maintaining fixed amounts of 40 & 10 wt% for PVA and EGDMA, respectively, and varying the amount of HEMA in the hydrogels. The results from swelling measurements to indicate the water absorption capabilities of full-IPN PVA/PHEMA hydrogels and comparison PVA/GA and PHEMA gels are shown in Figure 2.16. The full-IPN hydrogels showed significant, but different, swelling behaviour and reached equilibrium within 24 h.

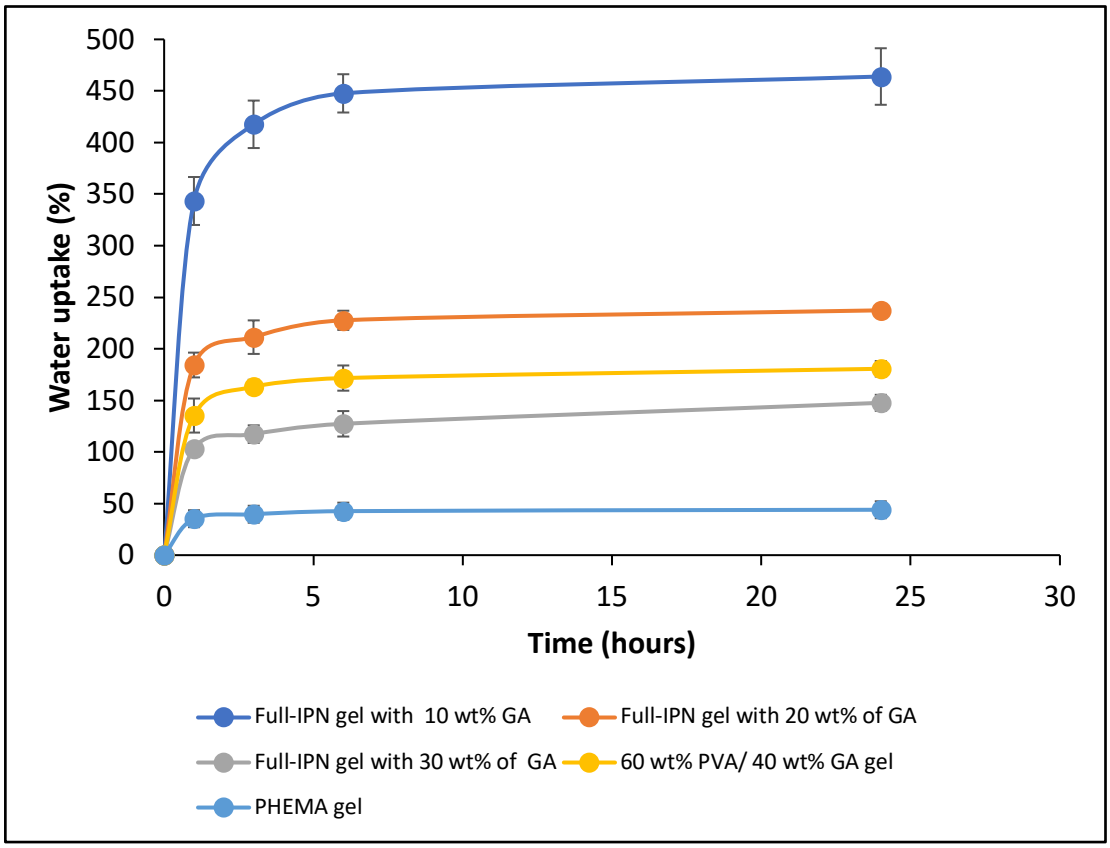

Figure 2.16. Water absorbing capabilities of full-IPN PVA/PHEMA hydrogels as a function of GA, PVA/GA gel, and PHEMA.

Moreover, the hydrogel containing 10 wt% GA exhibited a much higher water absorption capacity compared to other compositions. Significantly, when the GA ratio was increased from 10 to 20 wt%, the water uptake by the full-IPN hydrogel decreased substantially from 464 to 237%. The hydrogel prepared with 30 wt% GA showed the slowest rate and smallest amount of water absorption. Notably, the hydrogel containing 40 wt% of GA did not show any significant ability to absorb or retain water. This indicates that most hydroxyl groups are consumed during the crosslinking reaction, consequently, minimal hydrophilic sites are available to absorb water. The significant equilibrium swelling of the full-IPN hydrogels after exposure to water at 37 ^{o}C compared to their dried unswollen state is apparent in Figure 2.17.

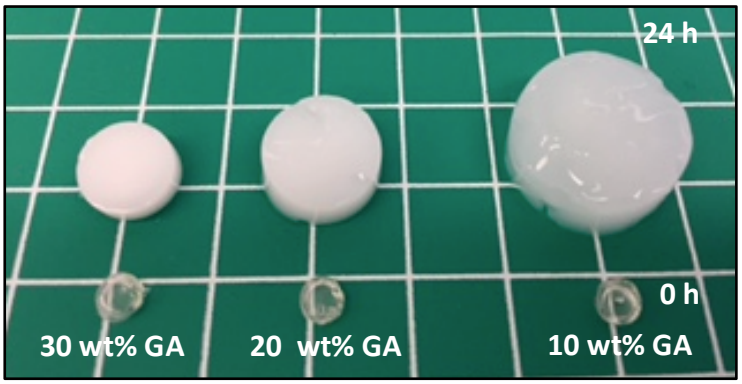

Figure 2.17. Images of full-IPN hydrogels as a function of GA ratio, showing unswollen state (lower) and equilibrium degree of swelling (upper) at 37 ^{o}C in water.

The difference in the water uptake ability of full-IPN hydrogels is attributed to the extent of crosslinking density that results in smaller pores and less free volume in the hydrogel network[130, 181]. Moreover, with increased amounts of GA in the gels, more hydroxyl groups in PVA are consumed in the crosslinking reaction. When aldehyde groups of GA react with hydroxyl groups of PVA, acetal rings and ether linkages are formed over most of the outer surface of the hydrogel network, creating a hydrophobic protective layer[181] that prevents water uptake (Figure 2.18). On the other hand, the water uptake by PVA/GA gel was relatively high compared to PHEMA because of the larger amount of pendant hydroxyl groups still present on the PVA compared to PHEMA backbone.

From the above discussion, it can be inferred, that water absorption by full-IPN hydrogels depends on several parameters, such as the crosslink density and presence of hydrophilic groups within the gel network.

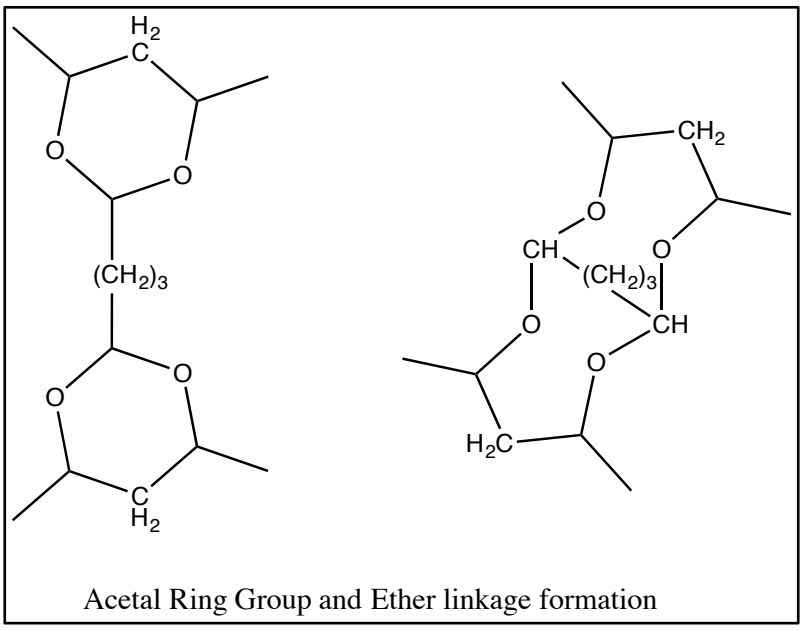

Figure 2.18. Acetal ring group and ether linkage formed by GA crosslinking of PVA[2].

2.4.6.2. *Full-IPN PVA/P(HBA-co-AA) hydrogels*

The water uptake of full-IPN PVA/P(HBA-co-AA) hydrogels as a function of HBA-to-AA ratio was investigated and compared to related simple hydrogels. The water absorption profiles are shown in Figure 2.19. Measurements of the water content of full-IPN co-polymer hydrogels were performed in triplicate and reached an equilibrium degree within 6 h. All full-IPN PVA/P(HBA-co-PAA) hydrogels exhibited similar water uptake profiles, with the hydrogel containing the higher amount of AA indicating the best water uptake because AA is more hydrophilic than HBA. The water absorption ability of the hydrogel is related to the hydrophilic groups, such as carboxyl of AA, and hydroxyl of PVA and HBA, that are available within the hydrogel structure. PAA is known to strongly associate with water because of carboxyl groups on the shorter alkyl polymer chain[182]. A similar water uptake was observed for hydrogels containing 20 & 27 wt% HBA. Noticeably, all the PVA/P(HBA-co-AA) hydrogels had significantly less water uptake than the full-IPN PVA/PHBA and PVA/PAA gels. However, a direct comparison of water uptake ability is

inadvisable because the simple hydrogels should have better water uptake ability because they contain a higher 65:35 ratio of hydrophilic-to-hydrophobic components compared to 60:40 for the PVA/copolymer hydrogels.

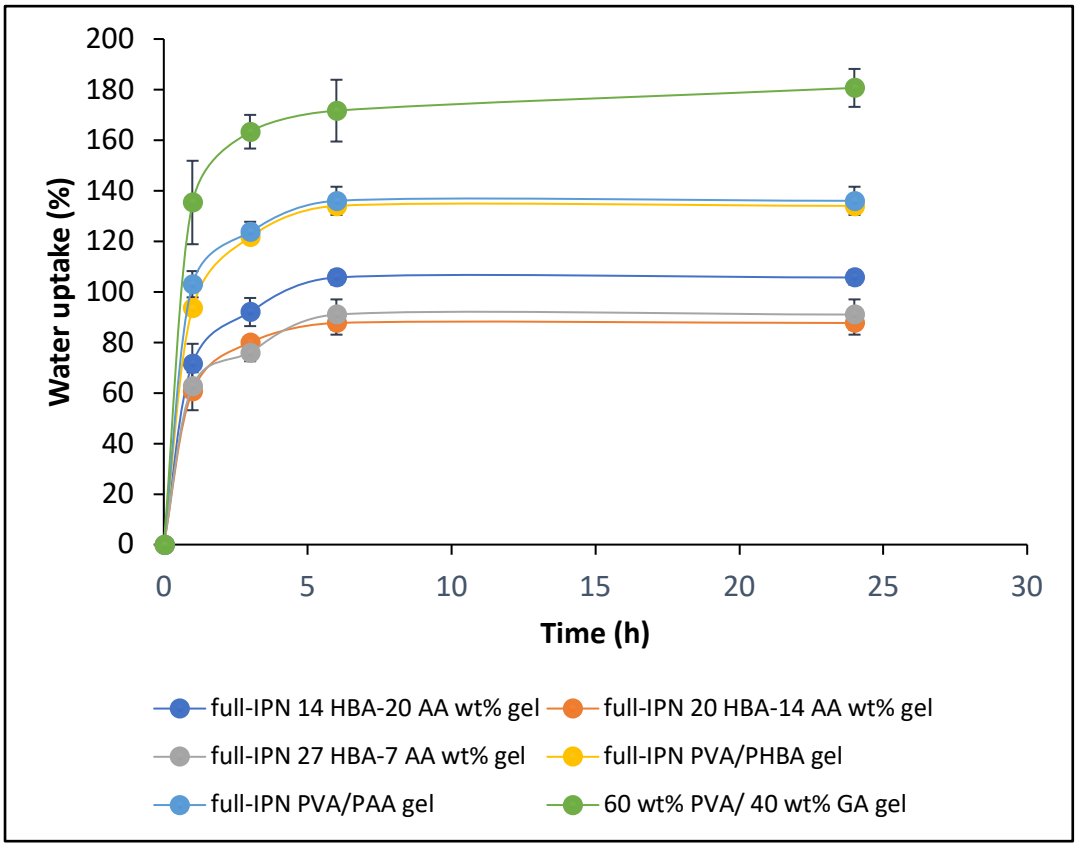

Figure 2.19. Water absorbing capabilities of full-IPN PVA/P(HBA-co-AA) as a function of HBA-to-AA ratio, full-IPN PVA/PHBA, PVA/GA, and full-IPN PVA/PAA hydrogels in deionised water at 37 °C.

An increased ratio of HBA-to-AA in the full-IPN resulted in decreased water content within the hydrogel. This effect could be due to additional hydrogen bonding between polymer components, specifically the hydroxyl groups of PVA or HBA, and carboxyl groups of AA. The PVA/GA gel shows the best water uptake because it still contains active polar sites after GA crosslinking, such as residual hydroxyl groups of PVA.

The similar water absorption of the full-IPN PVA/P(HBA-co-AA) hydrogels is exemplified in images of the hydrogel discs as shown in Figure 2.20, which indicate no

noticeable difference in the equilibrium degree of swelling at 37 °C despite changes to the HBA-to-AA ratio.

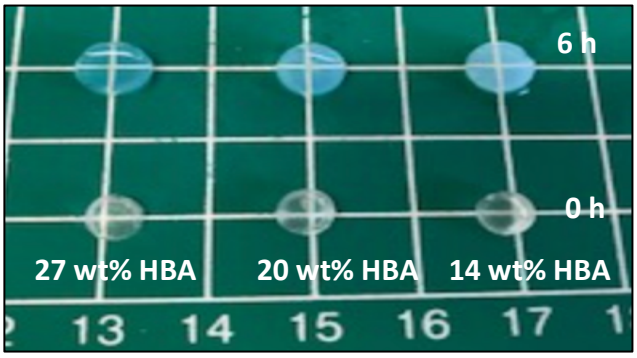

Figure 2.20. Images of full-IPN PVA/P(HBA-co-AA) hydrogels as a function of HBA (wt%) in dry (lower) and swollen (upper) states.

2.4.6.3. *Full-IPN PVA/P(MMA-co-IA) hydrogels*

The ability of hydrogels to absorb water is an important feature for different applications, especially as a system for drug delivery[183]. Water absorption of full-IPN PVA/P(MMA-co-IA) hydrogels as a function of MMA-to-IA ratio was investigated. In general, hydrogels with various amounts of MMA indicated similar water uptake profiles with improved water content at low amounts of MMA, as indicated in Figure 2.21. The better water uptake was due to the enhanced polar nature of the copolymer from the carboxyl groups of IA. The two carboxyl groups in each repeating unit of IA is known to enhance the ability to form hydrogen bonds with water[139]. Another reason for the better water content was the increased osmotic pressure inside the hydrogel from the presence of more IA that results in a high swelling degree[139]. The effect of PMMA and PIA on water uptake is indicated by the results using simple full-IPN PVA/PMMA and PVA/PIA hydrogels having the same ratio of components; the more hydrophilic PVA/PIA is 35% better.

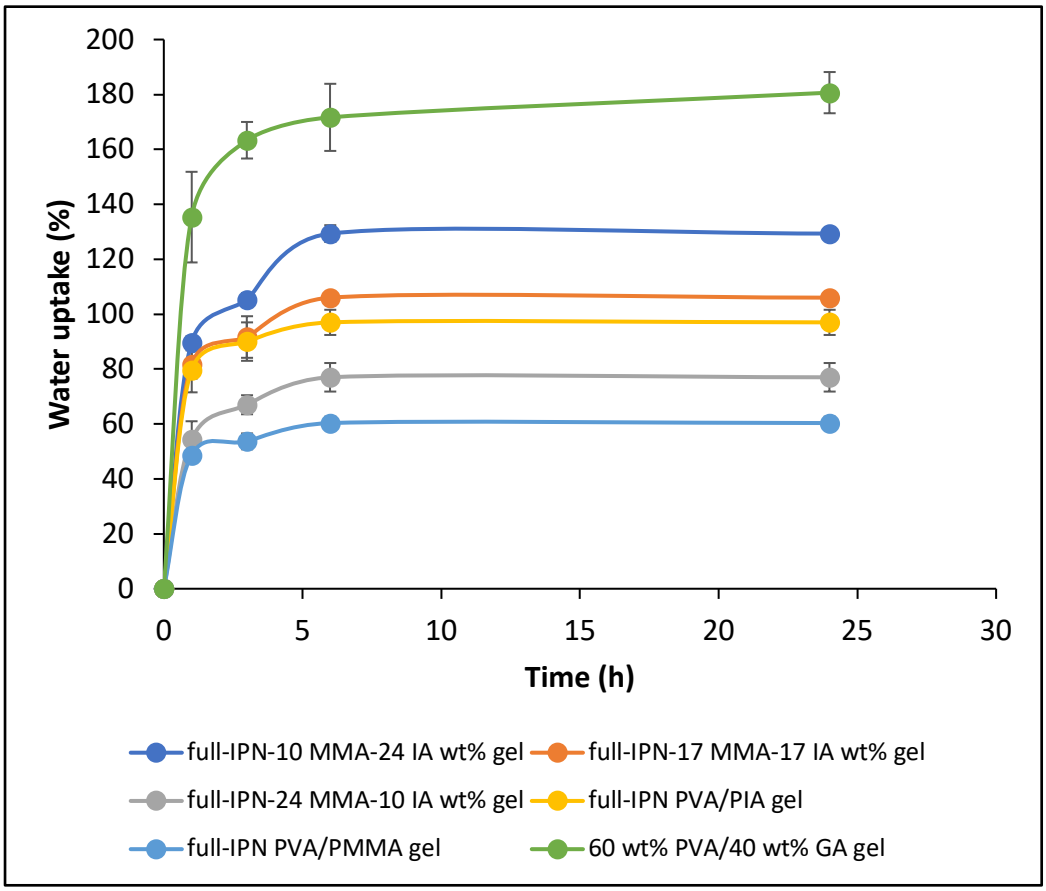

Figure 2.21. Water uptake profiles of full-IPN PVA/P(MMA-co-IA) as a function of MMA-to-IA wt% ratio (10:24, 17:17, & 24:10), full-IPN PVA/PIA gel, and full-IPN PVA/PMMA gel, PVA/GA gel.

All the hydrogels with different ratios of MMA reached an equilibrium swelling degree by 6 h. However, the increase in the amount of MMA within full-IPN hydrogels was accompanied by a relative decline in water absorption. The presence of hydrophobic segments in the hydrogel network is responsible for reduced water content. Consequently, the number of hydrophilic groups, such as COOH groups, was less along the polymer chains of the full-IPN.

Based on the information provided above, water diffusion into full-IPN hydrogels is affected by hydrophilic and hydrophobic characteristics of the polymer chains, and the formation of a full-IPN structure. However, it is obvious from the images of the swollen state of hydrogels with different ratios of MMA that there are big differences in the water uptake ability of the hydrogel samples (Figure 2.22).

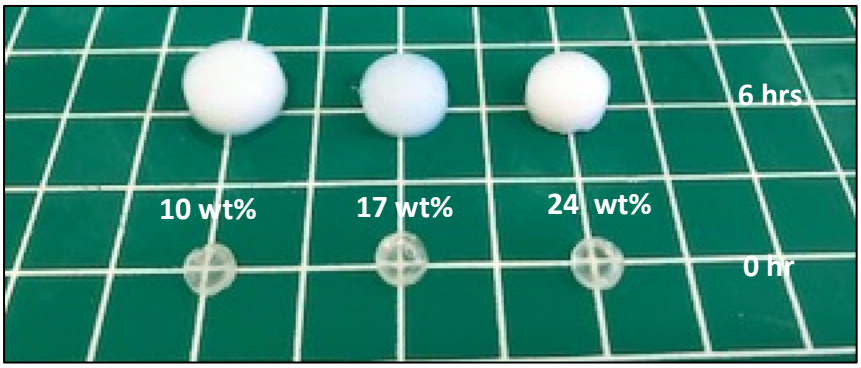

Figure 2.22. Images of full-IPN PVA/P(MMA-co-IA) hydrogels as a function of MMA amount (wt%) in dry (lower) and swollen (upper) states.

2.4.7. **pH-sensitivity**

2.4.7.1. *Full-IPN PVA/PHEMA hydrogels*

The physiochemical properties of full-IPN hydrogels used for biological or environmental applications is likely to be affected by the pH of the local environment. The effect of pH sensitivity on full-IPN PVA/PHEMA, PVA/P(HBA-co-AA) and PVA/P(MMA-co-IA) hydrogels prepared with different amounts of GA, HBA and AA, and MMA and IA, respectively, was investigated by monitoring the swelling and water uptake. The hydrogels were examined in a series of pH buffer aqueous solutions (3.4, 6.2, 7.2, & 8.2) at 37 ^{o}C. The effect of ionisation at pH 6.2, 7.2 & 8.2, which is more than one unit above the pK_a of the pendant acidic functional groups, of the different polymers was used to investigate water uptake and likely solute loading capacity of the hydrogels at or around physiological pH. Conversely, similar hydrogel performance was investigated at pH 3.4 at which the polymer functional groups are mostly unionized. Swelling profiles of full-IPN PVA/PHEMA as a function of GA ratio are presented in Figure 2.23.

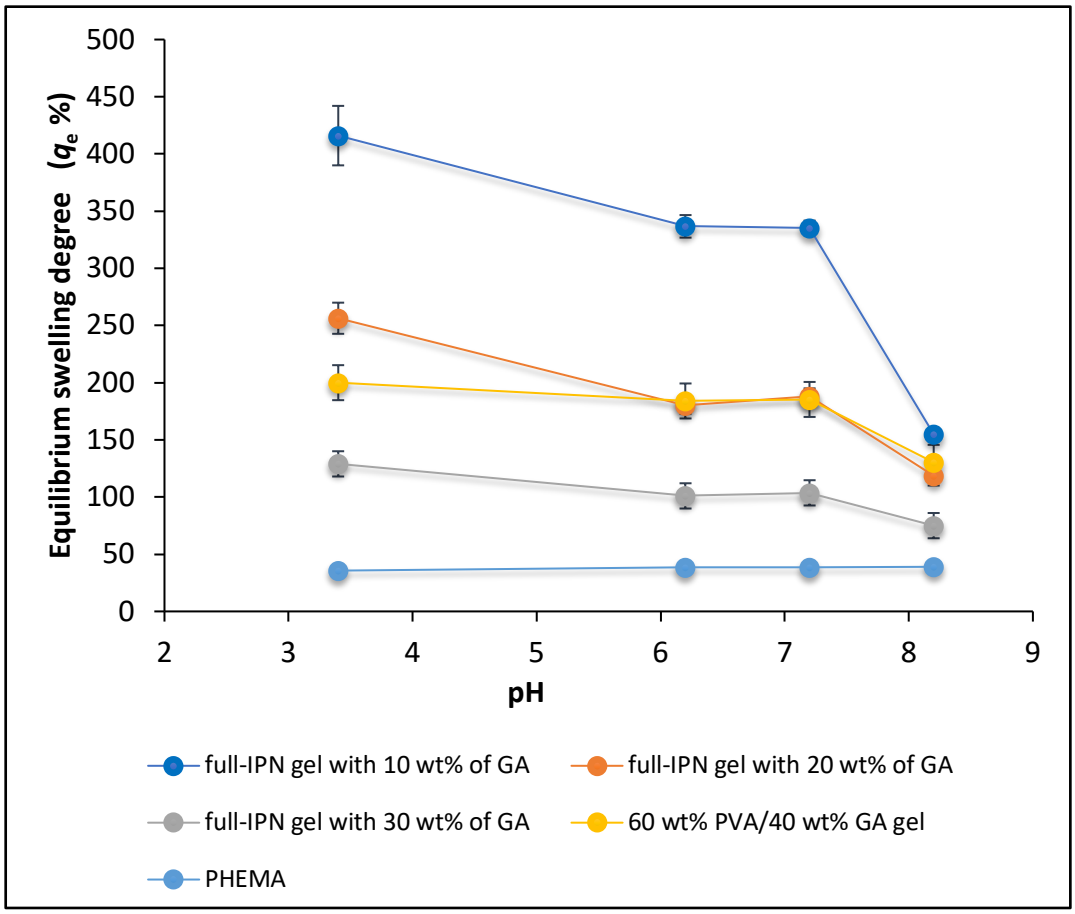

Figure 2.23. Profiles of pH sensitivity for PVA/GA, PHEMA and full-IPN PVA/PHEMA hydrogels with different amounts of GA (10, 20 & 30 wt%).

Noticeably, the equilibrium swelling degree of all full-IPN PVA/PHEMA hydrogels decreased as the pH was raised. The extent of the decreased swelling was more significant as the amount of GA was increased in the hydrogel. The combined effects of changing pH and amounts of GA significantly affect the hydrogen bonding capacity of PVA within the hydrogel. At higher pH and increased amounts of GA, the ability to form inter- and intra-molecular hydrogen bonds among the hydroxyl groups of PVA (Figure 2.24) is reduced, which effectively shrinks the 3D polymer network. In addition, hydrogen-bonding results in the formation of a tight or compact structure that restricts significant movement of polymer chains within the hydrogel network, which leads to a decrease in available free volume and reduced ability to absorb water. Significantly, there was a slight increase in the equilibrium swelling degree of full-IPN and PVA/GA hydrogels at pH 7.2. This result is against the general downward trend across the range of pH. It is inferred that some

residual acetate groups of PVA are ionized to -C-O-C(O^-)-CH_3 at pH 7 due to dehydrogenation of the methylene group and subsequent resonance stabilisation to form a vinyl group –[CH(OH)CH=C(O(CO^-)CH_3)CH_2]- within the polymer[183]. Consequently, the resultant charged polymer chains repel each other, leading to an expanded network space with increased internal volume[150]. The acetate groups are a result of incomplete hydrolysis to hydroxyl groups during the alkaline hydrolysis of poly(vinyl acetate) to PVA. The unexpected result at pH 7 is consistent with previous studies indicating increased pH-sensitive behaviour of hydrogels incorporating PVA at high pH of the surrounding media[184].

The amount of GA was shown to also affect the physical properties with reduced swelling as the ratio of GA was increased in the hydrogels. A combination of both low pH and amount of GA resulted in the best swelling and, by inference, water uptake. Under these conditions, the hydrogel network becomes highly hydrophilic, enabling the ready diffusion of water into the 3D hydrogel network. In previous studies, hydrogels composed of PVA containing 3 mol% of non-hydrolysed acetate groups showed increased swelling due to protonation of acetate groups at low pH[185].

The equilibrium degree of swelling of PVA/GA hydrogel also showed a similar, but not as significant, pH trend as full-IPN hydrogels. The swelling at pH 3.4 was about 20% more than at near neutral conditions of pH 6.2 or 7.2. A similar hydrogel has been previously shown to have a high swelling ratio in water and acetic acid due to the presence of more pendant aldehydic groups[130]. A previous study has reported that crosslinked PVA hydrogel showed pH-sensitive behaviour at pH 6 that was related to increased ionic strength that neutralised any negatively charged acetate groups[163].

The current results indicate no significant difference of equilibrium swelling degree of PHEMA at different pH. As such, this polymer is not pH-sensitive and does not respond to local environmental stimuli[138, 186].

The results clearly illustrate pH-sensitive behaviour of the PVA/GA hydrogel over pH 3.4 – 8.2. This is in contrast to some literature that reports that hydrogels of PVA cross-linked with GA are not pH sensitive, and that PVA exhibits an almost neutral response to pH stimuli[163, 187]. However, according to another study, PVA with a 87-89% degree of hydrolysis, composed of a copolymer of poly(vinyl alcohol-co-vinyl acetate), indicates pH-

sensitive behaviour because of the residual acetate groups in the inner region of the hydrogel network and can act as an amphiphilic system[163].

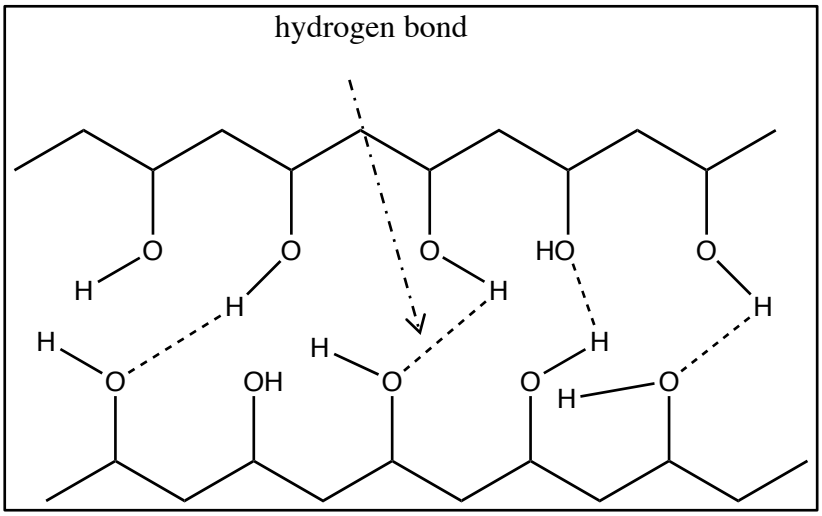

Figure 2.24. Formation of intermolecular hydrogen bonds between O-H groups of adjacent PVA chains.

2.4.7.2. *Full-IPN PVA/P(HBA-co-AA) hydrogels*

The various full-IPN hydrogels contain acidic functional groups that can be readily deprotonated by changes in pH that could affect the water uptake or swelling ability. The profiles of equilibrium swelling capacity in relation to pH of PVA/P(HBA-co-AA) hydrogels with different amounts of HBA-to-AA are shown in Figure 2.25. The hydrogels reached an equilibrium swelling degree within 3 h.

In general, the swelling capacity of all hydrogels was affected by pH. However, the PVA/GA and full-IPN PVA/PHBA gels showed a decrease in swelling as the pH was raised, whereas, full-IPN PVA/P(HBA-co-AA) and full-IPN PVA/AA gels exhibited increased swelling as the pH was raised, reaching a maximum at pH 7.2. The co-polymer hydrogel with the lowest HBA-to-AA ratio (14:20) had the highest equilibrium swelling capacity (q_e), indicating that AA has a more significant effect than HBA on the swelling capacity. The sharp increase in volume as indicated by q_e occurs at pH 7.2 which is higher than the pK_a of acrylic acid.

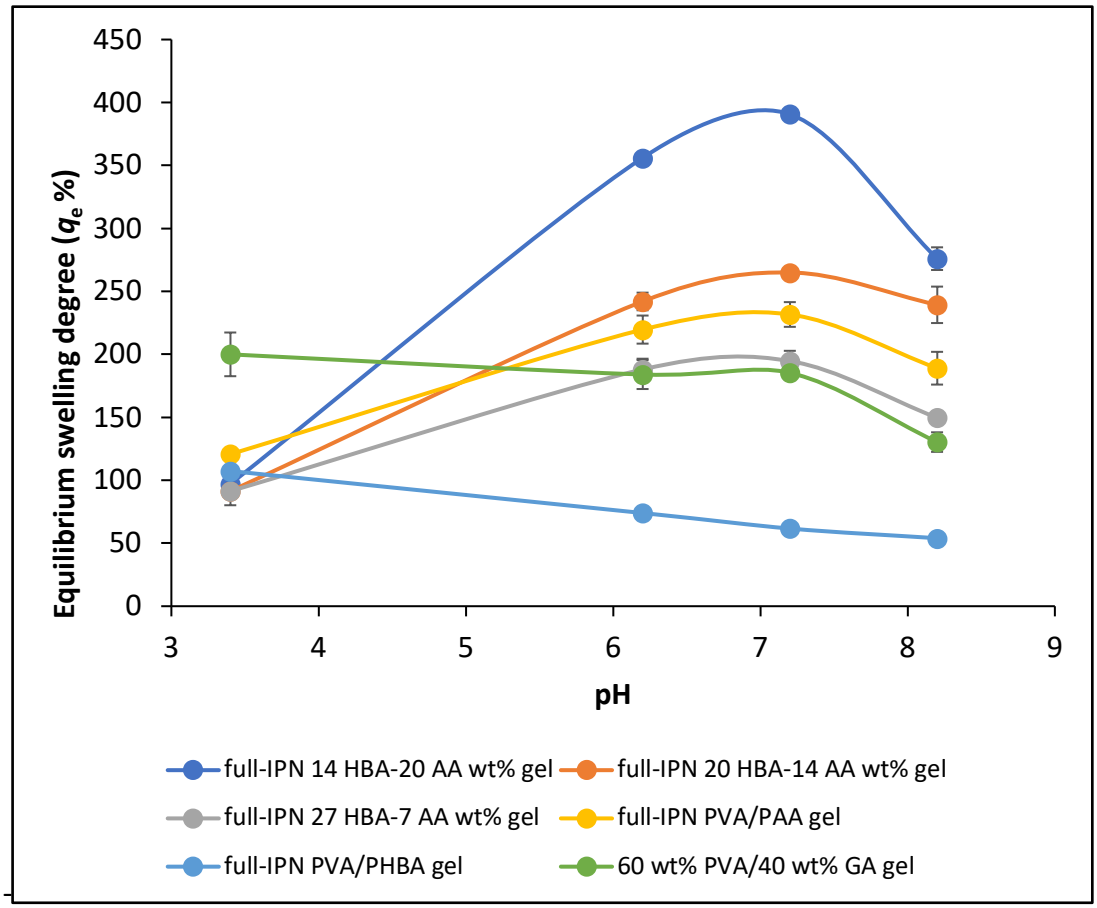

Figure 2.25. pH sensitivity profiles of full-IPN PVA/P(HBA-co-AA) as a function of HBA-to-IA ratio, full-IPN PVA/PHBA, full-IPN PVA/PAA, and PVA/GA hydrogels at 37 °C.

A significant decrease of q_e was noted at pH 8.2 that is consistent with previous studies. The reduced q_e resulted from ion-pairing of COO^- with Na^+ from the buffer to form -COONa under alkaline conditions. This increased the amount of mobile ion and reduced the hydrogen bonding capacity, leading to decreased osmotic pressure within the hydrogel[188-189].

However, other previous swelling studies over pH 2 – 12 of semi-IPN PVA/PAA hydrogels indicated pH-sensitive behaviour with the maximum swelling ratio observed at pH 12[123]. Additionally, the pH response of full-IPN PVA/PAA with various amounts of GA and EGDMA crosslinking reagents and different ionic strength of the swelling medium resulted in increased q_e as the pH was raised from 3 to 6[151]. These studies indicate that the type of polymer network and preparation methods have a significant effect on the physiochemical properties of hydrogels.

The differences in q_e bought about by different HBA-to-AA ratios in the co-polymer hydrogels is due to the pH-sensitivity of the carboxylate groups of AA with a pK_a of 4.5[47]. When the pH of the surrounding medium is 1 – 2 units above the pK_a, the carboxylate group is readily ionized, resulting in a significant increase in the extent of swelling. This results from electrostatic repulsion between neighbouring ionized carboxylate groups in P(HBA-co-AA) that causes expansion of the IPN and, consequently, improved water absorption capacity. However, at pH 3.2, which is below the pK_a, the swelling capacity of the IPN is reduced due to formation of hydrogen bonding between carboxylate groups of AA, and hydroxyl groups of PVA and HBA, respectively.

The results from this investigation using a full-IPN hydrogel containing P(HBA-co-AA) as a hydrophobic component indicate that the swelling capacity is very dependent on the composition of the IPN, presence and pK_a of ionizable functional groups (COOH in PAA), and pH of the solution or environment in which the hydrogel is used.

2.4.7.3. *Full-IPN PVA/P(MMA-co-IA) hydrogels*

Sensitivity to pH alterations in the surrounding environment was investigated by the equilibrium degree of swelling (q_e) of full-IPN PVA/P(MMA-co-IA) as a function of MMA-to-IA ratios, full-IPN PVA/PIA, full-IPN PVA/PMMA, and PVA/GA hydrogels and the results are indicated in Figure 2.26.

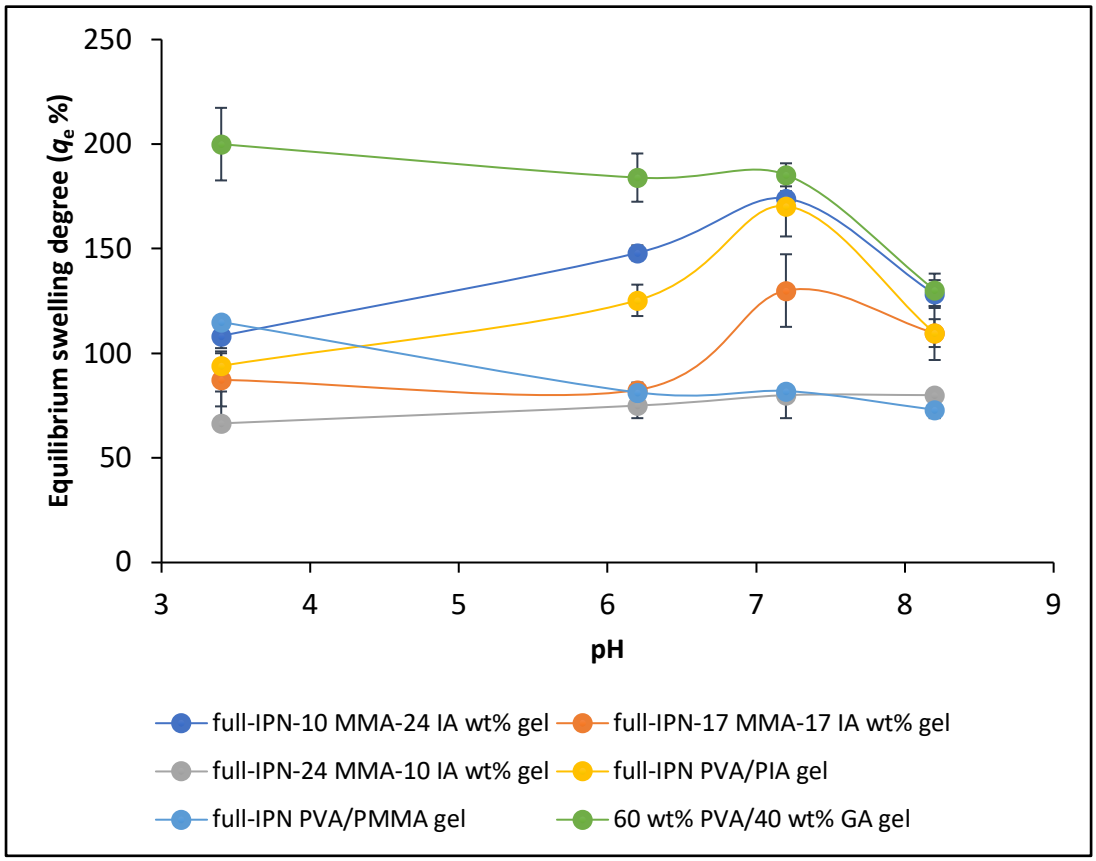

Figure 2.26. pH sensitivity profiles of full-IPN PVA/P(MMA-co-IA) with various ratio of MMA-to-IA, full-IPN PVA/PMMA, full-IPN PVA/PIA, and PVA/GA hydrogels.

As clearly shown in Figure 2.26, full-IPN PVA/P(MMA-co-IA) hydrogels are pH-sensitive with the q_e profiles of hydrogels with different MMA-to-IA ratio showing similar trends. The q_e was higher for all hydrogels at a pH above the pK_a of both carboxylic groups of IA (pK_{a1} = 3.85, pK_{a2} = 5.45)[7]. At pH 6, significant carboxylate groups of IA are present and as the pH is increased to 7 more carboxyl groups are converted to carboxylate, resulting in a significant increase in q_e[138, 183]. Consequently, these hydrogels are more hydrophilic. Additionally, the presence of carboxylate groups in the hydrogel network leads to repulsive forces between neighbouring polymer chains.

However, when the pH of the surrounding medium was below the pK_a of the carboxyl groups of IA, the full-IPN hydrogels show a reduced swelling degree. This is related to the extensive intramolecular hydrogen bonding between carboxyl groups of IA on neighbouring polymer chains[139 190], leading to the collapse of the free volume within

the full-IPN hydrogels. Previous studies of semi-IPN hydrogels composed of PVP, HEMA, and IA indicated a pH-sensitive behaviour with maximum q_e at pH 6[152].

The present study has shown that full-IPN PVA/P(MMA-co-IA) hydrogels are affected by pH and the carboxyl groups of IA have a significant effect on the equilibrium swelling behaviour.

2.4.8. **Water retention measurements**

2.4.8.1. *Full-IPN PVA/PHEMA hydrogels*

The ability of hydrogels to retain water in different environments is an important performance criterion for possible applications. The water retention of full-IPN PVA/PHEMA hydrogels with different amounts of GA, after drying at 30 ^{o}C are presented in Figure 2.27. The results are consistent with expectations that more water is lost from hydrogels containing high amounts of absorbed water or, conversely, more water is retained by hydrogels that absorb small amounts of water.

For instance, the 30 wt% GA hydrogel reached a water retention equilibrium ratio of 36% after 125 mins, whereas only 90 mins was needed for the 10 wt% GA hydrogel to reach an equilibrium value of 18%. The remarkable ability of the hydrogels to both absorb and retain water is related to the extent of crosslinking in the polymer network. Significant cross-linking hinders relaxation of polymer chains and mobility within the network, resulting in significant hydrogen bonding of absorbed water within the polymer network. Thus, even though highly cross-linked hydrogels do not absorb large amounts of water, they do retain significant amounts of absorbed water. The PVA/GA gel showed similar water retention to the 30 wt% GA hydrogel, indicating that a good proportion of absorbed water is retained within the polymer network. Even though the PHEMA hydrogel indicates high water retention (74%) this result must be considered in the context of the relatively small amount (40%) absorbed compared to the other hydrogels.

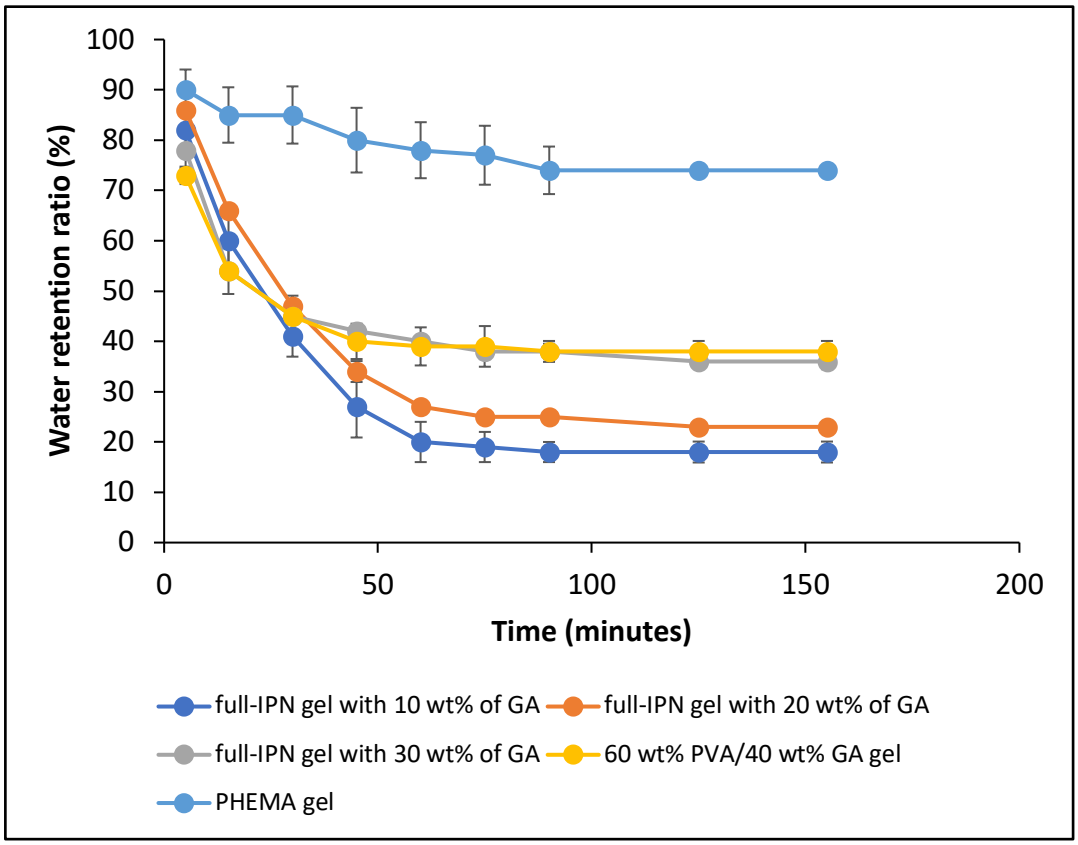

Figure 2.27. Water retention profiles of full-IPN PVA/PHEMA hydrogels as a function of GA, PVA/GA gel, and PHEMA hydrogels.

2.4.8.2. *Full-IPN PVA/P(HBA-co-AA) hydrogels*

As shown in Figure 2.28, the full-IPN PVA/P(HBA-co-AA) hydrogels with different amounts of HBA have, in general, similar water retention profiles and capacity. The hydrogels with 14 and 27 wt% HBA had the poorest water retention that was about 8% less than the 20 wt% HBA hydrogel with 51% water retention capacity. The results indicate that water retention, unlike water absorption, is not as dependent on the composition, that is HBA-to-AA ratio, or the internal volume of the hydrogel. This is attributed to the extensive hydrogen bonding that water molecules experience from all the polar groups within the IPN after absorption. This effect is intensified in hydrogels with extensive crosslinking that results in a compact structure with reduced pore size and restricted movement of polymer chains within the IPN.

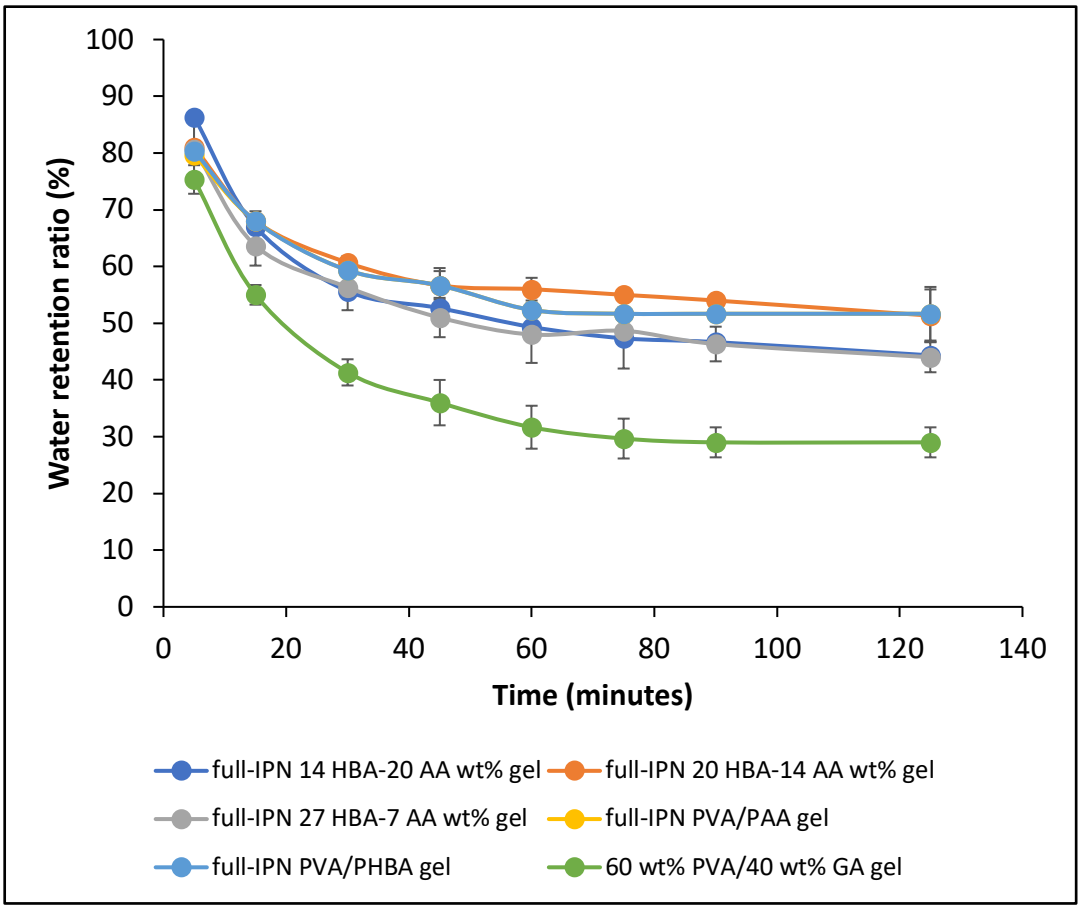

Figure 2.28. Water retention ratio profiles full-IPN PVA/P(HBA-co-AA) hydrogels as function of HBA ratios, full-IPN PVA/PHBA gel, full-IPN PVA/PAA gel, and PVA/GA gel.

2.4.8.3. *Full-IPN PVA/P(MMA-co-IA) hydrogels*

The water retention rate of full-IPN PVA/(P(MMA-co-IA) hydrogels as a function of MMA-to-IA ratio was compared to simple full-IPN PVA/PIA, full-IPN PVA/PMMA, and PVA/GA hydrogels. Water retention rate profiles of full-IPN PVA/(P(MMA-co-IA) with 10, 17 and 24 wt% MMA are shown in Figure 2.29. Hydrogels with 24 wt% MMA indicated high water retention of 73% compared to similar hydrogels with less MMA content. This is attributed to the presence of hydrophobic and hydrophilic segments of the hydrogel[139]. The movement of water molecules into and from the inner regions of the hydrogel network is restricted by significant hydrophobic interactions of pendant groups. Consequently, hydrogen bonds between water molecules and with the hydrophilic pendant groups within the IPN inhibit the loss of water. Water retention by PVA/GA was poor (38%) compared to full-IPN PVA/PIA (47%) and other full-IPN hydrogels. The results

indicate that hydrogels with a more non-polar nature and more compact structure due to extensive cross-linking in the hydrophilic and hydrophobic components have a better capacity to retain water.

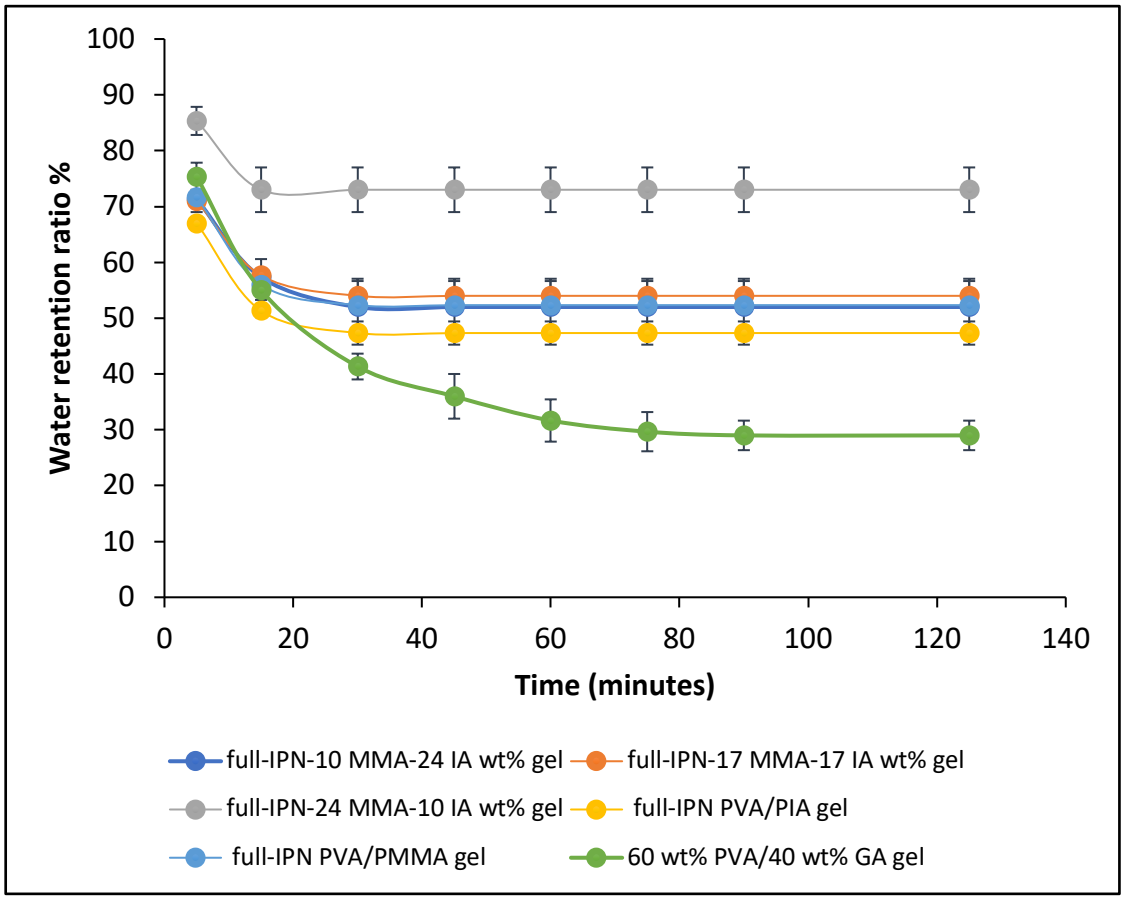

Figure 2.29. Water retention profiles of full-IPN PVA/P(MMA-co-IA) hydrogels with different amounts of MMA and IA, full-IPN PVA/PMMA gel, full-IPN PVA/PIA gel, and PVA/GA gel.

2.4.9. **Effect of pH on chemical configuration of full-IPN hydrogels**

2.4.9.1. *Full-IPN PVA/P(HBA-co-AA) hydrogels*

The effect of pH on the chemical configuration of full-IPN PVA/P(HBA-co-AA) hydrogels containing either 14 or 27 wt% HBA was investigated by infrared spectroscopy and the spectra are shown in Figure 2.30. The infrared stretching bands of COOH, OH, and C-O groups were affected by absorbed water at pH 3.4 and 7.2.

Spectra of hydrogels with 14 wt % HBA and 20 wt % AA showed a significant shift to 1556 cm^{-1} of the stretching band assigned to COOH at pH 7.2, which is indicative of an ionised carboxyl group[151]. A significant relative increase in the intensity of OH bands between 3345 – 3354 cm^{-1} was also observed. However, at pH 3.4, the hydrogel did not show any significant changes in the shape or intensity of characteristic bands due to association of hydrogen bonding between carboxylate groups of AA and hydroxyl groups of PVA.

The change in configuration of full-IPN PVA/P(HBA-co-AA) hydrogel containing 14 wt% HBA and 20 wt% AA at different pH is due to the extent of ionisation of carboxyl groups of the full-IPN. Acrylic acid has a pK_a of 4.5. Significant negatively charged sites exist along the polymer chains within the polymer network at pH 7.2. This results in electrostatic repulsion between carboxylate groups on neighbouring chains. The carboxylate groups also act as cation ion-exchange sites and electrostatically attract cations, such as sodium ions from the buffer solution.

On the other hand, the spectra of full-IPN PVA/P(HBA-co-AA) containing 27 wt% HBA and 7 wt% AA at pH 7.2 and 3.4 are mostly similar. The only significant difference is the band at 1567 cm^{-1} attributed to the symmetric and asymmetric stretching of carboxylate. The intensity of this band slightly increased at pH 7.2 due to the ionisation of carboxyl groups of PAA.

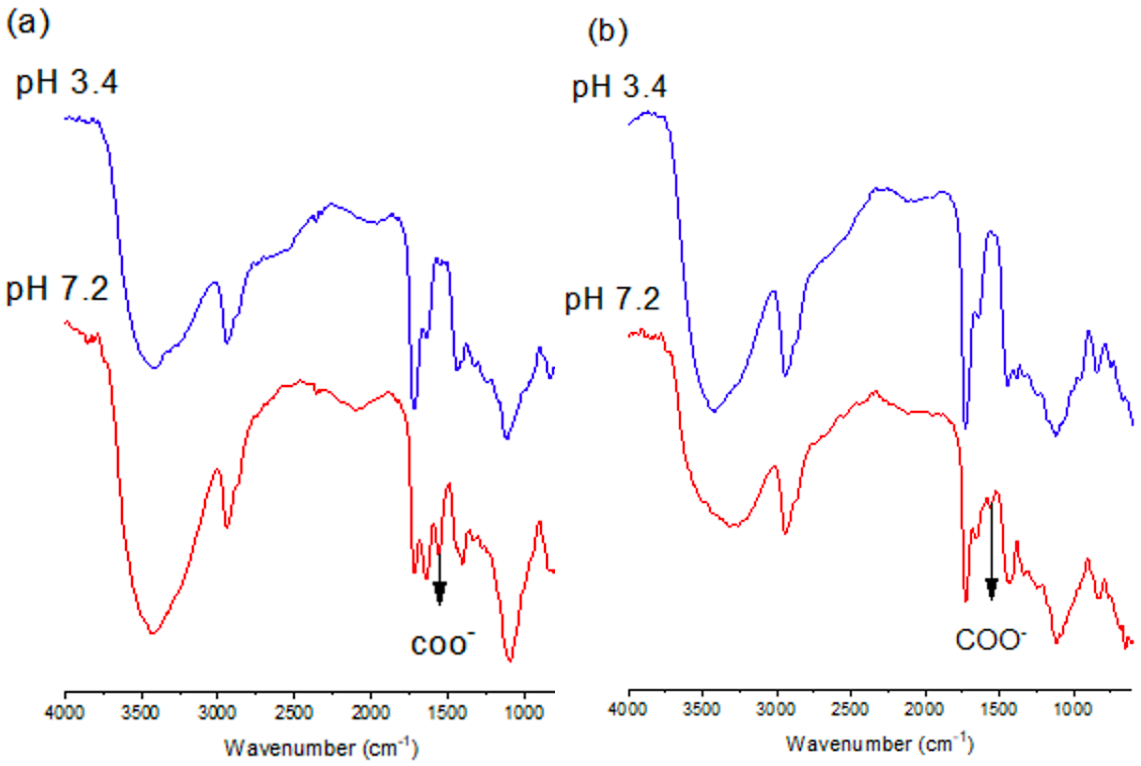

Figure 2.30. FTIR spectra of full-IPN PVA/P(HBA-co-AA) hydrogels as a function of HBA-to-AA ratio, 14:20 (a) 27:7 HBA (b), after reaching equilibrium at pH 3.4 (blue) and pH 7.2 (red).

2.4.9.2. *Full-IPN PVA/P(MMA-co-IA) hydrogels*

The pH of aqueous solutions has an effect on the chemical structure of hydrogels and this influence was investigated for full-IPN PVA/P(MMA-co-IA) at pH 3.4 and 7.2 using infrared spectroscopy. The spectra of hydrogels with wt% ratios of 10:24 and 24:10 of MMA-to-IA after reaching equilibrium at pH 7.2 and 3.4 are shown in Figure 2.31. Carboxyl groups of IA can respond to changes in pH of the surrounding media. Characteristic peaks of IA in the full-IPN hydrogels were affected by variations of pH. The hydrogel with the lower MMA-to-IA ratio, that is more IA, showed the presence of characteristic antisymmetric stretching frequency of carboxylate ion (COO^-) at 1562 cm^{-1}, resulting from the ionisation of COOH groups at pH 7.2. However, at pH 3.4, the COOH groups of PIA are fully protonated, so the peak due to COO^- is not observed. At the same time, no significant changes were noted in the infrared spectra of hydrogels prepared with the higher ratio of

MMA-to-IA at pH 3.4 and 7.2. due to the reduction of IA ratio on the surface of the network.

The results indicate that the components of the hydrophobic co-polymer network have a significant effect on the pH responsive behaviour of hydrogels. In this instance, variations of the amount of MMA and IA had affected the chemical nature of the hydrogel. Hydrophobic segments of the full-IPN hydrogel were not readily affected by pH changes of the surrounding medium. The more polar and readily ionised IA had a more significant effect than MMA on the pH response. A full-IPN PVA/P(MMA-co-IA) prepared with 10 and 24 wt% of MMA and IA, respectively, gave good pH response. This hydrogel could be useful for subsequent investigations for delivery or recovery of solutes involving chemistry that can be controlled by pH.

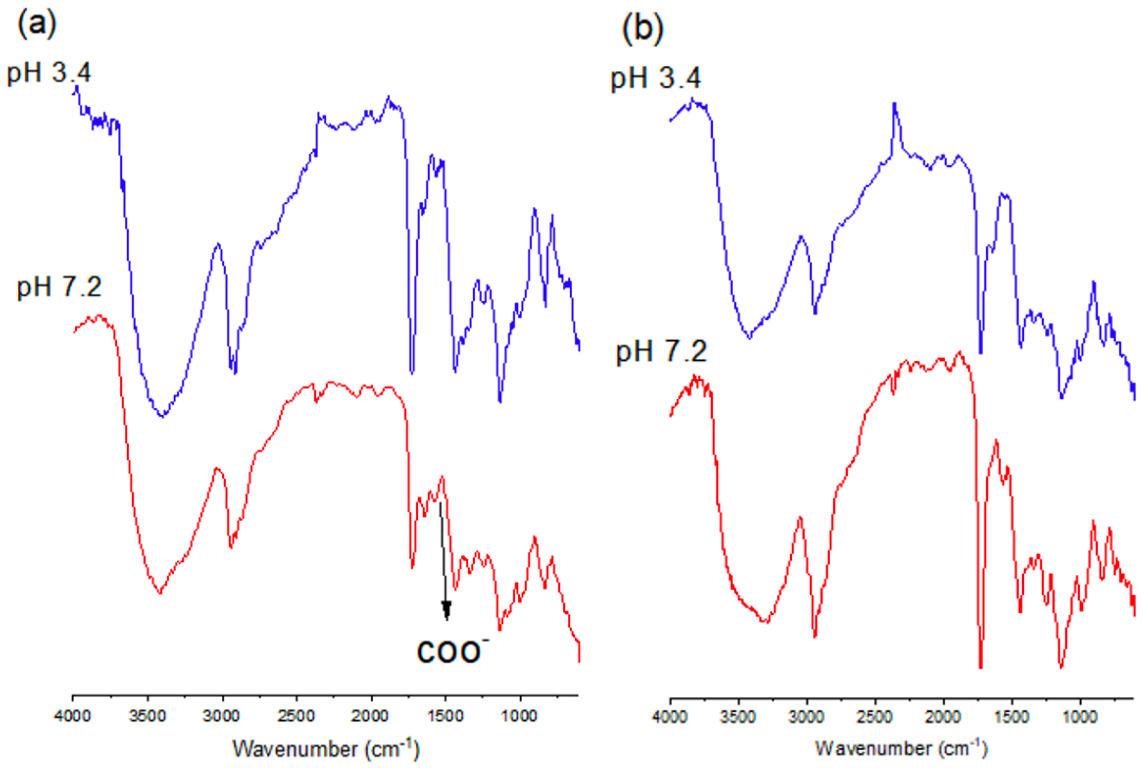

Figure 2.31. FTIR spectra of full-IPN PVA/P(MMA-co-IA) hydrogels as a function of MMA-to-IA ratio (10:24 wt%) (a) and (24:10 wt%) (b) after absorption of water at pH 3.4 (blue) and 7.2 (red) in the range of 4000-600 cm^{-1}.

2.4.10. **Thermal properties**

2.4.10.1. *Full-IPN PVA/PHEMA hydrogels*

The thermal stability of full-IPN hydrogels was investigated by TGA to get more information about the stability at different temperatures for a range of potential applications. The resultant thermograms of full-IPN PVA/PHEMA and PVA/GA hydrogels, and PVA and PHEMA polymers over the range 50 – 500 ^{o}C are presented in Figure 2.32.

Three stages of similar thermal decomposition were noted for the full-IPN PVA/PHEMA and PVA/GA hydrogels over the temperature range. The first stage of weight loss between 50 – 240 ^{o}C is attributed to the vaporisation of residual water trapped in the hydrogel network[143]. The second thermal decomposition was noticed from 250 – 350 ^{o}C and is attributed to cleavage and decomposition, such as dehydration, of side chains or pendant groups from the hydrogel[191]. A large weight-loss of (80%) occurred during the third and final decomposition stage between 400 – 500 ^{o}C. This final weight loss is related to the charring and decomposition, such as decarboxylation, of the backbone of the full-IPN. By comparison, the full-IPN and PVA/GA hydrogels indicated much better thermal stability than both PHEMA and PVA which underwent the onset of final decomposition at about 270 ^{o}C. The presence of the acetal and ether linkages, resulting from crosslinking between OH groups of PVA and aldehyde groups of GA, in PVA/GA are likely responsible for the extra thermal stability. PVA showed thermal degradation in one stage with the onset at 260 ^{o}C; consistent with earlier reports[144]. Noticeably, the PVA/GA hydrogel showed better thermal stability than the full-IPN hydrogel at higher temperatures of 300 – 500 ^{o}C.

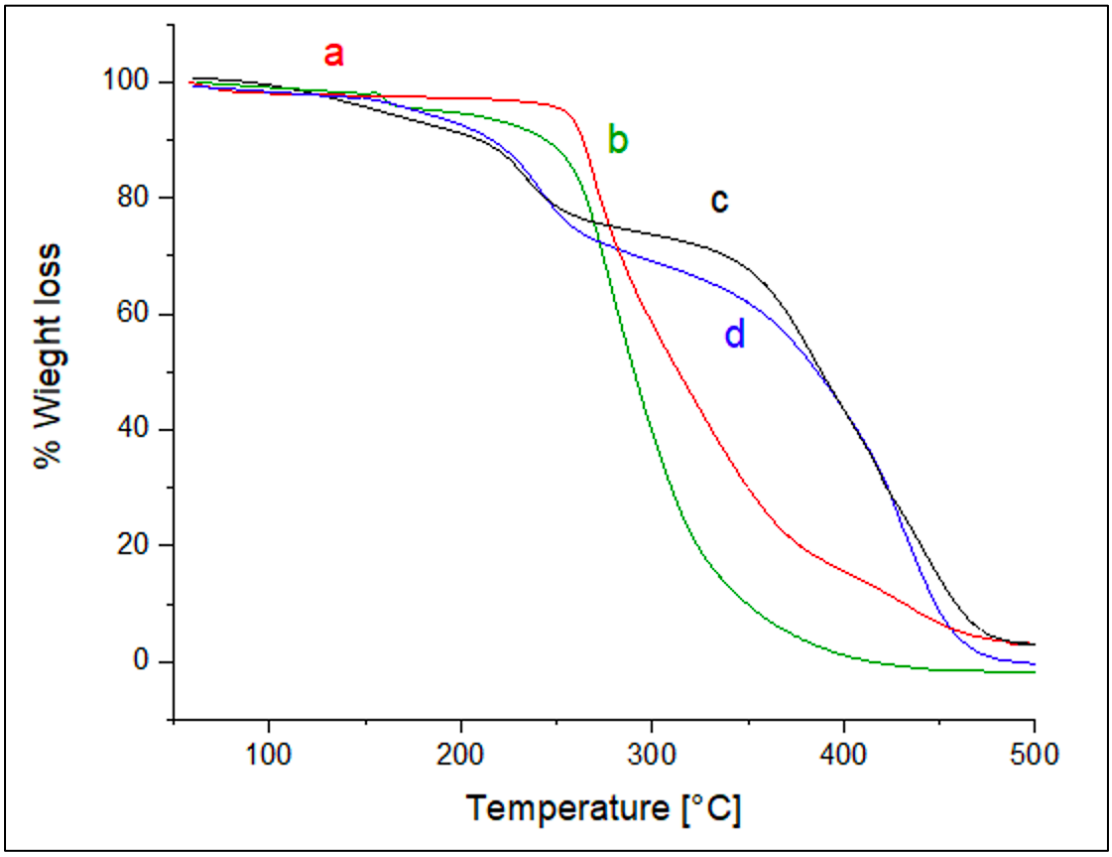

Figure 2.32. TGA curves of PVA (a), PHEMA (b), PVA/GA (c), and the full-IPN PVA/PHEMA1 (d) hydrogels.

The effect of GA cross-linking on the thermal properties of full-IPN hydrogels was also investigated by TGA. Similar thermogram profiles were obtained for hydrogels containing 10 or 20 wt% GA as shown in Figure 2.33. However, the hydrogel containing 20 wt% GA indicated better thermal stability over the complete temperature range with both a higher initial onset and final decomposition temperatures[181].

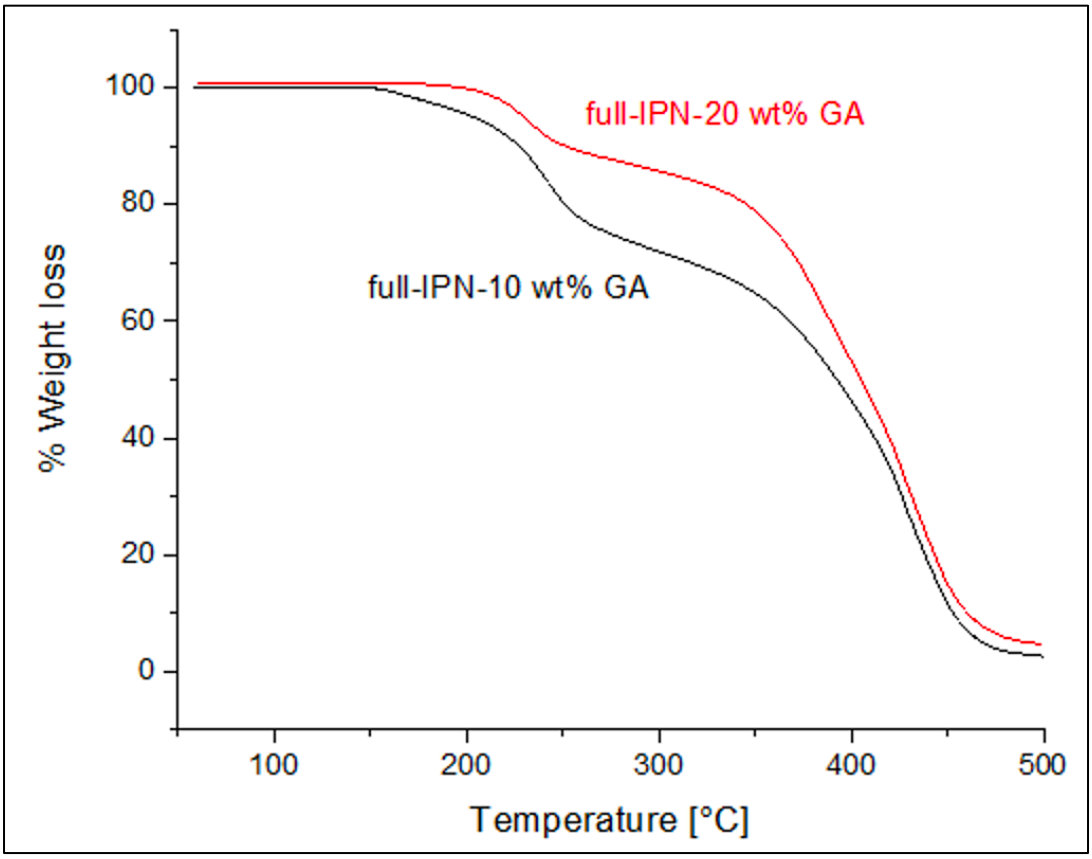

Figure 2.33. TGA curves of the full-IPN PVA/PHEMA hydrogels as a function of GA amount: 10 wt% (black), 20 wt% (red).

2.4.10.2. *Full-IPN PVA/P(HBA-co-AA) hydrogels*

The initial weight loss from full-IPN PVA/P(HBA-co-AA) hydrogel was observed between 50 – 350 °C due to loss of absorbed water (Figure 2.34). Additionally, a subsequent large weight loss was observed between 350 – 450 °C, which is attributed to the decomposition and fragmentation of the full-IPN. By comparison, the thermogram of full-IPN PVA/PAA indicated three decomposition regions: first stage (50 – 250 °C) corresponding to removal of weakly bound water; second stage (250 – 350 °C) indicating decomposition of pendant COOH groups of PAA; the third stage between 230 – 450 °C with a maximum weight loss of approximately 80% is attributed to the decomposition and charring of the IPN and polymer chains. The thermogram of PVA/GA had a similar profile to full-IPN PVA/PAA but showed earlier onset of the final two decomposition stages, indicating less thermal stability above 250 °C. Noticeably, the full-IPN PVA/PHBA hydrogel exhibited no apparent region of thermal stability with an early onset and gradual decomposition over the whole temperature range. The results indicate that thermal

stability of PVA is improved by using GA as a crosslinking agent, or in combination with PAA in full-IPN PVA/PAA or full-IPN PVA/P(HBA-co-AA) hydrogels. Formation of intermolecular hydrogen bonds between COOH groups of PAA, and OH groups of PVA are responsible for the improved thermal stability of full-IPN PVA/PAA and full-IPN PVA/P(HBA-co-AA) hydrogels.

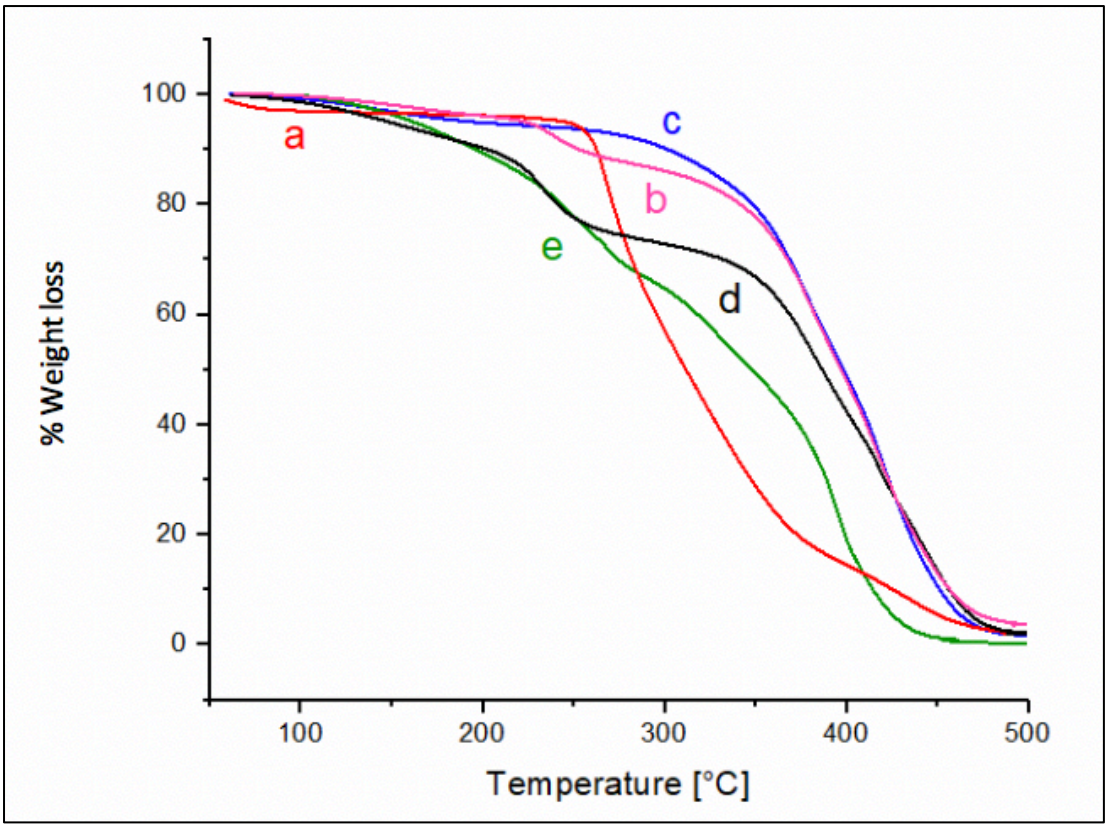

Figure 2.34. TGA curves of PVA (a) and full-IPN PVA/PAA (b), PVA/GA (d) full-IPN PVA/P(HBA-co-AA)1 (c), and full-IPN PVA/PHBA (e) hydrogels.

The effect of amounts of HBA, or more specifically the HBA-to-AA ratio, on the thermal properties of full-IPN PVA/P(HBA-co-AA) was investigated by TGA. As shown in Figure 2.35, no significant difference in thermal stability was observed. However, although both hydrogels exhibit similar thermal stability at lower temperatures, somewhat better thermal stability through the later decomposition stages at higher temperatures was observed for the hydrogel incorporating the higher amount of HBA.

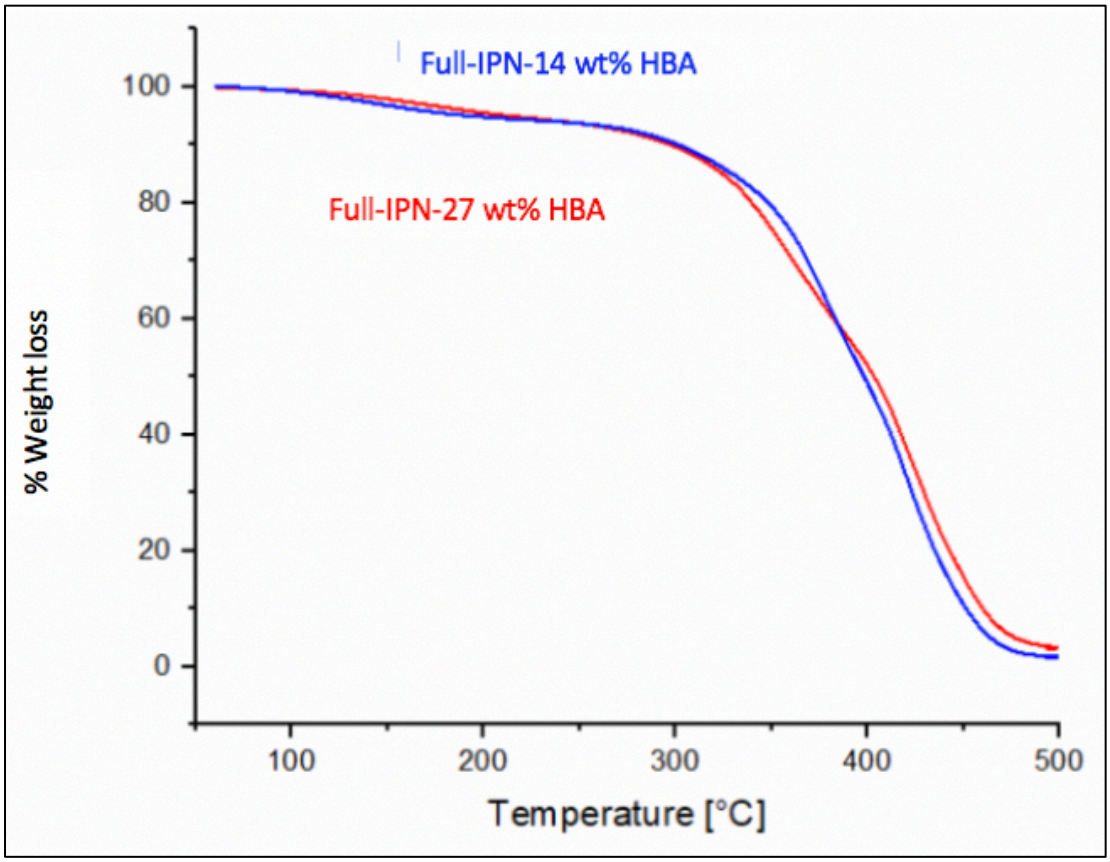

Figure 2.35. TGA curves of full-IPN PVA/P(HBA-co-AA) hydrogels as a function of HBA content: 14 wt% (blue), 27 wt% (red).

2.4.10.3. *Full-IPN PVA/P(MMA-co-IA) hydrogels*

Full-IPN PVA/P(MMA-co-IA) hydrogels had three decomposition phases as shown in Figure 2.36. The first decomposition was observed between 140 - 200 °C and is attributed to elimination of bound water trapped in the full-IPN gel. The second decomposition step was noted from 230 – 350 °C, with 20% weight loss, that is indicative of dehydration and decarboxylation from the pendant side chains of MMA and IA in the hydrogel[192]. The maximum weight loss occurred at 450–480 °C and is attributed to degradation of the main skeleton of the full-IPN hydrogel. The full-IPN PVA/PMMA hydrogel displayed similar thermal features to full-IPN PVA(P(MMA-co-IA). However, the thermogram of full-IPN PVA/PIA indicated two decomposition stages at 100 - 380 °C and 450 - 480 °C. The results indicate that MMA confers better thermal stability than IA in similar hydrogels. The somewhat better thermal stability of full-IPN PVA/P(MMA-co-IA) and PVA/PMMA at high temperatures compared to other hydrogels is due to several

factors, such as: crosslinking density, formation of full-IPN hydrogels, and the MMA content. The better thermal stability of PIA at higher temperatures is known[192].

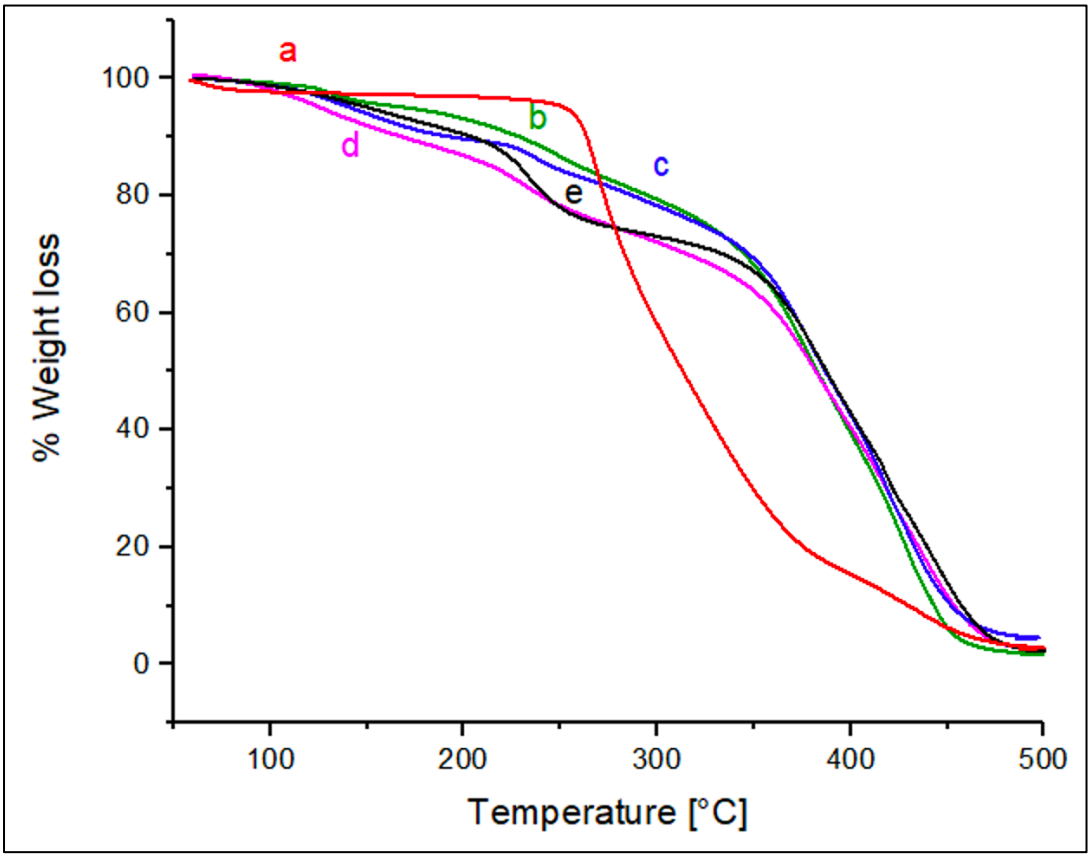

Figure 2.36. TGA curves of PVA (**a**), full-IPN PVA/PMMA (**b**), full-IPN PVA/P(MMA-co-IA)1 gel (**c**), full-IPN PVA/PIA gel (**d**), and PVA/GA gel (**e**).

The thermal stability of full-IPN PVA/P(MMA-co-IA) hydrogels with different amounts of MMA and IA was investigated and the resultant thermograms are shown in Figure 2.37. Similar weight loss profiles were noted, however, hydrogels with the lower 10 wt% amount of MMA had better thermal stability over the complete (50 - 500 °C) temperature range. This is a somewhat surprising result because earlier investigations had noted better thermal stability of PVA/PMMA compared to PVA/PIA hydrogels.

The better thermal stability of the full-IPN copolymer hydrogels at low amounts of MMA is due to the IA component containing additional carboxyl groups. This results in formation of more hydrogen bonds between OH groups of PVA and COOH groups of IA, providing additional non-covalent crosslinking and thermal stability in the full-IPN. This

result is consistent with known studies of PIA/PHEMA hydrogels that indicated improved thermal stability as the amount of IA increased from 0.2 to 0.35 mol%[138].

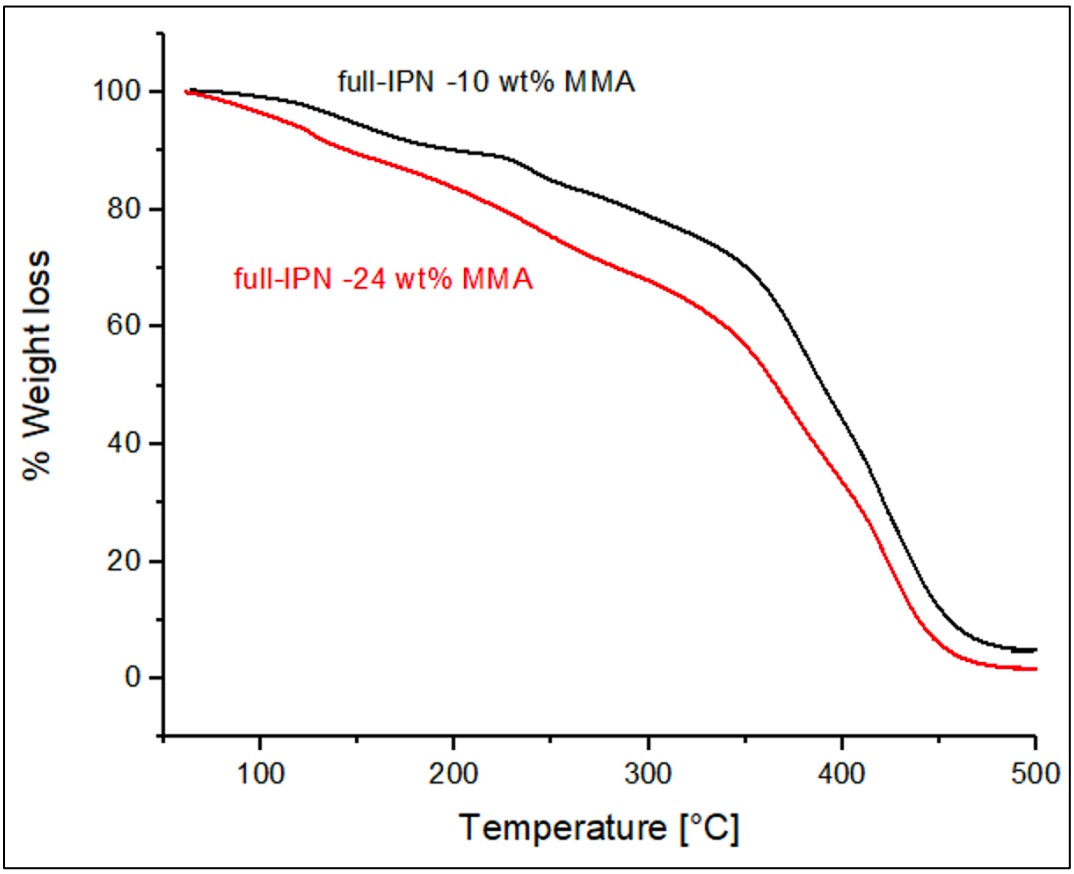

Figure 2.37. TGA curves of full-IPN PVA/P(MMA-co-IA) hydrogels as a function of MMA amount: 10 wt% (black), 24 wt% (red).

2.4.11. **Scanning electron microscopy (SEM)**

2.4.11.1. *Full-IPN PVA/PHEMA hydrogels*

Scanning electron microscopy (SEM) was used to evaluate the surface morphology and porosity of full-IPN PVA/PHEMA, PVA/P(HBA-co-AA), PVA/P(MMA-co-IA) and PVA/GA hydrogels. The SEM micrographs of the surface of swollen freeze-dried samples of PVA/GA and full-IPN PVA/PHEMA hydrogels at different magnifications are shown in Figures 2.38 (a) & (b). The pore structures of the swollen interiors of PVA/GA and full-IPN PVA/PHEMA hydrogels vary, depending on the hydrophilic nature of the monomer, the chemical composition, and the degree of crosslinking. The swollen freeze-dried sample of the full-IPN PVA/PHEMA hydrogel exhibited elliptical and mostly circular

small pores. The distribution of pore size varies from very small (2 μm) to quite large (5 μm) because of the inhomogeneous progress of the phase change reaction from liquid to gel state during polymerisation (Figure 2.41 (b)). In addition, the surface of the full-IPN gel was smooth and compact with thinner pore walls. However, crosslinked PVA/GA under the same condition exhibited larger pore size and much thicker pore walls (7 μm), and the pore distribution was more homogeneous (Figure 2.41 (a)). The pore size in both gels is controlled by the different extent of crosslinking within the polymer networks. In these hydrogels, PVA/GA and full-IPN PVA/PHEMA contain one and two, respectively, crosslinked networks. SEM was also used to examine the surface morphology of dried PVA/GA and full-IPN PVA/PHEMA hydrogels. No porous structures are observed on the surface of either hydrogel as shown in Figure 2.40. The surface of PVA/GA hydrogel shows large wrinkles and some cracks, consistent with the partial collapse of the crosslinked PVA network during the drying process[124].

2.4.11.2. *Full-IPN PVA/P(HBA-co-AA) hydrogels*

As shown in Figures (2.39 (c)), the micrograph of the surface of freeze-dried full-IPN PVA/(P(HBA-co-AA) gel revealed a smooth and homogeneous structure. Moreover, the analysis of the surface displayed a porous structure with different distributions and variety of pore sizes ranging from a small number of big channels to a large number of smaller pores. However, the surface pore distribution (Figure 2.42 (c)) involved smaller pores with thick walls.

Different porous structures, however, were observed in the full-IPN hydrogel, which indicates more components are joined to form this network. Other possible causes to take into consideration include crosslinking density and the hydrophilic properties of hydrogels.

The results from the SEM investigation support the results from the water uptake study that hydrophilic components, such as PVA, have the greatest effect on water uptake and result in more pores throughout the hydrogel. For this reason, PVA/GA exhibited better water uptake and more pore capacity compared to the series of full-IPN hydrogels.

2.4.11.3. *Full-IPN PVA/P(MMA-co-IA) hydrogels*

SEM micrographs of the swollen freeze dried and dried samples of full-IPN PVA/ P(MMA-co-IA) hydrogels are shown in Figure 2.39 (d). The surface of the freeze-dried hydrogel was revealed as rough and heterogenous with evidence of layers and low porosity, although with range of pore sizes. However, no porous structure was observed on the surface of the dried hydrogel.

The SEM investigation reveals that several factors can affect the morphological features of hydrogels, including crosslinking density in the polymer network, choice of monomers and composition of hydrogels, and the presence of hydrophobic aggregates on the surface or inside the matrix as result of residual unreacted monomers. However, these factors alone might not be responsible for the observed morphological features that might be affected by the drying process used to prepare samples for SEM. The freeze drying process is known to induce a honeycomb structure in hydrogels[146].

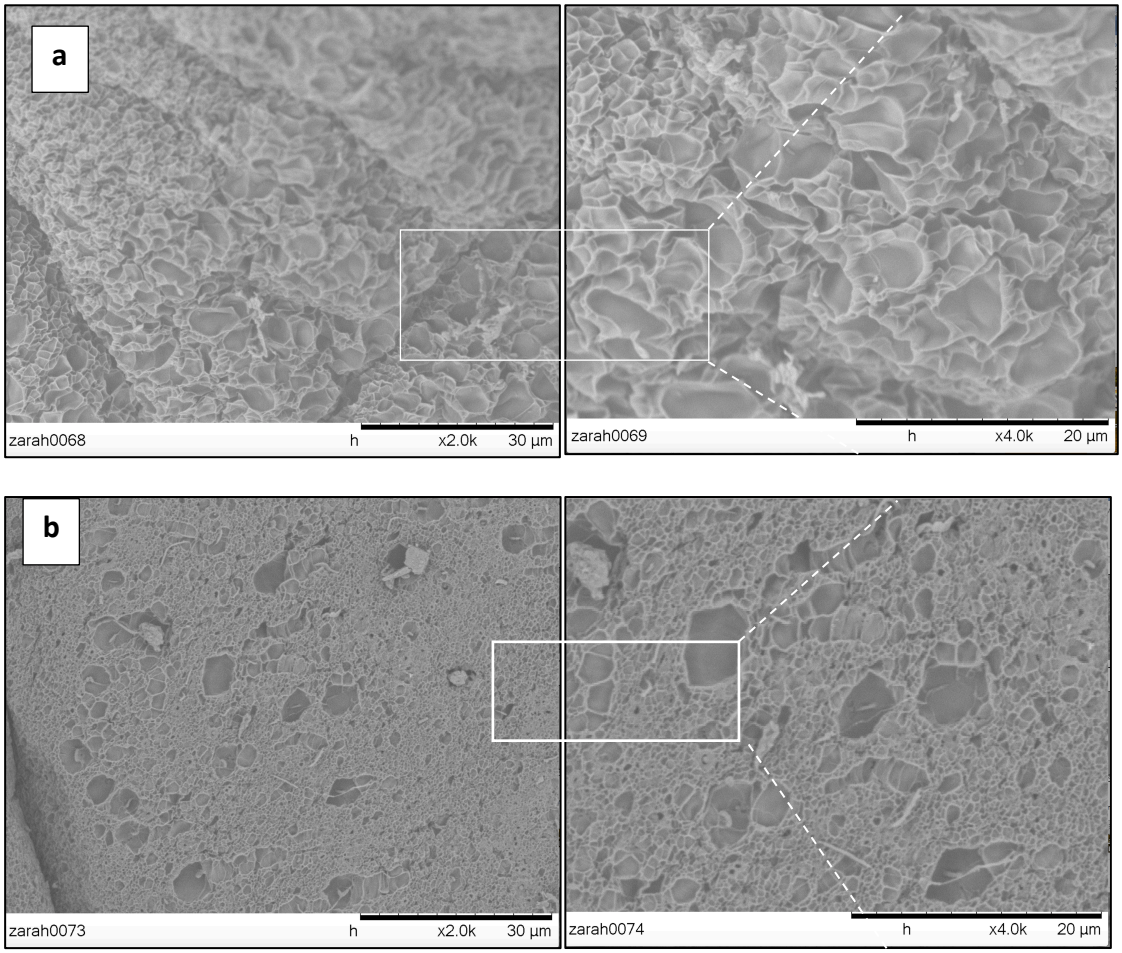

Figure 2.38. SEM images of the surface of swollen freeze-dried samples of PVA/GA (a) and full-IPN PVA/PHEMA1 (b) hydrogels.

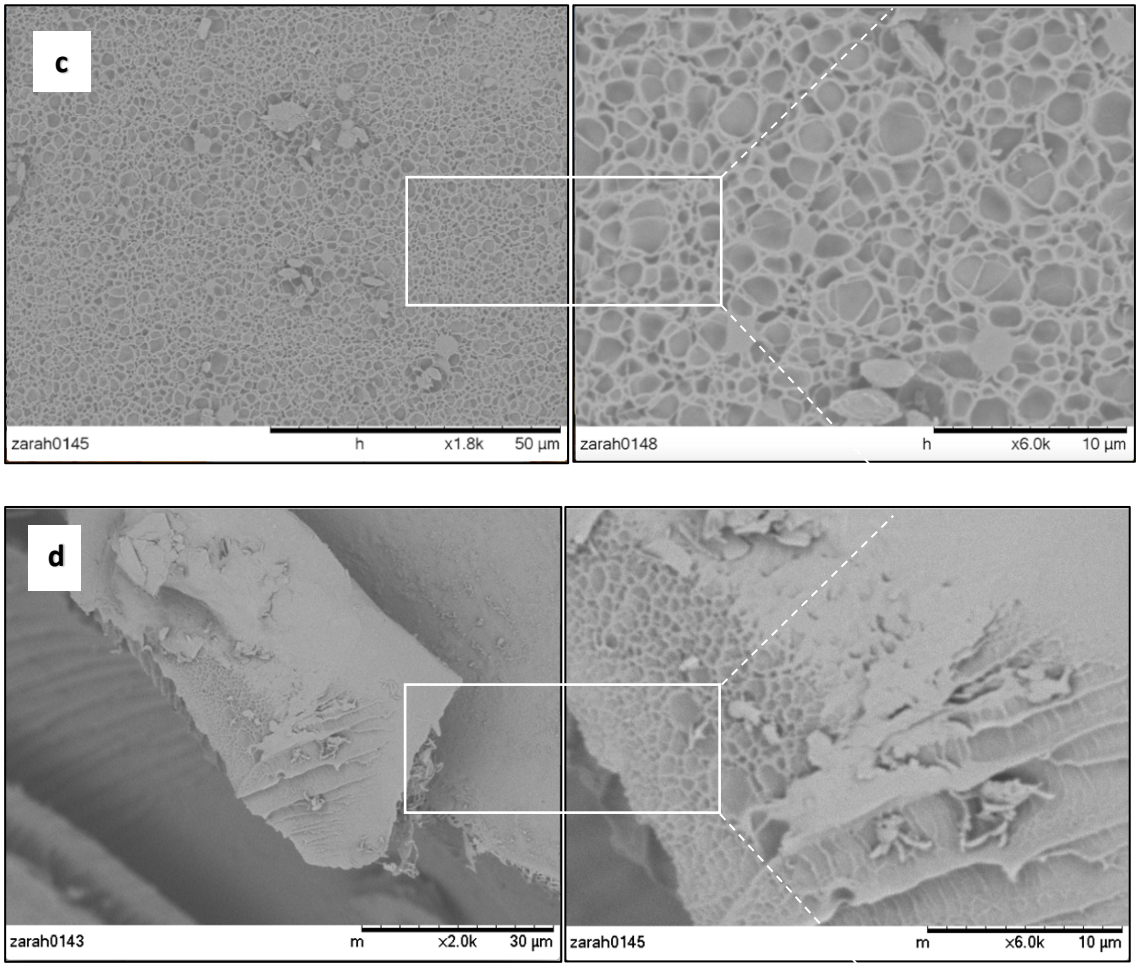

Figure 2.39. A swollen freeze-dried sample (surface) of the full-IPN PVA/P(HBA-co-AA)1 hydrogel (c), PVA/P(MMA-co-IA)1 (d) hydrogels.

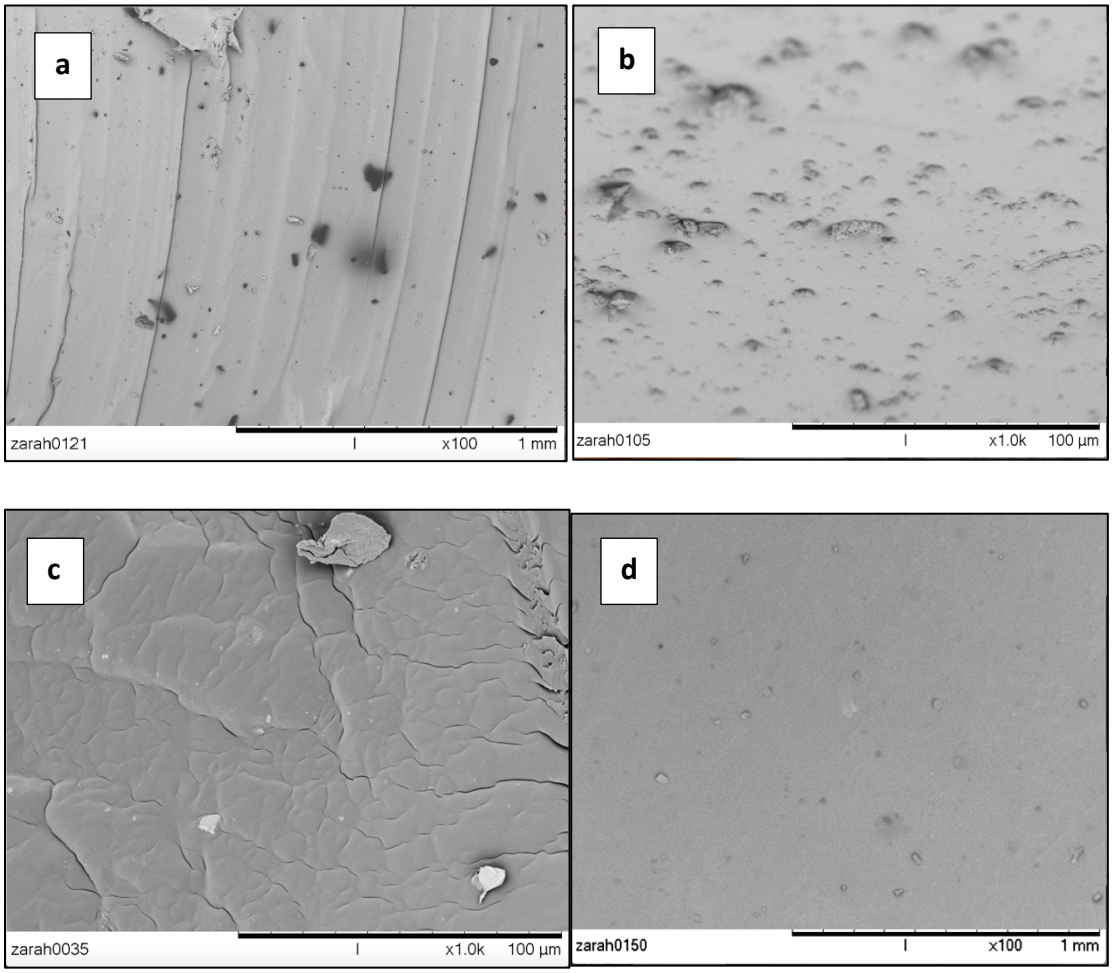

Figure 2.40. SEM images of dried samples of PVA/GA (a), full-IPN PVA/PHEMA1 (b), PVA/P(HBA-co-AA)1 (c), and PVA/P(MMA-co-IA)1(d) hydrogels.

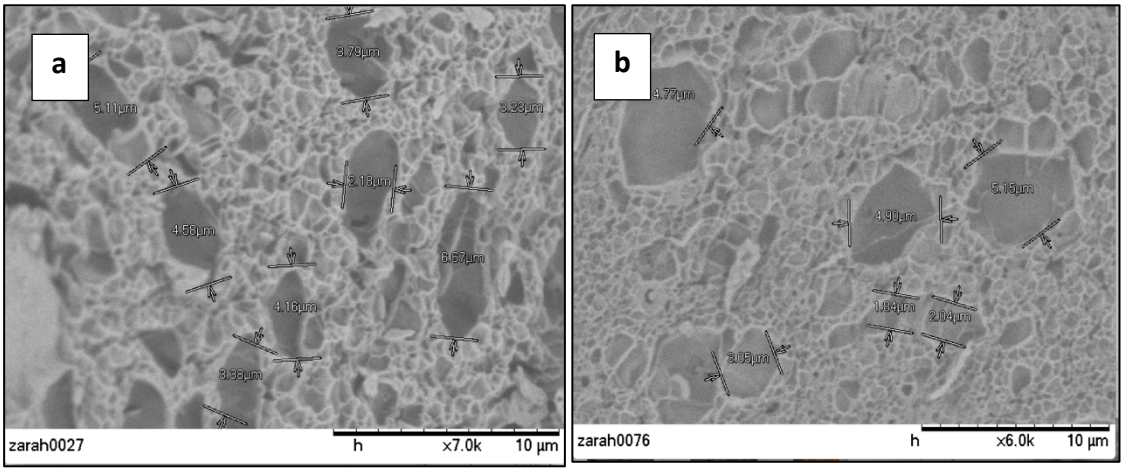

Figure 2.41. SEM images of pore distribution on surfaces of PVA/GA (a) and full-IPN PVA/PHEMA1 (b) hydrogels.

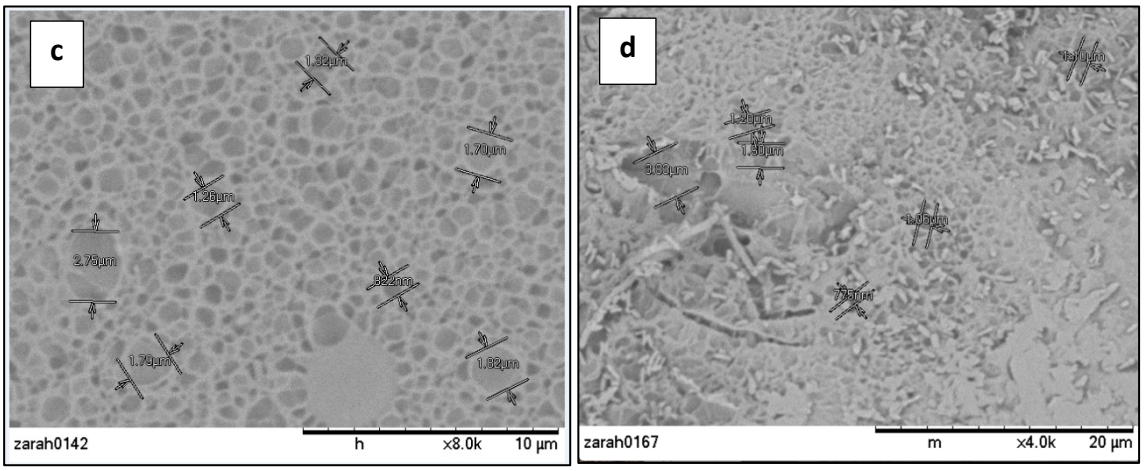

Figure 2.42. SEM images of pore distribution on surfaces of full-IPN PVA/P(HBA-co-AA) 1(c) and PVA/P(MMA-co-IA)1 (d) hydrogels.

2.5. Conclusion

Full-interpenetrating polymer network (full-IPN) hydrogels based on poly(vinyl alcohol) (PVA) cross-linked with glutaraldehyde (GA) as the hydrophilic polymer component with a series of hydrophobic polymers using different monomers, including 2-hydroxyethyl methacrylate (HEMA), acrylic acid (AA), itaconic acid (IA) as a hydrophilic monomer, 4-hydroxybutyl acrylate (HBA) and methyl methacrylate (MMA) as hydrophobic monomers, were prepared and investigated. A free radical polymerization reaction in the presence of ethylene glycol dimethacrylate (EGDMA) as crosslinker and azobisisobutyronitrile (AIBN) as initiator was used to prepare the hydrophobic polymers.

The series of full-IPN hydrogels containing different hydrophobic polymers were characterised by infrared spectroscopy and ToF-SIMS to indicate the composition of the hydrogels after preparation. Evidence of the successful preparation of the IPN was indicated by characteristic signals of the various polymer groups. Water absorption and retention capacity were determined, and pH-sensitivity studies of equilibrium swelling were performed in buffer solutions of pH 3.4, 6.2, 7.2 and 8.2 at 37 ^{o}C.

A series of full-IPN PVA/PHEMA hydrogels were prepared with 10, 20, 30, and 40 wt% GA as a crosslinking agent for the PVA network. Investigations revealed that the hydrogel with 10 wt% GA had significantly better water uptake and retention, and equilibrium swelling at pH 7.2.

The full-IPN PVA/P(HBA-co-AA) hydrogels were prepared with different wt% ratios of HBA-to-AA (14:20, 20:14 & 27:7) to investigate the effect of changed chemical character of the hydrophobic polymer on hydrogel properties. Increased amounts of HBA resulted in reduced water uptake and retention. The hydrogel with 14 wt% HBA and 20 wt% AA displayed significantly better equilibrium swelling at pH 7.2.

Similar studies were conducted using full-IPN PVA/P(MMA-co-IA) hydrogels prepared with 10:24, 17:17 and 24:10 wt% ratios of MMA-to-IA. The itaconic acid component had a significantly beneficial effect on hydrogel properties. The hydrogel with 24 wt% IA had markedly better water uptake and equilibrium swelling at pH 7. However, the best water retention was noted for the hydrogel containing the highest amount of MMA. The movement and loss of water from the IPN is likely inhibited because of the high hydrophobic content of pendant groups of MMA.

Overall, the full-IPN PVA/PHEMA hydrogel with 10 wt% GA showed better water absorption capacity compared to other hydrogels. Whereas, full-IPN PVA/P(MMA-co-IA) with 24 wt% MMA and 10 wt% IA offered the best performance in terms of water retention. The equilibrium degree of swelling of full-IPN PVA/PHEMA decreased with pH; maximum q_e was at pH 3.4 with a local maximum at pH 7.2. Whereas, full-IPN PVA/P(HBA-co-AA) and PVA/P(MMA-co-IA) containing acidic functional groups showed increased q_e as the pH was raised, reaching a maximum at pH 7.2. The pH response is affected by composition of the hydrogel network, the pH of the medium, and the pk_a of ionizable groups of PAA and PIA. A summary of the gel content, water absorption, water retention and equilibrium swelling properties of the hydrogels is presented in Table 2.7.

Table 2.7. Gel content (Gel%), water absorption (WU%), water retention (WR%), and equilibrium swelling (qe) of full-IPN hydrogels. (Refer to Table 2.1 for composition of the hydrogels)

Hydrogel	**Gel%**	**WU%**	**WR%**	***q_e (pH)***			
				3.4	**6.2**	**7.2**	**8.2**
Series 1							
PVA/PHEMA1	45	464	18	416	336	335	155
PVA/PHEMA2	69	237	23	256	180	188	118
PVA/PHEMA3	92	147	36	129	101	103	75
PVA/PHEMA4[1]	98						
PVA/GA	97	180	38	200	184	185	130
PHEMA	96	44	74	36	38	38	39
Series 2							
PVA/(HBA-co-AA)1	96	104	44	97	356	390	276
PVA/(HBA-co-AA)2	97	87	51	91	242	265	256
PVA/(HBA-co-AA)3	98	91	44	91	188	194	149
PVA/PAA	98	134	52	120	219	231	189
PVA/PHBA	92	136	52	107	74	61	54
Series 3							
PVA/P(MMA-co-IA)1	94	129	52	108	148	174	128
PVA/P(MMA-co-IA)2	96	106	54	87	83	130	109
PVA/P(MMA-co-IA)3	98	77	73	67	75	80	80
PVA/PMMA	98	60	52	115	81	82	73
PVA/PIA	97	97	47	94	125	170	109

Note [1]: WU%, WR%, and q_e results for PVA/PHEMA4 with 40 wt% GA.

Thermal stability of the resulting hydrogels was investigated over temperatures from 50 to 500 ^{o}C with the best thermal stability noted for full-IPN PVA/P(HBA-co-AA). Formation of intermolecular hydrogen bonds between COOH groups of PAA and OH groups of PVA are responsible for the improved thermal stability of full-IPN PVA/PAA and full-IPN PVA/P(HBA-co-AA) hydrogels.

The surface morphology and pore size of the hydrogels were investigated by SEM. The PVA/GA gel indicated a highly porous structure with a homogeneous surface, whereas a less porous structure was observed for the full-IPN PVA/P(MMA-co-IA) gel. The difference in distribution of pore size in PVA/GA and full-IPN hydrogels is determined by the amount of cross-linking, the composition of the network, and the chemical nature of the hydrophilic monomer.

The results from this investigation indicate that full-IPN PVA/PHEMA gel with low GA ratio is a good candidate as a hydrogel that displays good hydrogel properties and stability for applications of solute delivery and recovery.

Chapter 3: Extraction of Cu (II) using novel full-IPN hydrogels and Acorga P50 as carrier.

3.1. Introduction

Water that is contaminated with heavy metal ions has become a worldwide environmental problem that, even at low concentrations, has a significant effect on humans and the environment[121]. Among these heavy metal ions, copper is a common toxic contaminant in wastewater that can cause gastrointestinal disturbances in animals even from a short time exposure to a high level of copper[193]. A guideline limit of 1.3 mg/L for copper in drinking water has been set by the US Environmental Protection Agency (EPA)[194].

The release of copper ions into the environment takes place through various routes, including landfills, fossil fuel combustion, phosphate fertilizer production, wood production, copper industries (factories and mining), and natural sources[195]. To remove copper and other heavy metal ions from water, numerous approaches have been developed, such as membrane filtration, chemical precipitation, ion exchange, adsorption, and reverse osmosis, etc[21, 121, 193, 196].

The use of adsorption methods has gained considerable attention because of low cost, wide availability, high sorption capacity, and ease of handling [193, 197]. However, the lack of efficient adsorbents is a disadvantage that limits their use for the removal of Cu (II) from water[121]. In the recent decade, hydrogels with a three dimensional cross-linked network have been used as adsorbents, for the removal of Cu (II) ions, due to their ability to control the diffusion process, respond to external stimulus such as pH, ionic strength, high selectivity, high efficiency, and ease of operation[198]. The adsorption of heavy metals ions occurs by chemical interactions with polar functional groups of the hydrogel, such as $-NH_2$, -OH, and -COOH. For instance, the adsorption abilities of hydrogel adsorbents has been directly related to the extent of hydroxyl groups (-OH) in the material[121, 193].

Composite hydrogel beads were prepared from polyvinyl alcohol (PVA), chitosan (CS), and graphene oxide (GO) (PVA/CS/GO) by an instantaneous gelation approach. Different factors, including temperature, pH, adsorption and initial time, had an effect on Cu (II) adsorption. Pseudo-second-order reaction kinetics and Freundlich isotherms were

used to evaluate the adsorption process. The maximum adsorption ability of composite (PVA/CS/GO) (162 mg/g) was higher compared to binary (PVA/CS) hydrogels. Thermodynamic studies indicated that adsorption was an endothermic and spontaneous process[121]. Efficient removal of Cu (II) was characterised by using chitosan/PVA beads functionalized with poly(ethylene glycol). A maximum effective adsorption of 99.99 % was observed for an initial Cu (II) concentration of 25 mg/L at 45 °C and pH 5[199].

Other studies on Cu (II) adsorption have indicated maximum adsorption capacities of 0.64 mmol/g[200] and 0.36 mmol/g[201] for hydrogels prepared from poly(acrylic acid-co-methacrylamide) poly(AA-co-MA), and polyvinyl pyrrolidone (PVP) and acrylic acid (AA) (PVP/PAA), respectively.

A novel series of semi-IPN hydrogels composed of PVA, AA, and tourmaline (a boron silicate mineral) were tested as adsorbents for Cu (II) and Pb (II) and achieved maximum capacities of 2.98 mmol/g and 3.12 mmol/g, respectively[197]. Interpenetrating polymer network (IPN) hydrogels composed of carboxymethyl cellulose and poly(acrylic acid) have indicated a maximum adsorption capability of 250 mg/g^{-1} for Cu (II)[202].

Attempts to increase the hydrophilicity of the hydrogels resulted in a polymer matrix with low mechanical strength, which is not a desirable feature if adsorbents are to be reused for real-world applications for removal of Cu (II). Poor mechanical properties are the result of a highly swollen network. Hence, attention was paid to designing a robust hydrogel by copolymerisation of oligo(ethylene glycol) methacrylate and 2-vinyl-4,6-diamino-1,3,5-triazine that was cross-linked with N,N'-methylenebisacrylamide. Although, the materials demonstrated good mechanical stability, a reduced adsorption capacity of 1.1 mmol/g for Cu (II) was noted[203].

The technique of molecular imprinting (MI) has attracted interest in several fields due to the ease of preparation, low cost, high selectivity, and stability[204]. Wullff and Sarhan were the first to reveal the use of MI into organic polymers. The preparation of polymeric materials with molecular recognition elements have been investigated for potential applications involving sensing, catalysts and separating agents[112]. The process to prepare a MI polymer involves using a template during polymerization. The subsequent removal of the template from the polymer material results in cavities or molecular channels with a high selectivity for the desired analyte[205-206]. An ion-imprinted polymer

(IIP) is a specific type of molecularly imprinted membrane, having the same way of preparation. The difference between them is the use of 'ions'[190].

The use of molecular imprinting (MI) within an IPN could be a useful method to prepare a novel generation of adsorbent hydrogels with enhanced properties, including good mechanical strength and specific metal ion adsorption capacity. Some preliminary investigations have been reported. An IPN hydrogel imprinted with Cu (II) ions was prepared from acrylamide (AAm) and triethylene glycol divinyl ether (DVE-3) in the presence of ethylene glycol dimethacrylate (EGDMA) as a crosslinker were by UV-initiated simultaneous free radical/cationic hybrid polymerisation. A decreased adsorption capacity of the imprinted hydrogel was noted with a temperature increase from 303 K to 323 K, whereas improved adsorption occurred as the pH was increased from pH 2.5 to 5. Thermogravimetric analysis showed high thermal stability of the hydrogels and further analysis of thermodynamic parameters, such as the entropy (S), enthalpy (H) and Gibbs free energy (G), indicated that adsorption of Cu (II) was an exothermic and spontaneous process. A surface morphology study by SEM revealed significant changes to the hydrogel structure, involving a rougher surface with smaller pores, caused by copper adsorption[207].

Novel Cu (II)-imprinted microgels, composed of attapulgite (a clay material of magnesium aluminium phyllosilicate) as the support material, methacrylic acid (MAA) as the functional monomer, and EGDMA as a crosslinker have demonstrated a high affinity for Cu (II) over Mg (II) and Ca (II). The adsorption data were matched by a Freundlich isotherm model. At a pH above 4.5, the microgels were randomly spread throughout the buffer solution, however, an increase in pH resulted in larger particles. Whereas, at a pH below 4.5, the microgels were not well dispersed in the medium. The reusability of the microgels were assessed based on 5 adsorption cycles with about 15% regeneration loss[208].

The main disadvantage associated with the ion-imprinted polymer method is the incomplete removal of ions from the template, leading to reduced vacant cavities within the membrane[205]. Thus, the use of extractants in crosslinked PVA and full-IPN hydrogels could be a beneficial way to remove Cu (II) from aqueous solutions that needs subsequent investigation.

A metal ion extractant, commonly referred to as a carrier, are common reagents of an acidic or chelating chemical nature used for copper extraction[209] .The hydroxyoxime

reagents are widely used copper carriers that are classified as aldoxime or ketoxime depending on the side-chain attached, a hydrogen or short chain alkyl group, respectively, to the oxime group. The carriers have a hydrophobic chemical nature because of an attached long-chain alkyl group[210]. The chemical structure of hydroxyoxime reagents is shown in Figure 3.1.

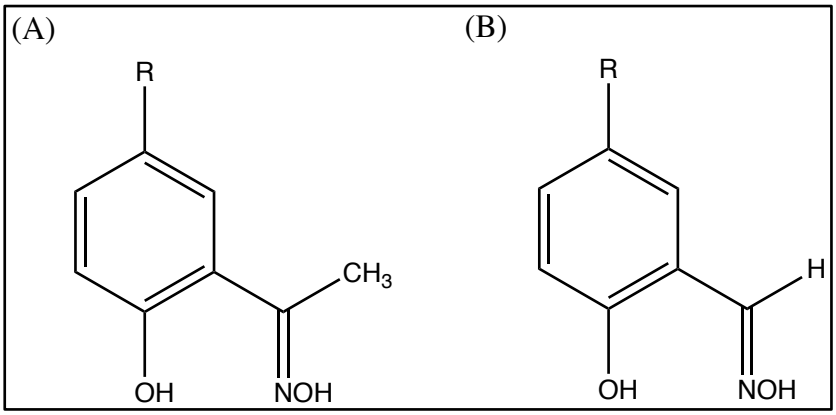

Figure 3.1. Chemical structures of ketoximes (A) and aldoximes (B) where R is typically C_9H_{19} or $C_{12}H_{25}$.

To improve the extraction performance for Cu (II), the 5-nonylsalicylaldoxime (Acorga P50) and Cu (II)-Acorga P50 complex were inserted as carriers into the crosslinked PVA and full-IPN hydrogels.

The aim of this current investigation is to prepare a series of novel full-IPN hydrogels and investigate the extraction performance for Cu (II). The hydrogels are based on PVA as a base hydrophilic polymer and the IPN contains hydrophobic, and hydrophilic monomers prepared from functional monomers, including 2-hydroxyethyl methacrylate (HEMA), 4-hydroxybutyl acrylate (HBA), Acrylic acid (AA), methyl methacrylate (MMA), and itaconic acid (IA). Either Acorga P50 or Cu (II)-Acorga P50 complex as carrier or Cu-carrier molecular imprinted templates, respectively, will be included during free radical polymerization to prepare the full-IPN. The chemical structure, microstructure, and the thermal stability (weight loss) of the resulting hydrogels will be characterised by FTIR, SEM, and TGA, respectively. Similar extraction and back-extraction conditions to those commonly used for Cu will be used, namely a feed solution at pH 2, and a 2 M H_2SO_4 stripping solution. The effect of the type of carrier template on extraction of Cu (II) ions

will be carried out in 50 mg/L pH 2. Batch extraction experiments of Cu (II) will be investigated by studying the effect of Cu (II) concentration and pH of the feed solution on extraction performance. The extraction data will also be assessed to compare the performance of hydrogels prepared with the different carrier molecular templates. The results from this study are expected to provide more information on novel polymeric adsorbents for Cu (II) extraction to benefit metal recovery and environmental remediation applications.

3.2. Experimental

3.2.1. Materials

Poly(vinyl alcohol) (PVA) (89,000 98,000, 99+% hydrolysed) (Aldrich), and ethylene glycol dimethyacrylate (EGDMA) (Aldrich) glutaraldehyde (GA) (Aldrich), itaconic acid (IA) (Aldrich), methyl methacrylate (MMA) (Aldrich), 2-hydroxyethyl methacrylate (HEMA) (Aldrich), 4-hydroxybutyl acrylate (HBA) (Aldrich), and acrylic acid (AA) (Aldrich) were used as reactants to prepare the hydrogels. MMA was purified by washing with 0.5 % NaOH. HEMA, HBA, AA were purified by passing through an activated alumina column chromatography and verified by ^{1}H-NMR. PVA, IA, EGDMA and GA were used as received. 2, 2'-Azobisisobutyronitrile (AIBN) initiator was purified by recrystallization from ethanol[156]. Dimethylsulfoxide (DMSO) was used as a solvent for polymerisation. Sulfuric acid (H_2SO_4) was used as catalyst. Acorga P50 (salicylaldoxime) was used as an extractant.

Copper standard for AAS (1,000 mg/L in 2% nitric acid) supplied by Sigma-Aldrich. Copper sulphate pentahydrate ($CuSO_4.5H_2O$) (Merck) was used to prepare copper solutions of different concentrations, including 25, 50, and 100 mg/L, adjusted to pH 2 with H_2SO_4. All solutions were prepared using deionized water.

3.2.2. Preparation of a Cu (II)-Acorga P50 complex

280 mL of Acorga P50 was placed in a beaker containing 40 mL of hexane. 100 mL of 500 mg/L of Cu^{2+} solution pH 2 was added to the beaker (this step is called liquid–liquid extraction preparation). The solution was stirred for 15 minutes, until an organic layer appeared. The organic layer (brown layer) was separated and washed three times with deionised water. The brown phase was dried using $MgSO_4$, then left to dry at room temperature to evaporate excess hexane. Preparation of Cu (II)-Acorga P50 complex is indicated in Scheme 3.1.

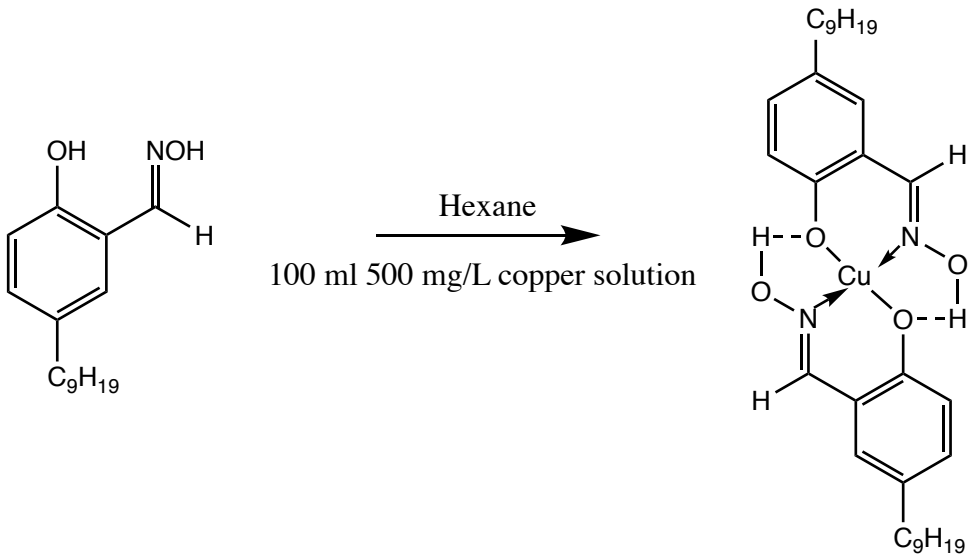

Scheme 3.1. Preparation of Cu (II)-Acorga P50 complex carrier.

3.2.3. **Preparation of Cu (II)-Acorga P50-complex-imprinted-full-IPN hydrogels, and Acorga P50-imprinted-full-IPN hydrogels.**

A different series of full-IPN hydrogels with Acorga P50 and Cu (II)-Acorga P50 complex as carriers were prepared and present as full-IPN poly(vinyl alcohol)/2-hydroxyethyl methacrylate PVA/HEMA, full-IPN poly(vinyl alcohol) /poly(4-hydroxy butyl acrylate-co-acrylic acid) PVA/P(HBA-co-AA), and full-IPN poly(vinyl alcohol/poly(methyl methacrylate-co-itaconic acid) PVA/P(MMA-co-IA). The crosslinked PVA gel containing carriers was prepared in one step, while the preparation of full-IPN hydrogels took two steps. The synthesis of the crosslinked PVA gel with carriers was done as follows: PVA was dissolved in 15 mL of DMSO in a three-neck round-bottom flask, a water condenser was attached, and the solution stirred using a magnetic stirrer bar. The solution was heated at 80 ^{o}C with continuous stirring at 800 rpm until it became transparent. The solution was cooled down to room temperature under a nitrogen gas cover to remove dissolved oxygen and was continuously stirred at slow speed. A constant amount of glutaraldehyde (GA) as the crosslinking agent and H_2SO_4 as catalyst were added to the PVA solution and stirred for 10 minutes. For full-IPN hydrogels, including Acorga P50 and Cu (II)-Acorga P50 complex, the first step was the same as the PVA gel preparation but with different amount of PVA depending on the full-IPN hydrogels' composition. In the second step, for dissolution, various amounts of monomers (HEMA, HBA, AA, MMA, and IA), fixed amount of the crosslinker of ethylene glycol dimethacrylate (EGDMA), and a small amount of

DMSO were added to the PVA solution. As an initiator, AIBN was placed in the full-IPN mixtures to start the polymerisation reaction. Acorga P50 and Cu (II)-Acorga P50 complex carriers were placed to the mixture of the PVA solution, and full-IPN solutions. The mixtures were stirred for 20 minutes under N_2 inert. The solutions were transferred to petri dishes and heated at 60 ℃ in an oven for 3 h. As the Cu (II)-Acorga P50-complex-imprinted-PVA/GA, full-IPN hydrogels were prepared, soft dark colour discs were obtained. The resulting discs were immersed in deionised water and the water was replaced each day for over one week to remove the unreacted monomers. The gel discs were dried at room temperature for one day and then in a vacuum until a constant weight was obtained. Similar non-imprinted PVA/GA and full-IPN hydrogels were prepared for comparison. The feed composition used in the synthesis of PVA/GA and full-IPN hydrogels, including Acorga P50 and Cu (II)-Acorga P50 complex for imprinted hydrogels, is presented in Table 3.1.

Table 3.1. Feed composition (wt%) used for hydrogel preparation.

Hydrogel	**PVA**	**GA**	**HEMA**	**HBA**	**AA**	**MMA**	**IA**	**EGDMA**
Acorga P50-PVA/GA	50	30	-	-	-	-	-	-
Cu (II)-Acorga P50-complex-PVA/GA	50	30	-	-	-	-	-	-
PVA/GA	60	40	-	-	-	-	-	-
Acorga P50-full-IPN PVA/PHEMA	40	30	5					5
Cu (II)-Acorga P50-complex-full-IPN PVA/PHEMA	40	30	5					5
Full-IPN PVA/PHEMA	40	30	20					10
Acorga P50-full-IPN PVA/P(HBA-co-AA)	40	20	-	5	10	-	-	5
Cu (II)-Acorga P50-complex-full-IPN PVA/P(HBA-co-AA)	40	20	-	5	10		-	5
Full-IPN PVA/P(HBA-co-AA)	40	20	-	10	20	-	-	10
Acorga P50-full-IPN PVA/P(MMA-co-IA)	40	20	-	-	-	5	10	5

Cu (II)-P50-complex-full-IPN PVA/P(MMA-co-IA)	40	20	-	-	-	5	10	5
Full-IPN PVA/P(MMA-co-IA)	40	20				10	20	10

AIBN = 0.1 g, H_2SO_4 = 0.1 mL, Acorga P50 = 20 wt %, Cu (II)-Acorga P50 complex = 20 wt%, and 20 mL DMSO.

3.2.4. **Stripping of Cu (II) from Cu (II)-Acorga P50-complex-imprinted PVA/GA, and full-IPN hydrogels.**

The Cu (II)-Acorga P50-complex-imprinted PVA/GA and full-IPN hydrogel discs were placed in a mesh to prevent physical damage and immersed in 100 mL of 2 M H_2SO_4 solution at room temperature. The solution was stirred at the optimum rate of 400 rpm for 10 days to ensure maximum release of copper. The resulting hydrogel discs were washed with deionised water. The discs were left to dry at room temperature for one day and then in a vacuum for another day. Finally, the discs were stored on filter paper in a petri dish. To monitor the release of copper, samples were collected for preparation for AAS measurements.

3.2.5. **Water uptake measurements**

The process of swelling study was explained in detail in chapter 2.

3.2.6. **Extraction and back-extraction of Cu (II)**

The extraction was carried out by immersing the hydrogel discs containing reagent or complex in a container containing 100 mL of 50 mg/L copper solution and stirred at the optimum rate of 400 rpm. The concentration of Cu (II) in the solution was monitored by removing 5 mL samples at regular time intervals and replacing each one with 5 mL of fresh 50 mg/L, pH 2. The taken amount was diluted with 2% HNO_3 for AAS analysis. The back-extraction profiles were structured by taking 5 mL of the stripping solution (100 mg/L, 2 M H_2SO_4) at regular time intervals. The samples were diluted with 2% HNO_3 for AAS measurement at 230 nm. The withdrawn sample volume was replaced with fresh 2 M H_2SO_4 to maintain a constant volume throughout the experiment. Calibration was conducted prior to each batch of analysis using Cu (II) standard solutions (2, 4, 6, 8, and 10 mg/L). All extraction and back-extraction experiments were carried out in triplicate. Hydrogel performance was evaluated by determining the extraction, back-extraction, and recovery factors as defined by the following expressions.

Extraction (percent), Ex (%) is the amount of analyte (copper) removed from the feed solution by the hydrogel according to the following equation:

$$\text{Ex (\%)} = \frac{C_{f,0} - C_{f,f}}{C_{f,0}} \text{ x } 100 \quad (1)$$

Where, $C_{f,0}$ and $C_{f,f}$ are the initial and final concentration of analyte in the feed solution.

Back-extraction (percent), BEx (%) is the amount of analyte (copper) recovered from the hydrogel by the stripping solution according to the following equation:

$$\text{BEx (\%)} = \frac{C_{s,f}}{C_{f,0} - C_{f,f}} \text{ x } 100 \quad (2)$$

Where, $C_{s,f}$ is the final concentration of analyte in the stripping solution.

Recovery Factor (percent), RF% is the amount of copper ions recovered after extraction and back-extraction experiments using the same membrane. Where, $C_{f,0}$ is the initial copper concentration in the feed solution, and $C_{s,f}$ is the final copper concentration in the stripping solution.

$$\text{RF (\%)} = \frac{C_{s,f}}{C_{f,0}} \text{ x } 100 \quad (3)$$

3.2.7. **Effect of Cu (II) concentration on extraction**

The extraction of Cu (II) at different feed concentrations (25, 50 and 100 mg/L at pH 2) was carried out by using the same process described for the extraction and back-extraction of Cu (II) in section 3.2.6.

3.2.8. **Effect of pH of feed solution on extraction of Cu (II)**

The extraction study of Cu (II) from a feed solution of 50 mg/L at pH 2 or 5 was done by the same method described for the extraction and back-extraction of Cu (II) in section 3.2.6. The pH of the feed solution was adjusted with 2 M H_2SO_4.

3.2.9. **Stability study**

To test the long-term stability of the Acorga P50-Cu (II)-Acorga P50-complex-imprinted PVA/GA, full-IPN hydrogels, the same hydrogel discs were dried and reused in

repeat experiments. The feed solution (50 mg/L, pH 2) and stripping solution (2 M H_2SO_4) were replaced with fresh solutions for each experiment.

3.2.10. **Kinetics**

The rate kinetics for the extraction of copper ions using Acorga P50 and Cu (II)-Acorga P50 -imprinted PVA/GA and full-IPN hydrogels was best determined using the equation for a first-order reaction.

$$\ln {C_{f,0}}/{C_{f,t}} = k \times t \quad (4)$$

Where $C_{f,0}$ is the initial concentration in the feed phase (mg/L), $C_{f,t}$ is the copper concentration in the feed phase at interval time, t is the extraction time (s), and *k* is the rate constant. The rate constant was calculated from the slope of linear plots (as confirmed by the correlation coefficient R^2) of ln ${C_{f,0}}/{C_{f,t}}$ versus time (s).

The permeability coefficient (*P*) was calculated using the following expression:

$$P = \frac{V}{A} \times k \quad (5)$$

Where A is the exposed area of the gel disc (m^2) and V is the volume of the feed solution (m^3).

3.3. Instrumental Analysis

3.3.1. **Infrared Spectroscopy (FTIR)**

The FTIR spectra of resulting Cu (II)- Acorga P50-complex-imprint, Acorga P50 PVA/GA, and full-IPN hydrogels were characterised by attenuated total reflectance-fourier transform infrared (ATR-FTIR) with a Zinc Selenide crystal using an Agilent Cary 600 series spectrometer. Spectra were recorded over 600 - 4000 cm^{-1} with a resolution of 4 cm^{-1}.

3.3.2. **Scanning electron microscopy (SEM)**

SEM was used to observe the specimen morphologies of prepared gels by using HITACHI TM3030 Plus SEM. The swollen hydrogels were dried using a freeze dryer (LABCONCO) at -80 ^{o}C for 24 h. The freeze–dried xerogels were loaded on the surface of an aluminium SEM specimen holder and sputter coated with gold for 2 minutes (Polaron sc7640 sputter coating) under vacuum prior to observation[7]. The magnification in this study was range of 100 to 10,000.

3.3.3. **Thermogravimetric Analysis (TGA)**

The thermal properties of Acorga P50, Cu (II)-Acorga P50-complex-imprinted PVA/GA, full-IPN PVA/PHEMA, full-IPN PVA/P(HBA-co-AA) full-IPN PVA/P(MMA-co-IA) hydrogels were investigated by TGA (TGA/DSC 1 STAR^{e} System (METTLER TOLEDO) over 50 -500 ^{o}C using nitrogen as purge gas, a heating rate of 10 ^{o}C/min and a sample mass of 8.5 mg.

3.4. Results and discussion

3.4.1. **Hydrogel preparation**

3.4.1.1. *Copper carrier complex*

In order to prepare the Cu (II)-Acorga P50 complex carrier, Cu (II) was reacted with Acorga P50 to form a complex between copper ions and the oxime and hydroxyl groups of the reagent. Thereafter, the resulting Cu (II) complex carrier was used as a template and inserted into the chemical matrix of crosslinked PVA, and free radical polymerisation of the acrylate monomers was initiated with AIBN in the presence of EGDMA as a crosslinker to prepare the full-IPNs. To prepare the hydrogels for adsorption experiments, the Cu (II) ions were released using 2 M H_2HO_4. The intention was to prepare hydrogels with Cu (II) bending sites having a particular orientation and appropriate cavities resulting from molecular imprinting. The synthetic routes for the preparation of the Cu (II)-Acorga P50 complex-imprinted PVA/GA, and full-IPN hydrogels is indicated in Scheme 3.2. The physical appearance of the hydrogel, including Cu (II)-Acorga P50 complex after preparation, washing with water, and drying, and release of Cu (II) is illustrated in Table 3.2.

Table 3.2. Images of the physical appearance of hydrogel with complex after preparation, washing with water, and drying, and after stripping of Cu (II).

After preparation	After washing with water	After drying	After stripping of Cu (II)
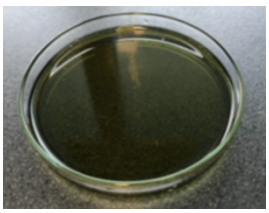	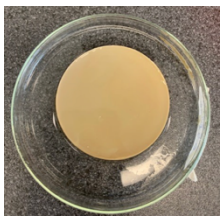		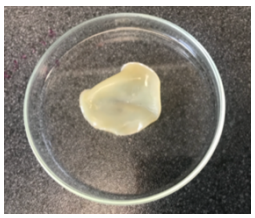

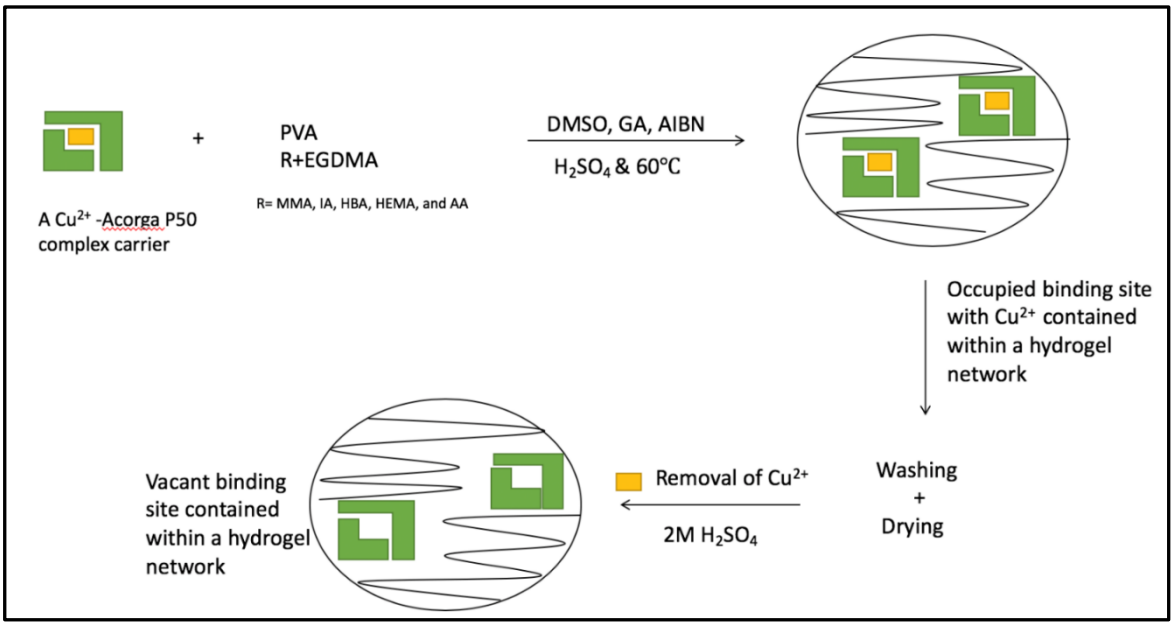

Scheme 3.2. Preparation of Cu (II)- Acorga (50)- complex-imprinted-PVA/GA, and full-IPN hydrogels.

3.5. Characterisation

3.5.1. FTIR analysis

The chemical structure of the reagent, and Cu (II)-complex-imprinted hydrogels was investigated using FTIR spectroscopy. The characteristic band at 1624 cm^{1} is attributed to the stretching vibration of C=N from the oxime group of Acorga P50 (as shown in Figure 3.2) and was used to confirm the presence of reagent in the hydrogels. Other characteristic peaks of Acorga P50 are at 2874 cm^{-1} attributed to aliphatic C-H groups, the C-O-H in-plane bend of the phenol group at 1390 cm^{-1}, and a weak peak at 1585 cm^{1} due to C=C of the aromatic group. In the case of the Cu (II)-Acorga P50 complex, the broad band located at 3381 cm^{-1} disappeared because the phenol groups are involved in copper chelation and can no longer participate in substantial hydrogen bonding. Moreover, all characteristic peaks of Acorga P50 appeared in the spectrum of Cu (II)-Acorga P50 complex, although with a slight shift in the wavenumber of bands, namely: 1610 cm^{-1} (C=N), 2872 cm^{1} (C-H), 1377–1324 cm^{-1} (C-O-H), 1580 cm^{-1} (C=C). The interpretation is consistent with previous results for similar reagents incorporated in membranes[211-213].

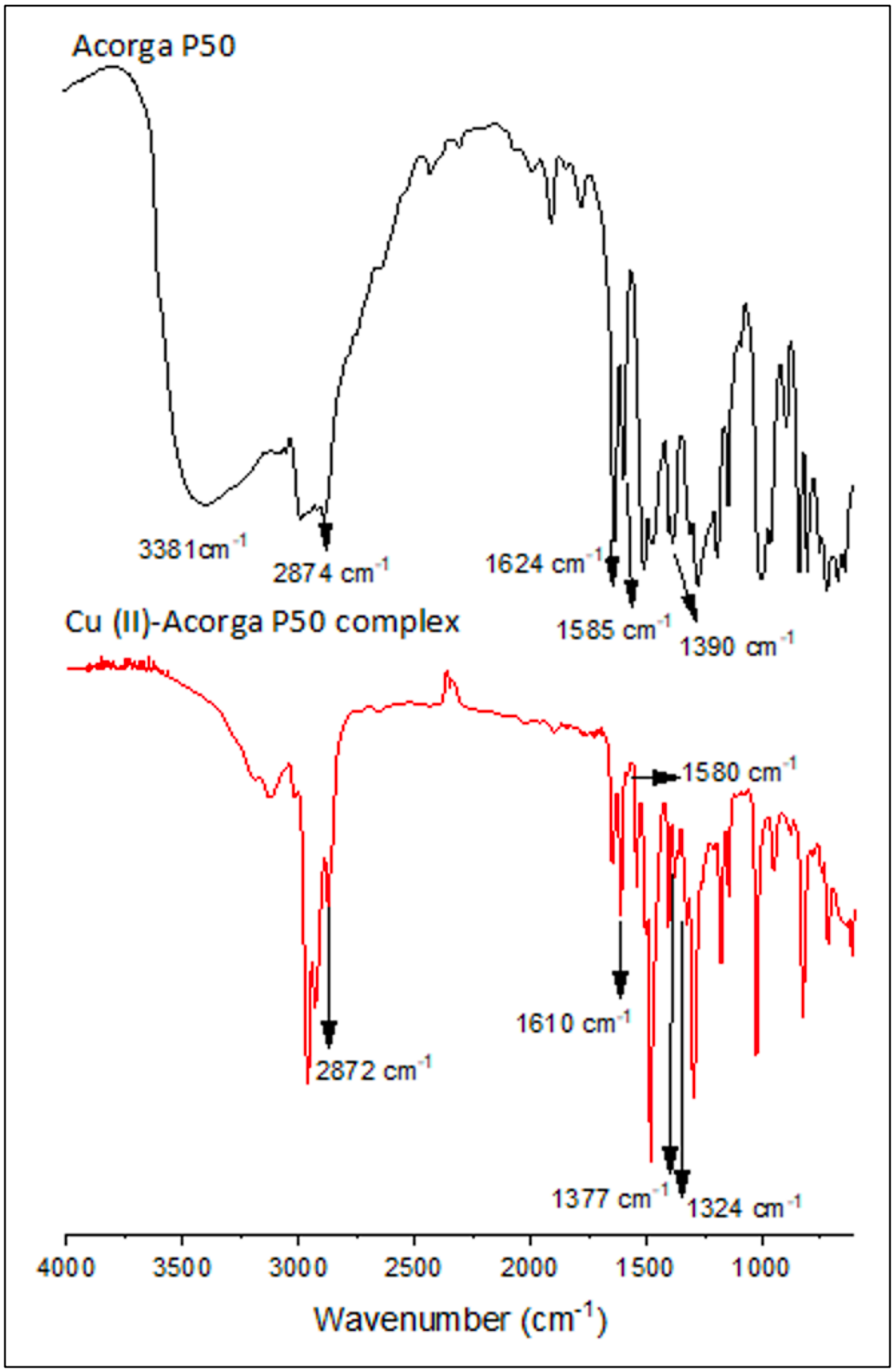

Figure 3.2. Spectra of Acorga P50 (top), and Cu (II)-Acorga P50 complex (bottom).

The spectra of the reagent and complex imprinted PVA/GA and series of full-IPN hydrogels are presented in Figures 3.3 and 3.4. The characteristic peaks of Acorga P50 are indicated in all spectra. However, there was a significant reduction in the intensity of C=O

groups of PHEMA, PAA, and PIA in the spectra of the Cu (II)-Acorga P50-complex imprinted full-IPN hydrogels, suggesting there is a strong molecular interaction between complex and hydrogels with the formation of covalent bonds. The results from FTIR analysis of PVA/GA and full-IPN gels were explained in detail in chapter 2. The FTIR spectra of all hydrogels, including reagent and complex loaded hydrogels, are included in the Appendix.

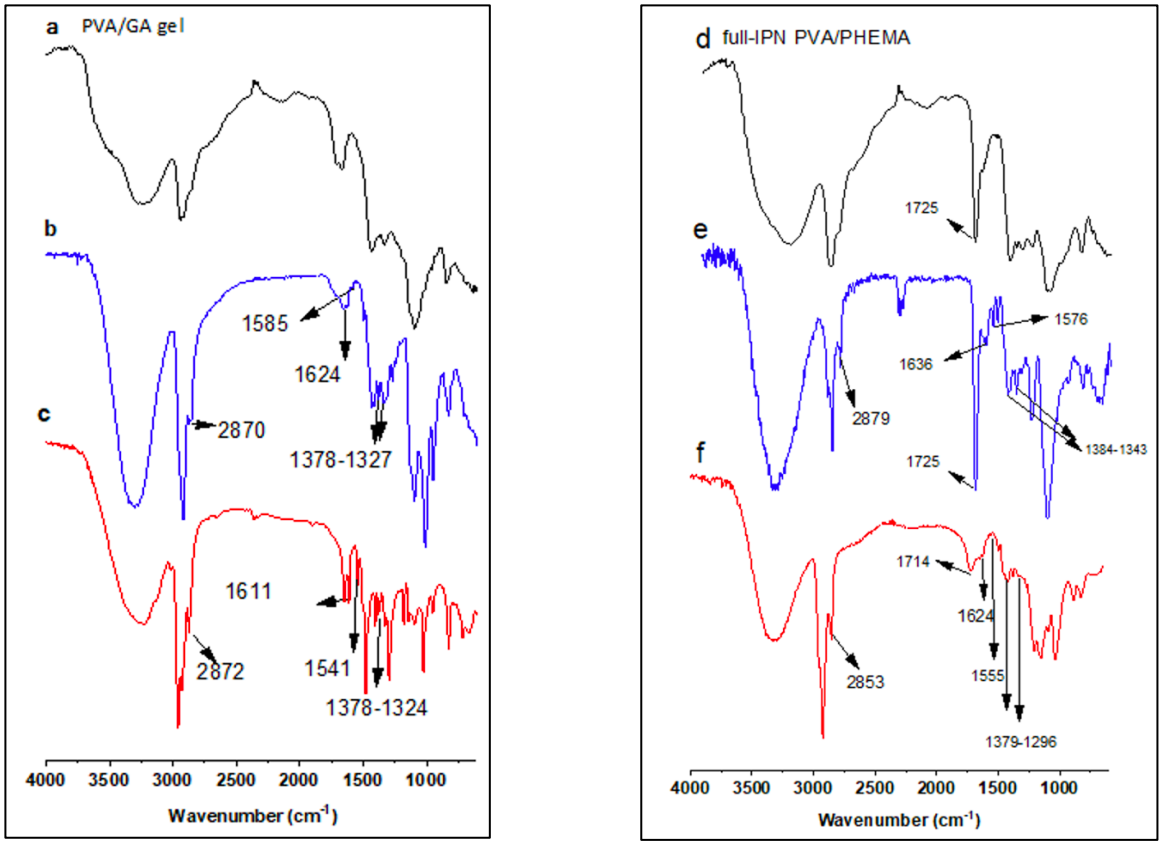

Figure 3.3. FTIR spectra of PVA/GA (a), Acorga P50 (b), and Cu (II)-Acorga P50 complex imprinted PVA/GA (c) hydrogels, full-IPN PVA/PHEMA (d), Acorga P50 (e), and Cu (II) Acorga P50-complex imprinted PVA/PHEMA (f) hydrogels.

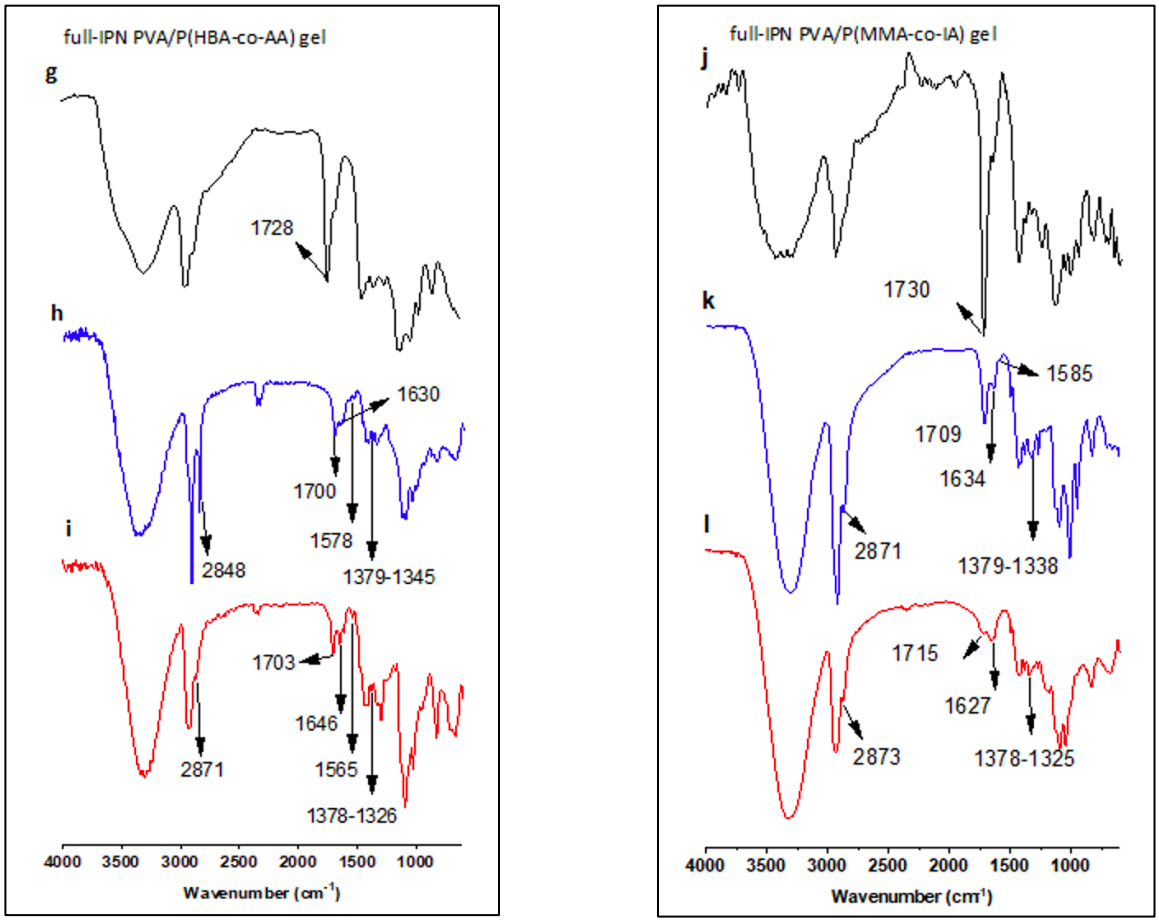

Figure 3.4. FTIR spectra of full-IPN PVA/P(HBA-co-AA) (g), Acorga P50 (h), and Cu (II)-Acorga P50-complex-imprinted-full-IPN PVA /P(HBA-co-AA) (i) hydrogels, full-IPN PVA/P(MMA-co-IA) (j), Acorga P50) (k), and Cu (II)-Acorga P50-complex-imprinted-full-IPN PVA /P(MMA-co-IA) (l) hydrogels.

3.5.2. **Water uptake measurements**

The ability of the hydrogels to absorb water is an important factor to consider when designing adsorbents to remove copper ions from aqueous solutions. The swelling induced by water uptake is proposed to facilitate copper movement and adsorption in the hydrogel. Swelling was investigated in deionised water at 37 °C and the results are shown in Figure 3.5. This temperature was chosen because the preliminary results might prove useful if the hydrogels are subsequently considered for biological applications. All samples have a similar water uptake profile and reach an equilibrium swelling degree within 6 h. The Cu (II)-Acorga P50-complex-imprinted-PVA/GA and full-IPN hydrogels after preparation indicated a higher water uptake compared to the hydrogels, including

Acorga P50. The complex imprinted-full-IPN PVA/P(MMA-co-IA) hydrogel indicated the largest uptake of water.

The swelling profiles indicate that the initial absorption of water was faster for the complex imprinted-PVA/GA and full-IPN hydrogels. Difference in the water uptake ability is attributed to the presence of hydrophilic functional groups, such as COOH groups of PIA and PAA, OH groups of PVA and PHEMA, and Cu (II) ions, which have a good affinity for water. Additionally, the presence of free aldehyde groups of GA are known to contribute to increased swelling of hydrogels in water[130]. Hydrogels imprinted with the reagent had the lowest water uptake. This is attributed to the existence of hydrophobic segments from molecular interactions of Acorga P50 units, which results in a reduced hydrophilic environment in the hydrogel network.

-

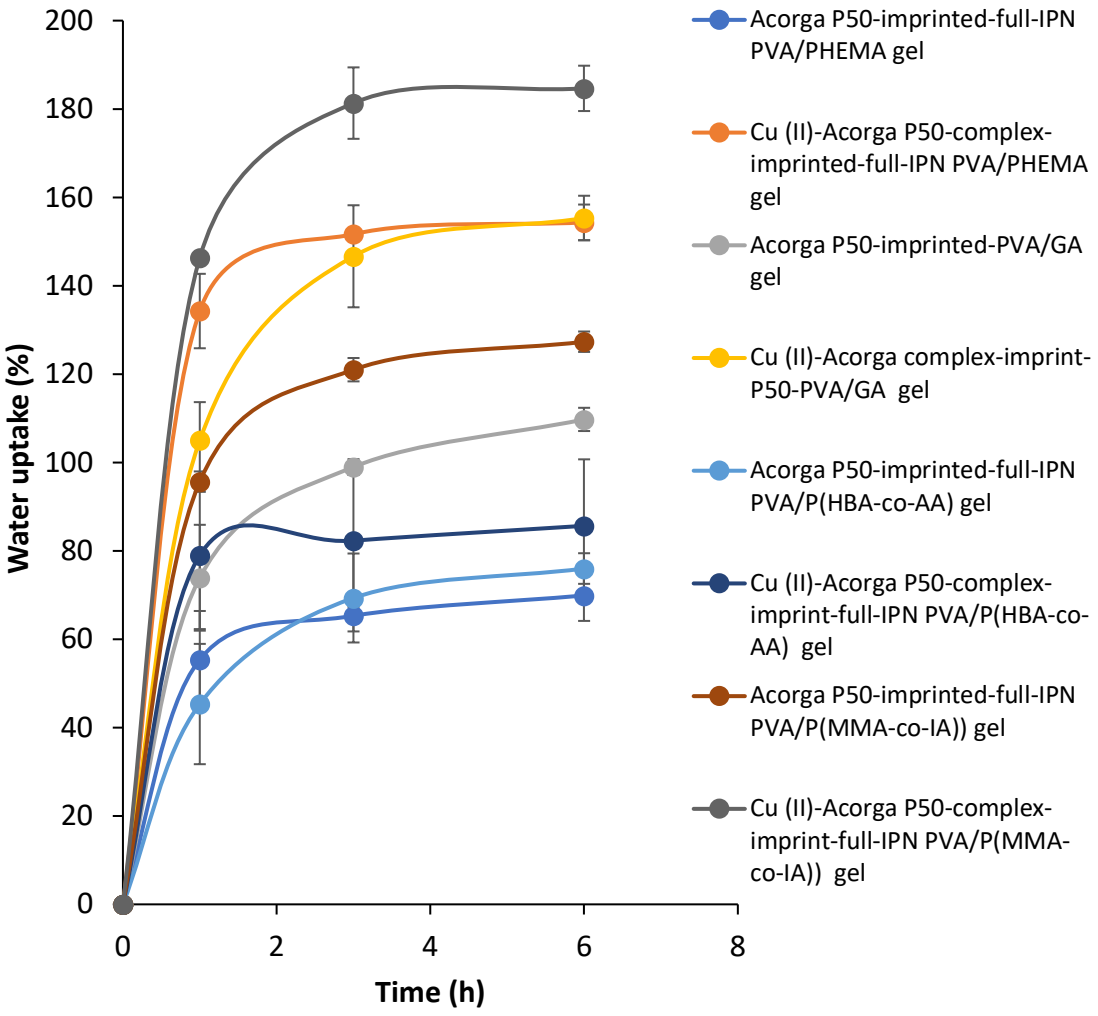

Figure 3.5. Water uptake of Acorga P50-PVA/GA, full-IPN PVA/PHEMA, PVA/P(HBA-co-AA), PVA/P(MMA-co-IA) hydrogels, and Cu (II)-Acorga P50 complex-imprinted-PVA/GA, full-IPN PVA/PHEMA, PVA/P(HBA-co-AA), and PVA/P(MMA-co-IA) hydrogels.

3.5.3. **Effect of carrier type on extraction of Cu (II)**

Extraction experiments were performed to investigate notable differences in performance of PVA/GA and full-IPN hydrogels prepared with different imprinted carrier type, either Acorga P50 reagent of Cu-Acorga P50 complex. The transient concentration profiles for the extraction and back-extraction of Cu (II) from aqueous solutions are shown in Figure 3.6. The errors bars of the extraction and back-extraction curves for the reagent imprinted PVA/GA and complex-imprinted full-IPN PVA/PHEMA hydrogels are considerably larger in comparison to the other hydrogels. This is a consequence of using the same hydrogels in three repeat cycles of extraction and back-extraction. During the first and second cycles, these particular hydrogels extract and retain a lot of copper. However, in the third cycle, significantly less copper is extracted because of retained copper. There is also some evidence of leaching of Acorga P50 from the hydrogels into the receiving solution. Consequently, both these factors reduce the amount of available carrier and contribute to the significantly reduced extraction and back-extraction performance during cycle 3.

In general, the complex imprinted-PVA/GA and full-IPN indicated a higher extraction efficiency (Table 3.3) for Cu (II) than similar hydrogels prepared with reagent. The full-IPN PVA/PHEMA complex based hydrogel indicated a similar extent but faster rate of Cu (II) extraction to that of the reagent imprinted PVA/GA hydrogel. The complex-imprinted full-IPN PVA/PHEMA, PVA/P(HBA-co-AA) and PVA/P(MMA-co-IA) hydrogels all extracted about 50 % of the available Cu (II) but took noticeably different times of 50, 120 and 150 hrs, respectively, to reach a steady-state equilibrium with the copper remaining in the feed. Almost full recovery of extracted copper was achieved during back-extraction for all hydrogels.

The reagent imprinted full-IPN PVA/PHEMA and PVA/P(HBA-co-AA) hydrogels indicated the poorest extraction of all hydrogels tested due to loss of Acorga P50 during the extraction and back-extraction processes. Presumably, the reagent could not form sufficient or strong enough molecular interactions with the hydrophobic polymer components when exposed to dynamic stirring during extraction and back-extraction.

The facilitated diffusion of Cu (II) in Acorga P50 hydrogels occurs by formation of a metal-carrier complex between Cu (II) in the feed solution and the oxime as well as phenol groups of Acorga P50 in the PVA/GA and full-IPN gels[214] (Figure 3.7).

Copper is removed from the Cu-Acorga P50 imprinted hydrogels by ion exchange with protons using 2 M H_2SO_4[211]. The conditioned hydrogels now contain imprinted vacant cavities within the IPN where copper can be extracted by rebinding to the chelation sites of the carrier that are exposed on the surface of the hydrogel (Figure 3.8). The back-extraction of Cu (II) reached equilibrium faster than the original extraction for all hydrogels. This result is related to the hydrophilic character of Cu (II) and the hydrophobic characteristics of the polymers in the hydrogels. Even though Cu (II) is chelated by Acorga P50, the reaction can be effectively reversed by a high acid concentration that regenerates the neutral form of the reagent and releases Cu (II) to its preferred aqueous environment. The difference in the extraction performance for copper ions is attributed to the size of the carrier template that creates different sized molecular imprinted cavities and the chemical nature of the components used to prepare the hydrophobic polymers within the IPN hydrogel. The insertion of Cu (II)-Acorga P50 complex as a molecular template within the IPN resulted in improved extraction performance for Cu (II) compared to similar hydrogels prepared using Acorga P50.

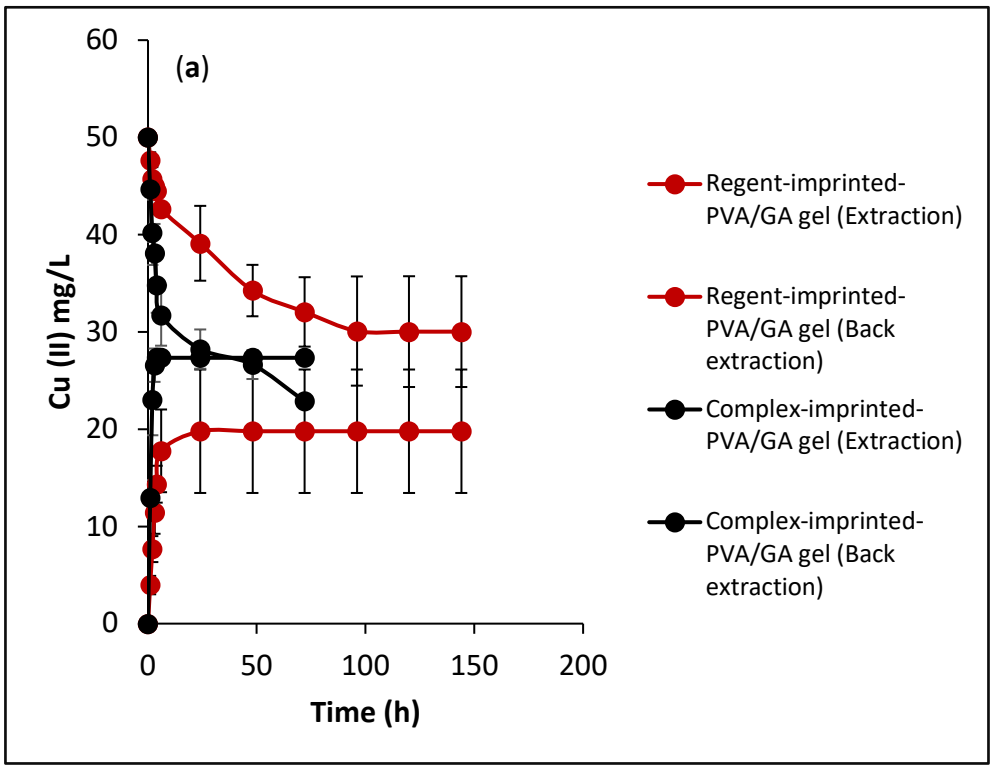
(a)
Cu (II) mg/L
Time (h)
0
10
20
30
40
50
60
0
50
100
150
200
Regent-imprinted-PVA/GA gel (Extraction)
Regent-imprinted-PVA/GA gel (Back extraction)
Complex-imprinted-PVA/GA gel (Extraction)
Complex-imprinted-PVA/GA gel (Back extraction)

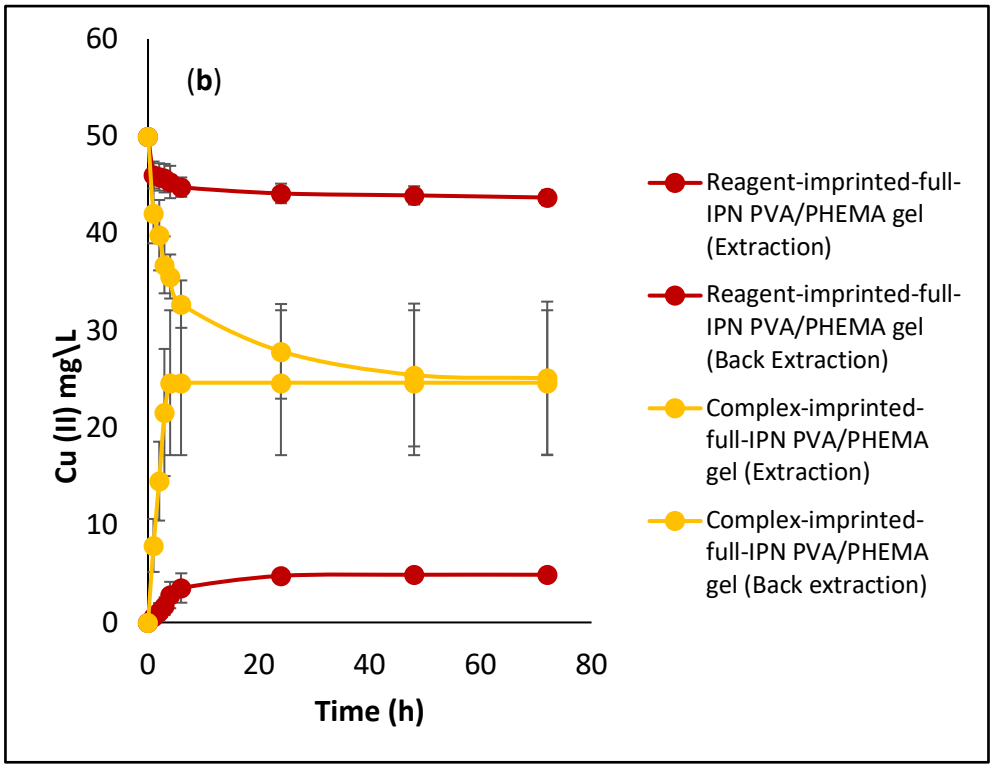
(b)
Cu (II) mg\L
Time (h)
0
10
20
30
40
50
60
0
20
40
60
80
Reagent-imprinted-full-IPN PVA/PHEMA gel (Extraction)
Reagent-imprinted-full-IPN PVA/PHEMA gel (Back Extraction)
Complex-imprinted-full-IPN PVA/PHEMA gel (Extraction)
Complex-imprinted-full-IPN PVA/PHEMA gel (Back extraction)

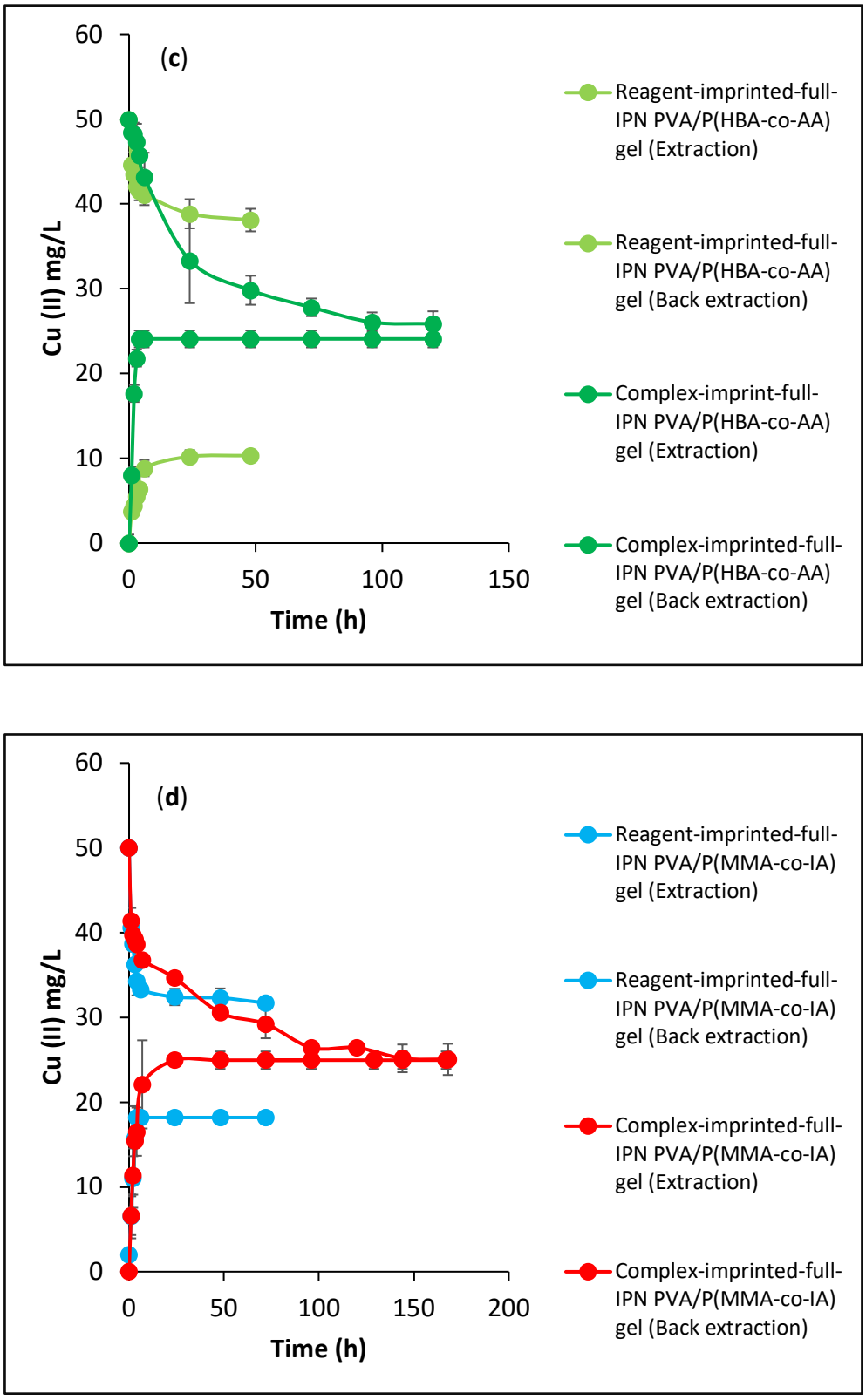

Figure 3.6. Extraction and back-extraction of Cu (II) using reagent and complex-imprinted hydrogels, PVA/GA (a), full-IPN PVA/PHEMA (b), full-IPN PVA/P(HBA-co-AA) (c), full-IPN PVA/P(MMA-co-IA) (d). Conditions: feed, 50 mg/L Cu (II) at pH 2; stripping, 2 M H_2SO_4; stirring rate, 400 rpm; at room temperature.

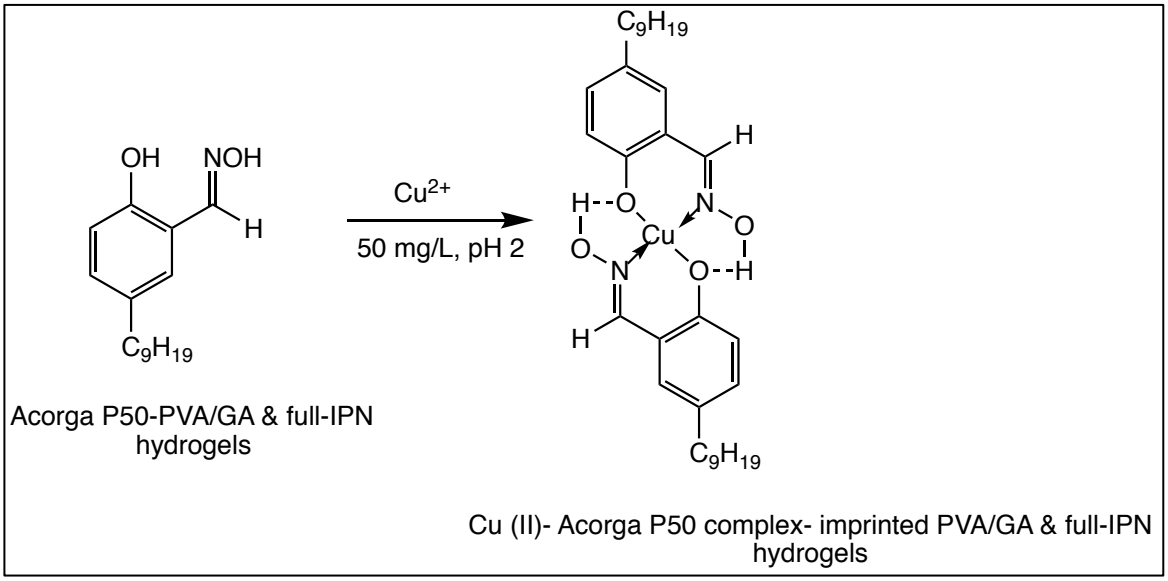

Figure 3.7. Process of Cu (II) extraction into Acorga P50-imprinted PVA/GA and full-IPN hydrogels.

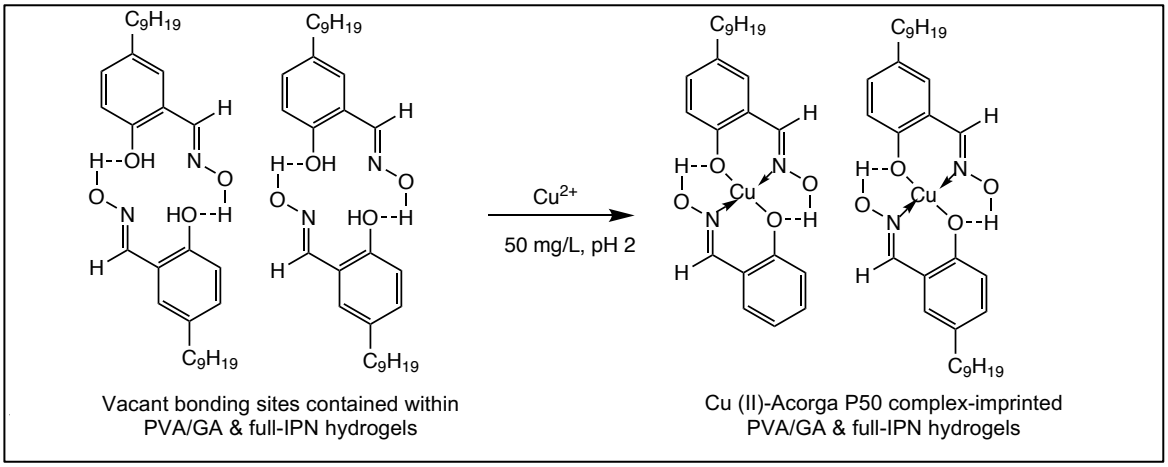

Figure 3.8. Process of Cu (II) extraction into Cu (II)-Acorga P50 complex-imprinted PVA/GA and full-IPN hydrogels.

3.5.4. **Effect of pH on extraction of Cu (II)**

The pH of the feed solution is an important consideration because it affects the extraction process of Cu (II) from aqueous solutions. This effect was investigated at pH 2 and 5 using the full series of reagent and complex imprinted hydrogels; the results are shown in Figures 3.10 - 3.13 and reported in Table 3.3. It is well-known that the solubility of Cu (II) can be affected by the pH of aqueous solutions. At a pH above 6, Cu (II) ions can precipitate as metal hydroxides and oxides[193]. The use of Acorga P50 for extraction of Cu (II) often uses a feed solution at pH 2. Therefore, the current extraction study for Cu (II) was performed using a feed concentration of 50 mg/L at pH 2 or 5.

Generally, the extraction performance by the reagent-imprinted PVA/GA and full-IPN PVA/PHEMA, full-IPN PVA/P(HBA-co-AA), full-IPN PVA/P(MMA-co-IA) hydrogels prepared with Acorga P50 for Cu (II) was better at pH 5, with the best extraction (57%) and recovery factor (51%) observed for full-IPN PVA/P(MMA-co-IA) (Fig. 3.13(g)). Full-IPN PVA/PHEMA and full-IPN PVA/P(HBA-co-AA) hydrogels had a similar Cu (II) recovery factor (~34%) at pH 5.

Conversely, the extraction performance at changed pH was different for the series of complex-imprinted compared to reagent-imprinted hydrogels. Similar extraction efficiencies of 56% and 50% were observed for PVA/GA and full-IPN PVA/PHEMA, respectively, at both pH 2 and 5. Whereas, full-IPN PVA/P(HBA-co-AA) had slightly better extraction at pH 2 compared to pH 5 with extraction efficiencies of 50% and 44%, respectively. The full-IPN PVA/P(MMA-co-IA) gels were the only member of the series to display a markedly different extraction performance affected by pH, with extraction efficiencies of 50% and 26% at pH 2 and 5, respectively. Although more Cu (II) was extracted at pH 2, a longer time was needed to reach equilibrium. In general, the time to reach extraction equilibrium was faster at pH 5 for all hydrogels regardless of the final extraction efficiency.

The effect of pH on the extraction of Cu using reagent-imprinted full-IPN PVA/P(HBA-co-AA) and PVA/(P(MMA-co-IA) is due to the -COOH groups on the backbone of polymers that are deprotonated at pH 5. The resulting $-COO^-$ groups lead to electrostatic repulsion between neighbouring ionised groups. Consequently, the carboxylate groups can form a complex with Cu (II). The binding sites (COO^-) in these

hydrogels enhance Cu (II) uptake[215]. In other words, complexation and electrostatic reactions play a significant role in copper extraction into the hydrogels containing Acorga P50.

Blank hydrogels without carrier (reagent or complex) were tested for copper extraction. The copper extracted at pH 5 is attributed to ionisation of functional groups, such as COOH groups of PIA (pK_{a1} = 3.85 and pK_{a2} = 5.45)[7] and PAA (pK_a 4.5)[47], and hydroxyl groups of PVA and PHEMA. This results in an increased number of negatively charged coordination sites for Cu (II) extraction[121]. The possible structure of the formation of complex between copper ions and COO^- ions on the surface of blank hydrogels at pH 5 is illustrated in Figure 3.9.

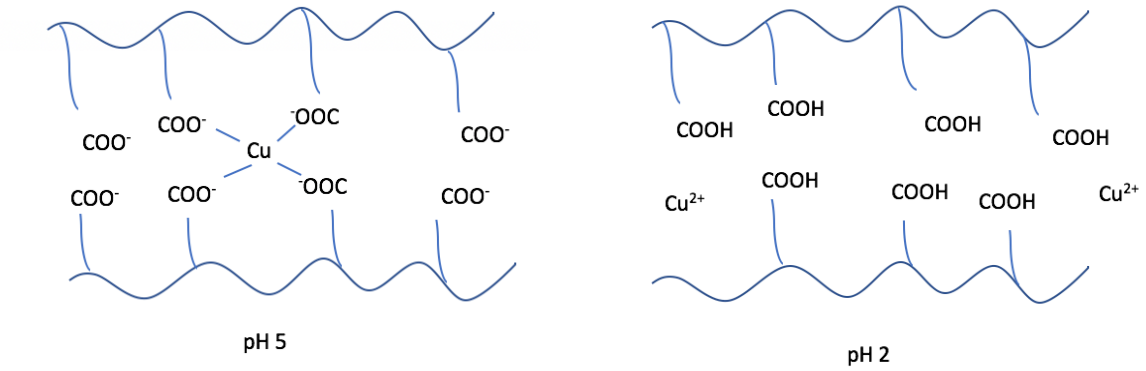

Figure 3.9. Structure of coordination complex between Cu (II) ions and carboxylate (COO^-) ions on the full-IPN gel at pH 5, and hydrogen bonding interaction at pH 2.

However, the blank hydrogels did not yield any copper extraction at pH 2 because of the formation of hydrogen bonds between COOH and OH groups.

It must be noted that a significant number of binding sites for Cu (II) are available due to the functional groups of the polymers within the hydrogel network. This could explain the significant (average 15%) extraction of the blank hydrogels and better extraction at pH 5.

Images of the physical appearance of the full series of reagent-imprinted, and complex-imprinted hydrogels after extraction and back-extraction of copper at pH 2 and pH 5 are shown in Table 3.4.

The Cu-imprinted-semi-IPN (PVA/PAA) hydrogel indicated a better copper adsorption in pH 5 due to the ionisation of COOH groups of PAA, leading to an increase in the adsorption sites for binding copper ions.

The evidence from this investigation confirms that a change of pH of the feed solution has a great effect on extraction performance. At pH 5, a better extraction performance and faster time to reach to equilibrium was observed for the reagent-loaded PVA/GA and full-IPN hydrogels compared to blank hydrogels and complex-loaded hydrogels. Two factors contribute to this pH effect: complexation of copper and electrostatic interactions between carrier and polar groups of the polymer chains.

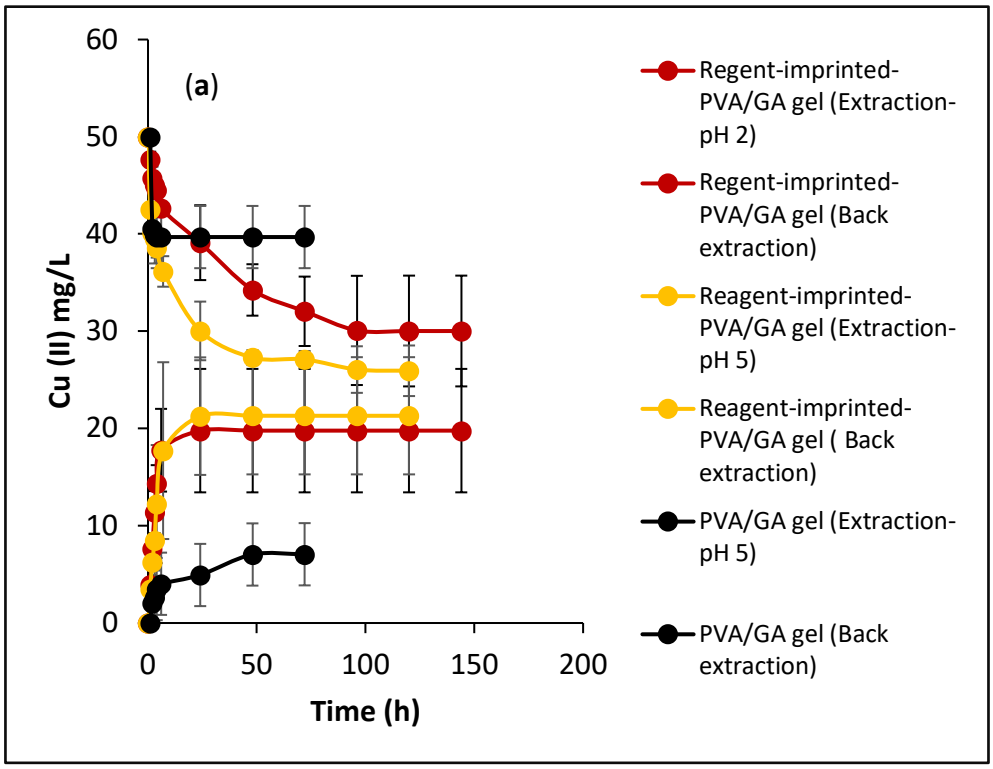

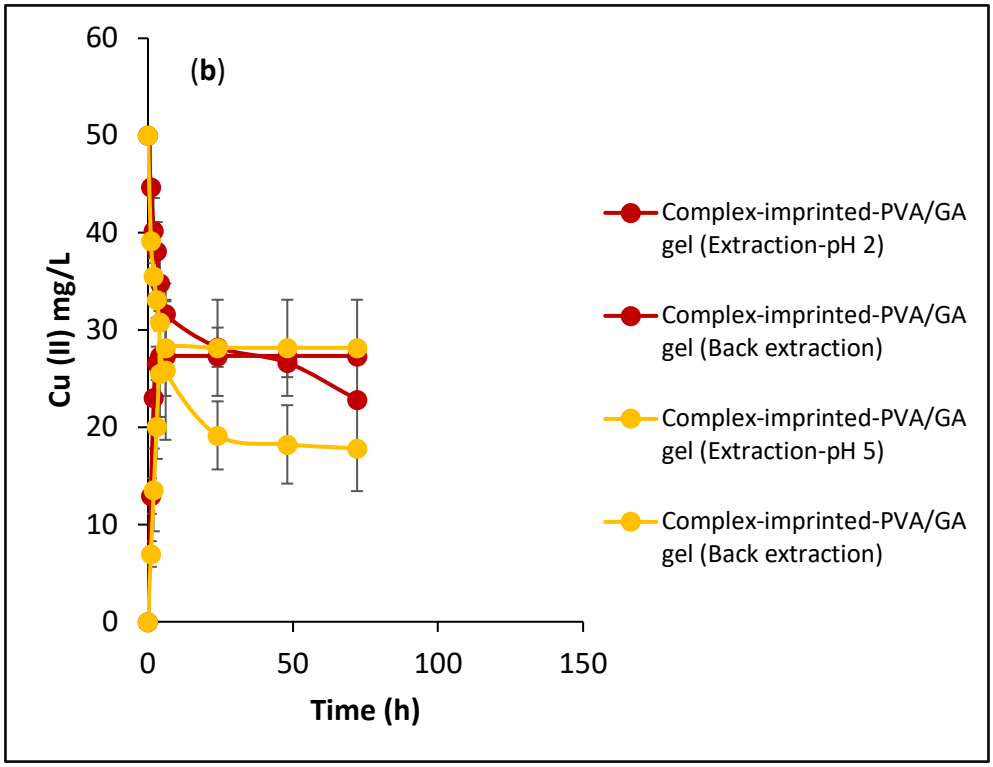

Figure 3.10. Extraction and back-extraction profiles of Cu (II) using reagent (a) and complex (b) imprinted-PVA/GA hydrogels. Conditions: extraction from Cu (II) 50 mg/L at pH 2 or pH 5, stirring rate of 400 rpm, room temperature 25 (±1)℃. Back-extraction used 2 M H_2SO_4.

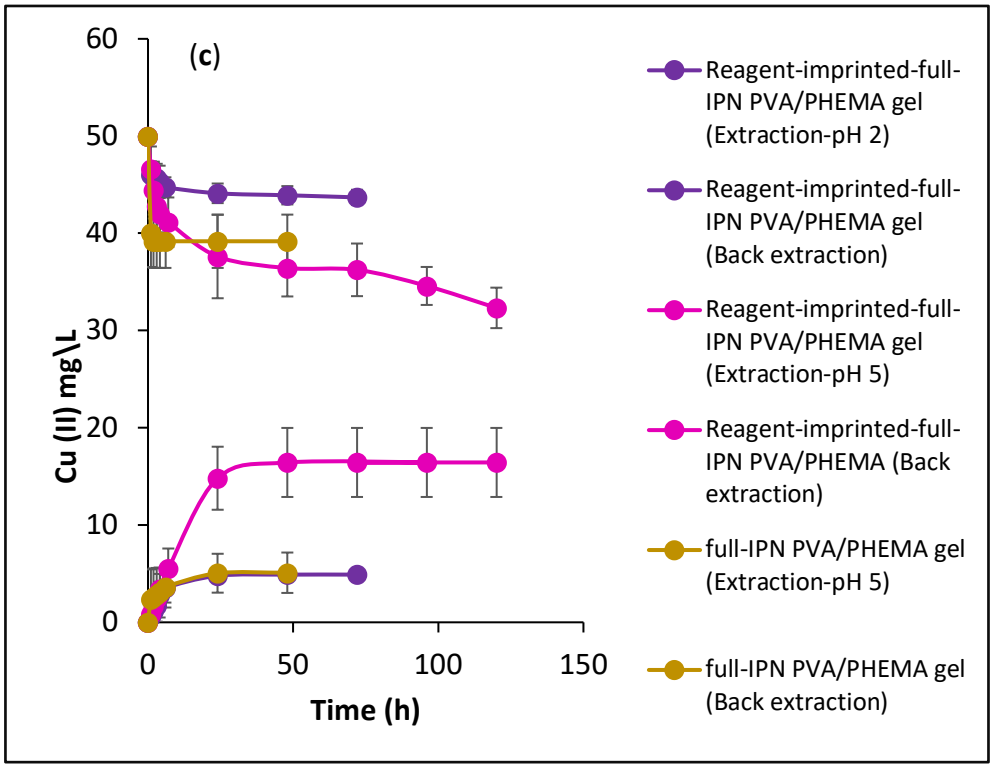

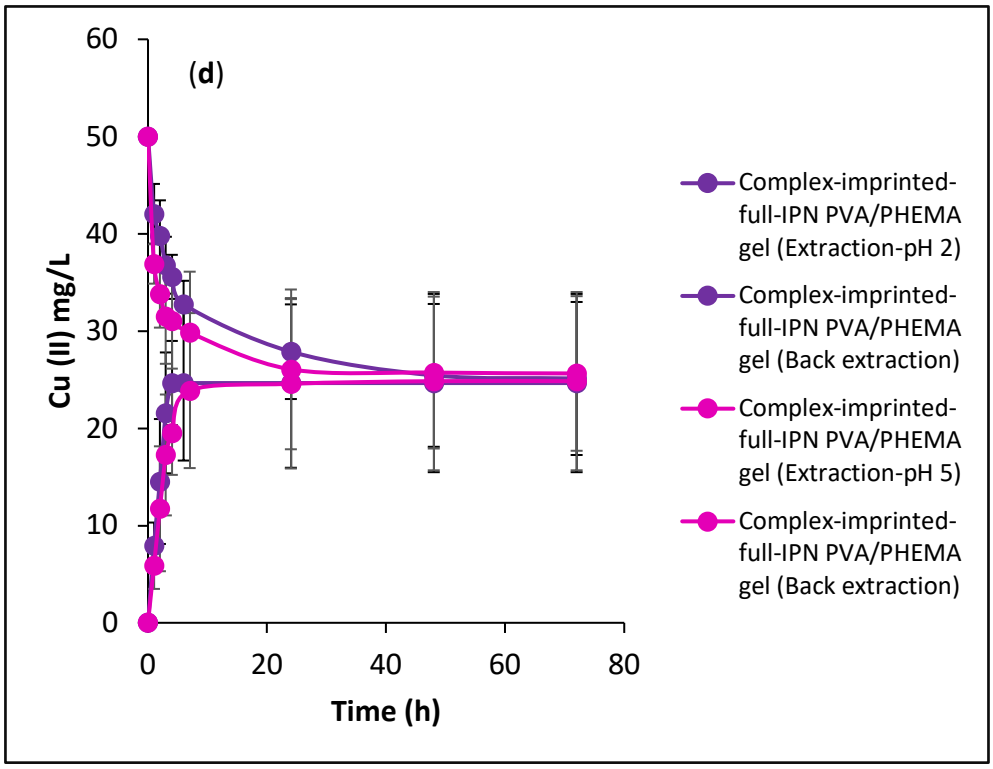

Figure 3.11. Extraction and back-extraction profiles of Cu (II) using reagent (c) and complex (d) imprinted-full-IPN PVA/PHEMA hydrogels. Conditions as for Fig. 3.10.

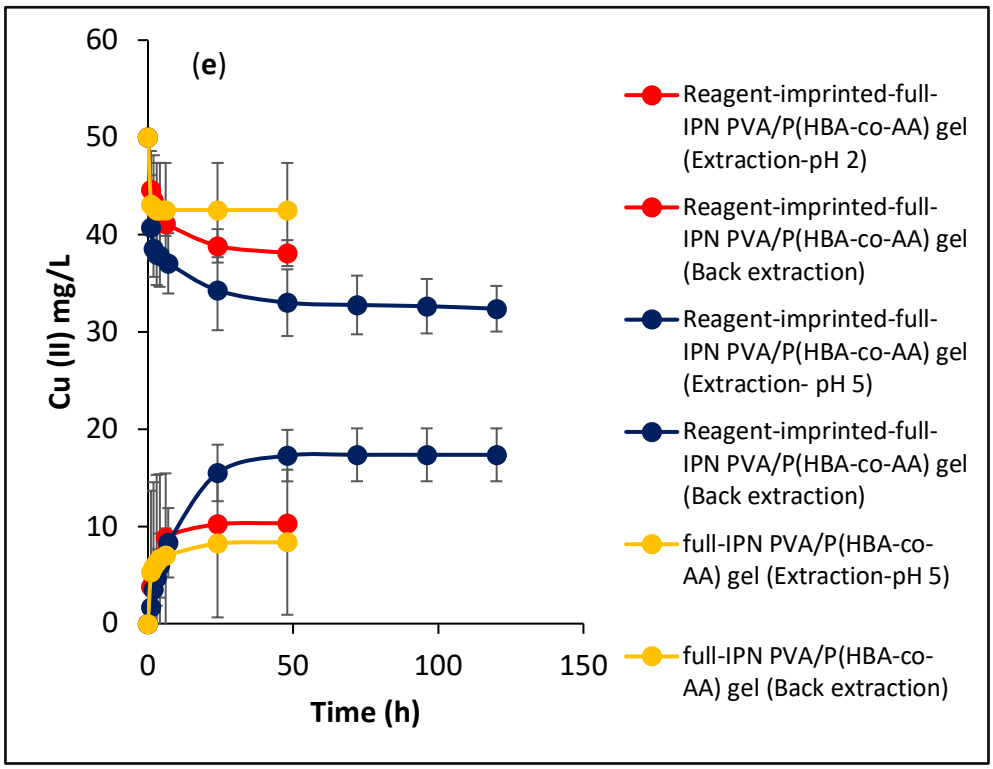

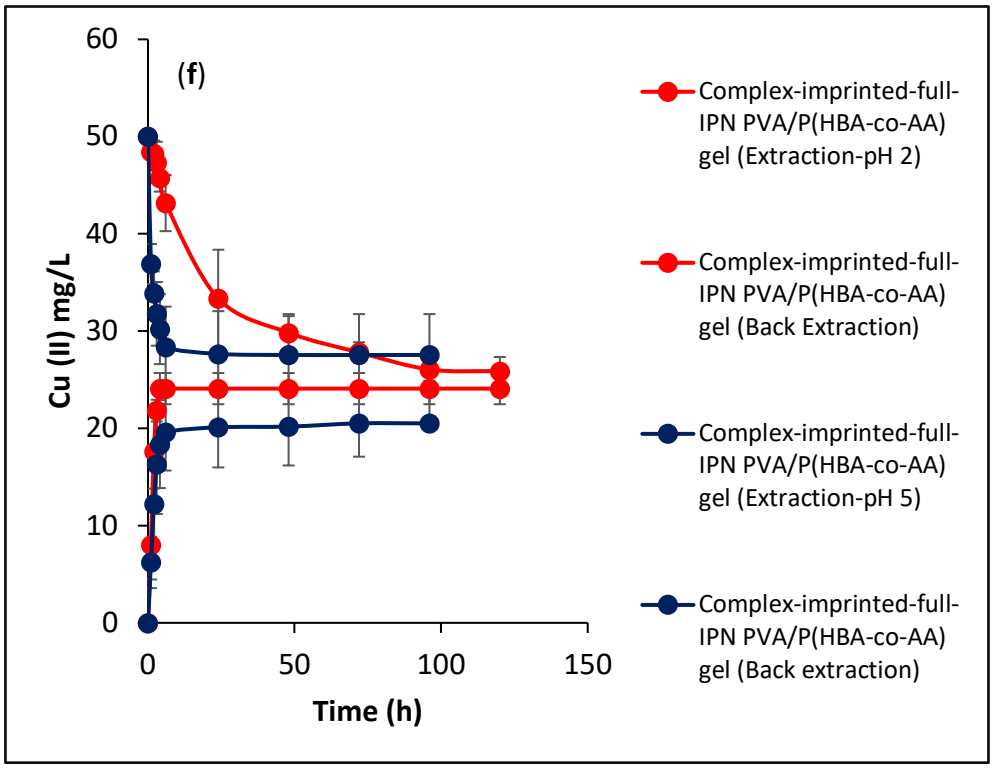

Figure 3.12. Extraction and back-extraction profiles of Cu (II) using reagent (e) and complex (f) imprinted-full-IPN PVA/P(HBA-co-AA) hydrogels. Conditions as for Fig. 3.10.

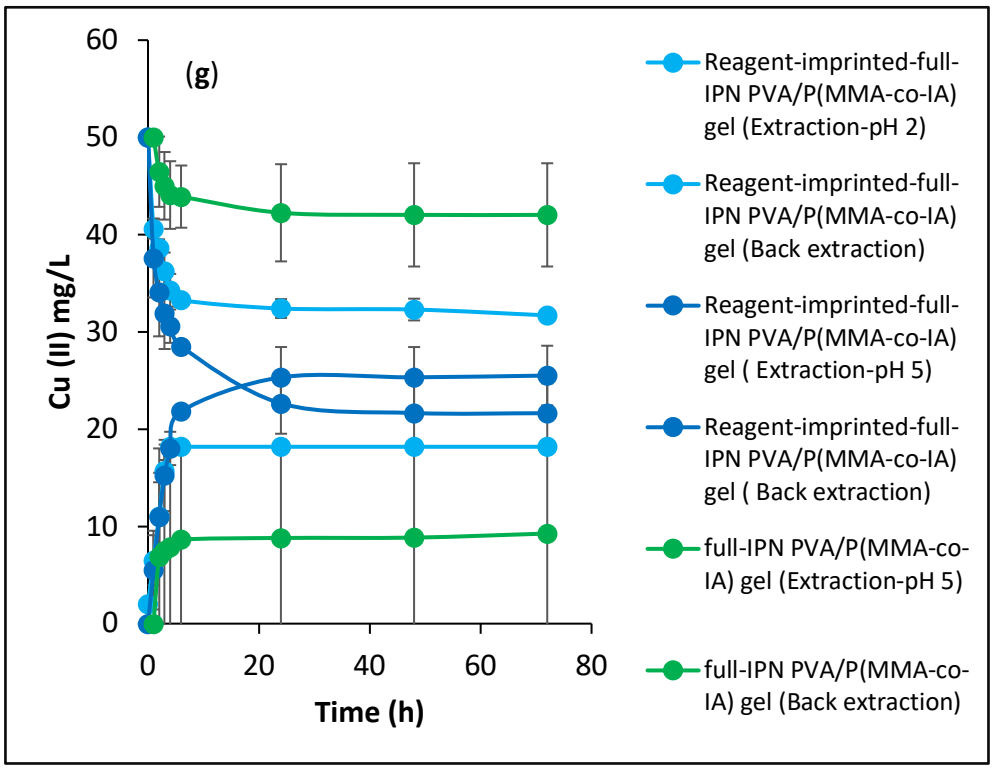

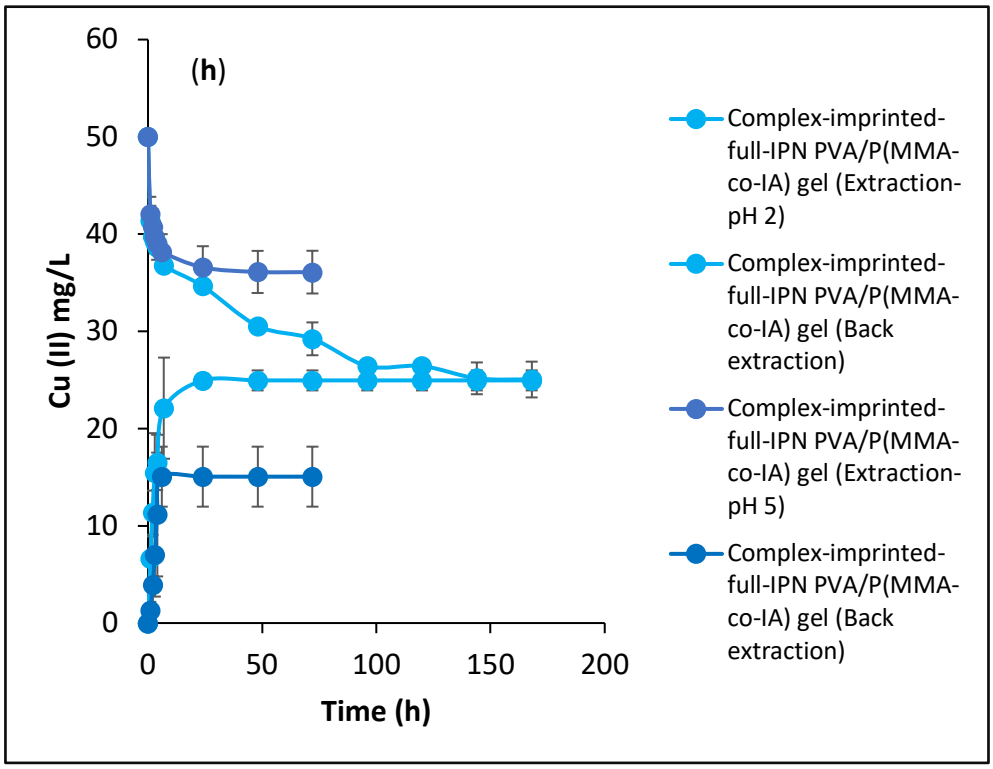

Figure 3.13. Extraction and back-extraction profiles of Cu (II) using reagent (g) and complex (h) imprinted-full-IPN PVA/P(MMA-co-IA) hydrogels. Conditions as for Fig. 3.10.

Table 3.3. Extraction performance indicators (extraction, back-extraction and recovery factor) for Cu (II) at pH 2 & 5 using the full series of reagent-imprinted and complex-imprinted hydrogels (where reagent is Acorga P50 and complex is Cu-Acorga P50).

Hydrogel	Ex (%)	BEx (%)	RF (%)	Eq time (hrs)	pH
PVA/GA					
complex	54	101	55	72	2
reagent	40	99	40	120	2
complex	64	88	56	72	5
reagent	48	89	43	48	5
blank	39	37	14	48	5
PVA/PHEMA					
complex	25	99	49	48	2
reagent	13	78	10	72	2
complex	49	102	50	24	5
reagent	35	93	33	48	5
blank	22	47	10	24	5
PVA/P(HBA-co-AA)					
complex	48	100	48	96	2
reagent	24	87	21	48	2
complex	45	91	41	24	5
reagent	35	99	35	48	5
blank	15	(112)	17	24	5
PVA/P(MMA-co-IA)					
complex	50	100	50	144	2
reagent	37	99	37	72	2
complex	28	(108)	30	6	5
reagent	57	90	51	24	5
blank	16	(116)	18	24	5

Data in brackets indicates significant difference of results from one of three replicate experiments.

Table 3.4. Images showing the physical appearance of Acorga P50 (reagent) and Cu (II)-Acorga P50 (complex) imprinted PVA/GA and full-IPN hydrogels after extraction and back-extraction of copper from an initial concentration of 50 mg/L at pH 2 & 5.

Hydrogel (extraction pH)	**Extraction**	**Back extraction**
PVA/GA		
complex (pH 5)	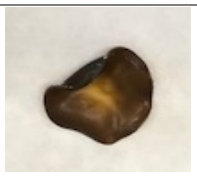	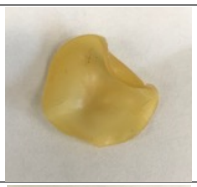
complex (pH 2)		
reagent (pH 2)		
reagent (pH 5)	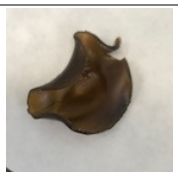	
blank (pH 5)		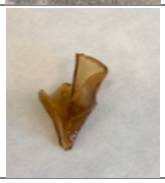
PVA/PHEMA		
complex (pH 5)	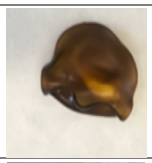	
complex (pH 2)	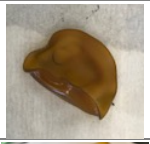	
reagent (pH 5)		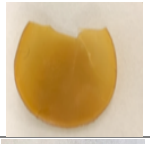
reagent (pH 2)		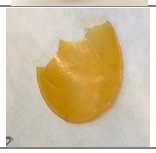

blank (pH 5)		
PVA/P(HBA-co-AA)		
complex (pH 2)		
complex (pH 5)		
reagent (pH 5)		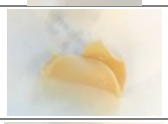
reagent (pH 2)		
blank (pH 5)		
PVA/P(MMA-co-IA)		
complex (pH 2)	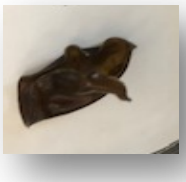	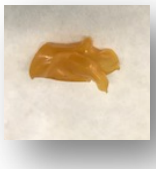
complex (pH 5)		
reagent (pH 5)		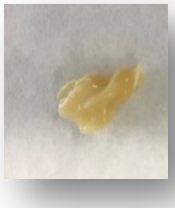
reagent (pH 2)		
blank (pH 5)		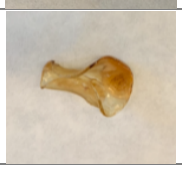

3.5.5. **Stability study**

In order to assess stability and reusability, the full series of reagent-imprinted and complex-imprinted hydrogels were reused in four consecutive cycles of extraction and back-extraction of Cu (II) involving the use of fresh feed and stripping solutions after each cycle. As indicated in Figure 3.14 and Table 3.5, the extraction performance, as indicated by permeability and recovery factor, showed a significant decrease after cycle 4 for reagent-based hydrogels. This is likely caused by leaching of Acorga P50 from the hydrogels into the stripping solution. This is possible because there are only weak non-covalent molecular interactions between Acorga P50 and the polymer chains. Consequently, it is easy for the carrier to be released from the IPN.

Compared to all other reagent-based and complex-based hydrogels, the full-IPN PVA/PHEMA reagent-based hydrogel indicated the sharpest drop in extraction performance after the fourth cycle. This could be related to residual copper ions from previous cycles being retained in the gel that limits the number of available binding sites for extraction of copper ions. The colour change of this hydrogel from pale amber after cycle 1 to tan-brown after cycle 4 is evidence of remaining copper ions in the hydrogel network. Effect of the number of cycles of extraction for Cu (II) on permeability and recovery factor using the Acorga P50-PVA/GA full-IPN hydrogels, and Cu (II)-Acorga P50-complex-imprinted PVA/GA-full-IPN hydrogels is demonstrated by comparing data from cycles 1 &4 s shown in Table 3.5.

It can be summarised that the complex-imprinted hydrogels offered better long-term performance as indicted by recovery factor after cycle 4 compared to similar reagent-based hydrogels. The best permeability was demonstrated by reagent-based PVA/P(HBA-co-AA) but, unfortunately, the initial recovery factor was low (44%) and decreased by 50% after the fourth extraction cycle. Both reagent-imprinted and complex-imprinted PVA/GA and full-IPN PVA/P(MMA-co-IA) hydrogels are indicated as offering reasonable performance for some repeat use applications for copper extraction. However, further investigations to improve stability for extended and repeated use applications are needed.

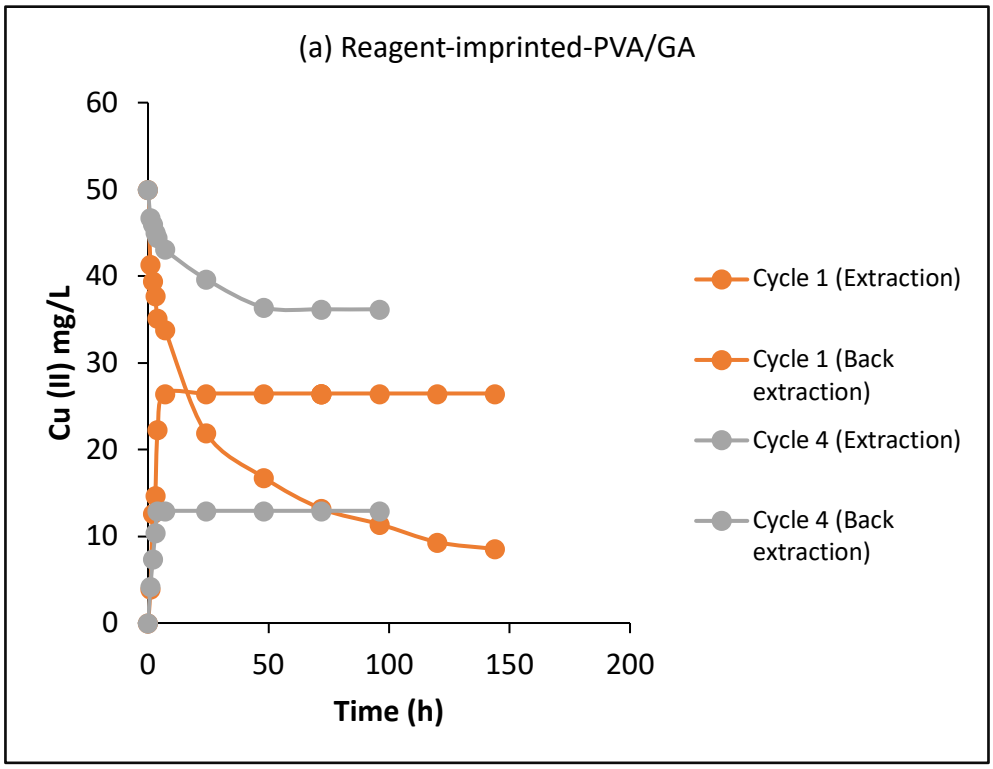
(a) Reagent-imprinted-PVA/GA
Cu (II) mg/L
Time (h)
0
10
20
30
40
50
60
0
50
100
150
200
Cycle 1 (Extraction)
Cycle 1 (Back extraction)
Cycle 4 (Extraction)
Cycle 4 (Back extraction)

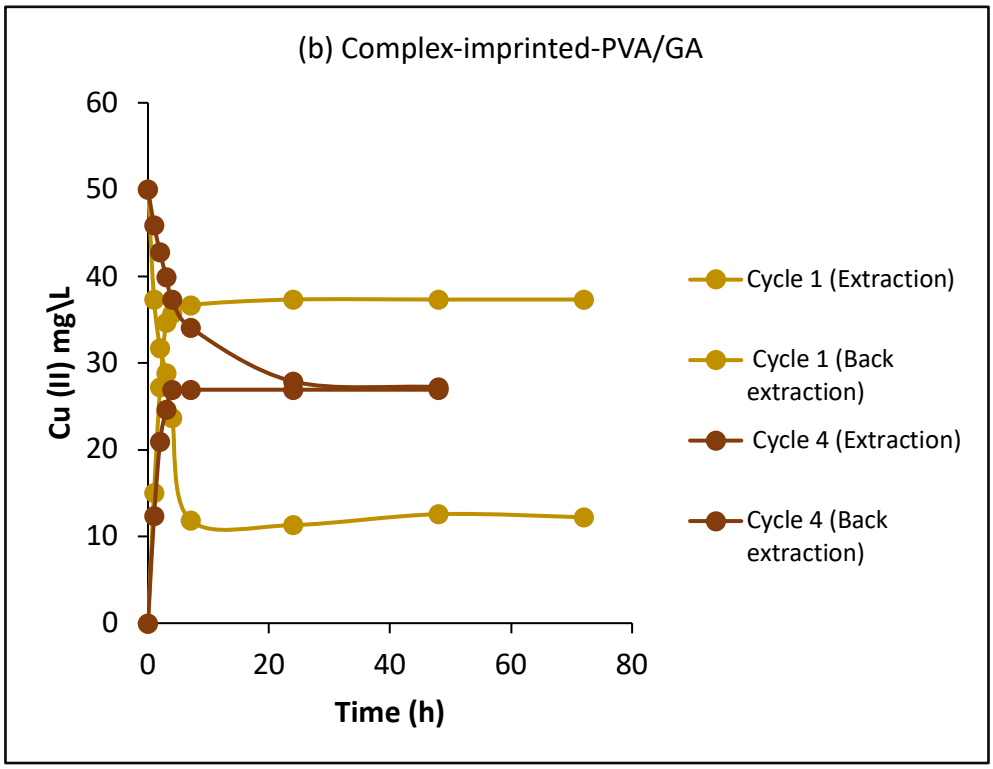
(b) Complex-imprinted-PVA/GA
Cu (II) mg\L
Time (h)
0
10
20
30
40
50
60
0
20
40
60
80
Cycle 1 (Extraction)
Cycle 1 (Back extraction)
Cycle 4 (Extraction)
Cycle 4 (Back extraction)

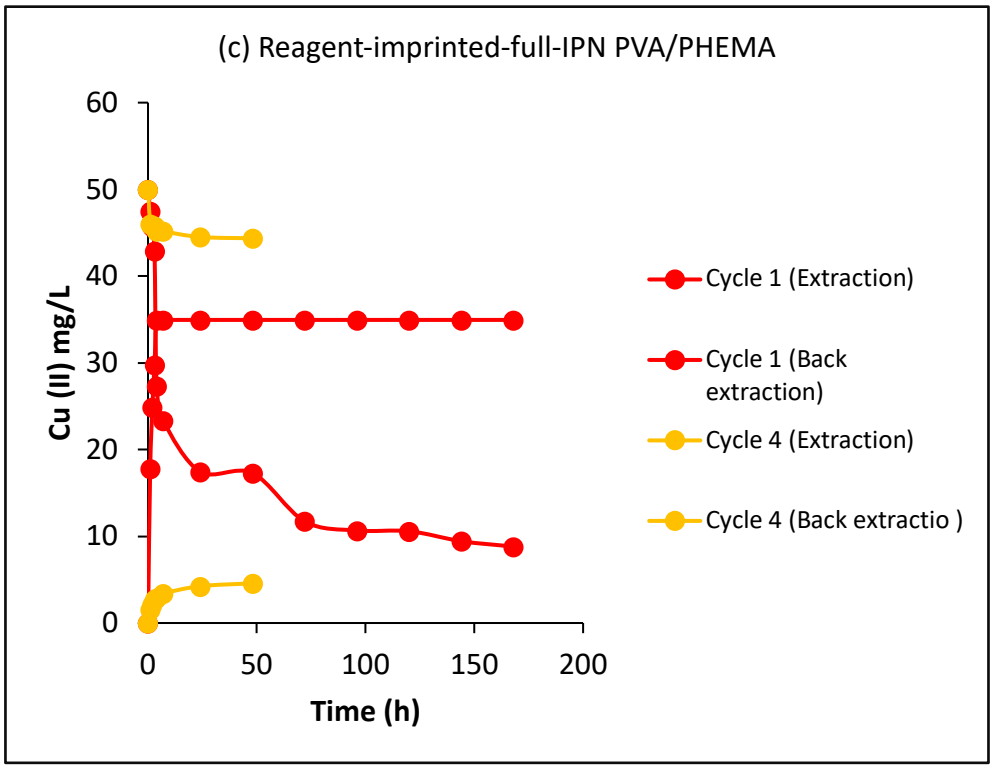
(c) Reagent-imprinted-full-IPN PVA/PHEMA
Cu (II) mg/L
Time (h)
0
10
20
30
40
50
60
0
50
100
150
200
Cycle 1 (Extraction)
Cycle 1 (Back extraction)
Cycle 4 (Extraction)
Cycle 4 (Back extractio)

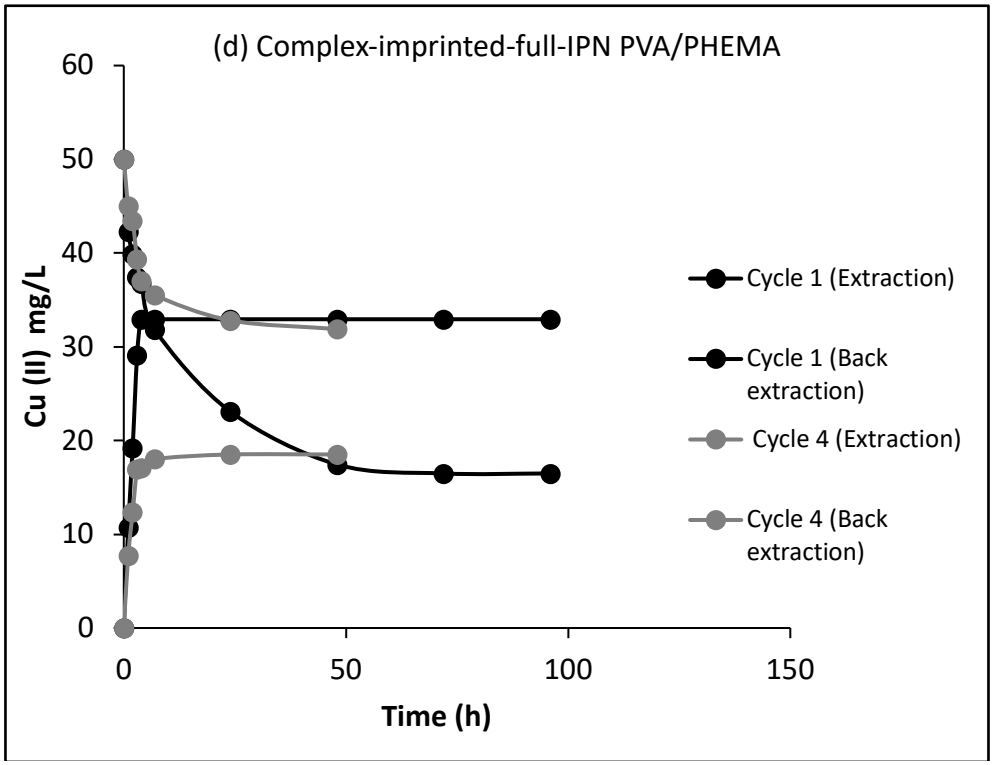
(d) Complex-imprinted-full-IPN PVA/PHEMA
Cu (II) mg/L
Time (h)
0
10
20
30
40
50
60
0
50
100
150
Cycle 1 (Extraction)
Cycle 1 (Back extraction)
Cycle 4 (Extraction)
Cycle 4 (Back extraction)

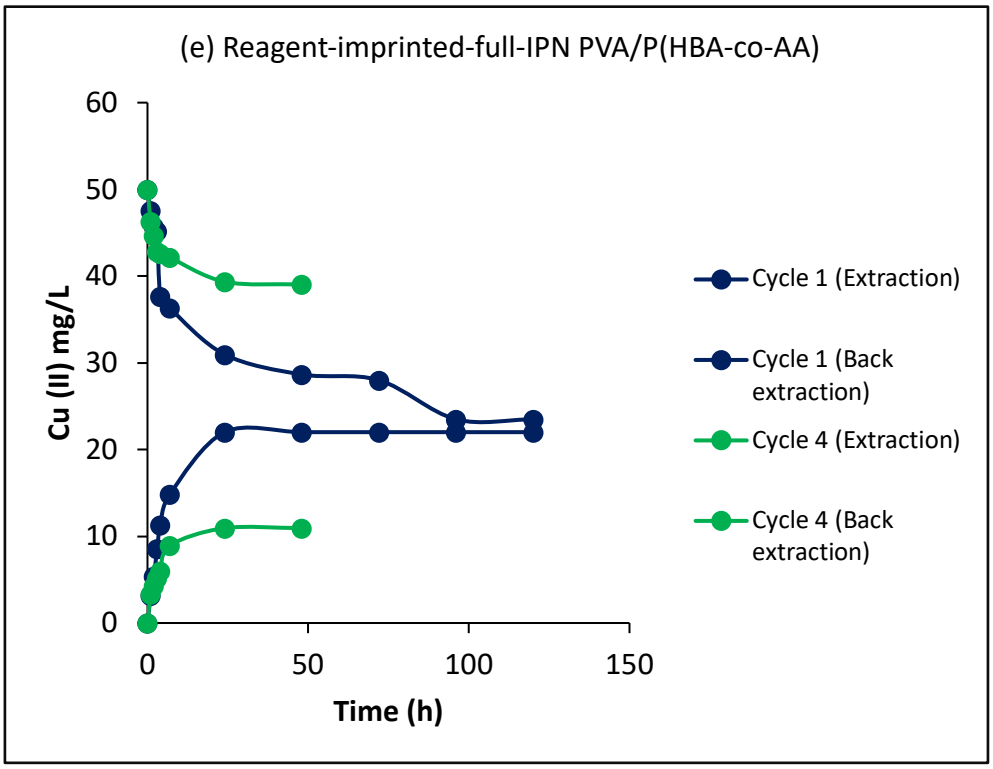
(e) Reagent-imprinted-full-IPN PVA/P(HBA-co-AA)
Cu (II) mg/L
Time (h)
0
10
20
30
40
50
60
0
50
100
150
Cycle 1 (Extraction)
Cycle 1 (Back extraction)
Cycle 4 (Extraction)
Cycle 4 (Back extraction)

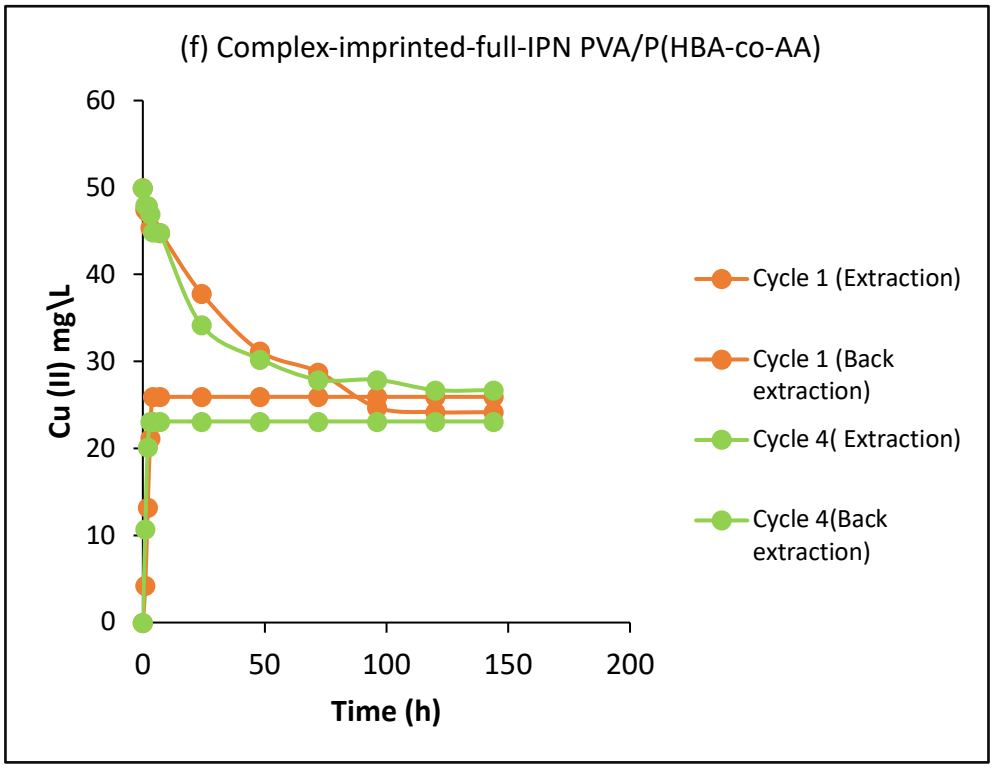
(f) Complex-imprinted-full-IPN PVA/P(HBA-co-AA)
Cu (II) mg\L
Time (h)
0
10
20
30
40
50
60
0
50
100
150
200
Cycle 1 (Extraction)
Cycle 1 (Back extraction)
Cycle 4(Extraction)
Cycle 4(Back extraction)

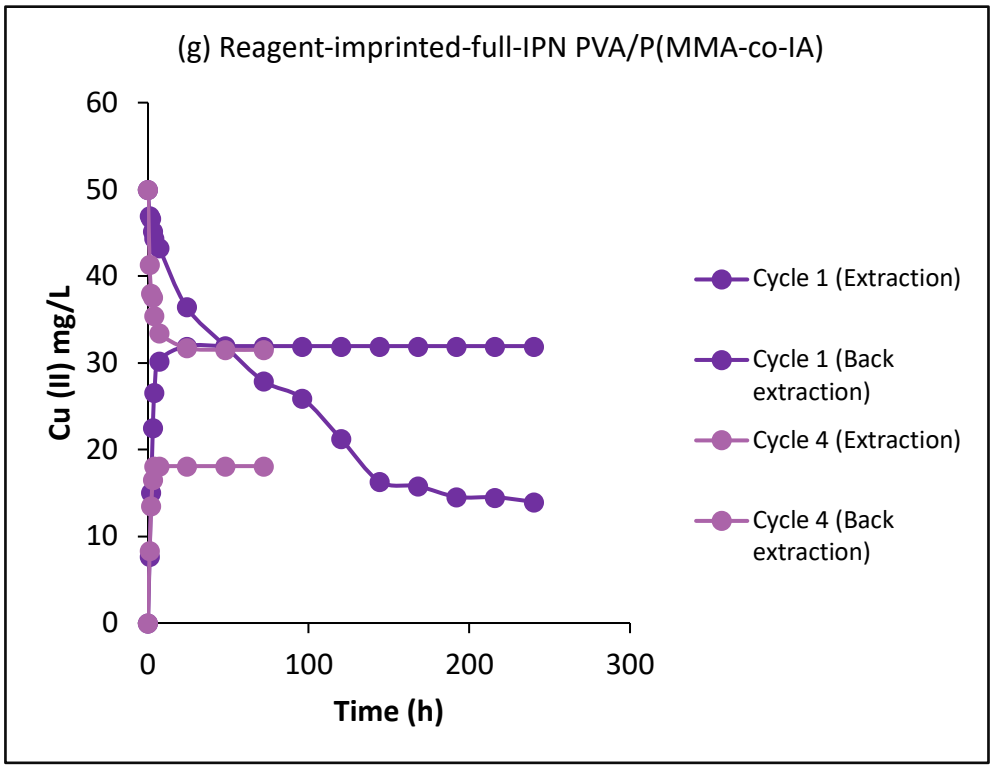

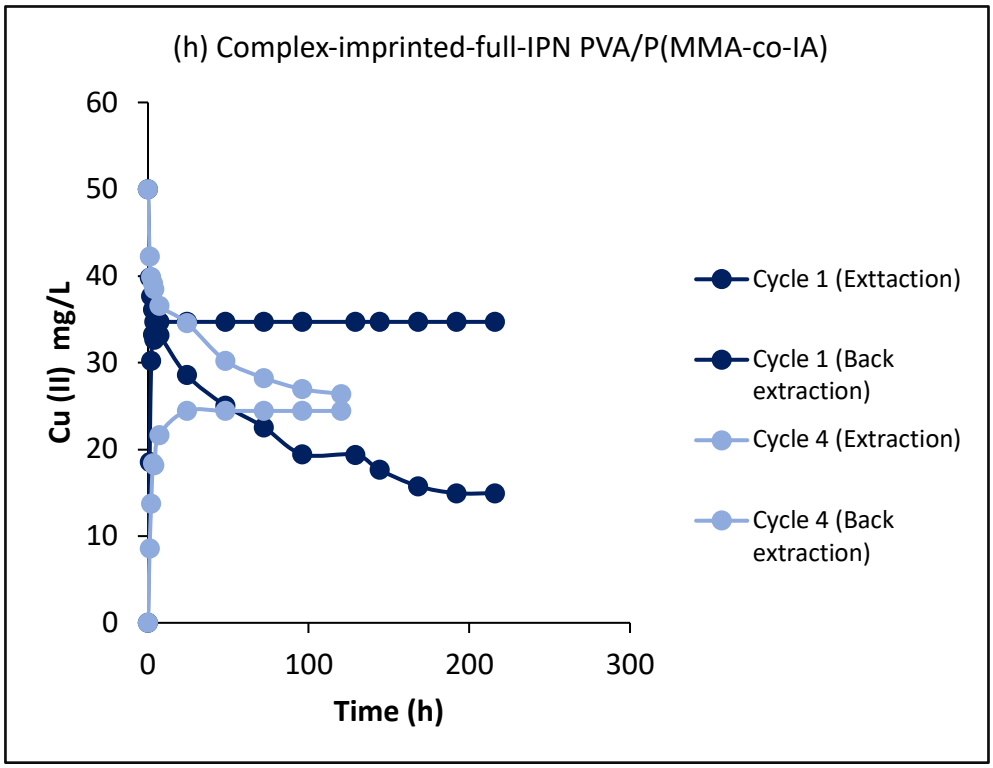

Figure 3.14. Comparison of first and fourth extraction and back-extraction cycles for Cu (II) using reagent (a) and complex (b) imprinted PVA/GA hydrogels, reagent (c) and complex (d) imprinted full-IPN PVA/PHEMA hydrogels, reagent (e) and complex (f) imprinted full-IPN PVA/P(HBA-co-AA) hydrogels, reagent (g) and complex (h) imprinted-

full IPN PVA/P(MMA-co-IA) hydrogels. Conditions: feed, 50 mg/L of copper, pH 2; stripping, 2 M H_2SO_4.

Table 3.5. Effect of number of extraction cycles for Cu (II) on permeability and recovery factor using reagent-loaded and complex-loaded PVA/GA and full-IPN hydrogels.

Hydrogel	Permeability (x 10^{-7}, m^{-2} s^{-1})			Recovery factor (%)		
	Cycle 1	Cycle 4	Change (%)	Cycle 1	Cycle 4	Change (%)
PVA/GA						
Reagent	16.7	5.4	-67	53	26	-51
Complex	32.4	15.2	-53	75	54	-28
PVA/PHEMA						
Reagent	49.8	1.5	-97	70	9.2	-87
Complex	10.7	15.2	+42	66	37	-44
PVA/P(HBA-co-AA)						
Reagent	171	10.4	-91	44	22	-50
Complex	1.11	1.23	+11	52	46	-12
PVA/P(MMA-co-IA)						
Reagent	22.8	17.6	-22	64	36	-44
Complex	18.7	8.9	-53	69	49	-29

3.5.6. **Effect of Cu (II) concentration**

The effect of initial copper concentration on extraction of Cu (II) was carried out in a series of experiments using initial concentrations of 25, 50 and 100 mg/L at pH 2. The extraction and back-extraction profiles of Cu (II) using the full series of reagent-based and complex-based hydrogels are indicated in Figure 3.15. In general, as the concentration of feed solution increased from 25 to 100 mg/L, the permeability and recovery factor were noted to decrease for all hydrogels (Table 3.6). However, the complex-imprinted full-IPN PVA/P(HBA-co-AA) gel indicated the highest permeability when the concentration of feed phase was 100 mg/L. The best permeabilities of 3.62 x 10^{-6} and 2.43 x 10^{-6} m^{-2} s^{-1} were obtained using complex-based PVA/GA and full-IPN reagent-based PVA/P(MMA-co-IA), respectively, at Cu (II) 25 mg/L. This is explained by the decreased rate of formation of Cu (II)-Acorga complex at the feed/hydrogel interface at increased concentration of Cu (II). In addition, the decline in copper permeability as the initial copper concentration increases is due to the limited number and restricted availability of vacant coordination sites on the surface of hydrogels.

This investigation indicates that the permeability and recovery factor of Cu (II) using reagent-based and complex-based hydrogels are compromised from feed solutions with concentrations below 100 mg/L.

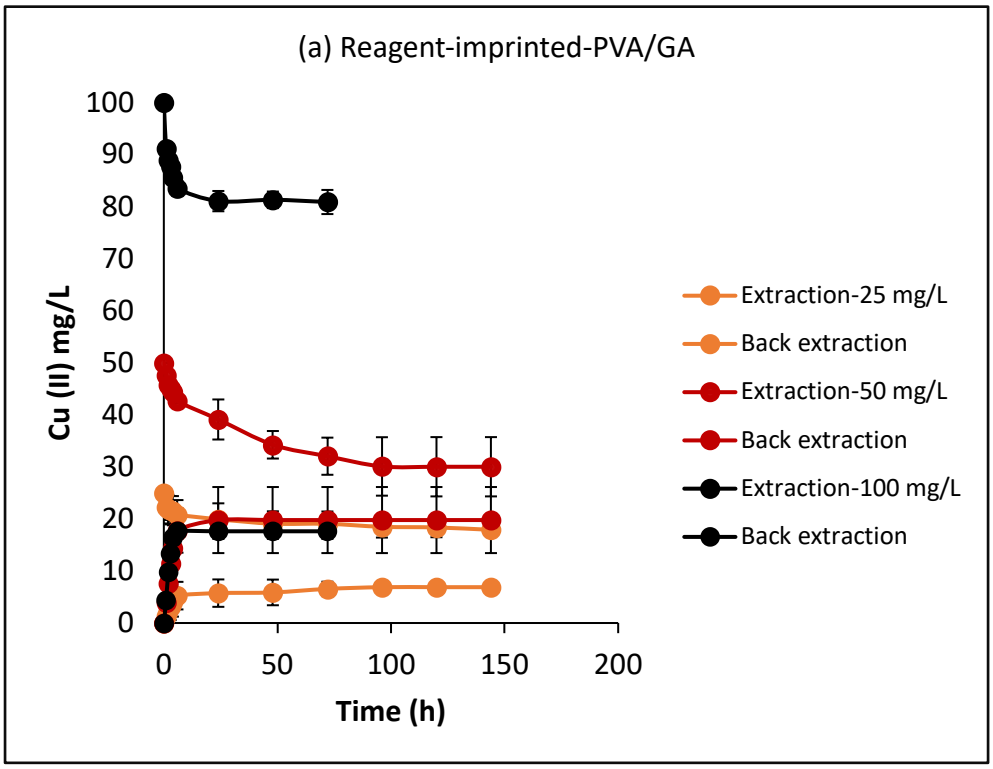
(a) Reagent-imprinted-PVA/GA
Cu (II) mg/L
Time (h)
0
10
20
30
40
50
60
70
80
90
100
0
50
100
150
200
Extraction-25 mg/L
Back extraction
Extraction-50 mg/L
Back extraction
Extraction-100 mg/L
Back extraction

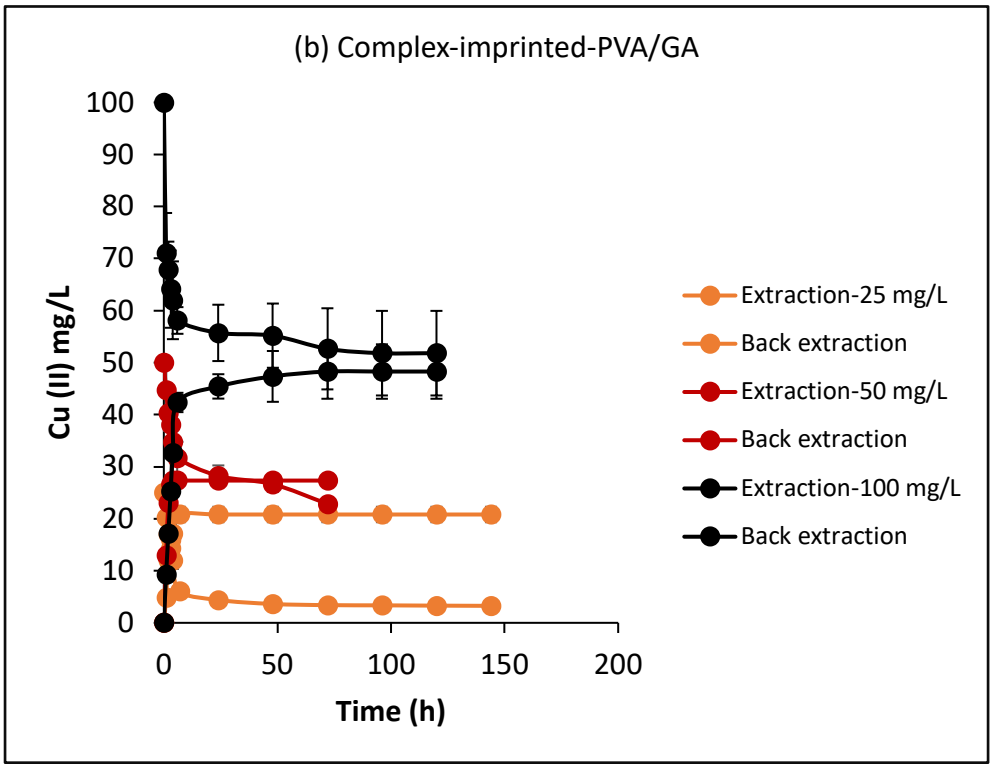
(b) Complex-imprinted-PVA/GA
Cu (II) mg/L
Time (h)
0
10
20
30
40
50
60
70
80
90
100
0
50
100
150
200
Extraction-25 mg/L
Back extraction
Extraction-50 mg/L
Back extraction
Extraction-100 mg/L
Back extraction

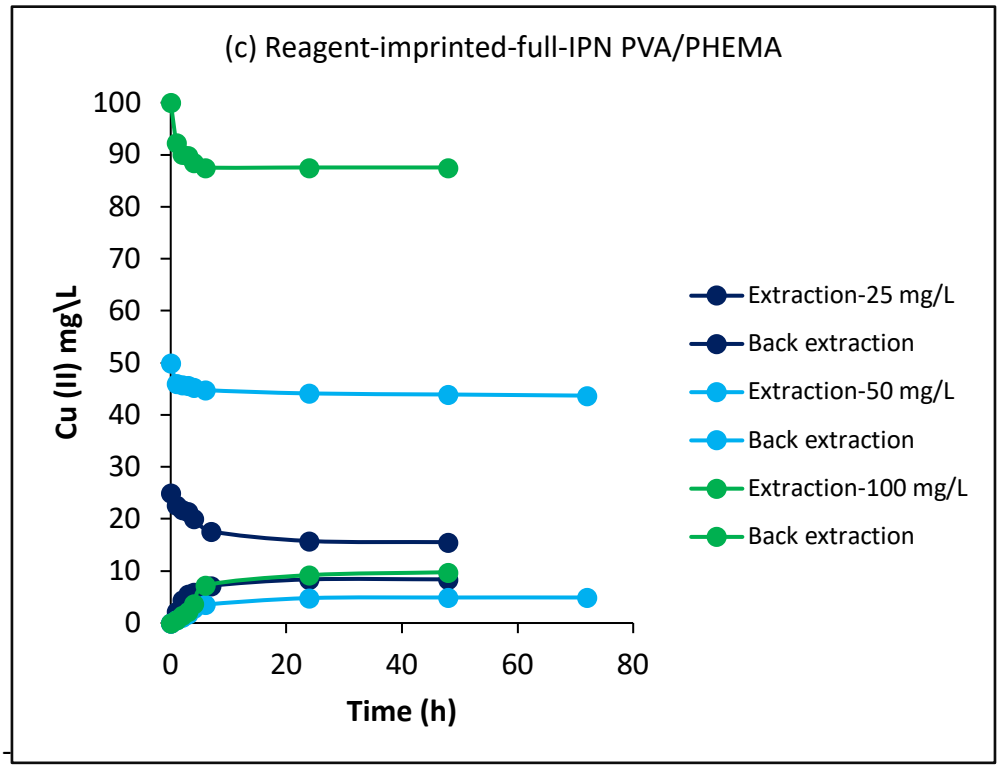
(c) Reagent-imprinted-full-IPN PVA/PHEMA
Cu (II) mg\L
Time (h)
0
10
20
30
40
50
60
70
80
90
100
0
20
40
60
80
Extraction-25 mg/L
Back extraction
Extraction-50 mg/L
Back extraction
Extraction-100 mg/L
Back extraction

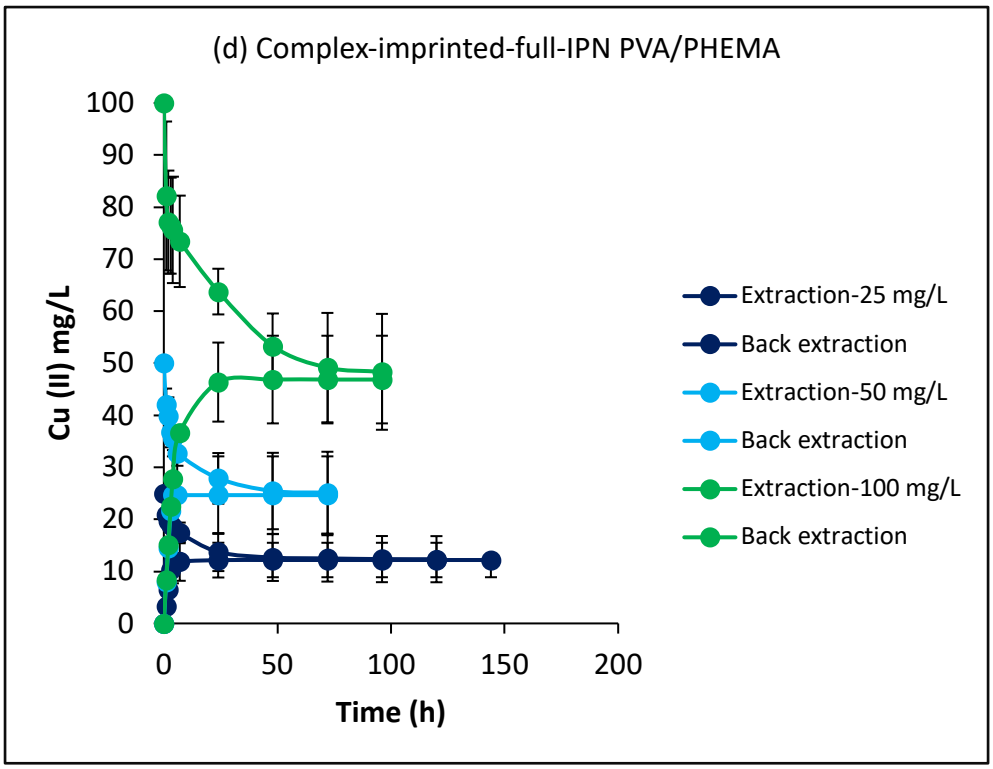
(d) Complex-imprinted-full-IPN PVA/PHEMA
Cu (II) mg/L
Time (h)
0
10
20
30
40
50
60
70
80
90
100
0
50
100
150
200
Extraction-25 mg/L
Back extraction
Extraction-50 mg/L
Back extraction
Extraction-100 mg/L
Back extraction

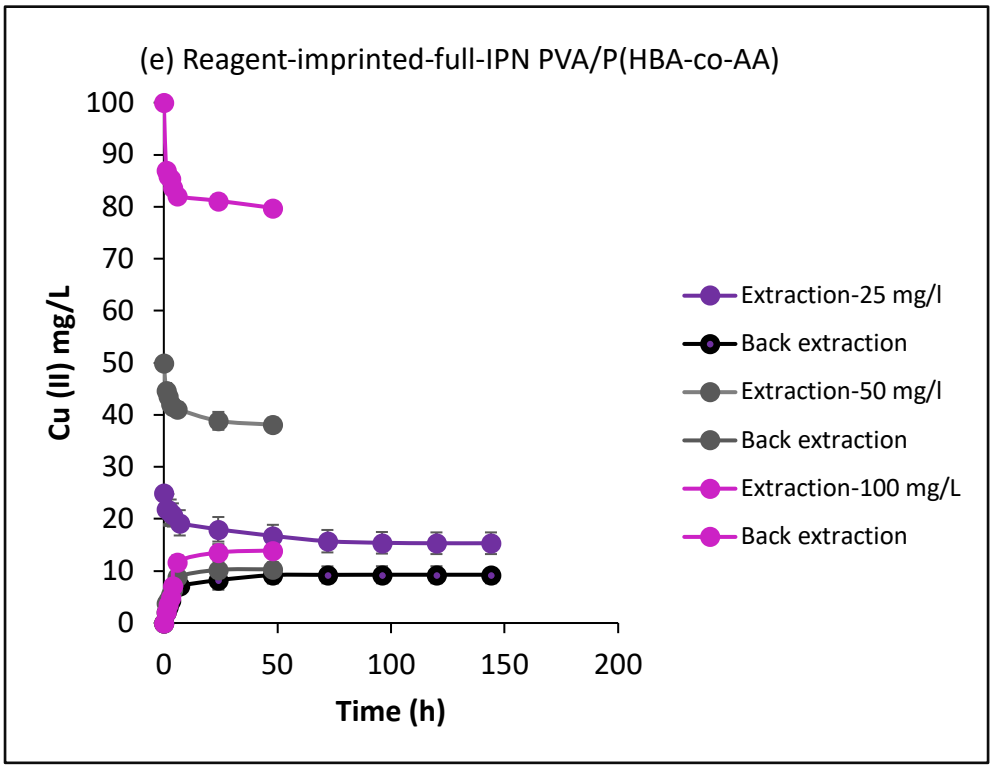
(e) Reagent-imprinted-full-IPN PVA/P(HBA-co-AA)
Cu (II) mg/L
Time (h)
0
10
20
30
40
50
60
70
80
90
100
0
50
100
150
200
Extraction-25 mg/l
Back extraction
Extraction-50 mg/l
Back extraction
Extraction-100 mg/L
Back extraction

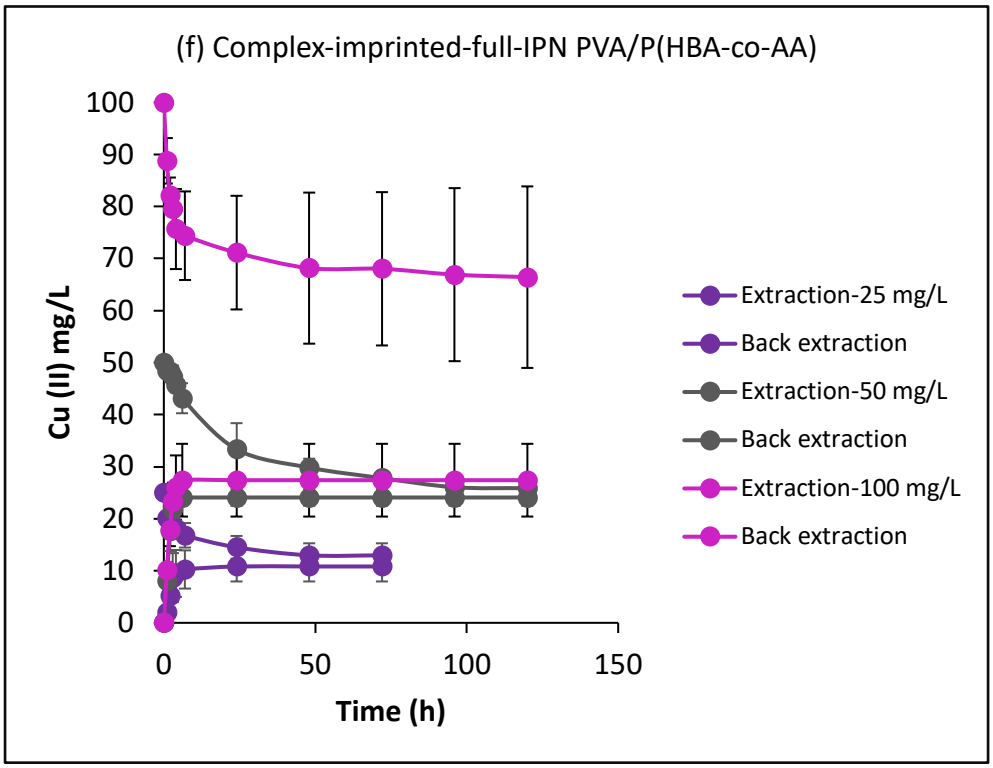
(f) Complex-imprinted-full-IPN PVA/P(HBA-co-AA)
Cu (II) mg/L
Time (h)
0
10
20
30
40
50
60
70
80
90
100
0
50
100
150
Extraction-25 mg/L
Back extraction
Extraction-50 mg/L
Back extraction
Extraction-100 mg/L
Back extraction

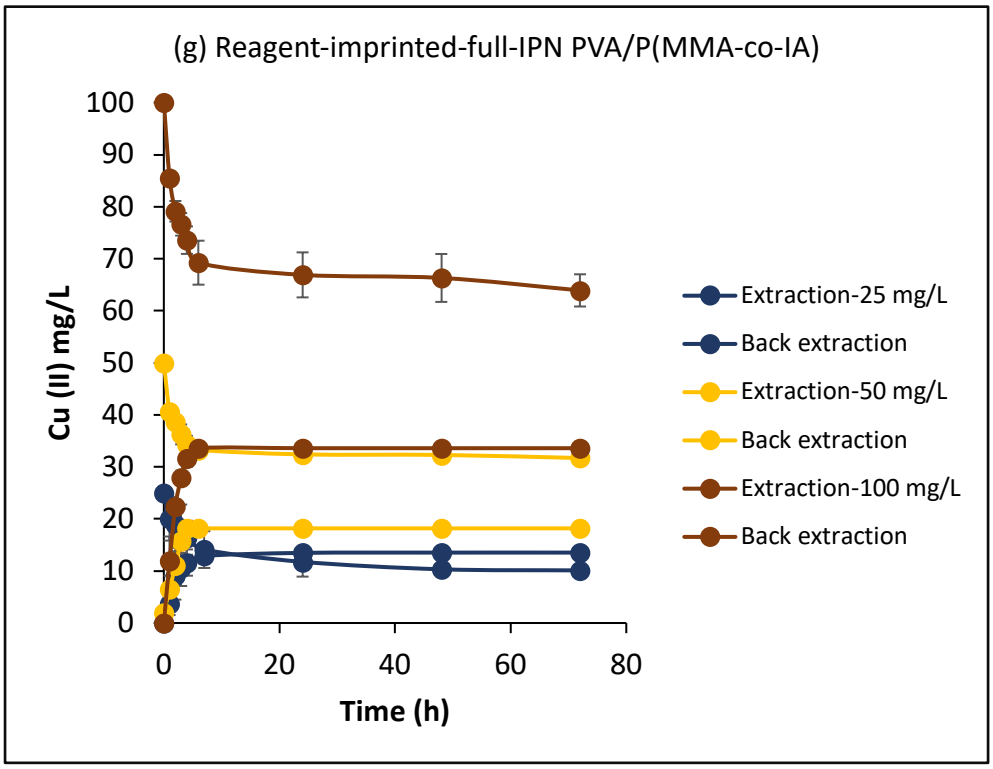

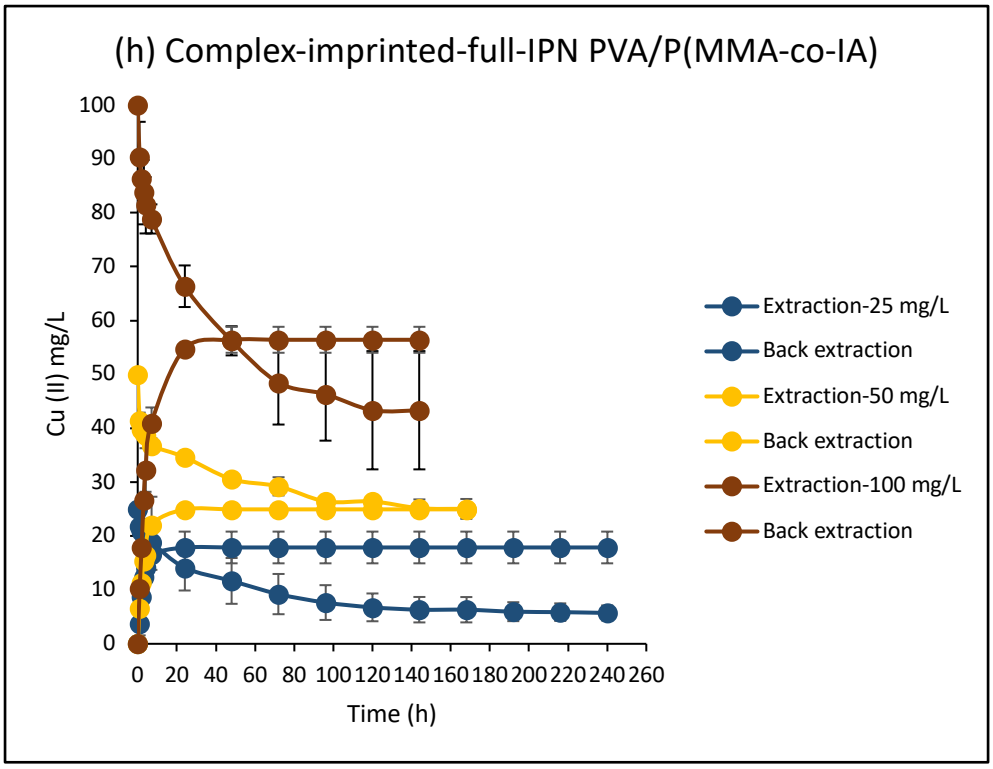

Figure 3.15. Effect of initial copper concentration on extraction of Cu (II) using the reagent (a) and complex (b) imprinted PVA/GA hydrogels, reagent (c) and complex (d) imprinted full-IPN PVA/PHEMA hydrogels, reagent (e) and complex (f) imprinted full-IPN PVA/P(HBA-co-AA) hydrogels, reagent (g) and complex (h) imprinted full-IPN PVA/P(MMA-co-IA) hydrogels.

Table 3.6. Effect of initial concentration of Cu (II) on permeability and recovery factor using reagent-imprinted-PVA/GA, full-IPN PVA/PHEMA, PVA/P(HBA-co-AA), and PVA/P(MMA-co-IA) hydrogels, complex-imprinted-PVA/GA, full-IPN PVA/PHEMA, PVA/P(HBA-co-AA), and PVA/P(MMA-co-IA) hydrogels.

Hydrogel	**Permeability (x 10^{-7}, m^2 s^{-1})**			**Recovery factor (%)**		
	Concentration (mg/L)					
	25	**50**	**100**	**25**	**50**	**100**
PVA/GA						
Reagent	2.95	6.97	6.25	28	40	18
Complex	36.2	17.7	12.3	83	55	48
PVA/PHEMA						
Reagent	11.1	1.44	3.75	34	10	10
Complex	12.5	12.9	8.10	49	49	47
PVA/P(HBA-co-AA)						
Reagent	69.0	8.81	4.43	37	21	14
Complex	7.42	4.31	2.60	43	48	28
PVA/P(MMA-co-IA)						
Reagent	24.3	21.5	18.2	54	36	34
Complex	11.2	6.46	11.4	72	50	57

3.5.7. **Kinetic study**

To understand the kinetics of the extraction process for Cu (II) using the full series of reagent-based and complex-based hydrogels, pseudo-first order reactions conditions were applied using equation 4 to interpret the experimental data. The rate constants (*k*) were calculated from the slope of plots of ln ($C_{s,0}/C_{s,t}$) versus time (shown in Figures 3.16 - 3.19) and the results are summarised in Table 3.7. The kinetic plots at all concentrations and for all hydrogels show good agreement with first-order kinetics as indicated by values of the correlation coefficient.

Based on the kinetic investigation, two hydrogels were identified as having better rates of extraction across the concentration range. Specifically, PVA/P(MMA-co-IA) and PVA/GA were the best of the reagent-based and complex-based, respectively, hydrogels. In particular, complex-based PVA/GA had the overall best rate of extraction at low concentration (25 mg/L) and a similar rate to reagent-based PVA/P(MMA-co-IA) at higher (50 & 100 mg/L) concentrations.

The kinetic investigation indicates that the extraction of copper by the reagent-based and complex-based hydrogels follows a pseudo-first order equation for all hydrogels except for complex-imprinted-full-IPN PVA/PHEMA.

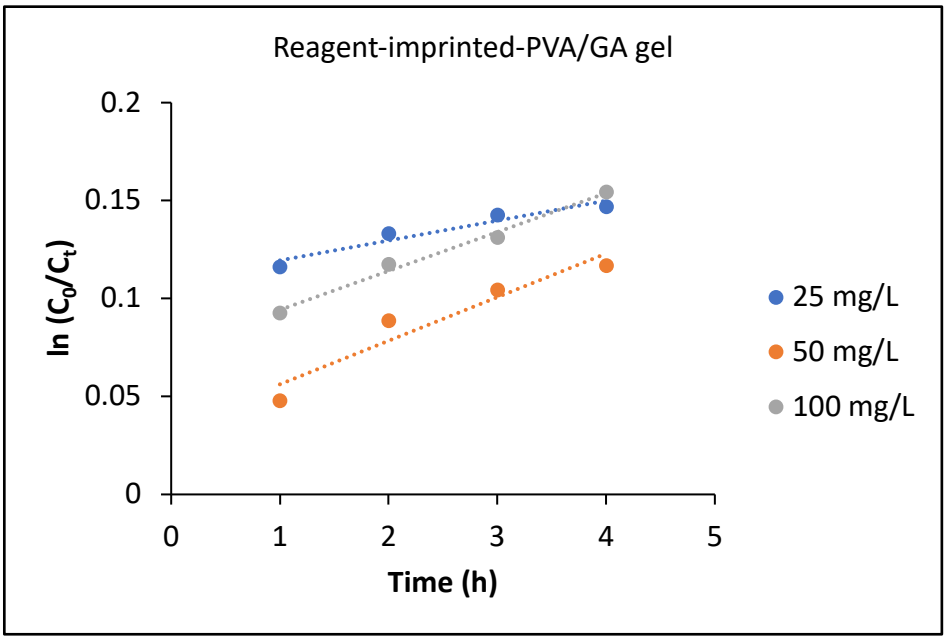

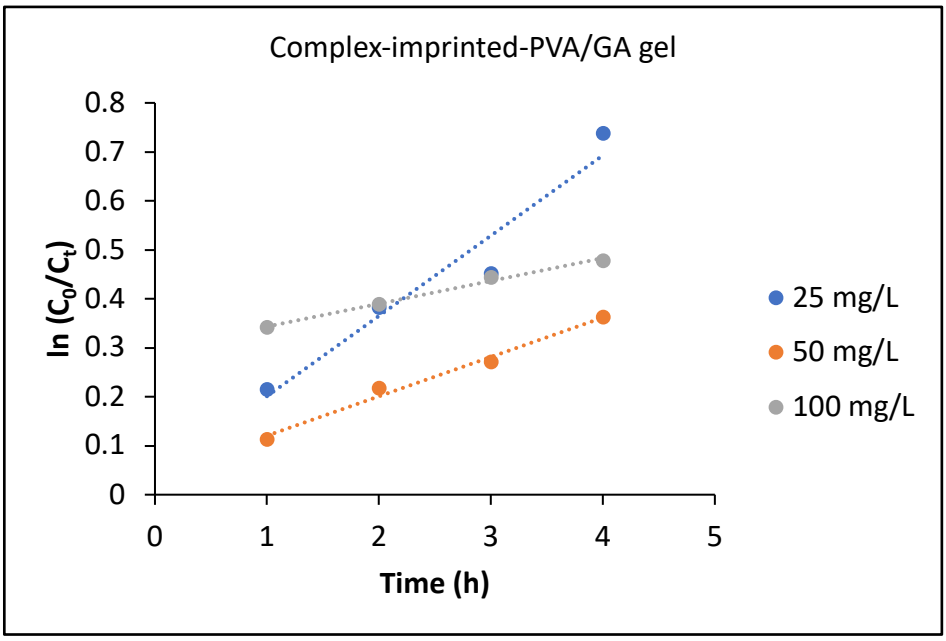

Figure 3.16. Kinetic plot for extraction of Cu (II) by reagent-imprinted-PVA/GA gel, and complex-imprinted-PVA/GA gel.

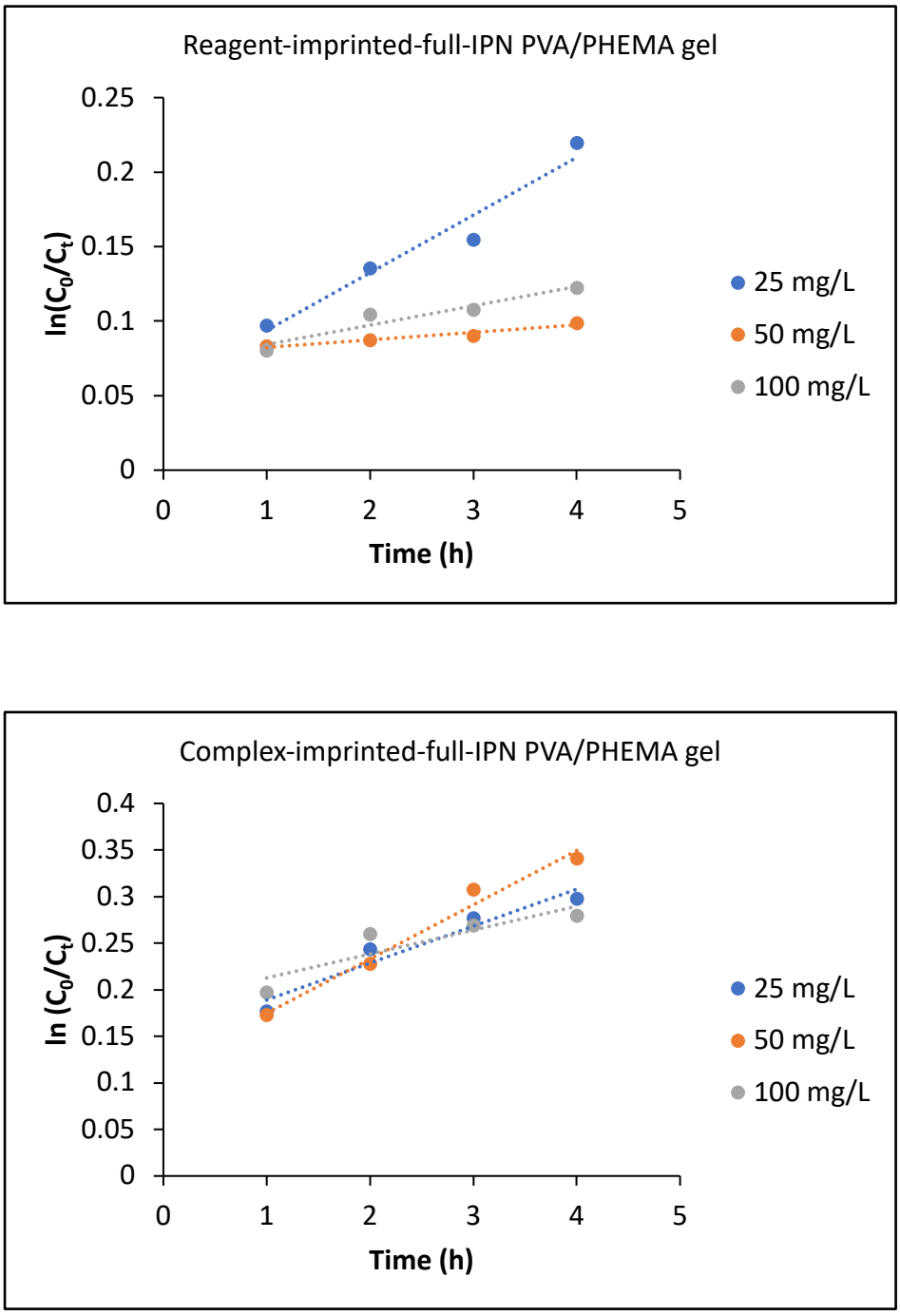

Figure 3.17. Kinetic plot for extraction of Cu (II) by reagent-imprinted-full-IPN PVA/PHEMA gel, and complex-imprinted-full-IPN PVA/PHEMA gel.

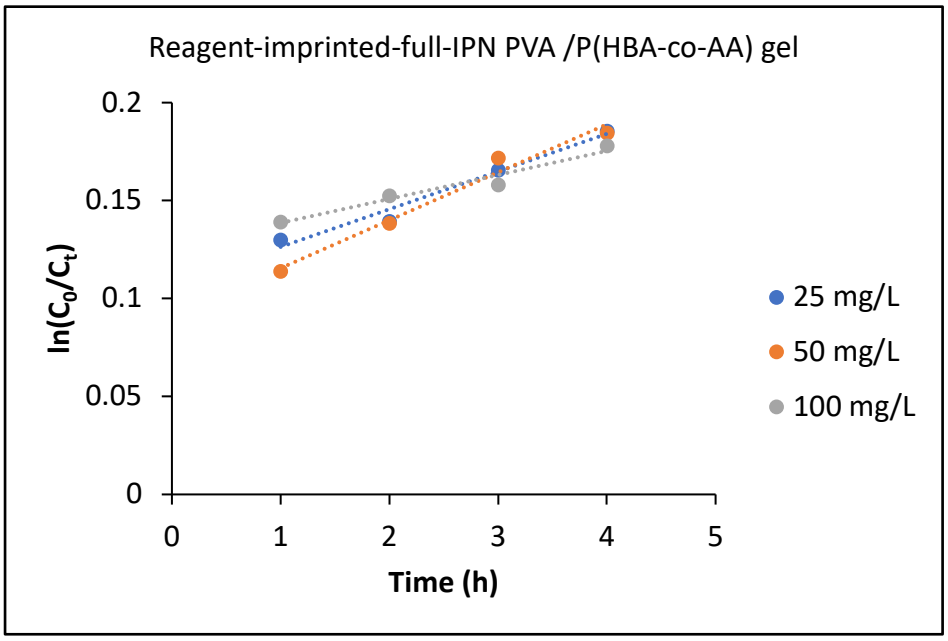

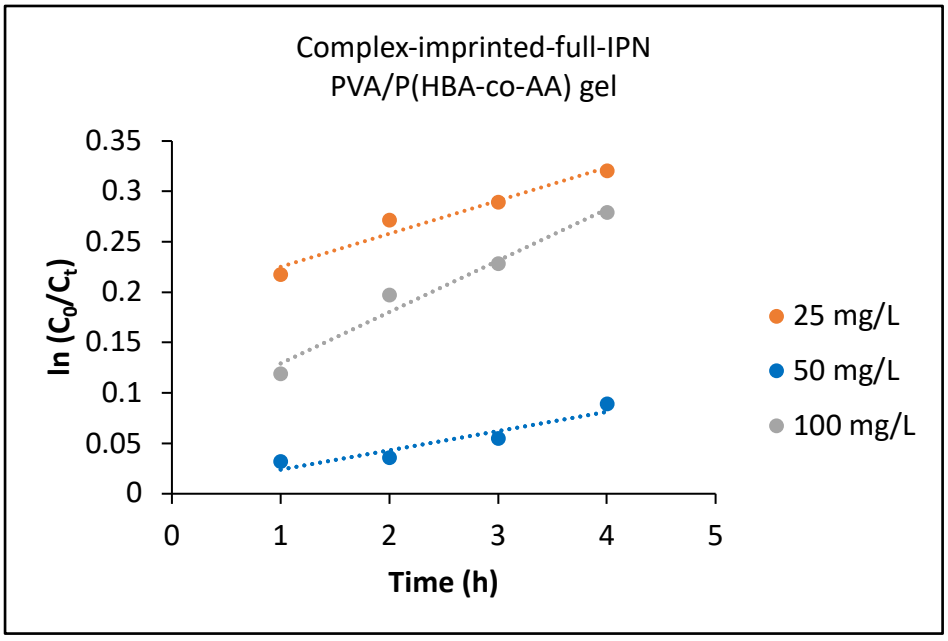

Figure 3.18. Kinetic plot for extraction of Cu (II) by reagent-imprinted-full-IPN PVA/P(HBA-co-AA) gel, and complex-imprinted-full-IPN PVA/P(HBA-co-AA) gel.

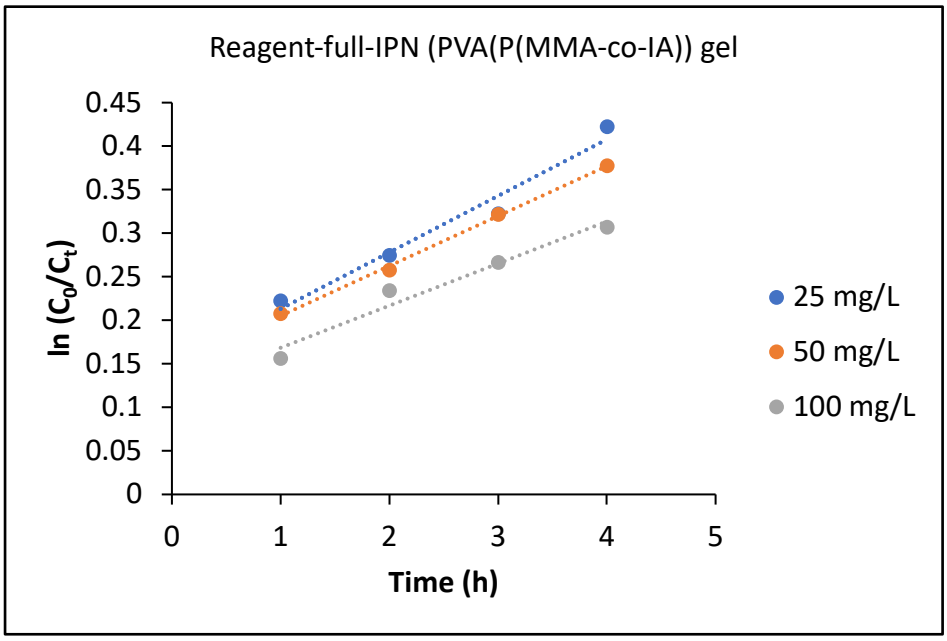

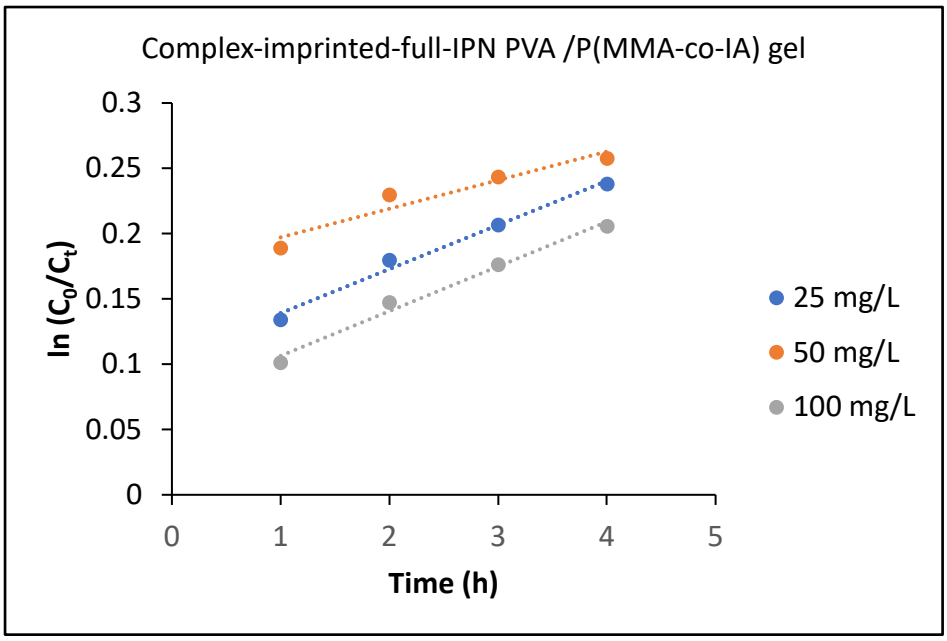

Figure 3.19. Kinetic plot for extraction of Cu (II) by reagent-imprinted-full-IPN PVA/P(MMA-co-IA), and complex-imprinted-full-IPN PVA/P(MMA-co-IA) hydrogel.

Table 3.7. Kinetic rate constant for the extraction of Cu (II) from different feed concentrations using reagent-based and complex-based PVA/GA and full-IPN hydrogels.

Hydrogel	**25 mg/L**		**50 mg/L**		**100 mg/L**	
	k **(h^{-1})**	**R^2**	***k*** **(h^{-1})**	**R^2**	***k*** **(h^{-1})**	**R^2**
Acorga P50						
PVA/GA	0.0102	0.9262	0.022	0.9175	0.0199	0.9896
PVA/PHEMA	0.0387	0.9497	0.005	0.9443	0.013	0.9229
PVA/P(HBA-co-AA)	0.0192	0.972	0.0245	0.9739	0.0123	0.9553
PVA/P(MMA-co-IA)	0.0649	0.9665	0.0573	0.9979	0.0484	0.9595
Cu (II)-Acorga P50						
PVA/GA	0.1639	0.9412	0.0804	0.9871	0.0466	0.9919
PVA/PHEMA	0.0397	0.9357	0.0582	0.9784	0.0257	0.7973
PVA**/**P(HBA-co-AA)	0.0329	0.9552	0.0201	0.9445	0.051	0.9691
PVA**/**P(MMA-co-IA)	0.0337	0.9866	0.0219	0.919	0.0342	0.9865

3.5.8. **Thermal properties**

Thermal stability at different temperatures is an important criterion if hydrogels are to be used for a range of applications including controlled drug release in biomedicine. The series of reagent-based and complex-based hydrogels were investigated by TGA over 50 – 500 ^{o}C and the thermograms are presented in Figures 3.20 & 3.21. The hydrated hydrogels were examined after preparation and after stripping of copper to ascertain if the presence of copper affected the thermal stability

As indicated in Figure 3.20 and 3.21, the use of reagent and complex as carrier templates in the hydrogel network had a great effect on the thermal properties of crosslinked PVA/GA, and full-IPN hydrogels as a function of temperature. It is remarkable that the thermograms of reagent-based and complex-based hydrogels had different thermal behaviour after preparation and after stripping of copper ions. After preparation, similar thermograms (b) involving a two-step degradation and weight loss were observed for complex-imprinted PVA/GA and full-IPN hydrogels, with the later presenting better thermal stability than the former. In terms of the TGA profiles of reagent-based hydrogels (a), however, different decomposition stages of weight loss were observed, with two and three stages for PVA/GA and full-IPN hydrogels, respectively.

After stripping of copper, the thermograms of complex-based and regent-based hydrogels indicated four weight loss stages over the temperature range. In general, reagent-based hydrogels showed a higher degradation rate than similar complex-based hydrogels.

The first decomposition step was recorded between 50 – 150 ^{o}C for all hydrogels and is attributed to the evaporation of entrapped water. As the temperature increased from 150 to 450 ^{o}C, two further thermal decomposition phases due to likely degradation of carrier and side chains of polymers, including decarboxylation, within the hydrogel network. A subsequent weight loss occurred above 450 ^{o}C that was related to the final decomposition of any remaining crosslinking or IPN structure within the hydrogels and decomposition of the polymers. The reagent-based hydrogels had slightly better thermal stability between 50 – 150 ^{o}C) coinciding with temperatures for practical application. No significant differences were noted at 50 -100 ^{o}C, indicating both carrier-type hydrogels offer good thermal stability for biomedical applications.

The TGA investigation indicated that both reagent-based and complex-based hydrogels before the removal of copper had good thermal stability at lower temperature, whereas a reduced thermal stability over the same temperature range was observed for these hydrogels after stripping of copper. However, at increased temperatures from 400 to 500 ^{o}C, the copper containing hydrogels had improved thermal stability compared to pre-extraction hydrogels. The presence of copper within the hydrogel network increases the heat capacity that confers thermal stability, requiring a higher temperature to degrade the IPN of the hydrogels.

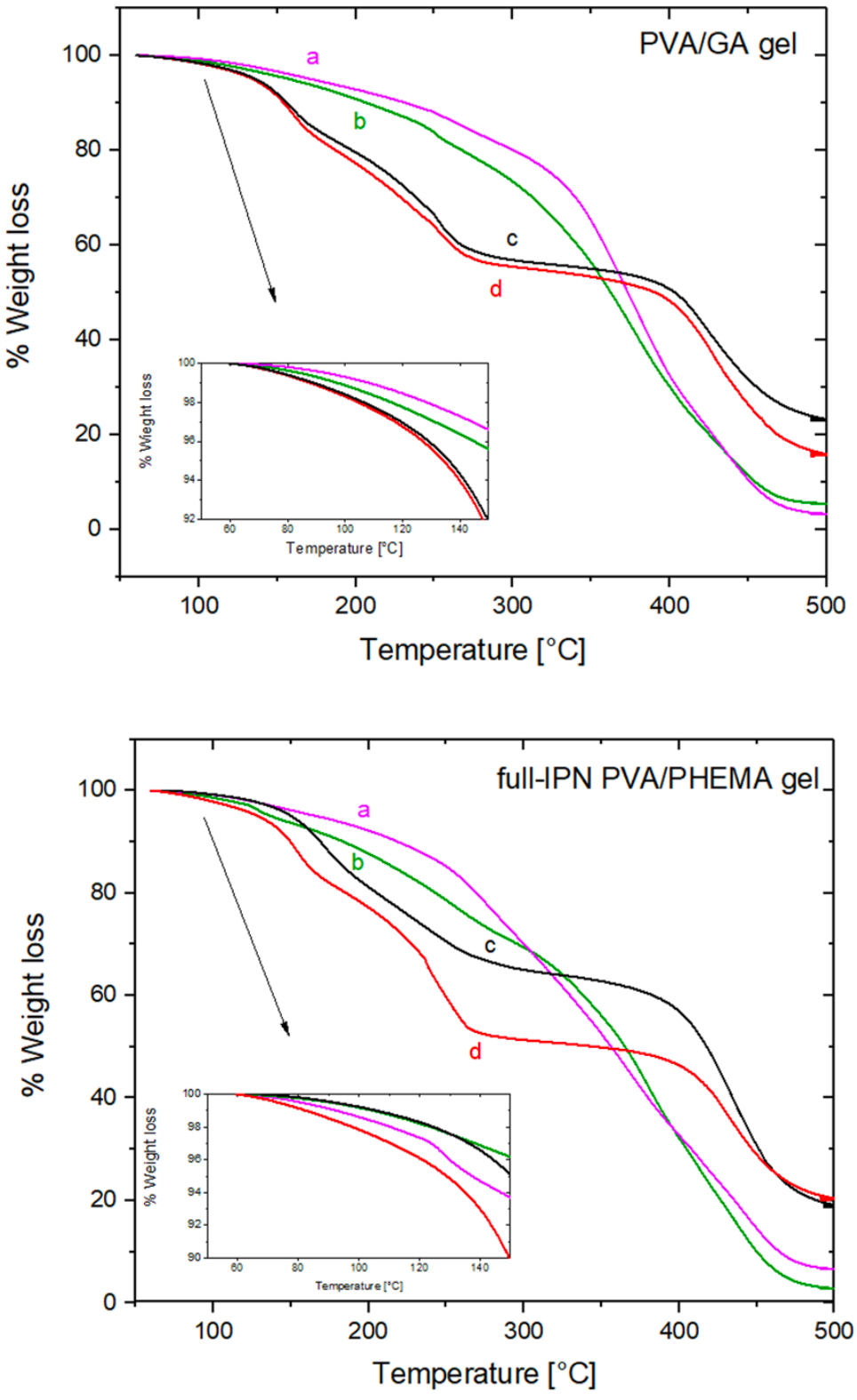

Figure 3.20. TGA curves of reagent (a) and complex (b) imprinted PVA/GA gels after preparation, reagent (c) and complex (d) imprinted PVA/GA gels after stripping of Cu (II) (upper); and, reagent (a) and complex (b) imprinted full-IPN PVA/PHEMA gels after preparation, and reagent (c) and complex (d) imprinted full-IPN PVA/PHEMA gels after stripping of Cu (II) (lower).

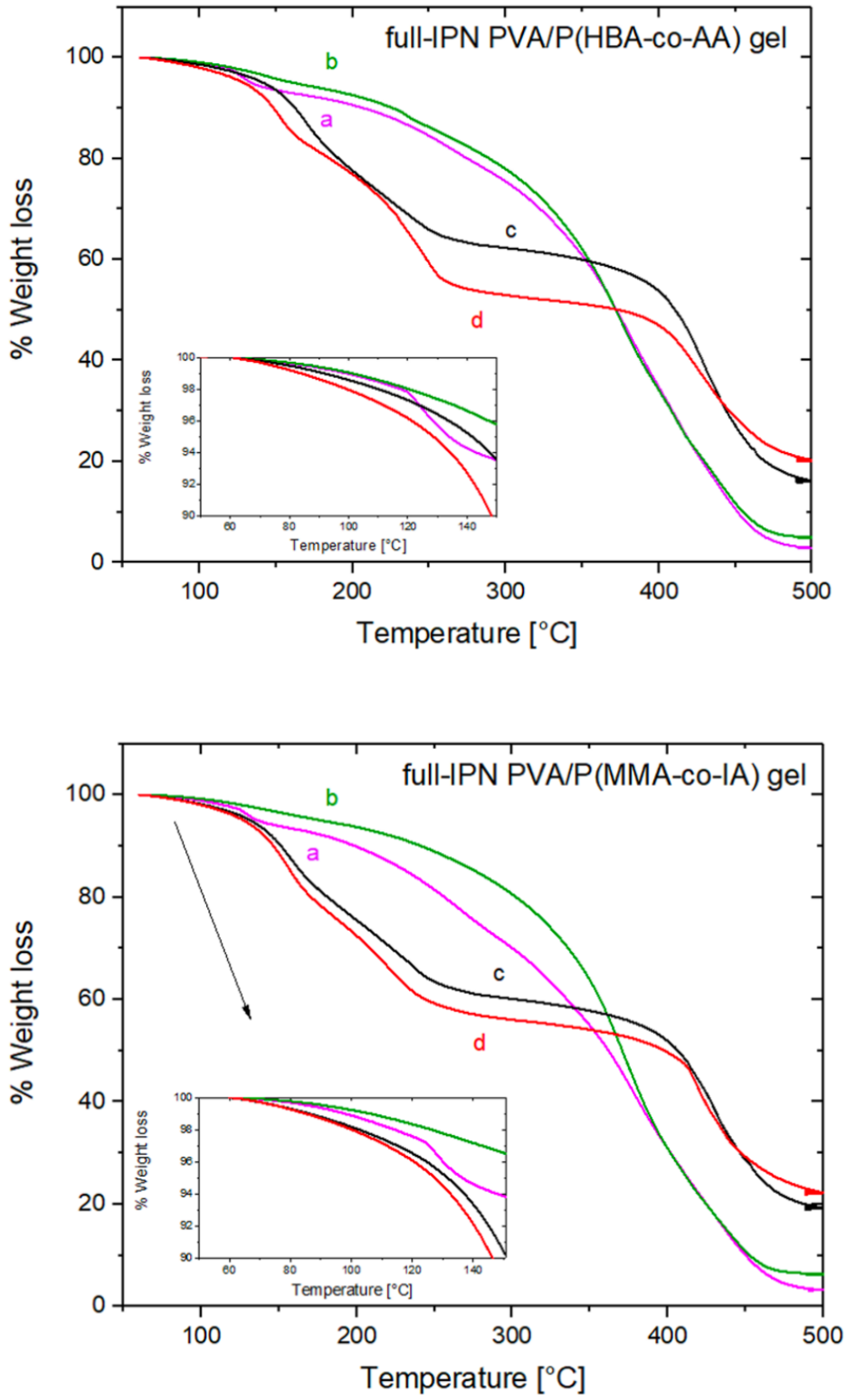

Figure 3.21. TGA curves of reagent-(a) and complex (b) imprinted full-IPN PVA/P(HBA-co-AA) gels after preparation, reagent (c) and complex (d) imprinted full-IPN PVA/P(HBA-co-AA) gel after stripping of Cu (II) (upper); and, reagent (a) and complex (b) imprinted full-IPN PVA/P(MMA-co-IA) gels after preparation, and reagent (c) and complex (d) imprinted full-IPN PVA/P(MMA-co-IA) gels after stripping of Cu (II) (lower).

3.5.9. **Scanning electron microscopy (SEM)**

The surface morphology and microstructure of hydrogels can affect the extraction performance. To investigate these effects, the full series of hydrogels after preparation, and after use in extraction and back-extraction experiments were examined using SEM and the micrographs are shown in Figures 3.22-3.25.

Differences in the surface morphology of reagent-based and complex-based hydrogels were apparent. For instance, the complex-based hydrogels after preparation, have a distribution of surface pores and bubbles, as shown in Figure 3.22. These surface features contain templated sites for copper recognition and extraction. However, the same hydrogels after stripping of Cu (II) (Figure 3.23) have a more uniform distribution of surface pores of similar size. Also, no surface bubbles are now apparent, presumably these surface features are disrupted as copper (II) is stripped from the hydrogel. The complex-imprinted PVA/GA had a higher number of larger cavities compared with other hydrogels. Whereas, a larger number of small cavities were observed on the surface of complex-based PVA/P(HBA-co-AA) after stripping of copper. The variation in the distribution of cavities of the various hydrogels, which is readily apparent in Figure 3.26, is attributed to polymer composition and the presence of functional groups that have different interactions with the reagent and complex. The larger number of surface pores increases the surface area that enhances the mass transfer of copper resulting in improved adsorption kinetics. A similar effect on extraction rate due to surface morphology has been noted for a novel Cu (II)-imprinted semi-IPN PVA/PAA hydrogel that had a rougher surface after being used for extraction[167].

Noticeably, the SEM images of the reagent-based hydrogels after preparation indicated a smooth, homogeneous surface with a larger pore size as indicated in Figure 3.24. A consistent distribution of porous layers was observed across the surface of reagent-based full-IPN PVA/PHEMA and PVA/P(HBA-co-AA) hydrogels. However, after several uses in the extraction and back-extraction process, a less porous surface structure was noted (Figure 3.25). The postulated reason for this was the loss of Acorga P50 content from the hydrogel, resulting in a collapse of pores in the hydrated full-IPN. In other words, less binding sites are available in the hydrogel as Acorga P50 partitions to the aqueous phase. Approximate pore size and pore count from representative surface areas of the

hydrogels are indicated in Table 3.8. The SEM observations support the results from the extraction study (section 3.19).

The surface morphology features of full-IPN hydrogels is affected by the size of carrier template used during preparation. Use of Cu (II)-Acorga P50 complex as a template during the polymerisation process to prepare PVA/GA and full-IPN hydrogels generated more stable cavities as sites for enhanced extraction of copper compared to similar Acorga P50 reagent hydrogels.

Table 3.8. Range of pore size and pore count from representative surface areas of complex-imprinted-PVA/GA, and full-IPN hydrogels and reagent-imprinted PVA/GA, and full-IPN hydrogels after stripping of Cu (II).

Hydrogel	**Pore count (approximate)**	**Pore size (μm, range)**
Complex-imprinted-PVA/GA gel	80	6-8
Complex-imprinted-full-IPN PVA/PHEMA	160	2-6
Complex-imprinted-full-IPN PVA/(HBA-co-AA)	300	2-3
Complex-imprinted-full-IPN PVA/(MMA-co-IA)	170	2-5
Reagent-imprinted-PVA/GA gel	185	2-3
Reagent-imprinted-full-IPN PVA/PHEMA	140	3-4
Reagent-imprinted-full-IPN PVA/(HBA-co-AA)	100	4-8
Reagent-imprinted-full-IPN PVA/(MMA-co-IA)	90	1-2

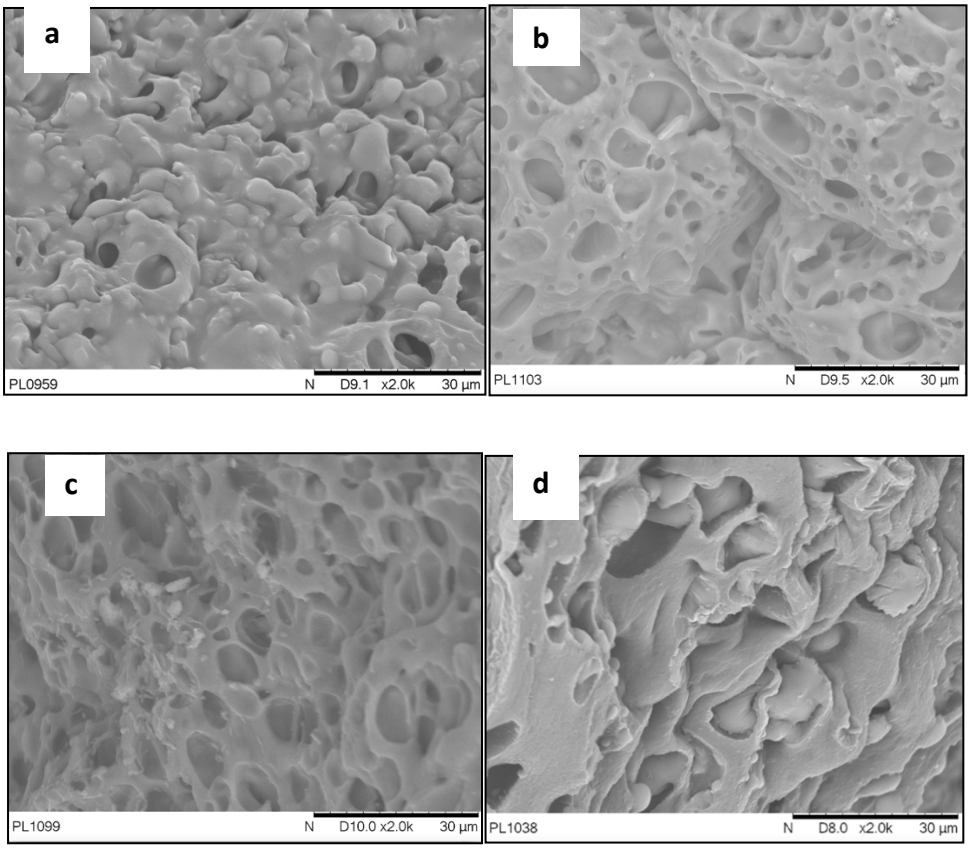

Figure 3.22. SEM images of complex-based hydrogels after preparation: PVA/GA (a), full-IPN PVA/PHEMA (b), full-IPN PVA/P(HBA-co-AA) (c), and full-IPN PVA/P(MMA-co-IA) (d).

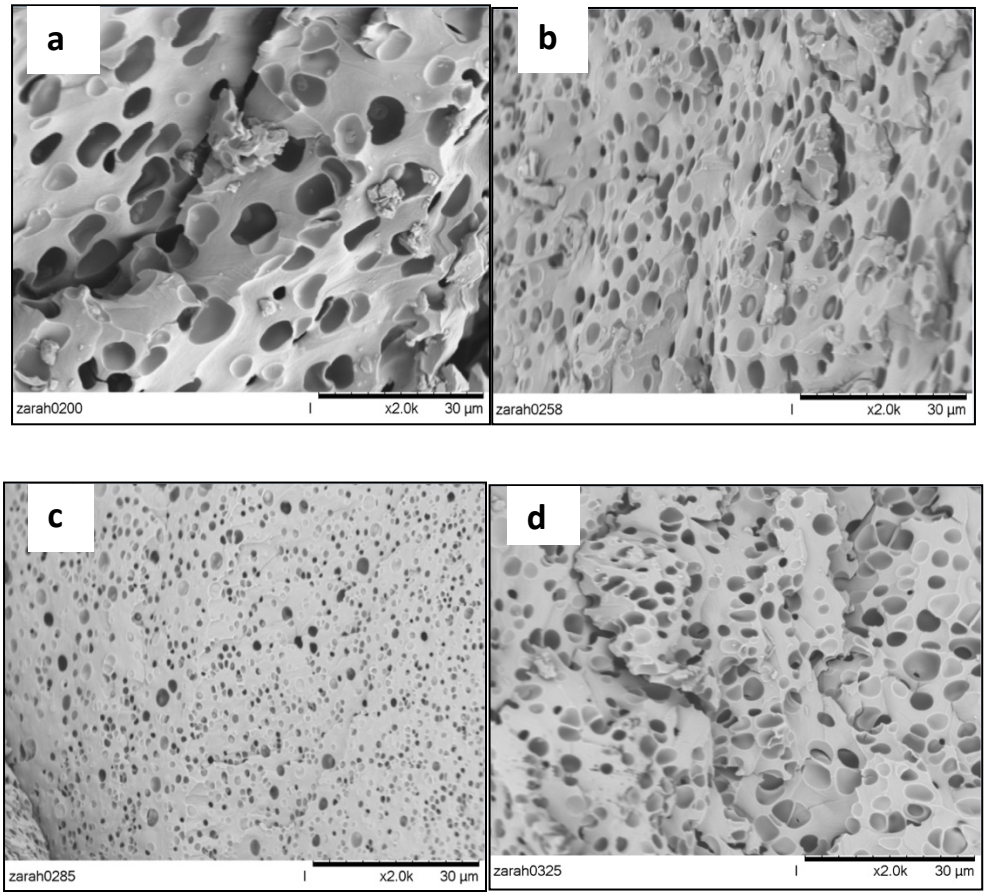

Figure 3.23. SEM images of complex-based hydrogels after stripping of Cu (II): PVA/GA (a), full-IPN PVA/PHEMA (b), full-IPN PVA/P(HBA-co-AA) (c), and full-IPN PVA/P(MMA-co-IA) (d).

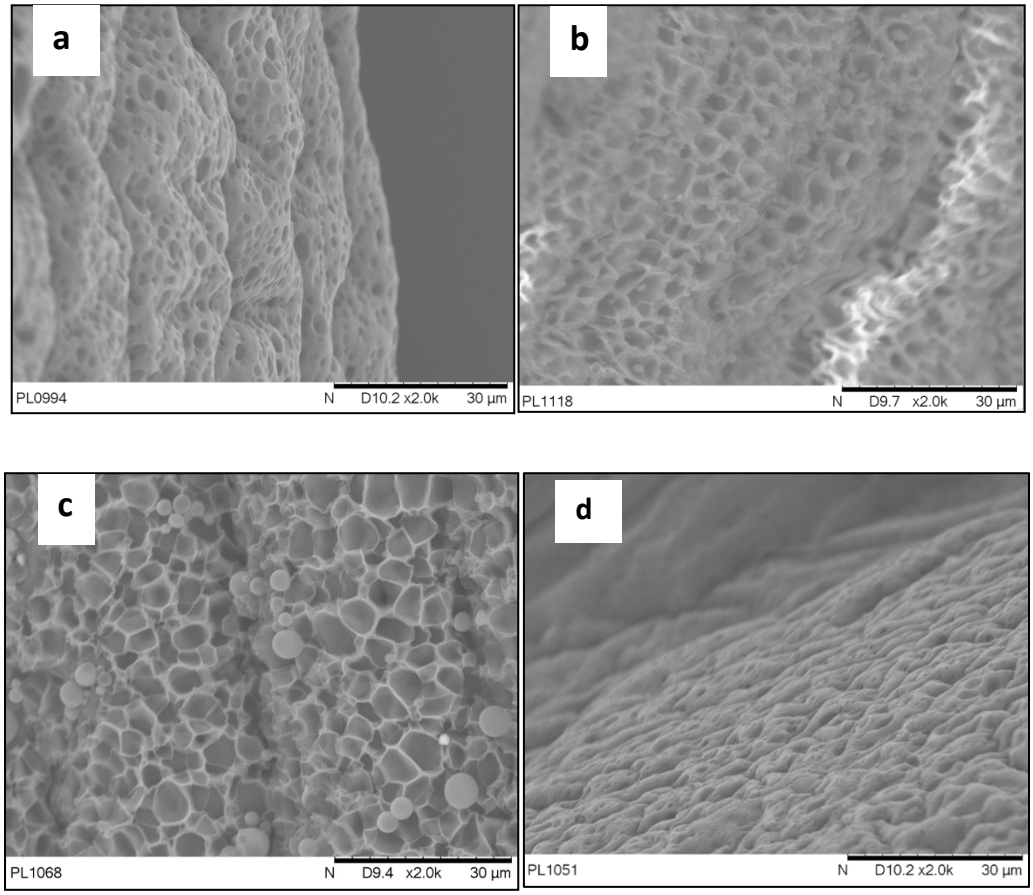

Figure 3.24. SEM images of reagent-based hydrogels after preparation: PVA/GA (a), full-IPN PVA/PHEMA (b), full-IPN PVA/P(HBA-co-AA) (c), and full-IPN PVA/P(MMA-co-IA) (d).

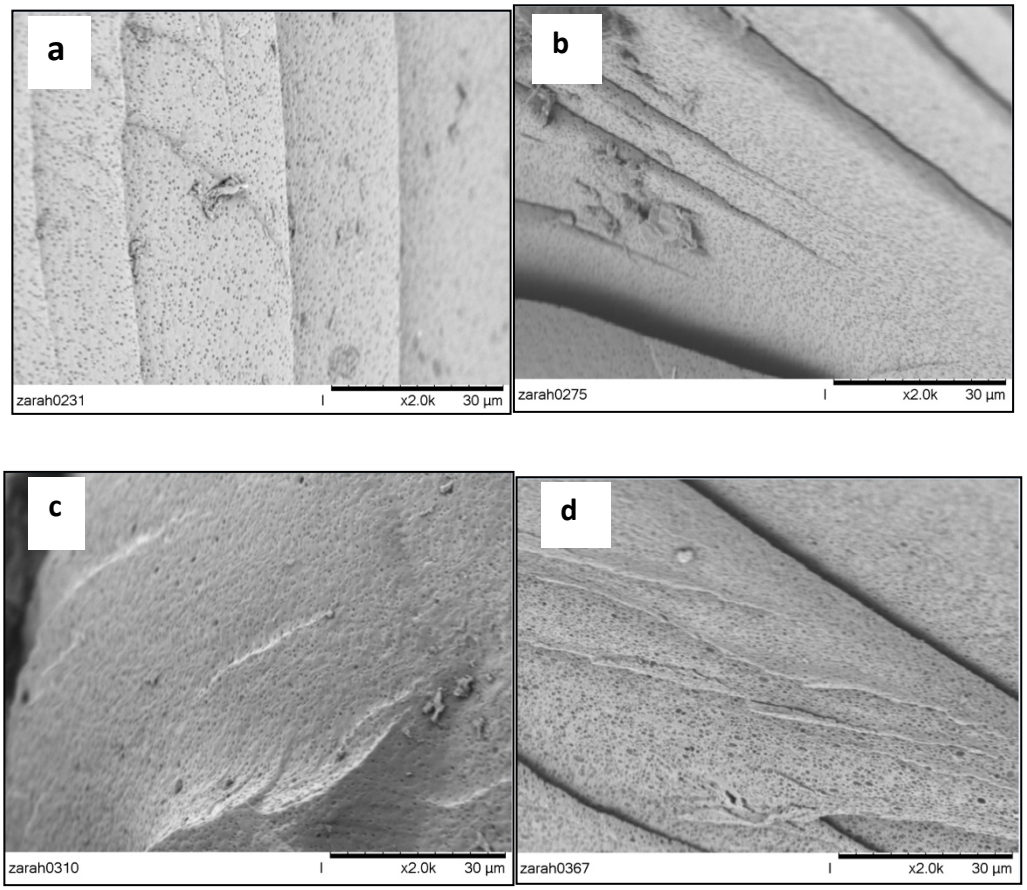

Figure 3.25. SEM images of reagent-based hydrogels after stripping of Cu (II); PVA/GA (a), full-IPN PVA/PHEMA (b), full-IPN PVA/P(HBA-co-AA) (c), and full-IPN PVA/P(MMA-co-IA) (d).

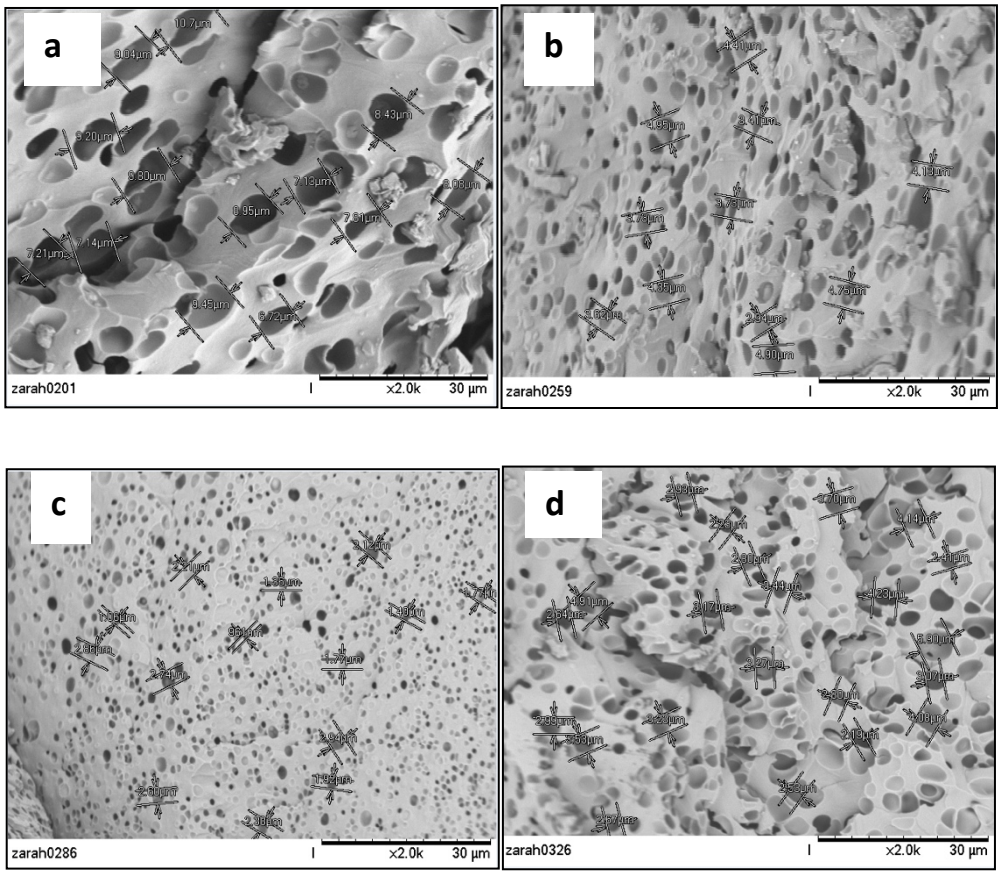

Figure 3.26. Distribution of pore size of complex-based hydrogels after stripping of Cu (II): PVA/GA (a), full-IPN PVA/PHEMA (b), full-IPN PVA/P(HBA-co-AA) (c), and full-IPN PVA/P(MMA-co-IA) (d).

3.6. Conclusion

A novel series of crosslinked PVA/GA and full-IPN hydrogels containing either Cu (II)-Acorga P50 complex or Acorga P50 reagent as molecular templates for a copper carrier were prepared and tested as adsorbents to extract Cu (II) from aqueous solutions.

Full-IPN hydrogels were prepared using different monomers, including HEMA, HBA, AA and IA, where used in a free radical polymerisation process to prepare a series of full-IPN PVA/PHEMA, PVA/P(HBA-co-AA) and PVA/P(MMA-co-IA) hydrogels. Investigation using FTIR indicated that Cu (II)-Acorga P50-complex could be successfully used as a molecular carrier imprint during preparation of the hydrogel and the Cu (II) successfully removed using 2 M H_2SO_4. The influence of type of carrier template on Cu (II) extraction performance was investigated and showed better extraction using complex-imprinted hydrogels.

The effect of pH of the feed solution on the extraction of Cu (II) was examined at pH 2 and 5, with better extraction performance noted at pH 5 for the reagent-based PVA/GA and full-IPN hydrogels. Some extraction of copper was noted at pH 5 for non-carrier imprinted hydrogels due to the Cu (II) interaction with the polar side chains of the polymers; although, the extraction was substantially less than for similar carrier-imprinted hydrogels.

As the initial Cu (II) concentration in solution increased from 25 to 100 mg/L, the initial permeability values and extraction efficiency of copper decreased due to the limited number of available extraction sites on the surface of the hydrogel. A kinetic investigation at different concentrations showed the extraction process followed a first-order reaction model. Further insights into the physical properties of the hydrogels were revealed by SEM and TGA investigations. The presence of many surface pores, especially after stripping of copper from the template, was revealed by SEM. The resulting increased surface area was related to the observed enhanced extraction performance a result of insertion of copper ions as template, which was confirmed by SEM. The thermal stability, as revealed by TGA, at low temperatures was similar for both series of carrier-imprinted hydrogels. However, mid-range and high-end temperature stability was better for reagent-based and complex-based hydrogels, respectively. On the basis of these investigations, complex-based cross-linked PVA/GA and reagent-based full-IPN

PVA/P(MMA-co-IA) were identified as promising hydrogels for use as adsorbents for copper extraction.

Chapter 4: Extraction of naproxen from aqueous solutions using novel Aliquat 336-full-IPN hydrogels.

4.1. Introduction

The production of hydrogel adsorbents and biosorbents has increased rapidly in the last two decades. According to Ding et al., this has generated significant attention in the treatment and purification of water from various pollutants[216]. The motive for this interest results from the availability of various methods of preparing and modifying hydrogels with regards to either chemical or physical binding through crosslinking, grafting, blending, ion-imprinting methods and impregnation to enhance mechanical and adsorption properties. Maleki et al. stated that immobilisation and functionalisation of hydrogel sorbents can be done with some reactive groups, such as carboxyl, hydroxyl, and amino, after proper treatment[217]. This helps to create 3D network structures, which are effective in adsorption of inorganic and organic pollutants from water. These structures also have a high capacity to swell and retain water[218]. Novel adsorbent hydrogels composed of sodium alginate modified with amine derivative were prepared and used to efficiently remove methyl blue from water[219]. An investigation was carried out on the removal of methyl orange onto newly prepared hydrogel including TiO_2 and polyacrylamide[220]. The preparation of 3D graphene hydrogels was done and they were used to remove ofloxacin from aqueous solutions[221]. The removal of tetracyclinae by hydrogels based on double-metal/cross-linked alginate and graphene was investigated by advanced Fenton reaction[222]. The removal of some antibiotics from aqueous solutions was enhanced using triple-network nanocomposite hydrogels composed of sodium alginate and carbon nanotubes-graphene oxide[223].

Naproxen (Figure 4.1) is a nonsteroidal anti-inflammatory drug used to reduce fever, pain, and ongoing inflammation. It can be detected in water as result of waste from households and hospitals. The concentration of naproxen in wastewater has been reported from 0.37 - 1.70 µg/L to 23.21 µg/L in Australia[224]. Additionally, naproxen can be found in groundwater due to landfill leachate and manufacturing residues[225].

The Pisum sativum pods biochar/ starch hydrogel N-PSPB/SHGL, which is a newly designed nanosorbent hydrogels was successfully synthesised and used for removal of Cr (VI) and naproxen drug (NAP). The maximum swelling capacity of N-PSPB/SHGL was observed (500.0%) at room temperature. The stability of nanosorbent was assessed based on 10 adsorption cycles with about regeneration by 0.1 mol/L HCl. N-PSPB/SHGL has confirmed excellent capacity values as 309.82 and 420.13 mg g^{-1} for NAP drug and Cr(VI), respectively[226].

Oxidized starch/CuO bionanocomposites were prepared and an investigation done on its strengths as an antibacterial colon drug delivery system. FT-IR and XRD techniques were used to verify the successful formation of the CuO-nanoparticles (CuO NPs) within the oxidized starch hydrogel matrix. SEM image disclosed the development of the white spherical spots that are associated with the formation of CuO NPs with a mean diameter of 35–40 nm within the hydrogel network. Results of the investigation to show the swelling and NPX loading degree revealed that an increase in the concentration of Cu2þ from the 0 to 0.01 M increased the swelling, however, additional increase in this concentration to 0.03 caused a decrease of the swelling. The highest value of naproxen release for was observed for C2 coded bio-nanocomposite near to 70%[227].

There are several criteria in choosing extractants in preparation of PIMs, including their ability to form hydrogen bonding and participate in dipole-dipole reactions[228]. Consequently, the active functional groups of polymers in hydrogels are also able to participate in dipole-dipole interactions.

Aliquat 336 (Figure 4.1) is a phase-transfer catalyst that is composed of a mixture of quaternary ammonium chloride[229] and that has been used widely as a basic carrier in preparation of PIMs to accelerate the extraction of polar organic solutes, including phenylalanine, phenols, and carboxylic acids[230].

James et al. prepared the first PIMs that contained PVC and Aliquat 336—they were used as ion-selective electrodes more than four decades ago[231]. For the extraction and transport of organic compounds, there have been a few studies performed on PIMs that were limited to carbohydrates[230].

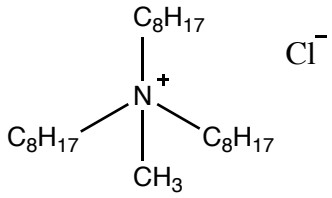

Aliqaut 336

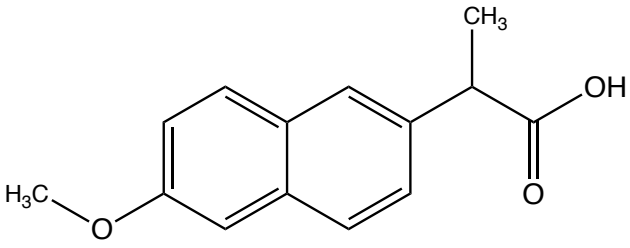

Naproxen, $pK_a = 4.2$

Figure 4.1. Chemical structure of Aliquat 336 and Naproxen.

The selective extraction of a particular organic from a mixture of similar compounds by PIMs, which have a mostly hydrophobic character, is somewhat problematic because the selective chemistry is not as specific compared to the extraction of metal ions. The hydrophilic nature of hydrogels provides an environment that is useful for absorption of organic compounds with a polar nature from aqueous solutions. Hydrogels as a system for the delivery of drugs has been widely investigated, however, extraction of organic solutes using hydrogels incorporating extractants has yet to be reported.

The insertion of Aliquat 336 into a hydrogel network would be a useful way to prepare a new generation of adsorbents to remove organic solutes from aqueous solutions. The hydrogels obtained by the method of interpenetrating polymeric networks is convenient for fabricating materials with improved mechanical stability. The use of Aliquat 336 as a carrier and its immobilisation in a full-IPN matrix has not been investigated.

The aim of this current work is to load Aliquat 336 as a basic carrier within a series of full-IPN of hydrogels prepared from poly(vinyl alcohol) (PVA) as the base polymer and using different monomers, such as 2-hydroxy ethyl methacrylate (HEMA), 4-hydroxybutyl

acrylate (HBA), acrylic acid (AA), methyl methacrylate (MMA), and itaconic acid (IA). The chemical structure of Aliquat 336-functionalised PVA/GA full-IPN hydrogels will be investigated by Fourier-transform infrared spectroscopy (FTIR). Aliquat 336 can likely be trapped in a full-IPN matrix by participating in strong dipole-dipole interactions between quaternary ammonium cations with hydroxyl groups of PVA and carboxyl groups of PIA. Naproxen was selected as a model organic solute for the extraction study because it exists as an anion at pH 7. Water uptake studies will be performed at 37°C to investigate the effect of Aliquat 336 on the swelling behaviour of hydrogels. Extraction studies of naproxen will use a feed solution of 125 mg/L at pH 7 and back-extraction performed using 1 M NaCl at pH 9. The kinetics of naproxen extraction through hydrogel samples will also be investigated. The thermal and morphological properties of the Aliquat 336 PVA/GA full-IPN hydrogels will be studied using thermogravimetric analysis (TGA) and scanning electron microscopy (SEM).

4.2. Experimental

4.2.1. Materials

Poly(vinyl alcohol) (PVA) (99+% hydrolysed) (Aldrich), and Ethylene glycol dimethyl acrylate (EGDMA) (Aldrich) Glutaraldehyde (GA) (Aldrich), Itaconic acid (IA) (Aldrich), and, Methyl methacrylate (MMA) (Aldrich), 2-hydroxyethyl methacrylate (HEMA). (Aldrich), 4-hydroxybutyl acrylate (HBA) (Aldrich), and Acrylic acid (AA) (Aldrich) were used as reactants to prepare the hydrogels. MMA was purified by washing with 0.5% NaOH. HEMA, HBA, AA were purified by passing through an activated alumina column chromatography and verified by ^{1}H-NMR. PVA, IA, EGDMA and GA were used as received. 2, 2'-Azobisisobutyronitrile (AIBN) initiator was purified by recrystallization from ethanol[156]. Dimethylsulfoxide (DMSO) was used as a solvent for polymerisation. Sulfuric acid (H_2SO_4) was used as catalyst. Naproxen was supplied from Whittlesea Pharmacy. Sodium chloride (NaCl) (Aldrich) was used to prepare a stripping solution and the pH adjusted with 1 M NaOH. Sodium dihydrogenphosphate dihydrate ($NaH_2PO_4.2H_2O$), and Disodium hydrogenphosphate heptahydrate ($Na_2HPO_4.7H_2O$) were used to prepare a sodium phosphate buffer solution.

4.2.2. Preparation of Aliquat 336-full-IPN hydrogels

Aliquat 336-full-IPN hydrogels were prepared by using the same method used to prepare full-IPN hydrogels, with Acorga P50 and Cu (II) Acorga P50 complex as carriers by replacing these carriers with Aliquat 336.

The feed composition used for hydrogel preparations is reported in Table 4.1. Images of the physical appearance of the Aliquat 336 containing PVA/GA and full-IPN hydrogels are shown in Figure 4.2. The method to prepare Aliquat 336 PVA/GA and full-IPN hydrogels is indicated in Scheme 4.1.

Table 4.1. Feed composition used to prepare PVA/GA, and full-IPN hydrogels containing Aliquat 336.

Hydrogel	**PVA (wt%)**	**GA (wt%)**
Aliquat 336 -PVA/GA	50	30
Aliquat 336- full-IPN PVA/PHEMA	40	30
Aliquat 336-full-IPN PVA/P(HBA-co-AA)	40	20
Aliquat 336-full-IPN PVA/P(MMA-co-IA)	40	20

AIBN= 0.1 g, H_2SO_4= 0.1 mL, EGDMA= 0.5 wt %, HEMA = 5 wt%, HBA = 5 wt%, AA = 10 wt%, MMA = 5 wt%, IA = 10 wt %, Aliquat 336 = 20 wt%, and 20 mL DMSO.

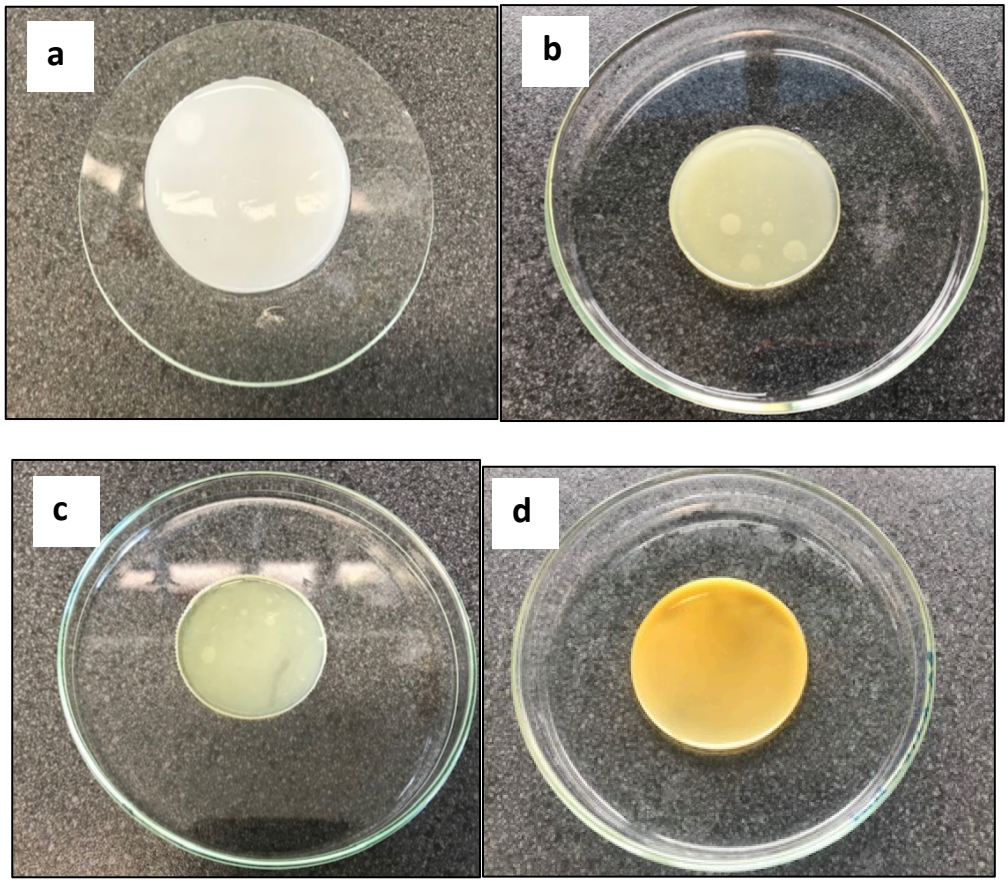

Figure 4.2. Images of the physical appearance of Aliquat 336-PVA/GA gel (a), full-IPN PVA/PHEMA gel (b), full-IPN PVA/P(HBA-co-AA) gel (c), and full-IPN PVA/P(MMA-co-IA) gel (d).

4.2.3. **Water uptake measurements**

The process for the swelling study was explained in detail in chapter 2.

4.2.4. **Extraction and back-extraction study**

To investigate the extraction of naproxen, Aliquat 336 PVA/GA, Aliquat 336-full-IPN PVA/PHEMA, Aliquat 336-full-IPN PVA/(PHBA-co-AA), and Aliquat 336-full-IPN PVA/P(MMA-co-IA) hydrogels were placed in 100 mL aqueous solution of naproxen (125 mg/L, pH 7) and allowed to reach equilibrium for six days at room temperature. The extraction profile of naproxen by full-IPN hydrogels was constructed by withdrawing 0.1 mL and diluting with pH 7 buffer at regular times; removed amount was replaced with fresh naproxen solution. Samples were analysed by UV spectroscopy (Cary UV-Vis

spectrophotometer). The equilibrium concentration of naproxen was determined from the appropriate calibration graph obtained with the solutions of known concentrations of naproxen. The back-extraction profile was determined by sampling 0.1 mL of the stripping solution (100 mg/L, 1 M NaCl, pH 9) at regular time intervals. Samples were diluted with pH 9.0 buffer for UV-Vis measurement at 230 nm. The withdrawn samples were replaced by fresh NaCl solution.

4.3. Characterisation

4.3.1. Infrared Spectroscopy

The chemical structure of the PVA/GA, full-IPN PVA/PHEMA, full-IPN PVA /P(HBA-co-AA), and full-IPN PVA/P(MMA-co-IA) hydrogels with Aliquat 336 was investigated by FTIR spectroscopy. The instrument details and measurement process were explained in detail in the previous section.

4.3.2. Scanning electron microscopy (SEM)

The process of using SEM to investigate the surface morphology was explained in the chapter 2.

4.3.3. Thermogravimetric Analysis (TGA)

The process of using TGA to investigate the thermal properties was explained in the chapter 2.

4.3.4. Extraction kinetics

The kinetic study was carried out in the same way as reported in chapter 3.

4.3.5. Proton Nuclear Magnetic Resonance (^{1}H-NMR)

The effectiveness of the back-extraction process to remove naproxen from the hydrogels was investigated by ^{1}H-NMR. The back-extraction solution containing naproxen

was extracted with chloroform. The organic phase was separated and dried with a drying agent. The resulting solid was dissolved in dimethyl sulfoxide-d6 and the ^{1}H-NMR spectrum acquired. The extracted solid was confirmed as naproxen by comparison of the acquired spectrum with that of a spectrum of pure naproxen.

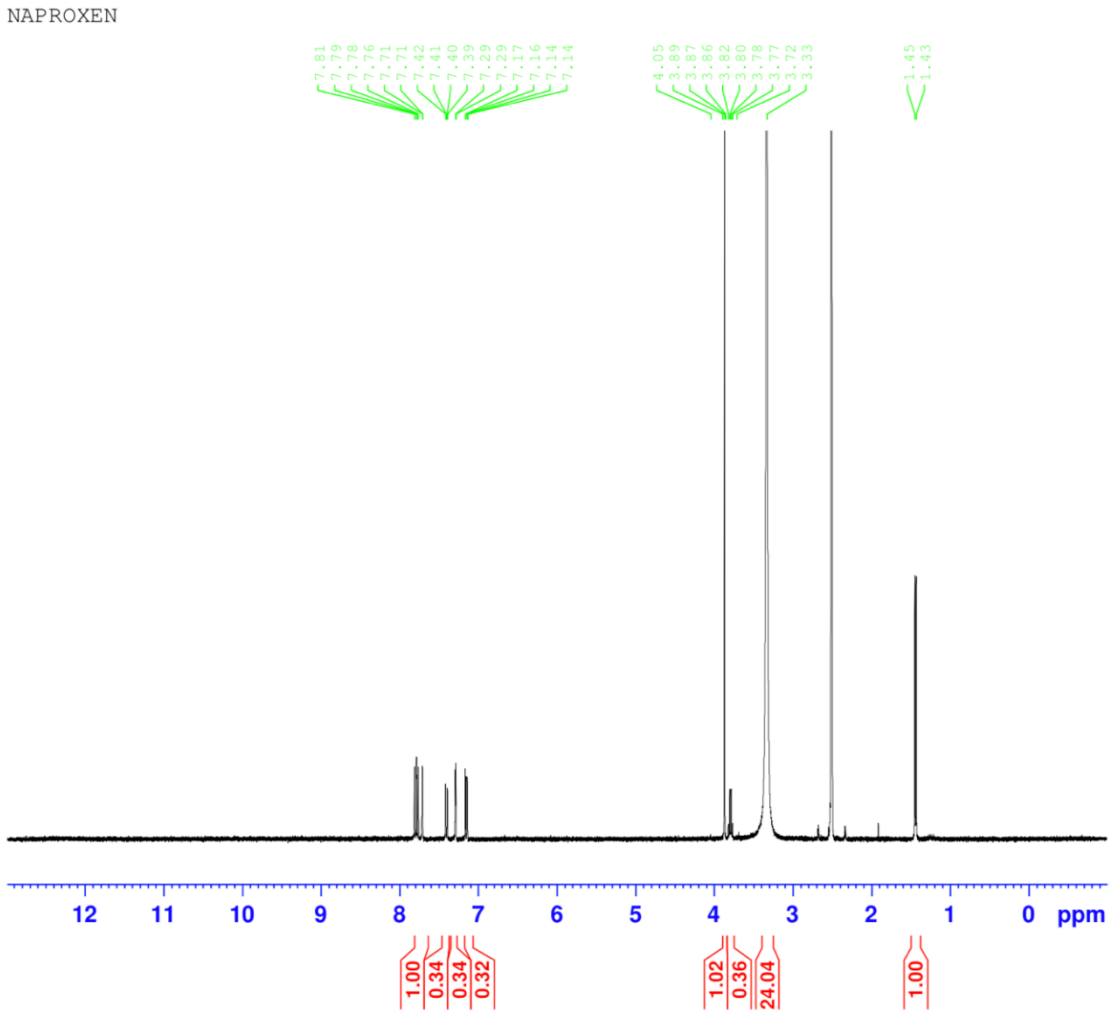

Figure 4.3. 1H-NMR spectrum of naproxen extracted after the back-extraction process.

4.4. Results and discussion

4.4.1. **Hydrogel preparation**

Aliquat 336 can penetrate crosslinked PVA and full-IPN hydrogels by van Der Waals interactions between hydrophobic alkyl chains of Aliquat with the hydrophobic polymer chains, and ion- ion interactions between negatively charged carboxyl groups of hydrophilic polymers and positively charged ammonium group of Aliquat. The method to prepare hydrogels loaded with Aliquat 336 is presented in Scheme 4.1.

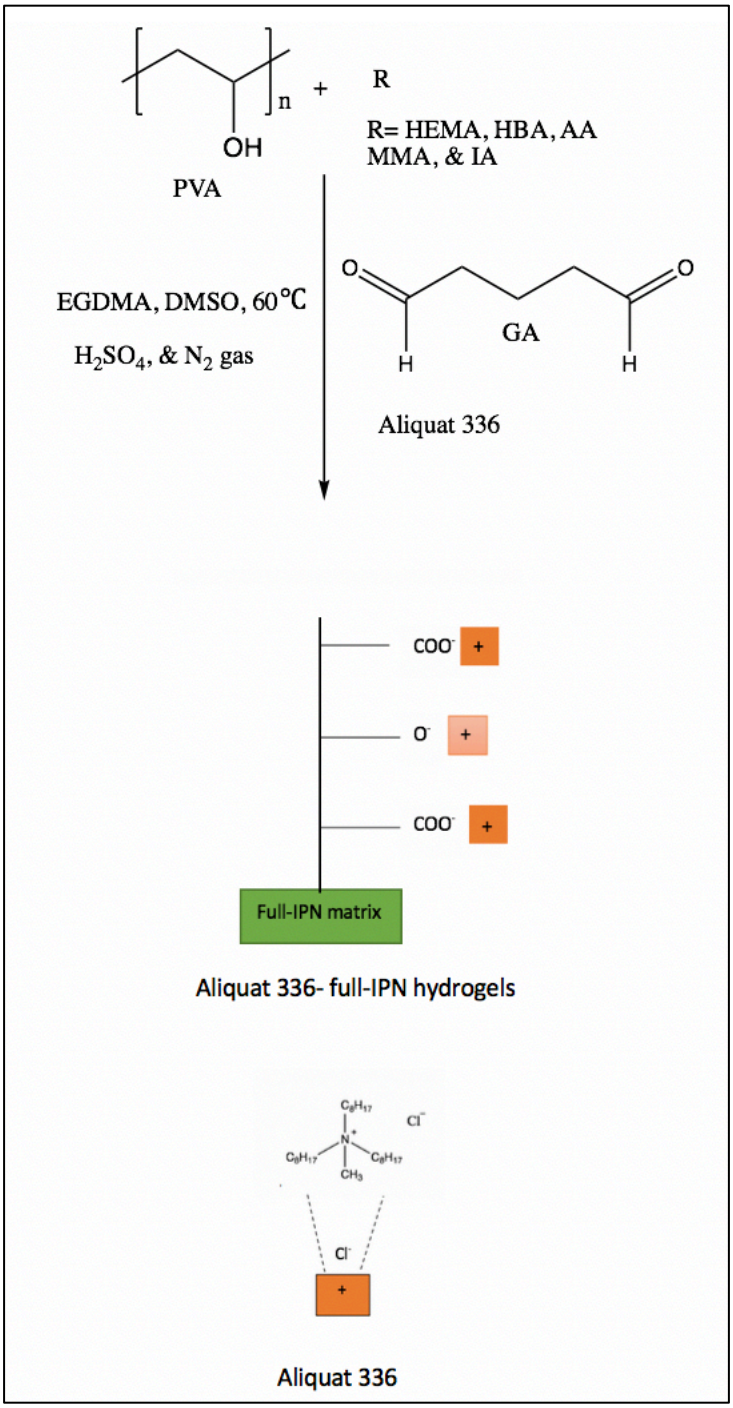

Scheme 4.1. Preparation of Aliquat 336-PVA/GA, and full-IPN hydrogels.

4.4.2. **Infrared analysis**

The chemical structure of the PVA/GA and the series of full-IPN hydrogels with Aliquat 336 were investigated by FTIR spectroscopy. As shown in Figures 4.4 and 4.5, characteristic bands attributed to quaternary ammonium groups at 1,466 and 1,377 cm^{-1}, and other peaks at 2,924 and 2,855 cm^{-1} due to CH_3 group were assigned by reference to

a pure sample of Aliquat 336[232]. The assignment of Aliquat bands observed in the FTIR spectra of hydrogels are reported in Table 4.2.

All characteristic peaks of Aliquat 336 are apparent in the PVA/GA and full-IPN hydrogels, with little shift in wavenumbers, which confirmed that Aliquat 336 was successfully incorporated into the hydrogels. For instance, bands assigned to ν(C-H) from methyl were observed at 2,924 and 2,855 cm^{-1}, and quaternary ammonium at 1,466 and 1,377 cm^{-1}. A strong intensity band due to ν(O-H) from the water content of Aliquat is observed at 3359 cm^{-1}. In the hydrogels, a significant band due to ν(O-H) is now observed at 3400 cm^{-1}, however, although the band is broader than for Aliquat it is not as broad as similar bands in hydrogels without Aliquat. This is likely due to decreased amounts of free water in the hydrogel that has been replaced with Aliquat. Another likely reason is the strong ion-ion interactions between quaternary ammonium cations of Aliquat and negatively charged carboxyl groups of the polymer. Other significant bands, such as ν(C=O) at 1726 cm^{-1} of carboxylate groups, from the hydrophobic, and hydrophilic polymer components confirm the successful preparation of the full series of Aliquat containing hydrogels. A full interpretation of FTIR spectra of PVA/GA and the series of full-IPN hydrogels (without Aliquat 336) is explained in Chapter 2. The FTIR spectra of all hydrogels, including Aliquat 336 loaded hydrogels, are included in the Appendix.

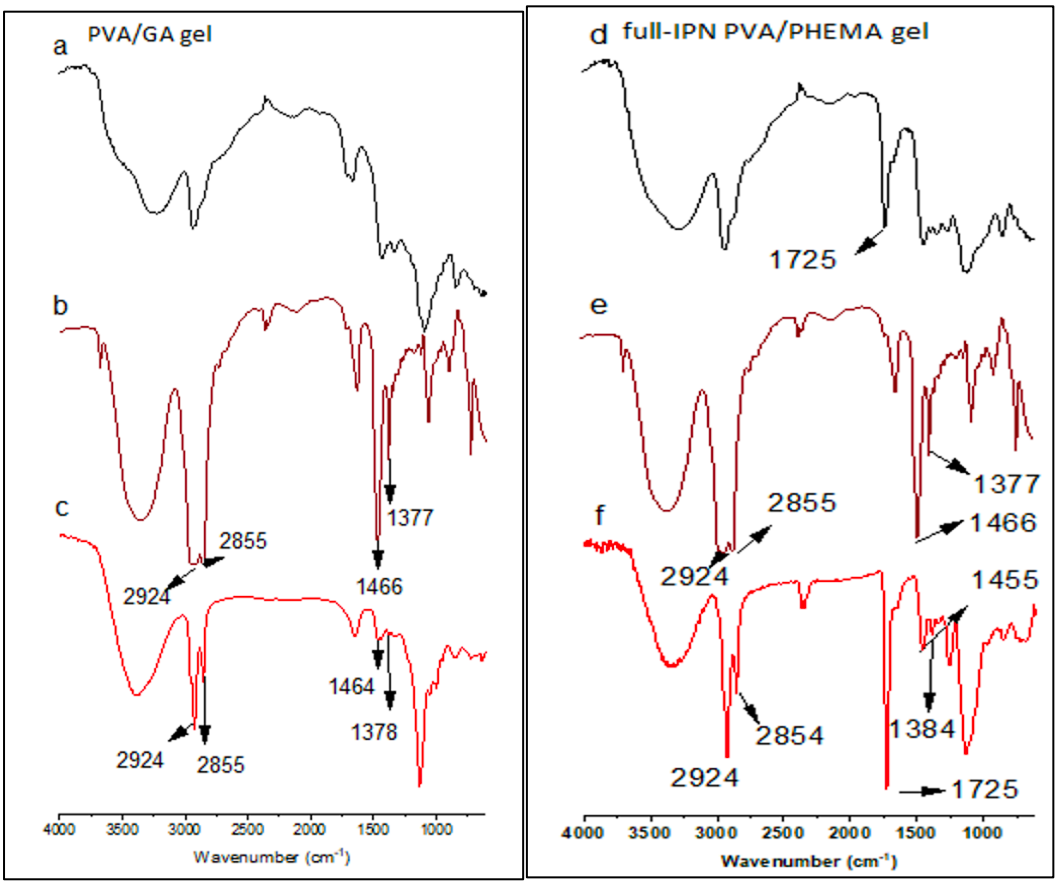

Figure 4.4. FTIR spectra of PVA/GA gel (a), Aliquat 336 (b), and Aliquat 336-PVA/GA gel (c); full-IPN PVA/PHEMA gel (d), Aliquat 336 (e), and Aliquat 336-full-IPN PVA/PHEMA gel (f).

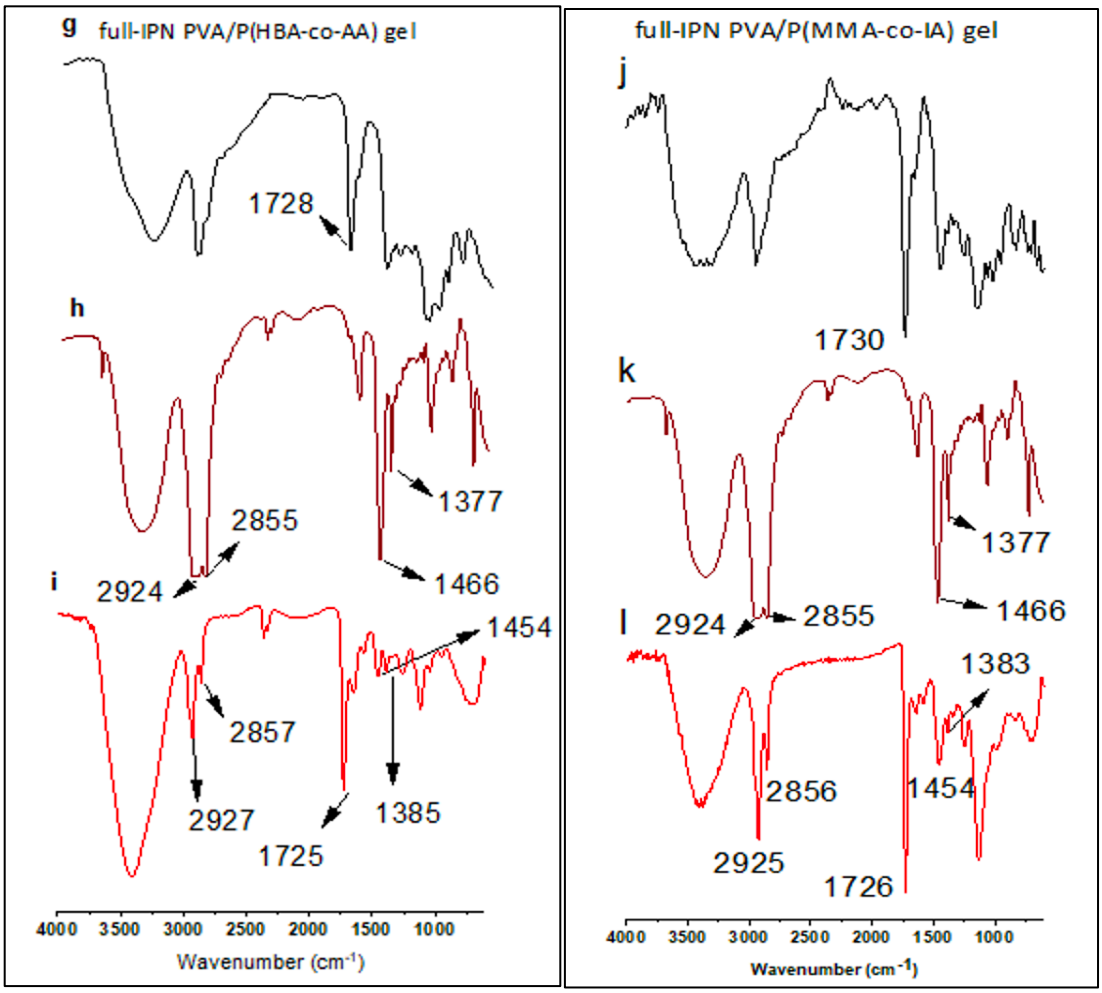

Figure 4.5. FTIR spectra of full-IPN PVA/P(HBA-co-AA) gel (g), Aliquat 336 (h), and Aliquat 336- full-IPN PVA/ P(HBA-co-AA) gel (i); full-IPN PVA/P(MMA-co-IA) gel (j), Aliquat 336 (k), and Aliquat 336- full-IPN PVA/P(MMA-co-IA) gel (l).

Table 4.2. Assignment of bands observed in FTIR spectra of PVA/GA and full-IPN hydrogels containing Aliquat 336.

Hydrogels (with Aliquat)	**Band position (cm^{-1})**	
	$-CH_3$	$-NR_1R_2R_3(CH_3)$
PVA/GA	2924-2855	1464-1378
PVA/PHEMA	2924-2854	1455-1384
PVA/P(HBA-co-AA)	2927-2857	1454-1385
PVA/P(MMA-co-IA)	2925-2956	1454-1383

4.4.3. **Water uptake**

Aliquat 336 has known hydrophilic characteristics due to the ionic liquid and polar nature of the quaternary ammonium cation and chloride counter-anion, which contribute to improved water uptake of the resulting hydrogels[233]. The effect of Aliquat 336 as a basic carrier on water uptake of PVA/GA and the series of full-IPN hydrogels was investigated in deionised water at 37°C. The water uptake profile of each hydrogel is shown in Figure 4.6.

The results of water uptake measurements indicate that all hydrogels showed significant swelling behaviour with full-IPN hydrogels having a similar capacity (200%), reaching equilibrium within six h. However, PVA/GA required more time to reach equilibrium because of the substantial water adsorption capacity (400%); double that of full-IPN hydrogels.

The results indicate that the difference in water uptake is attributed to the various polymer matrix components that confer different hydrophilic characteristics and water uptake ability to the hydrogels. In PVA/GA, the more hydrophilic nature means a greater affinity for water. The reduced water uptake of full-IPN hydrogels is related to hydrophobicity of the network and the strong ion-ion interaction between the Aliquat 336

cation and COO- during the polymerisation process, leading to reduced binding sites for absorbing water, as well as smaller pore size. Water absorption by PVA/GA and full-IPN hydrogels loaded with Aliquat 336 followed a similar trend to the carrier free hydrogels. The water uptake by PVA/GA was relatively high compared to full-IPN PVA/P(HBA-co-AA) and PVA/P(MMA-co-IA) because of more pendant hydroxyl groups still present on PVA compared to the full-IPN backbone. However, the full-IPN PVA/PHEMA hydrogel with a lower amount of GA indicated a similar water content to the PVA/GA gel with Aliquat 336.

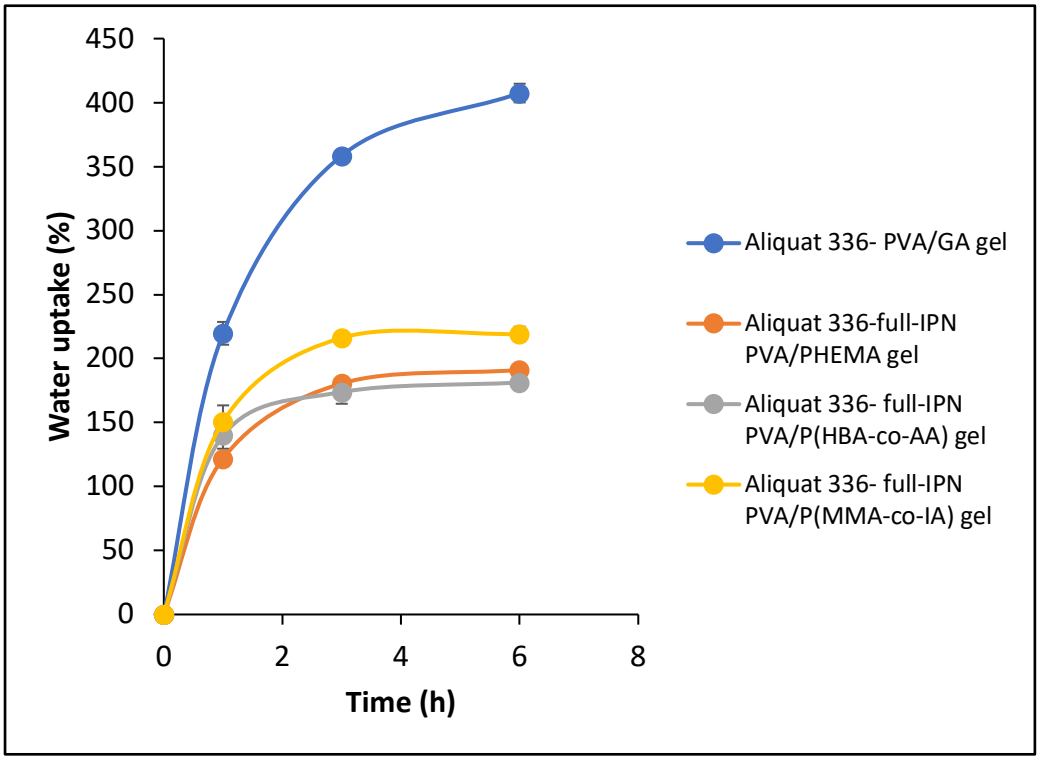

Figure 4.6. Water uptake by hydrogels containing Aliquat 336: PVA/GA and full-IPN PVA/PHEMA, PVA/P(HBA-co-AA) and PVA/P(MMA-co-IA).

4.4.4. **Extraction of Naproxen**

The effect of incorporating Aliquat 336 as an effective carrier in PVA/GA and full-IPN hydrogels was studied during extraction and back-extraction experiments using naproxen as a test solute. The transient extraction profiles for all hydrogels are shown in Figure 4.8 and 4.9.

Aliquat 336 needs to be incorporated into the hydrogel to facilitate the extraction of naproxen through the formation of an ion-pair complex of Aliquat-naproxen. The pKa of the carboxylic group of AA (4.5)[47], IA (pK_{a1} = 3.85 and pK_{a2} = 5.45)[7], and naproxen is 4.2[234]. Thus, in a pH 7 phosphate buffer solution, these carboxyl groups are ionised and naproxen exists as an anion in the feed solution (Figure 4.7).

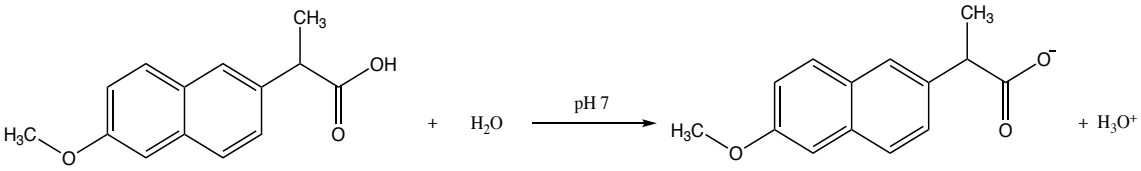

Figure 4.7. Ionization of COOH group to carboxylate ions of naproxen at pH 7 (PBS).

Preliminary extraction experiments of naproxen using hydrogels without Aliquat were performed, but no extraction was noted. The lack of extraction was attributed to ionisation of the carboxyl groups of PAA and PIA, and naproxen to COO^- at pH 7. Thus, naproxen is electrostatically repelled by the ionized polymer groups within the hydrophilic environment and, consequently, no extraction occurs.

Generally, PVA/GA indicated better extraction than the full-IPN hydrogels that all had a similar extraction efficiency for naproxen (Table 4.3). The more hydrophobic nature of full-IPN PVA/P(HBA-co-AA) contributed to the lower extraction efficiency. Conversely, the better extraction of PVA/GA is attributed to the hydrophilic environment within and on the surface that provides more carrier-naproxen interaction sites for effective extraction.

The process of diffusion of naproxen in the hydrogels is initiated by formation of an ion-pair complex between the carboxylate of deprotonated naproxen anion in the feed and the quaternary ammonium cation of Aliquat on the hydrogel surface. Other factors can affect the extraction of naproxen, including the carrier amount, charged sites of polymers, and hydrophilic-hydrophobic nature of the hydrogel.

The back-extraction was significant less than the extraction ability for all hydrogels (Table 4.3) with the best back-extraction noted for PVA/GA and full-IPN PVA/PHEMA. The recovery of naproxen after a complete cycle of extraction and back-

extraction is an important performance indicator. Expectedly, the combined better extraction and back-extraction of PVA/GA delivered the best percent recovery of naproxen. Similar performance was noted for PVA/PHEMA and PVA/P(MMA-co-IA) and substantially less recovery of naproxen was noted using PVA/P(HBA-co-AA).

Naproxen loaded in the hydrogels is released by dissociation from and replacement in the ion-pair with chloride from the stripping solution. The low back-extraction performance is attributed to the strong ion-pair interaction between naproxen and Aliquat 336. Consequently, this affects ion-exchange of the hydrophobic naproxen anion with chloride, even at a reasonably high concentration, in the hydrophilic water environment within the hydrogel. The process of extraction and back-extraction of naproxen by Aliquat 336 hydrogels is shown in Scheme 4.2.

Permeability of naproxen using the full series of Aliquat 336 hydrogels is reported in Table 4.3. The permeability results compliment the extraction results, indicating PVA/GA as the best performing hydrogel.

Nanofiber mats made of PVA have been prepared by electrospinning and used as carriers for transdermal delivery of non-steroidal anti-inflammatory drugs, including naproxen (NAP), sodium salicylate (SS), diclofenac sodium (DS), and indomethacin (IND). The drug delivery performance of nanofiber matts was evaluated by total immersion and transdermal diffusion using pig skin and compared to PVA cast films. Results from the total immersion method indicated the total amount of NAP, SS, DS, and IND released from the nanofiber mats was 98, 97, 76 and 42%, respectively. Whereas, 76, 96, 38, and 30% of NAP, SS, DS, and IND, respectively, was released from the PVA films[235].

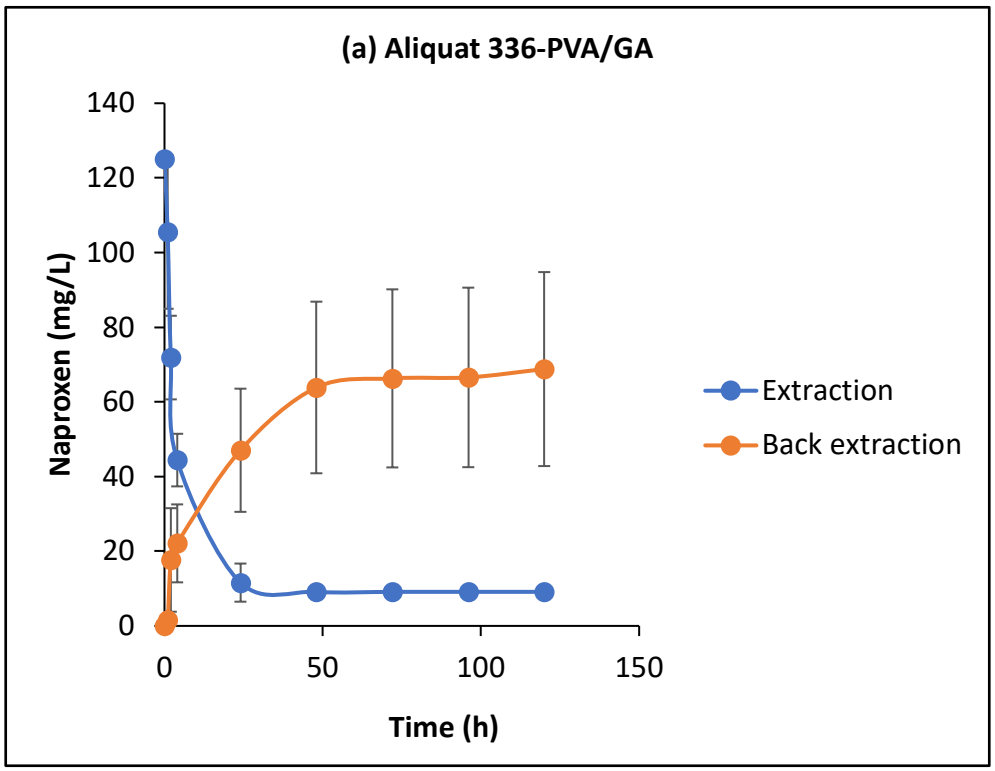

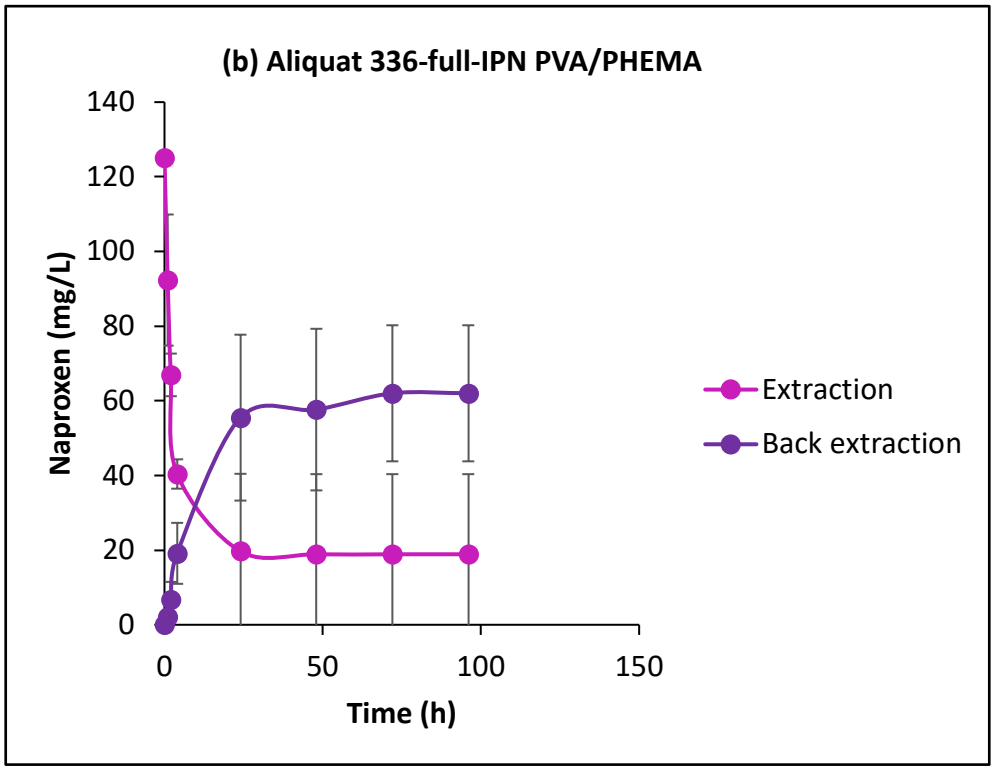

Figure 4.8. Extraction and back-extraction profiles of naproxen using Aliquat loaded hydrogels: PVA/GA (a), full-IPN PVA/PHEMA (b), Conditions: extraction, 125 mg/L naproxen, pH 7; back-extraction, 1 M NaCl, pH 9.

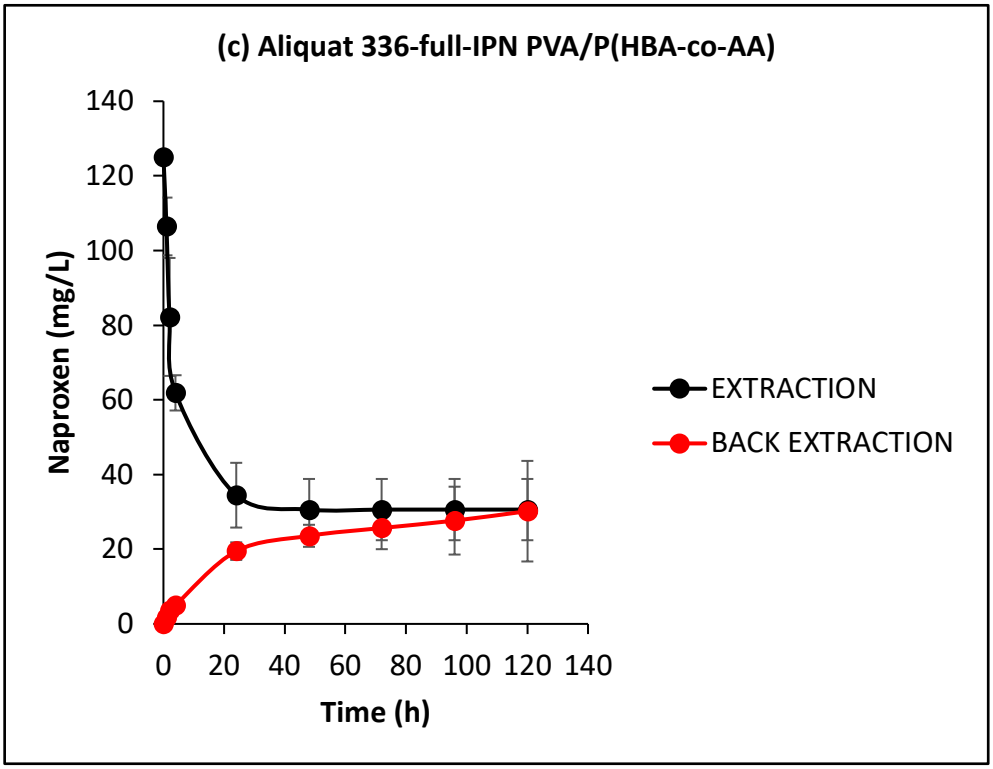

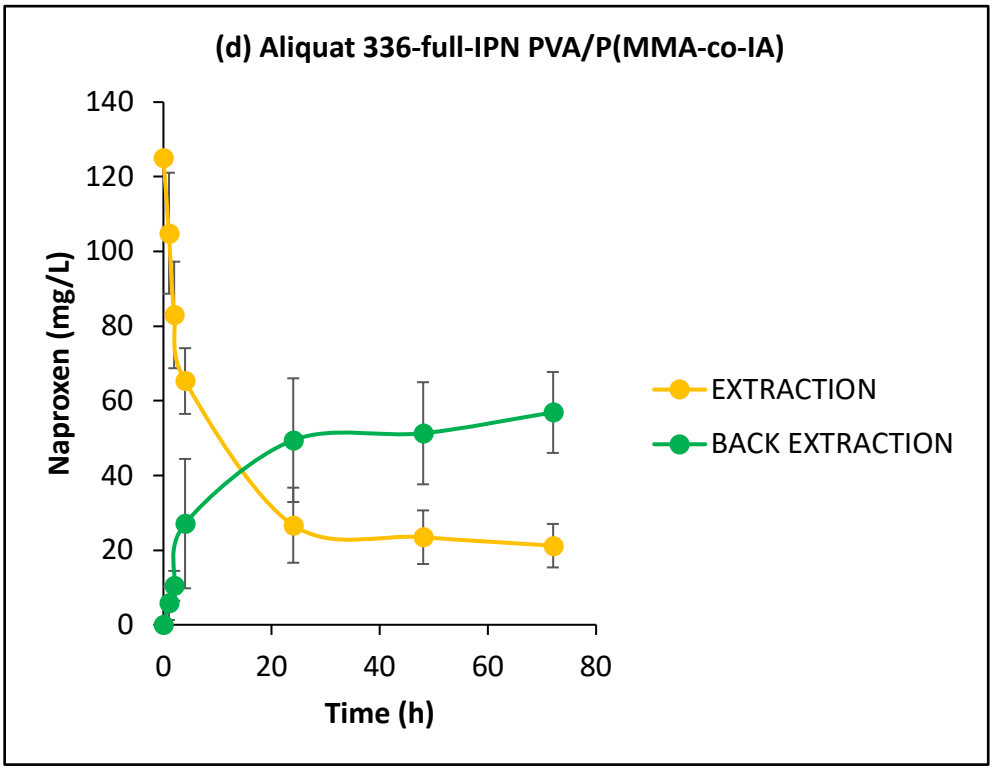

Figure 4.9. Extraction and back-extraction profiles of naproxen using Aliquat loaded hydrogels: full-IPN PVA/P(HBA-co-AA) (c), full-IPN PVA/P(MMA-co-IA) (d), Conditions as for Fig. 4.8.

Table 4.3. Permeability and extraction performance indicators for naproxen using Aliquat 336-PVA/GA and Aliquat 336-full-IPN hydrogels.

Hydrogel	**Permeability (x 10^{-7}, m^2 s^{-1})**	**Extraction (%)**	**Back-Extraction (%)**	**Recovery Factor (%)**
Aliquat 336-PVA/GA	23.4	93	59	55
Aliquat 336-full-IPN PVA/PHEMA	1.59	85	58	50
Aliquat 336 -full-IPN PVA/P(HBA-co-AA)	2.17	76	32	24
Aliquat 336 -full-IPN PVA/P(MMA-co-IA)	2.77	83	55	46

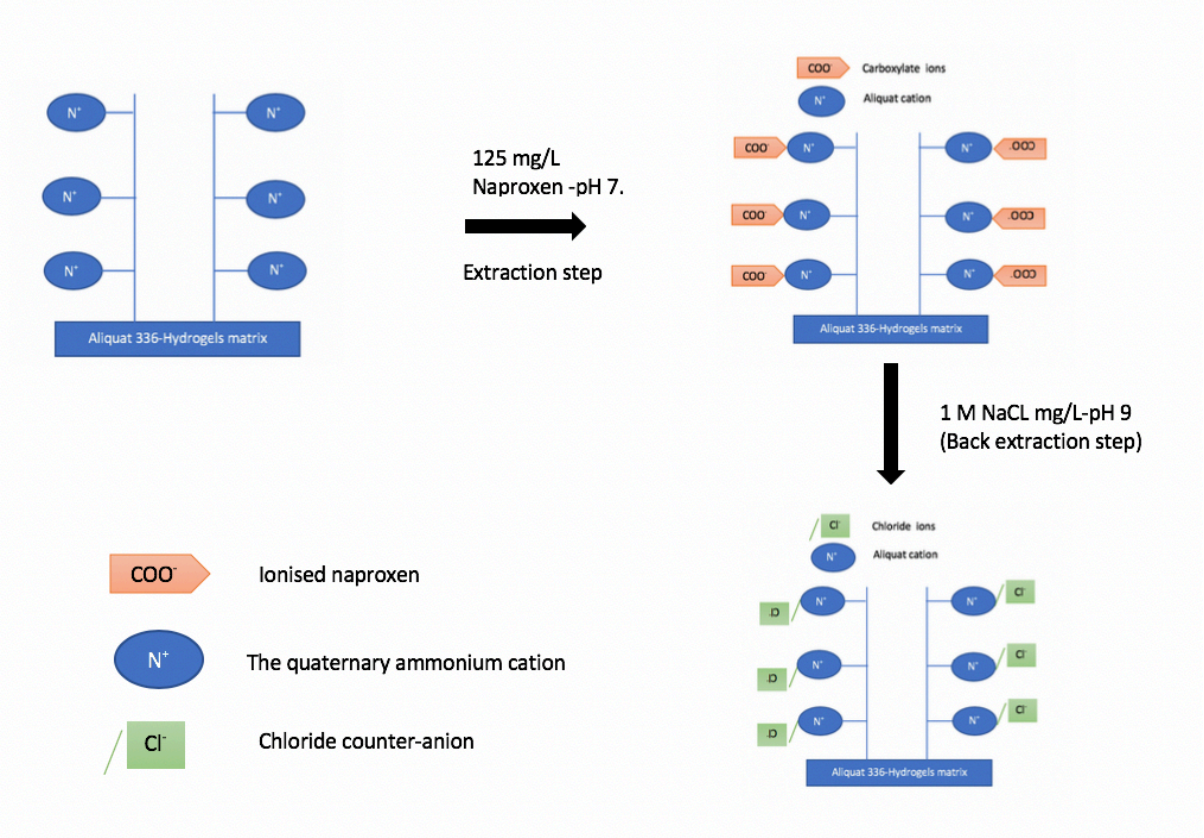

Scheme 4.2. Extraction and back-extraction process of naproxen using the Aliquat 336-hydrogels matrix.

4.5. Characterisation of the hydrogels containing Aliquat loaded with Naproxen

4.5.1. Infrared analysis

The presence of naproxen in the Aliquat336-PVA/GA and series of full-IPN hydrogels after extraction, and back-extraction was investigated by FTIR spectroscopy and the spectra are shown in Figures 4.10 and 4.11. The bands at 1,683, 1,631, and 1,591 cm^{-1} in the spectrum of naproxen are attributed to the skeletal stretching vibration of the aromatic ring[234]. These bands shifted to lower wavenumber when naproxen was absorbed by the hydrogels, indicating formation of an Aliquat-naproxen ion-pair. The C-H stretching vibration of the polymer backbone is indicated by a band at 2,923 cm^{-1} that decreased in intensity for PVA/GA, PVA/PHEMA and PVA/P(MMA-co-IA) after back-extraction of naproxen. This is evidence of chloride associated with the polymer backbone resulting from the anion process to exchange naproxen with chloride in the stripping solution.

However, in the spectrum of PVA/P(HBA-co-AA) after back-extraction, there is little difference in the intensity of these bands, more naproxen remained in the hydrogel network — this observation agrees with the result from the extraction study. The presence of naproxen in the stripping solution was also confirmed by ^{1}H-NMR.

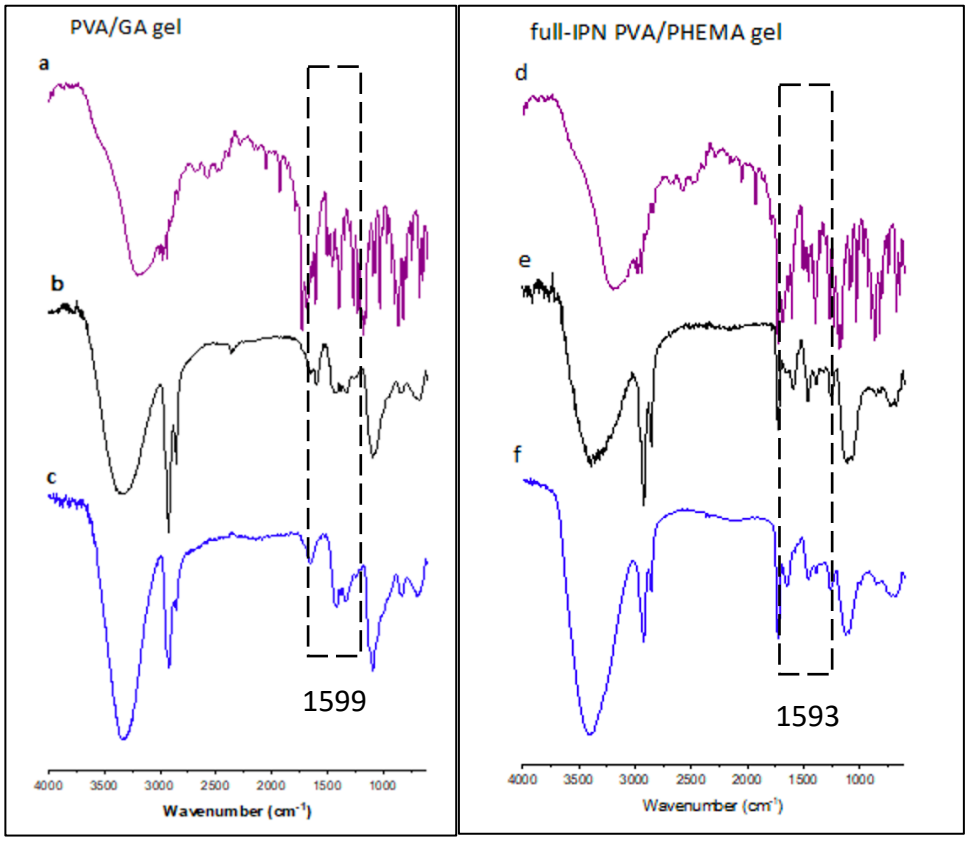

Figure 4.10. Infrared spectra of naproxen (a), Aliquat 336-PVA/GA gel after extraction of naproxen (b), Aliquat 336 PVA/GA gel after back-extraction of naproxen (c); naproxen (d), Aliquat 336 full-IPN PVA/PHEMA after extraction of naproxen (e), and Aliquat 336 full-IPN PVA/PHEMA after back-extraction of naproxen.

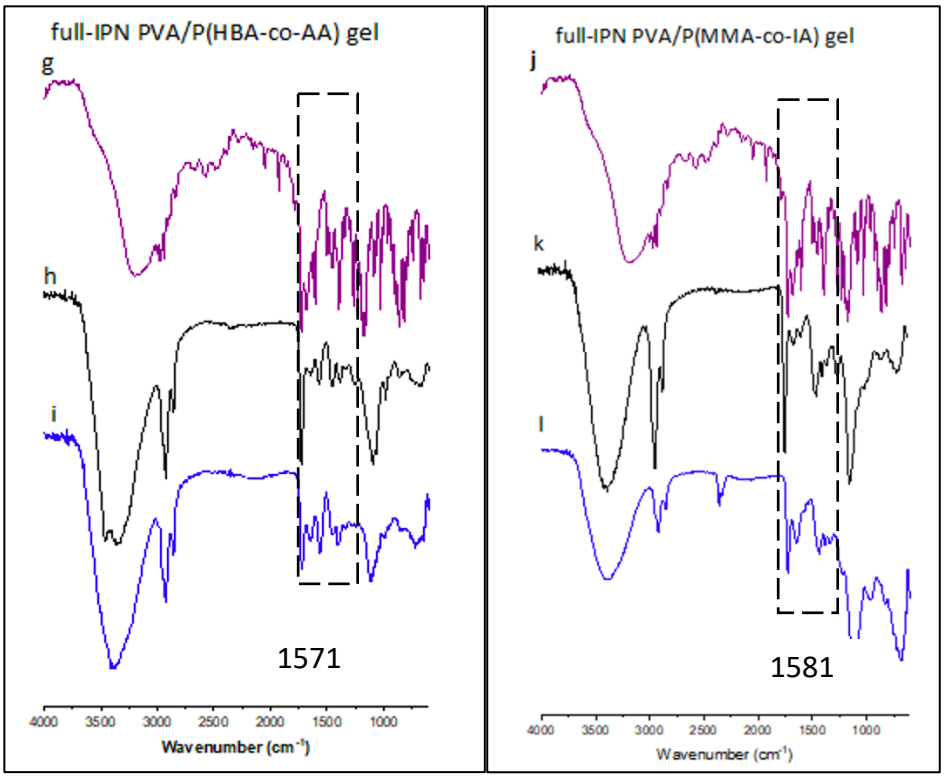

Figure 4.11. Infrared spectra of naproxen (g), Aliquat 336 full-IPN PVA/P(HBA-co-AA) gel after extraction of naproxen (h), Aliquat 336 full-IPN PVA/P(HBA-co-AA) gel after back-extraction of naproxen (i); naproxen (j), Aliquat 336 full-IPN PVA/P(MMA-co-IA) after extraction of naproxen (k), and Aliquat 336 full-IPN PVA/P(MMA-co-IA) after back-extraction of naproxen (l).

4.5.2. **Extraction Kinetics**

The kinetics of naproxen extraction using the full series of Aliquat impregnated hydrogels was investigated to provide further information to identify the best performance (Figures 4.12 & 4.13). The extraction data was shown to be a good fit by regression values with a pseudo first-order rate equation. Rate constants (*k*) were calculated from plots of ln $[nap]_0/[nap]_t$ versus time and are reported in Table 4.4. As shown, full-IPN PVA/PHEMA had the best rate and along with PVA/GA these two hydrogels had significantly better rates compared to the two other hydrogels.

The release kinetics from electrospun PVA mats and PVA cast films loaded with 20 wt% naproxen using a pig skin release method has been investigated. The results indicated Fickian diffusion with rate constants (*k*) for drug release from mats and films of 0.021 and 0.023 $s^{-0.5}$, respectively[235]. Compared to this study, the Aliquat-loaded hydrogels indicated better rates of naproxen extraction.

Table 4.4. Kinetic parameter for the rate of extraction of naproxen using Aliquat 336 impregnated PVA/GA and full-IPN hydrogels.

Hydrogel	***k*** **(h^{-1})**	**R^2**
Aliquat 336-PVA/GA	0.267	0.9876
Aliquat 336-PVA/PHEMA	0.282	0.9966
Aliquat 336-PVA/P(HBA-co-AA)	0.179	0.9860
Aliquat 336-PVA/P(MMA-co-IA)	0.164	0.9793

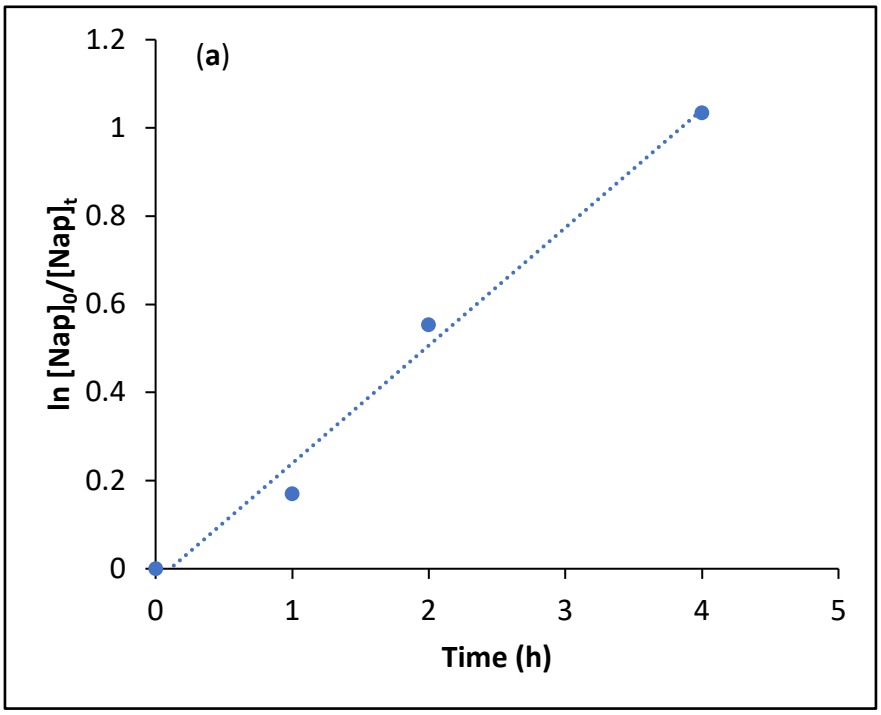

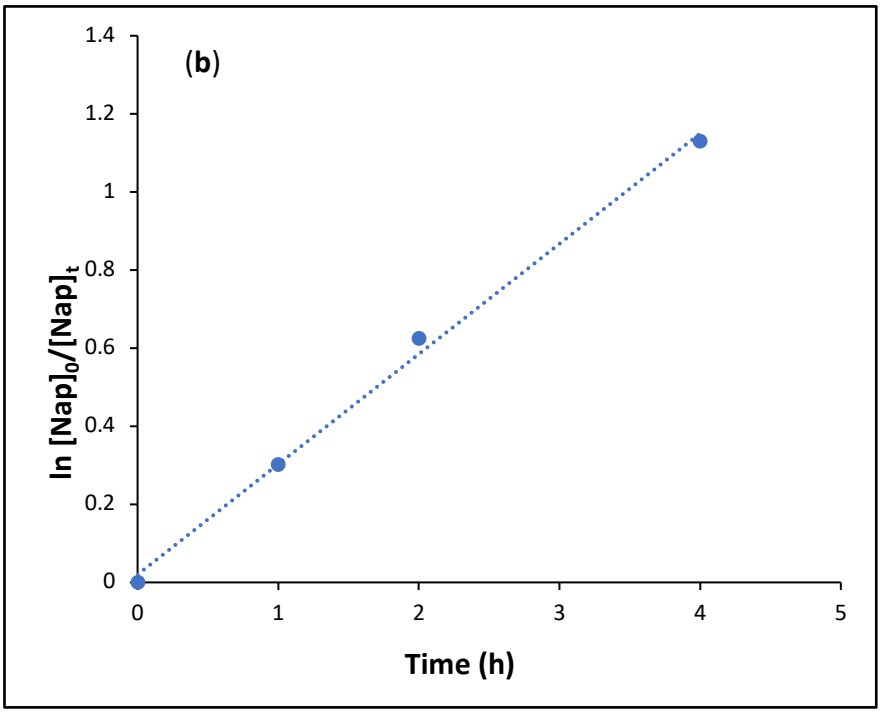

Figure 4.12. Kinetic plot for extraction of naproxen by Aliquat 336 PVA/GA gel (a), and Aliquat 336 PVA/PHEMA gel (b). Conditions: extraction, 125 mg/L naproxen, pH 7; back-extraction, 1 M NaCl, pH 9.

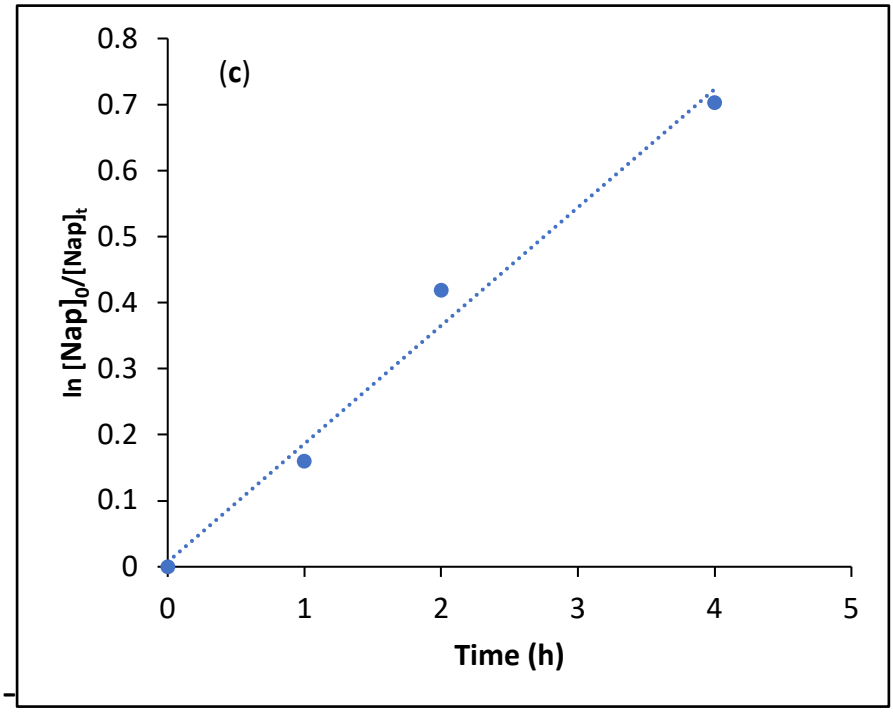

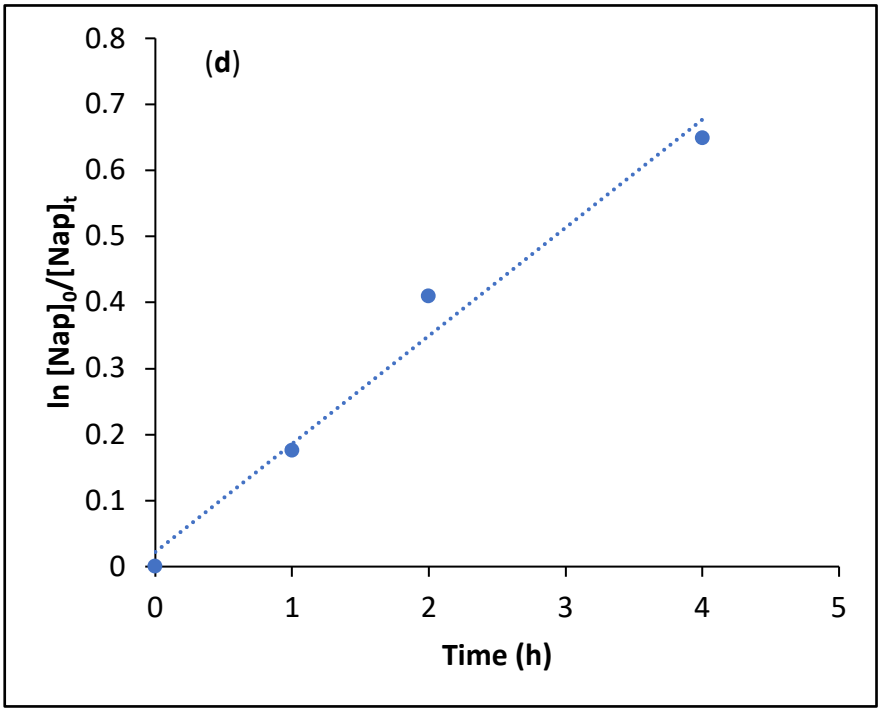

Figure 4.13. Kinetic plot for extraction of naproxen by Aliquat 336 PVA/P(HBA-co-AA) gel (c), and Aliquat 336 PVA/P(MMA-co-IA) gel (d).

4.5.3. **Thermal properties**

A thermogravimetric analysis (TGA) was used to investigate the effect of Aliquat 336 on the thermal properties of the full series of hydrogels. The thermograms of hydrogels after preparation and after use in extraction, and back-extraction experiments of naproxen are shown in Figures 4.14 and 4.15. In general, the thermograms of hydrogels after back-extraction of naproxen show better thermal stability compared to the same hydrogels after preparation.

The Aliquat impregnated hydrogels had substantially better thermal stability at lower temperatures. This is clearly indicated by a significant 50 ^{o}C improvement to 300 ^{o}C before significant weight loss associated with removal of bound water from the network. In the presence of Aliquat, water is more strongly retained thorough additional hydrogen bonding with the carrier, not just with polar regions of the polymers. This confers a more rigid structure by displacing free water from the hydrogel network. The effect is most obvious for PVA/GA and PVA/PHEMA. Two decomposition stages were clearly observed in the series of Aliquat 336 hydrogels before adsorption of naproxen (after preparation) —the first from 50 - 350°C, and the second between 350 - 500°C. Weight loss of Aliquat at 233 ^{o}C is known from TGA investigations of PIMs composed of CTA, bis(2-ethylhexyl) sebacate (BEHS) and Aliquat 336[233].

Significantly, the naproxen released hydrogels experienced weight loss over three stages of decomposition and had even better initial thermal stability. The first stage, involving the loss of water, ranged from 50 - 200°C for PVA/GA and full-IPN PVA/PHEMA and over a reduced range of 50 - 150°C for full-IPN PVA/P(HBA-co-AA) and PVA/P(MMA-co-IA) hydrogels. The additional thermal stability is attributed to the larger Aliquat-naproxen ion pair that displaces more free water and confers extra structural rigidity to the network. The stage of second decomposition ranged from 200 - 350°C for PVA/GA, and a slightly better upper temperature of 380°C for the full-IPN PVA/PHEMA. However, an earlier onset of weight loss over the range 150 - 350°C was noted for full-IPN PVA/P(HBA-co-AA) and PVA/P(MMA-co-IA) hydrogels. This second weight loss is associated with the decomposition of Aliquat and naproxen within the network. The final stage of weight loss occurred above 400 ^{o}C for all hydrogels and is associated with the breakdown of the IPN and the decomposition of polymer chains.

The incorporation of Aliquat within the IPN conferred additional thermal stability to hydrogels as indicated by TGA investigations. This effect was particularly noticeable for PVA/GA and full-IPN PVA/HEMA. The improved thermal stability extends the effective operating temperature range and indicates likely enhanced reusability for applications involving practical operating temperatures of 50 – 150 ^{o}C. Thermal stability was further enhanced for hydrogels after back-extraction to release naproxen. Improved thermal stability results from the structural rigidity imposed by carrier impregnation and solute loading that displaces free water from within the IPN of the hydrogel.

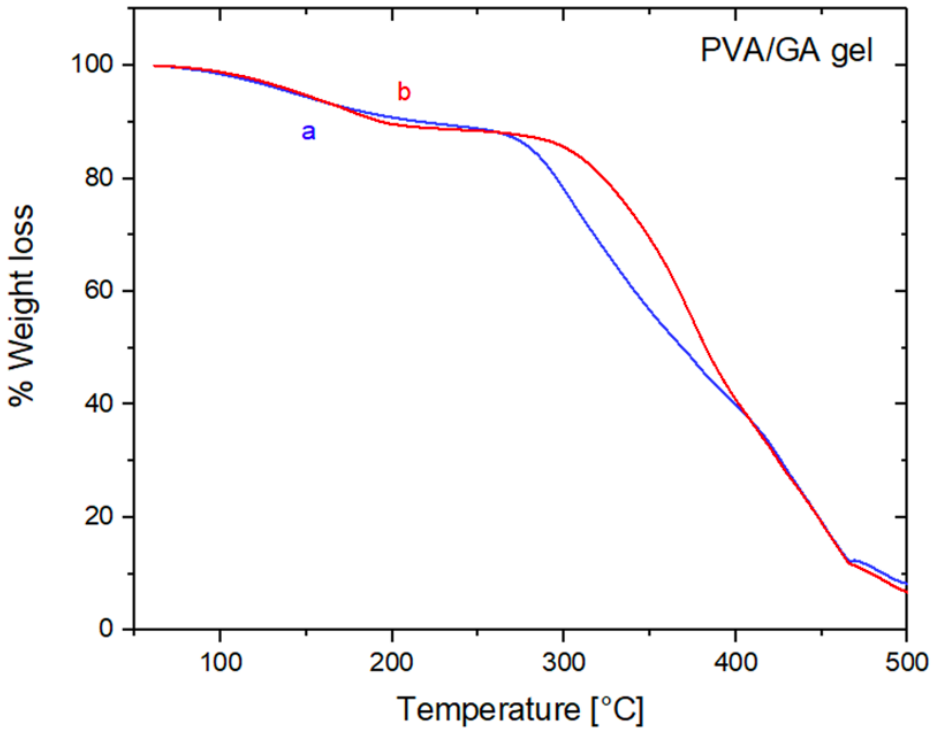

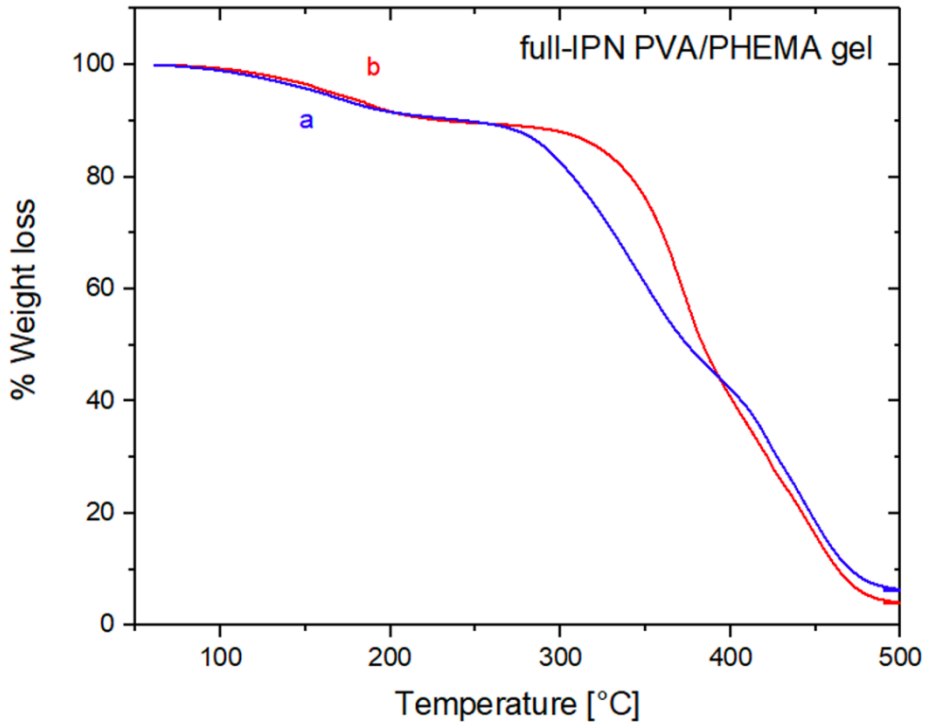

Figure 4.14. TGA profiles of Aliquat 336-PVA/GA (a) gel after preparation, Aliquat 336 PVA/GA (b) gel after back-extraction of naproxen, and Aliquat 336- full-IPN PVA/PHEMA (a) gel after preparation, and Aliquat 336 full-IPN PVA/PHEMA (b) gel after back-extraction of naproxen.

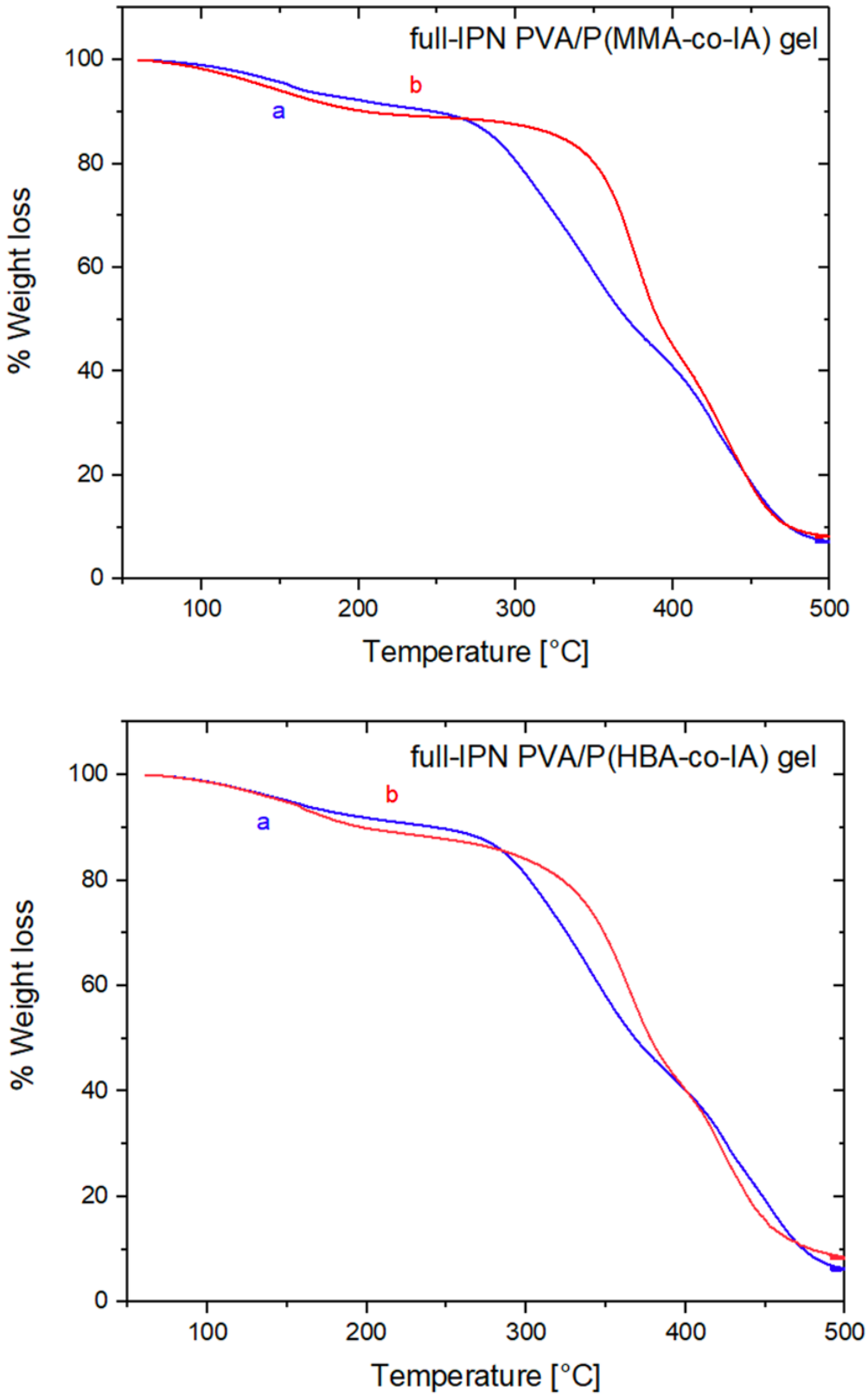

Figure 4.15. TGA profiles of Aliquat 336-full-IPN PVA/P(HBA-co-AA) (a) gel after preparation, Aliquat 336-full-IPN PVA/P(HBA-co-AA) gel after back-extraction of naproxen (b), and Aliquat 336- full-IPN PVA/P(MMA-co-IA) (a) gel after preparation, and Aliquat 336-full-IPN (PVA/P(MMA-co-IA) (b) gel after back-extraction of naproxen.

4.5.4. **Scanning electron microscopy (SEM)**

The surface morphology of the Aliquat 336 impregnated full series of hydrogels after preparation and after back-extraction of naproxen was investigated by SEM; the resulting micrographs are shown in Figures 4.16 - 4.17. Previous investigations of similar hydrogels without Aliquat using SEM were reported in Chapter 2. The results indicated that hydrogels without Aliquat had a porous structure with the different size of pores affected by the composition and types of monomers used, and the cross-linking between polymers within the IPN.

The addition of Aliquat 336 into the hydrogels resulted in distinctly separated layers on the surface, without the same obvious porous structure observed for similar hydrogels without Aliquat. Noticeably, the hydrogel composition affected the packing of layers with close packing apparent for PVA/GA. This indicates addition of Aliquat results in the micropores being filled with carrier, creating smooth layers on the hydrogel surface. This is consistent with the known effects of using Aliquat 336 as a component in PIMs whereby Aliquat acts as a plasticiser between polymer chains, resulting in a homogenous membrane. Investigations of the surface morphology of PIMs composed of PVC and Aliquat 336 found that low amounts of Aliquat resulted in dense, thin, and nonporous membranes[236]. However, transparent and homogenous membranes with irregular pore shapes were obtained when an increased amount of Aliquat up to 40% was used. Another study illustrated that PIMs based on CTA and Aliquat 336 had a nonporous and uniform structure[233].

The surface morphologies of all the hydrogels with Aliquat 336 were different after back-extraction. The SEM images of surface PVA/GA, PVA/PHEMA, and PVA/P(MMA-co-IA) after back-extraction indicate each hydrogel had a different cavity size, whereas no cavities where readily apparent for PVA/P(HBA-co-AA). In the case of full-IPN PVA/P[MMA-co-IA) gel, a uniform distribution of pores was observed. In addition, PVA/GA has a smooth surface, whereas PVA/P(MMA-co-IA) has a rough and irregular surface.

Images of PVA/PHEMA reveal a porous hydrogel consisting of homogeneous layers across the surface and many small pores after preparation, whereas a range of mostly larger sized internal pores are revealed after back-extraction. Surface images of PVA/P(HBA-co-AA) after back-extraction reveal a multi-layered structure. This could be a

factor in the noted reduced extraction because the multi-layers act to impede the adsorption and permeation of naproxen.

Surface morphology studies of hydrogels of poly(2-hydroxyethyl acrylate/itaconic acid) (P(HEA/IA)) has been reported. Before loading the hydrogels with oxaprozin (OXA), the surface had a coral-like, wavy texture with microchannels. However, after loading of OXA within the network, the surface was less wavy because the microchannels were now filled with OXA[190].

The difference in SEM results for the series of hydrogels with and without naproxen in the current investigation is related to several factors, including hydrophilic and hydrophobic features, composition of the IPN, and the strong ion-ion interactions between the quaternary ammonium of Aliquat and negatively charged carboxyl groups of the polymer.

In summary, the incorporation of Aliquat 336 as basic carrier of anions in the matrix of PVA/GA and full-IPN hydrogels during preparation produces a surface with distinctly separated layers, where the micropores are filled with carrier. The SEM images of similar hydrogels after back-extraction to remove naproxen indicated varied surfaces with different pore sizes. The PVA/GA, full-IPN PVA/PHEMA, and full-IPN PVA/P(MMA-co-IA) hydrogels including carrier indicated a more porous structure with homogeneous surface compared to full-IPN PVA/P(HBA-co-AA) gel. The SEM indication of relative pore size supports the outcomes from extraction experiments of naproxen, which indicated PVA/GA, full-IPN PVA/PHEMA and full-IPN PVA/P(MMA-co-IA) had the best extraction performance.

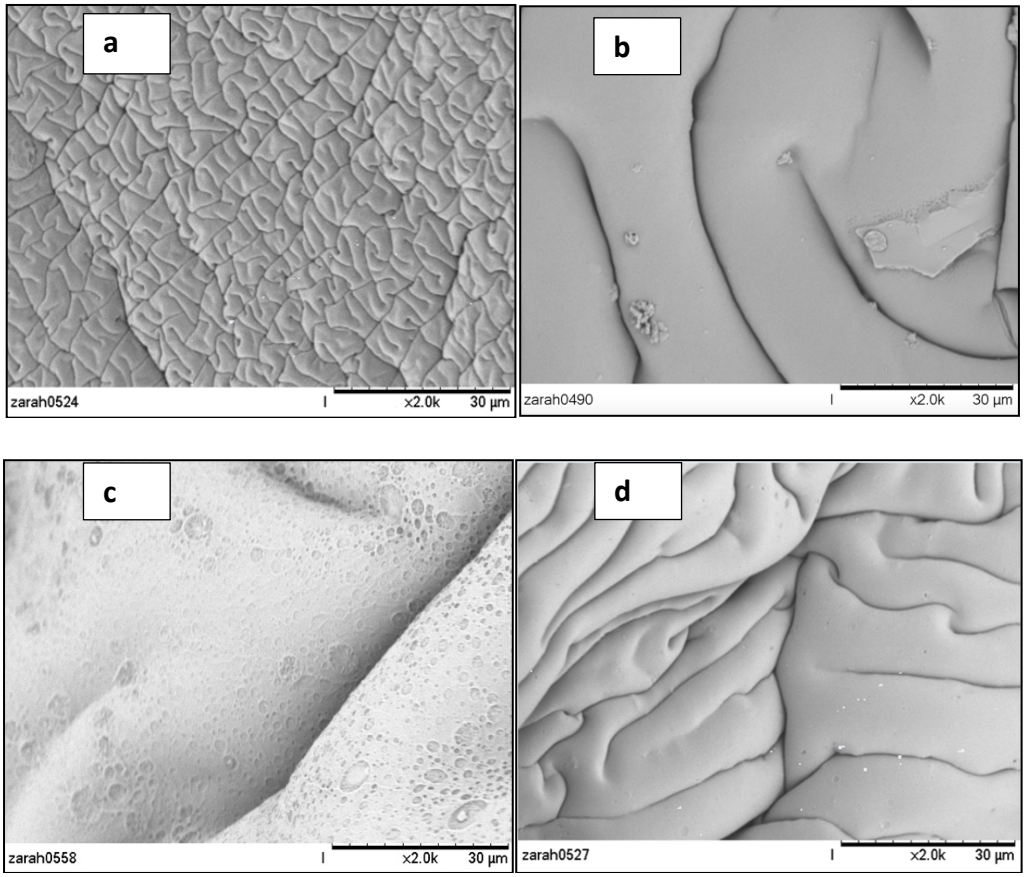

Figure 4.16. SEM images of surface of freeze-dried gel samples of Aliquat 336 PVA/GA (a), full-IPN PVA/PHEMA (b), full-IPN PVA/P(HBA-co-AA) (c), and full-IPN PVA/P(MMA-co-IA) (d) after preparation.

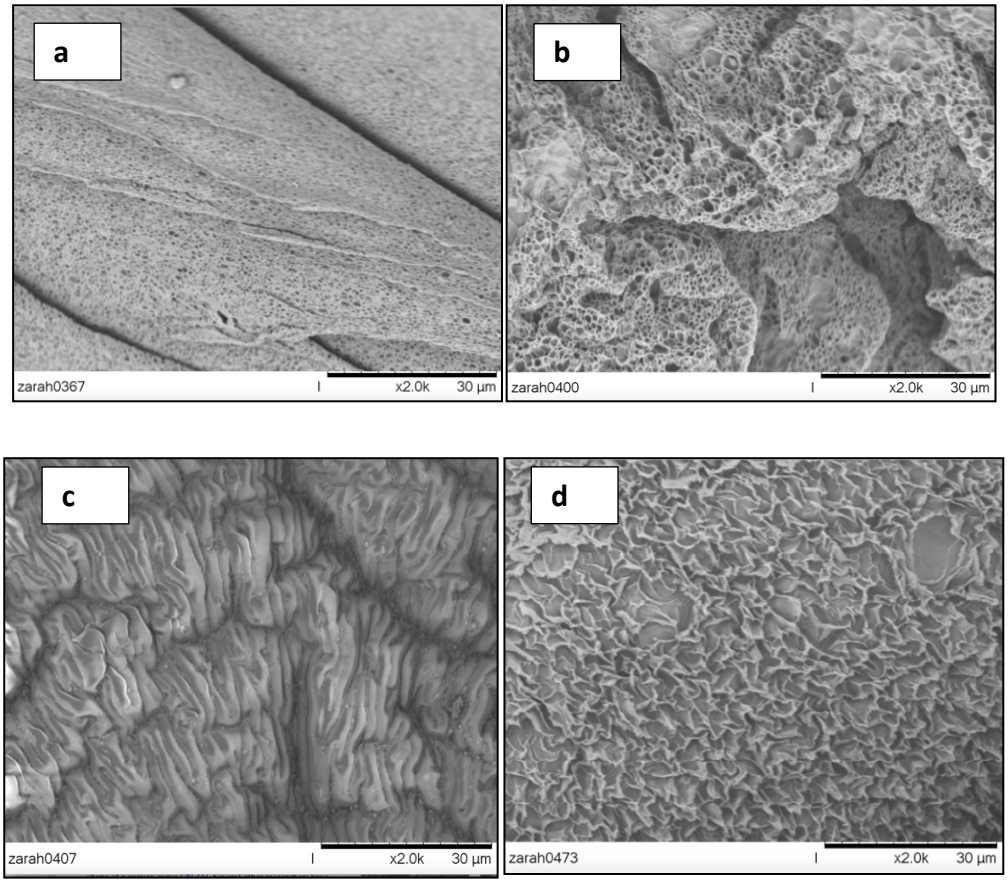

Figure 4.17. SEM images of surface of freeze-dried gel samples of Aliquat 336 PVA/GA (a), full-IPN PVA/PHEMA (b), full-IPN PVA/P(HBA-co-AA) (c), and full-IPN PVA/P(MMA-co-IA) (d) after back-extraction.

4.6. Conclusion

In the present study, novel Aliquat 336 hydrogels were prepared from PVA, 2-hydroxyethyl methacrylate (HEMA), 4-hydroxybutyl acrylate (HBA), acrylic acid (AA), methyl methacrylate (MMA), and itaconic acid (IA) by free radical copolymerisation. Aliquat 336 as a basic carrier of anions was successfully incorporated in cross-linked PVA/GA, full-IPN PVA/PHEMA, full-IPN PVA/P(HBA-co-AA), and full-IPN PVA/P(MMA-co-IA) hydrogels. The ability of the carrier impregnated hydrogels to function as effective adsorbents was investigated using naproxen as a test solute. All hydrogels effectively extracted naproxen, with PVA/GA delivering the best performance as indicated by rate of extraction and efficiency. The properties of Aliquat loaded hydrogels were compared to similar non-loaded hydrogels. Thermal stability of the hydrogels over practical operating temperatures was improved by the presence of entrapped Aliquat and extracted naproxen. Surface morphology studies revealed that Aliquat hydrogels had smooth surfaces with small pores and micro-channels filled with Aliquat 336. Improved thermal stability and surface homogeneity was linked to Aliquat displacing water and promoting a more regular structure throughout the polymer network. This preliminary study has demonstrated the ability to incorporate Aliquat 336 as a suitable carrier for naproxen. This work opens an avenue for further research to explore the use of carrier loaded hydrogels as extractants for highly mobile organic anions in aqueous environments.

Chapter 5: Summary and Future Work

5.1. Summary

Hydrogels are a special class of polymers with unique properties that make them of interest to materials scientists. The ability to absorb large amounts of water make hydrogels ideal candidates as useful biomaterials for different applications. However, the high content of absorbed water results in a material with a low mechanical strength. Despite this limitation, research has focused on preparing hydrogels with stimuli-responsive characteristics. The preparation of hydrogels that are mechanically robust but still exhibit rapid diffusion and a high response rate[237] is still a challenge. Hydrogels prepared as interpenetrating polymer networks (IPNs) have better mechanical stability. This approach was used to prepare a series of full-IPN hydrogels containing hydrophilic and hydrophobic polymer components in this research project.

The first study involved the preparation of a number of full-IPN hydrogels based on poly(vinyl alcohol) (PVA) crosslinked with glutaraldehyde (GA) and using a variety of different monomers, including 2-hydroxyethyl methacrylate (HEMA), 4-hydroxybutyl acrylate (HBA), acrylic acid (AA), methyl methacrylate (MMA) and itaconic acid (IA). Hydrogels were prepared by free radical polymerization of the monomers in the presence of ethylene glycol dimethacrylate (EGDMA) as a crosslinking agent. The series of hydrogels included full-IPN PVA/PHEMA, full-IPN PVA/P(HBA-co-AA), and full-IPN PVA/P(MMA-co-IA). The chemical composition of the hydrogels was investigated by FTIR and ToF-SIMS.

The contribution to thermal stability and responsive characteristics of the hydrogels from using crosslinked PVA was investigated with 10, 20 or 30 wt% of GA in full-IPN PVA/PHEMA. Similarly, the effect of the hydrophobic component on hydrogel properties was investigated by varying the ratio of HBA to AA (14:20, 20:14 & 27:7) in full-IPN PVA/P(HBA-co-AA), and MMA to AA ratio (10:24, 17:17 & 24:10) in full-IPN PVA/P(MMA-co-IA). Water uptake and retention, and pH-sensitive behavior of the hydrogels was investigated. Significantly better water absorption was indicated for PVA/PHEMA with 10 wt% GA compared to other full-IPN hydrogels. All hydrogels indicated pH-sensitive behavior due to the polar nature of the pendant polar groups of the polymers.

Water retention studies at 30 ^{o}C of the series of full-IPN hydrogels with different amounts of GA and MMA revealed the best water retention at 30 wt% GA and 24 wt% MMA for PVA/PHEMA, and PVA/P(MMA-co-IA), respectively.

The thermal stability of the hydrogels was investigated by thermogravimetric analysis (TGA) and revealed that PVA/P(HBA-co-AA) and full-IPN PVA/P(MMA-co-IA) were more stable than PVA/GA, and PVA/PHEMA. Additionally, full-IPN PVA/PAA had good thermal stability. The formation of intermolecular hydrogen bonds between COOH groups of PAA and PIA, and OH groups of PVA is responsible for the improved thermal stability.

Surface morphology of the hydrogels was investigated by scanning electron microscopy (SEM). A highly porous structure and dense homogeneous surface was indicated for PVA/GA that indicates a high ability to retain large amounts of water. A reduced porous nature with smaller pores, however, was revealed for the other hydrogels, indicating that extensive crosslinking throughout the IPN components significantly reduces porosity. Full-IPN hydrogels with high amounts of GA, HBA or MMA had low porosity and smooth surfaces, and the appearance of robust and transparent films.

The second study in this research involved an investigation of using full-IPNs as specific adsorbents for copper using Acorga P50 as carrier. The novel adsorbents incorporated Acorga P50 or Cu (II)-Acorga P50 complex and were prepared by free radical polymerization as a series of full-IPN PVA/PHEMA, PVA/P(HBA-co-AA) and PVA/P(MMA-co-IA) hydrogels. The carrier and Cu (II)-carrier complex were successfully retained within the hydrogels after preparation as indicated by FTIR. Weak van der Waals interactions between the carrier and hydrophobic regions in the hydrogel contribute to the stability of the hydrogels. The robust nature of the hydrogels was exemplified by the use of 2 M H_2SO_4 to remove Cu (II) ions from the hydrogels prepared with copper-carrier complex. The full-IPN hydrogels were used as adsorbents to remove Cu (II) from aqueous solutions and the extraction capacity was compared to single network PVA/GA.

All hydrogels prepared with Cu (II)-carrier complex had better extraction of Cu (II) compared to hydrogels prepared with carrier. The large complex acts as a template during preparation that produces more free volume and open channels within the hydrogel network, resulting in better diffusion of Cu (II). The effects of pH and initial Cu (II) concentration on extraction performance was studied using carrier-based hydrogels.

Maximum extraction efficiency occurred at pH 5 consistent with the pK_a of the ionisable groups. Extraction efficiency and permeability of Cu (II) decreased for all hydrogels when the concentration of the feed increased from 25 to 100 mg/L.

Surface morphology studies of the hydrogels after stripping of copper suggest the presence of a more open porous structure. This is consistent with the larger template initially used during preparation. Good thermal stability of the hydrogels over 50 – 100 ^{o}C was noted before extraction, however, after stripping of copper ion using the same samples, better thermal stability was observed at higher temperatures due to the heat capacity of copper. Analysis of the extraction data indicated good agreement with first-order kinetics. Reusability of the carrier loaded PVA/GA and full-IPN hydrogels was assessed over four consecutive extraction and back-extraction cycles. Results indicated that complex-loaded hydrogels had better reuse performance and potential as adsorbents to remove copper ions from aqueous environments.

The third study as part of this research examined the preparation and use of full-IPN hydrogels prepared with Aliquat 336 as adsorbents for organics. Naproxen was selected as a representative target solute because it is deprotonated at a pH that is useful for physiological and environmental studies. Aliquat 336 is a basic carrier for anions and can form an Aliquat-naproxen ion-pair complex. The successful loading of Aliquat 336 in the hydrogels was indicated by FTIR. A better extraction rate and efficiency was achieved by PVA/GA compared to full-IPN hydrogels. Modelling of the extraction data indicated a good agreement with first-order kinetics.

All Aliquat loaded hydrogels showed a smooth surface with a minimum of small pores before extraction, whereas after back-extraction a more porous structure was observed on the surface of all hydrogels except PVA/P(HBA-co-AA). The low porosity is consistent with the dual chemical nature of Aliquat, whereby it acts as a phase transfer conduit between hydrophobic and hydrophilic domains in the hydrogel. The higher porosity is consistent with the better results from extraction experiments. Improved thermal stability was noted for all hydrogels after back-extraction of Naproxen due to the Aliquat-naproxen ion-pair providing extra molecular connectivity between polymer chains.

The results from this research demonstrate that the chemical nature of full-IPN hydrogels can be utilized to load selective reagents during preparation to achieve good

extraction with some selectivity of target solutes from aqueous environments. The full-IPN hydrogels demonstrated good chemical and mechanical stability that might be useful for extractions under more aggressive reaction conditions, such as prolonged temperatures at 50 – 60 ^{o}C, to achieve better extraction performance compared to crosslinked PVA/GA hydrogels. Despite the improved stability of full-IPN hydrogels, the extraction performance, as indicated by permeability and recovery factor, was less than crosslinked PVA/GA hydrogels. This investigation provides a stimulus to further investigate the use of full-IPN hydrogels as useful adsorbents for other inorganic and organic chemicals from aqueous environments for analytical measurements and remediation purposes.

5.2. Future work

The results from the research reported in this thesis indicate that a reagent to target specific solutes can be successfully incorporated in full-IPN hydrogels prepared using a variety of different monomers. The hydrogels can be used as transparent and robust films in extraction experiments with reuse capability demonstrated over four extraction cycles. If the hydrogel materials are to be used as adsorbents for small- or large-scale commercial applications, the robust nature of the material should be further examined.

Young's modulus and an ultimate tensile strength test can be used to assess the mechanical properties of the materials[238] The preparation of fine powders by milling of freeze-dried hydrogels can also be investigated as a means of increasing the surface area and extraction performance.

The full-IPN hydrogels used for all experiments in this research were prepared from PVA as the main hydrophilic polymer. Various other polymers, such as cellulose triacetate (CTA), could be used to prepare full-IPN hydrogels for investigation.

The use of CTA could improve the mechanical features and water content of the materials. CTA is used widely to prepare polymer inclusion membranes (PIMs) due to its abilities to produce thin membranes with good mechanical strength and deliver effective transport of small organic compounds and metal ions[201]. CTA is a polar polymer containing

acetyl and hydroxy groups that can form intramolecular hydrogen bonds, resulting in a crystalline structure. The presence of crystalline domains in CTA is responsible for improved mechanical strength[236]. Physiochemical properties of hydrogels prepared from PVA or CTA with similar hydrophobic monomers could be assessed to determine whether CTA provides any beneficial advantages.

Further experiments using Acorga P50 loaded full-IPN hydrogels are needed using real environmental samples to assess the interference of other chemicals, such as iron and zinc, on copper extraction. The selectivity for other metals could be examined in experiments at different pH. The positive results from using Acorga P50 is encouraging. This indicates the possibility of loading other carriers for particular metals in similar full-IPN hydrogels. The hydrophobic hydrogel content can be modified by varying the amount and use of different monomers to achieve effective loading of different carriers.

The results reported using Aliquat 336 loaded full-IPN hydrogels were also encouraging. However, the back-extraction efficiency of naproxen using 1 M NaCl from the hydrogels is poor, being only 32 - 43%. Methods to improve the back-extraction need to be considered, such as using 2 M NaCl to increase the concentration of chloride to affect the extraction equilibrium to release deprotonated naproxen from the Aliquat-naproxen ion pair. The use of an ion-pair reagent along with NaCl in the stripping solution should also be investigated as a means to facilitate the back-extraction of naproxen. Nevertheless, the promising preliminary results indicate that it would be worthwhile to broaden the investigation of using Aliquat 336 loaded full-IPNs as adsorbents of other deprotonated organic and inorganic anions.

Appendix

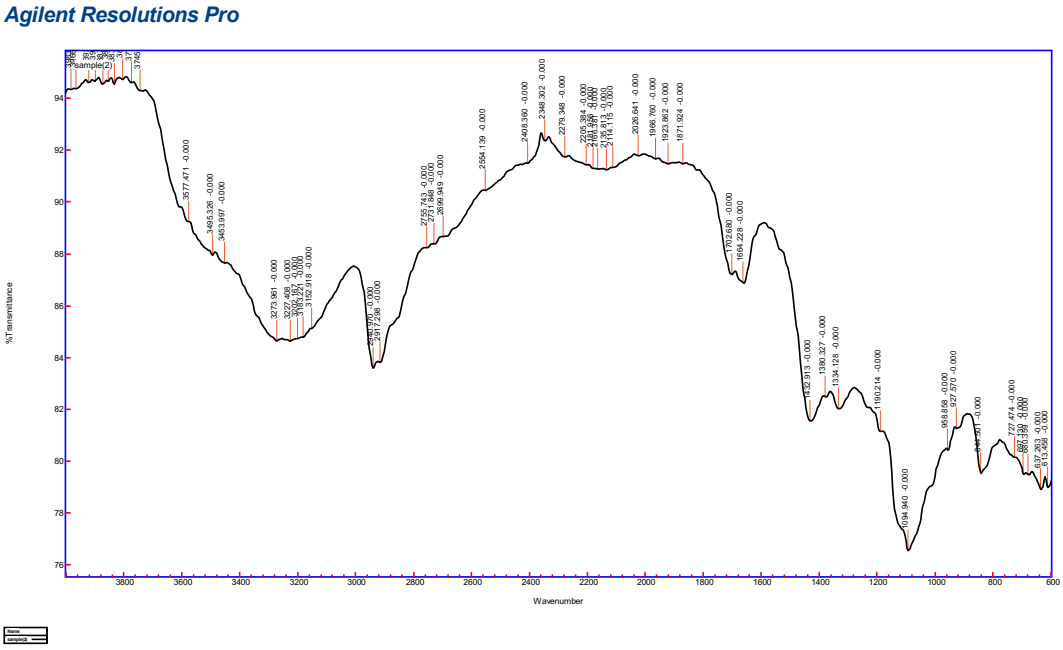

Figure A1. FTIR spectrum of PVA/GA gel.

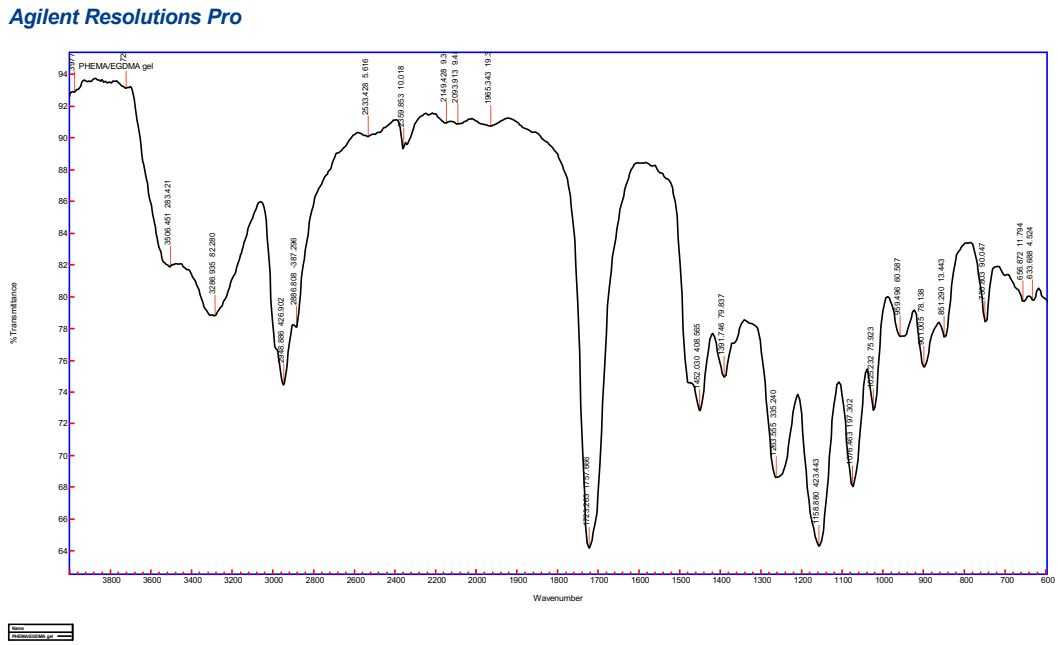

Figure A2. FTIR spectrum of PHEMA gel.

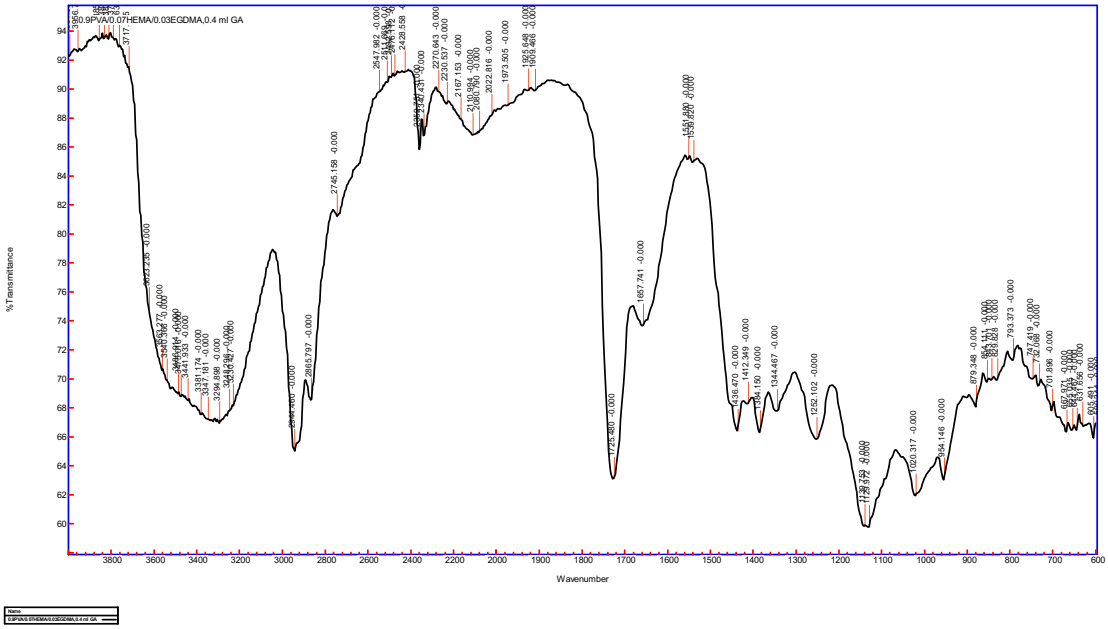

Figure A3. FTIR spectrum of full-IPN PVA/PHEMA gel.

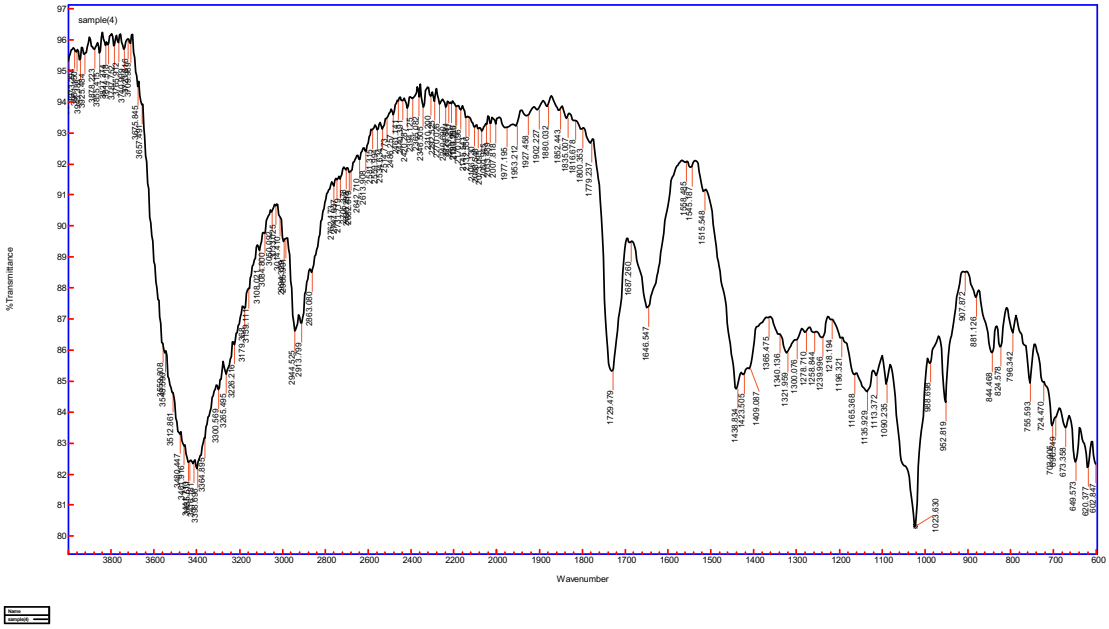

Figure A4. FTIR spectrum of full-IPN PVA/PHBA gel

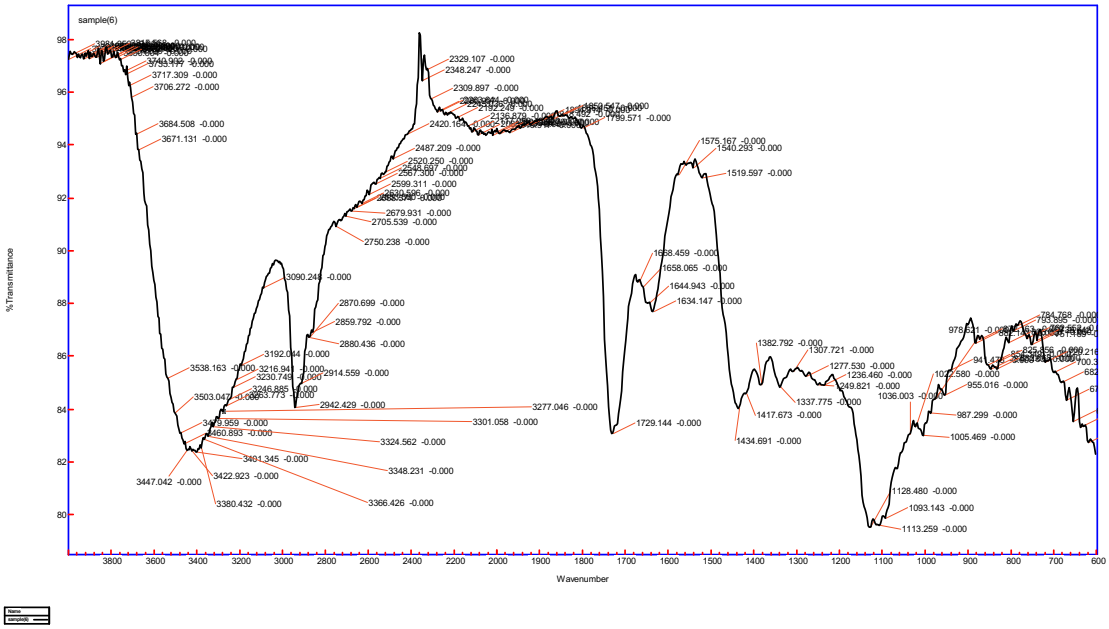

Figure A5. FTIR spectrum of full-IPN PVA/PAA gel.

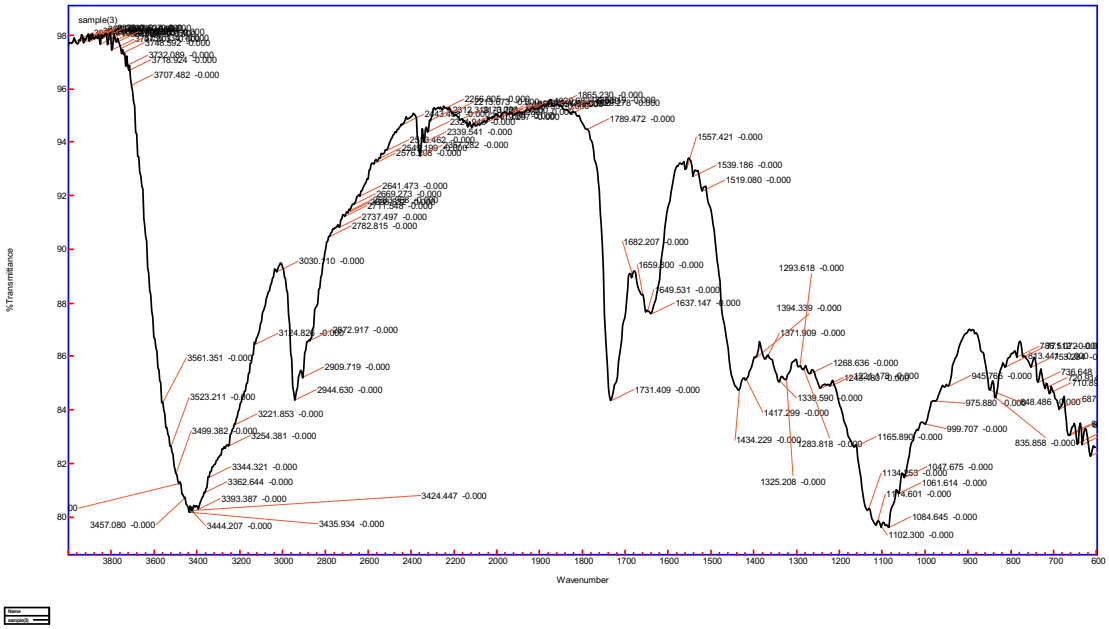

Figure A6. FTIR spectrum of full-IPN PVA/P(HBA-co-AA) gel.

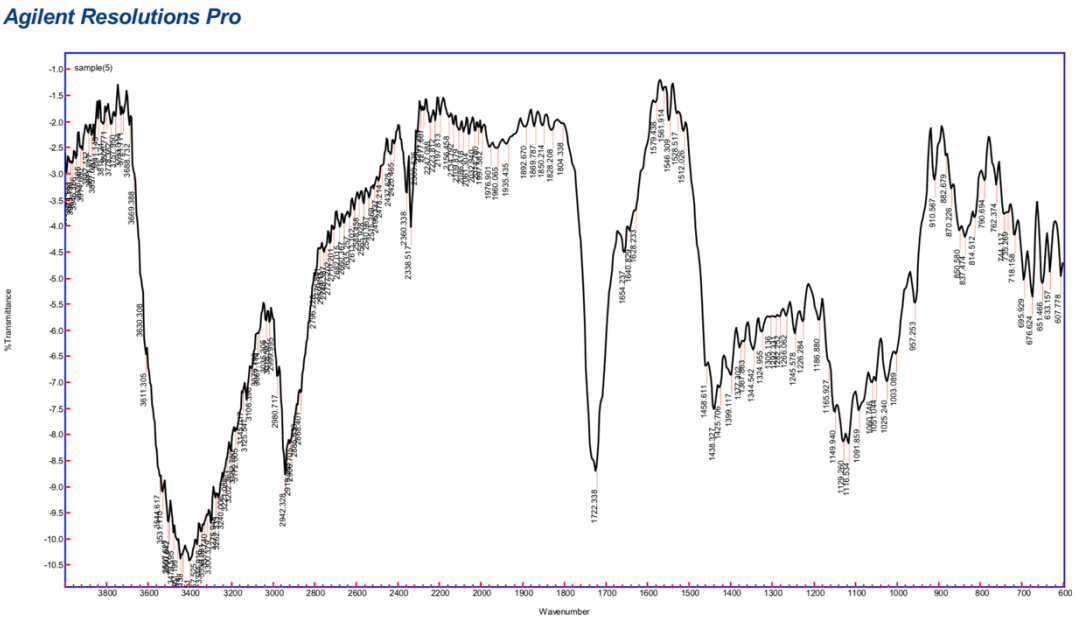

Figure A7. FTIR spectrum of full-IPN PVA/PIA gel.

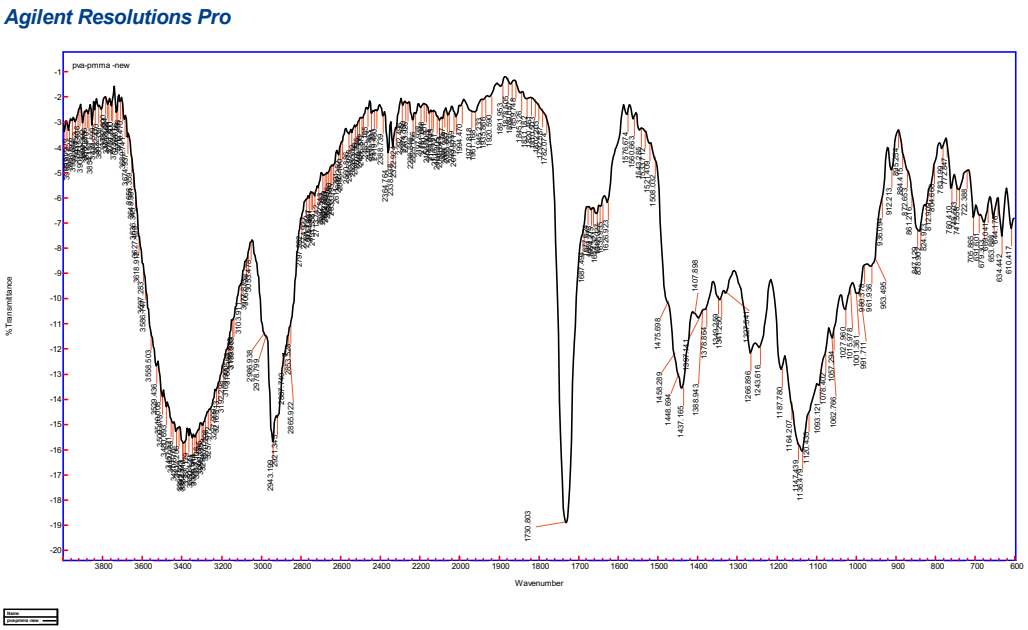

Figure A8. FTIR spectrum of full-IPN PVA/PMMA gel.

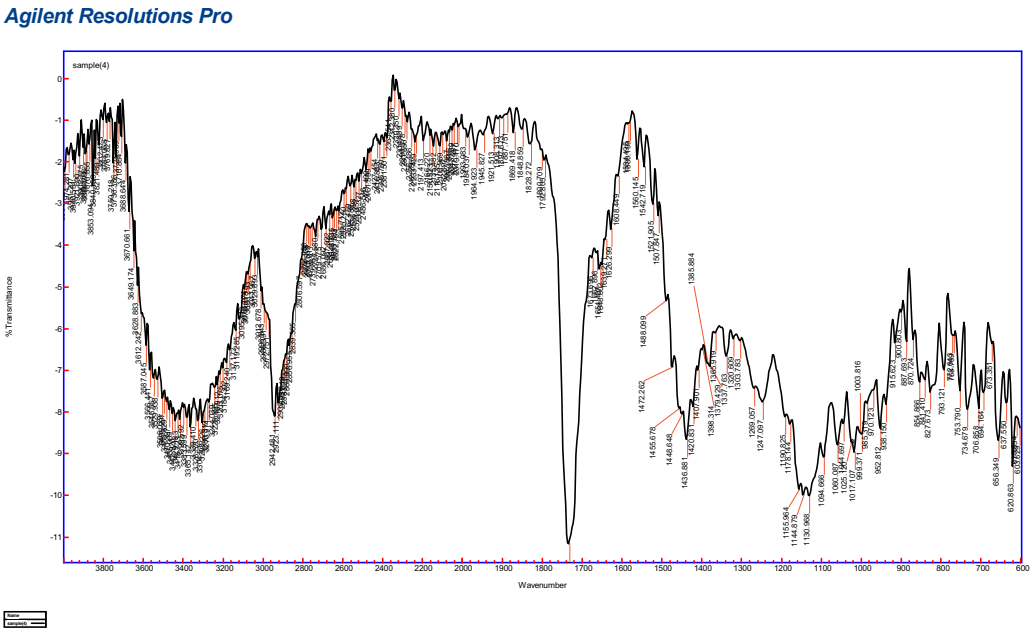

Figure A9. FTIR spectrum of full-IPN PVA/P(MMA-co-IA) gel.

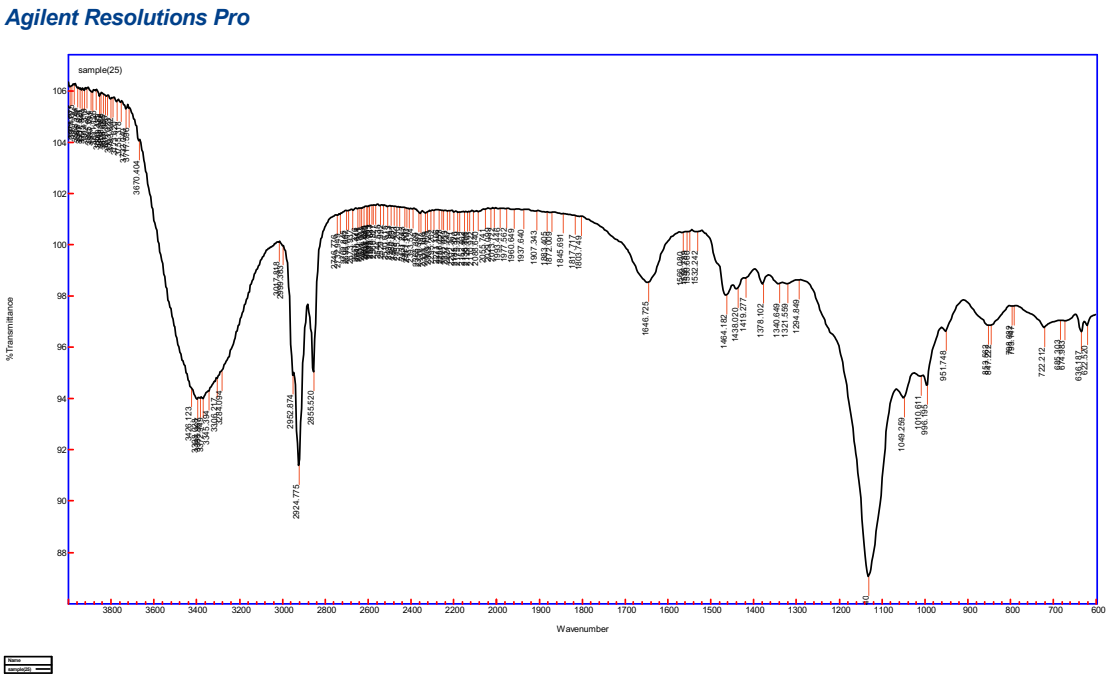

Figure A10. FTIR spectrum of Aliquat 336-PVA/GA gel.

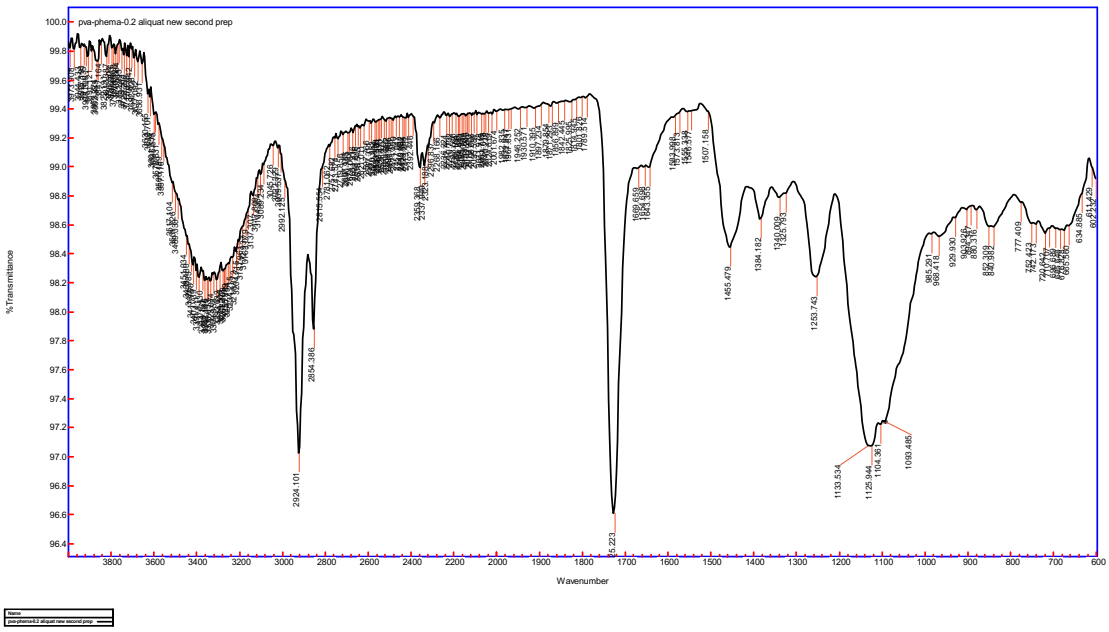

Figure A11. FTIR spectrum of Aliquat 336-full-IPN PVA/PHEMA gel.

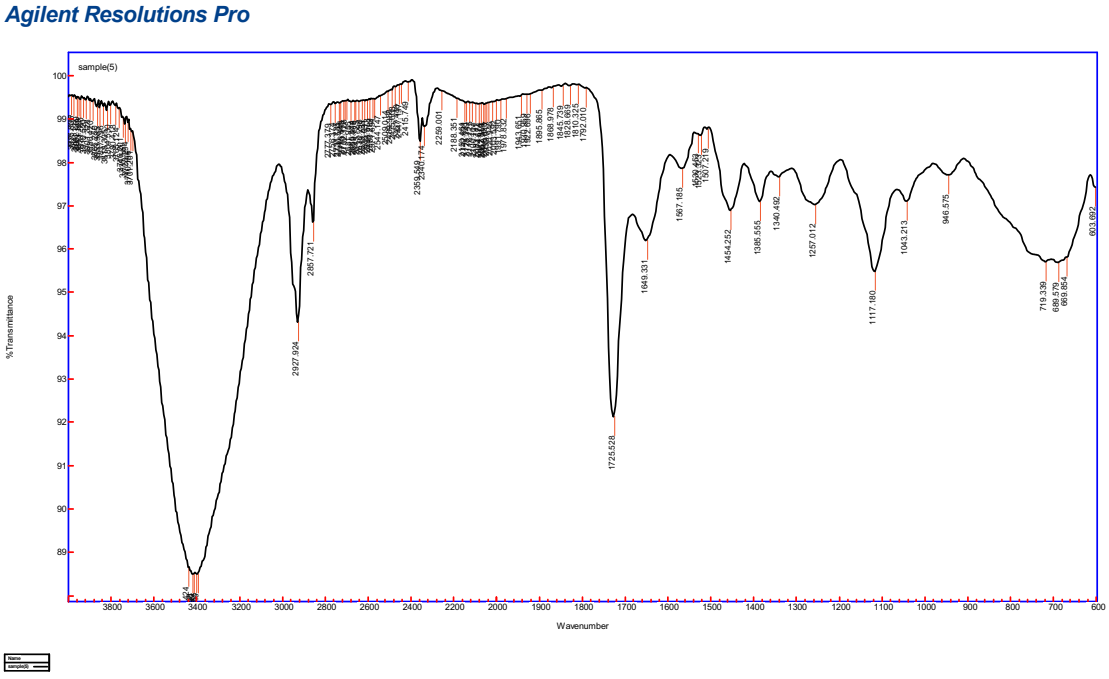

Figure A12. FTIR spectrum of Aliquat336-full-IPN PVA/P(HBA-co-AA) gel.

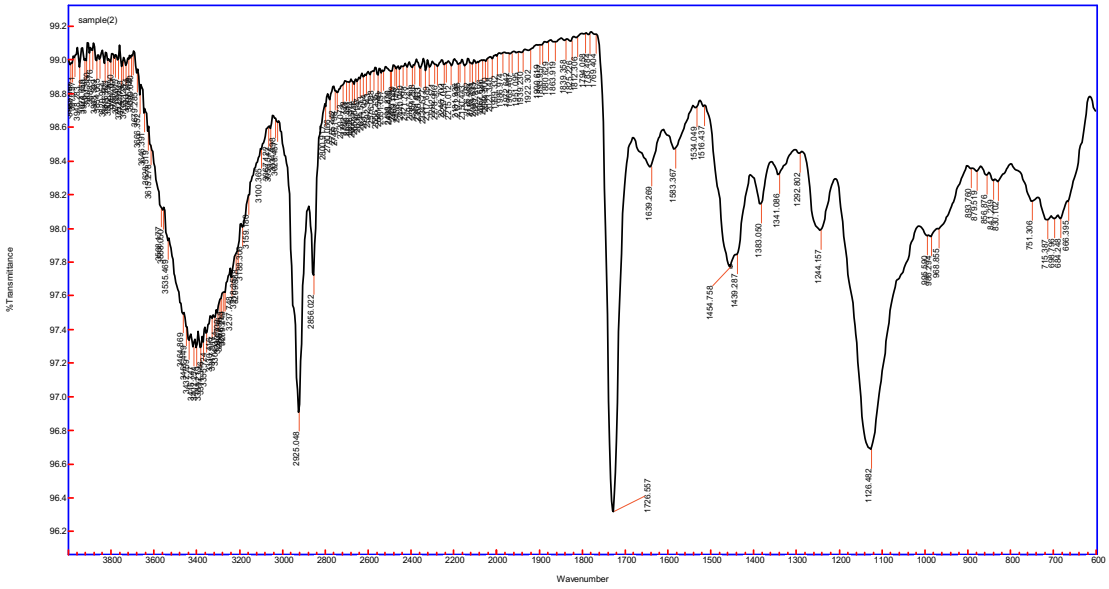

Figure A13. FTIR spectrum of Aliquat 336-full-IPN PVA/P(MMA-co-IA) gel.

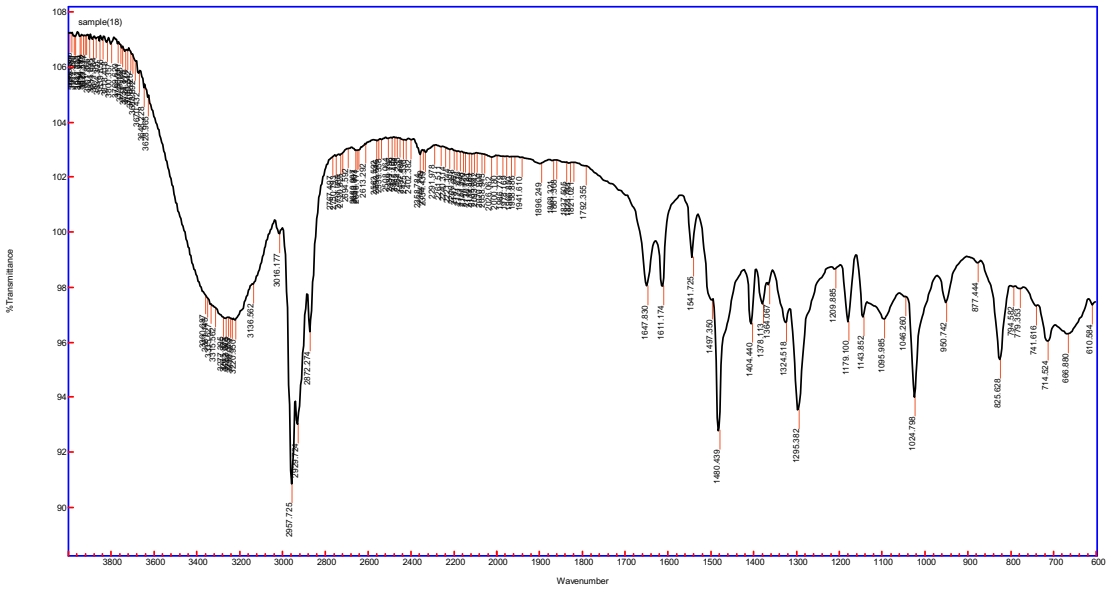

Figure A14. FTIR spectrum of Cu (II)-Acorga P50-complex-imprinted-PVA/GA gel.

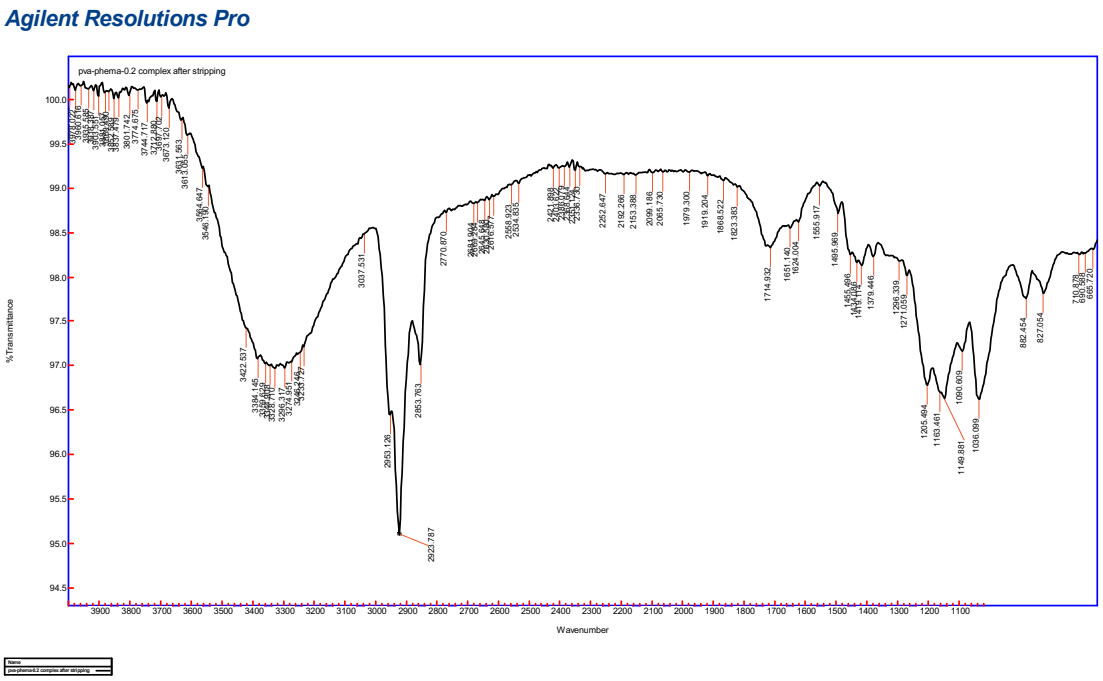

Figure A15. FTIR spectrum of Cu (II)-Acorga P50-complex-imprinted-full-IPN PVA/PHEMA gel.

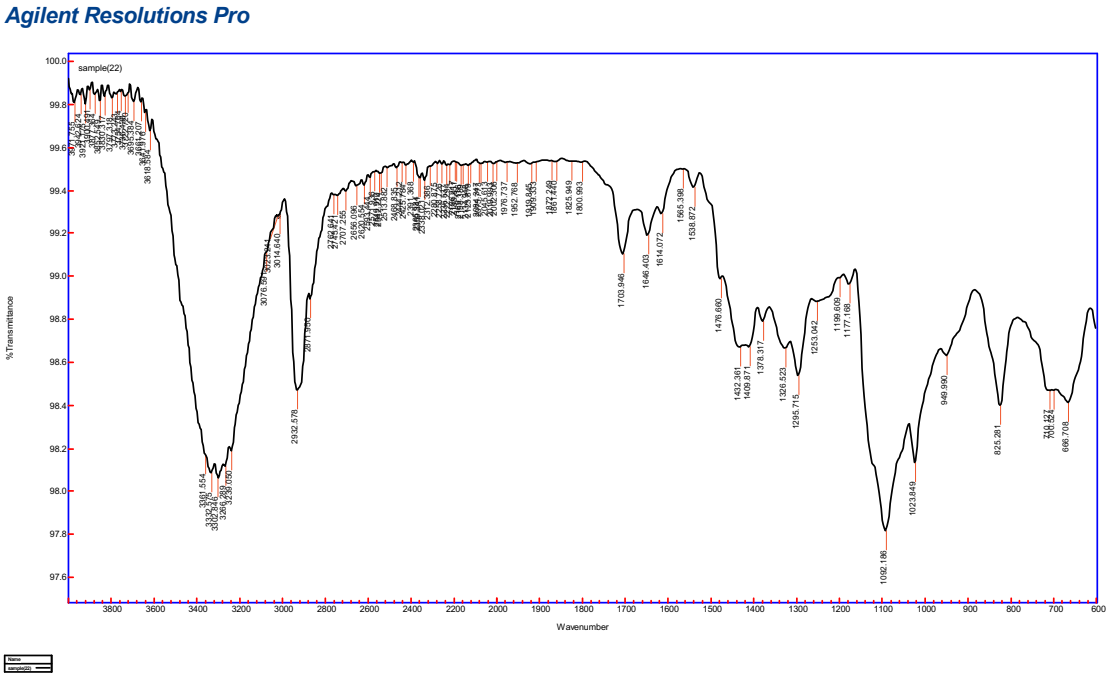

Figure A16. FTIR spectrum of Cu (II)-Acorga P50-complex-imprinted-full-IPN PVA/P(HBA-co-AA) gel.

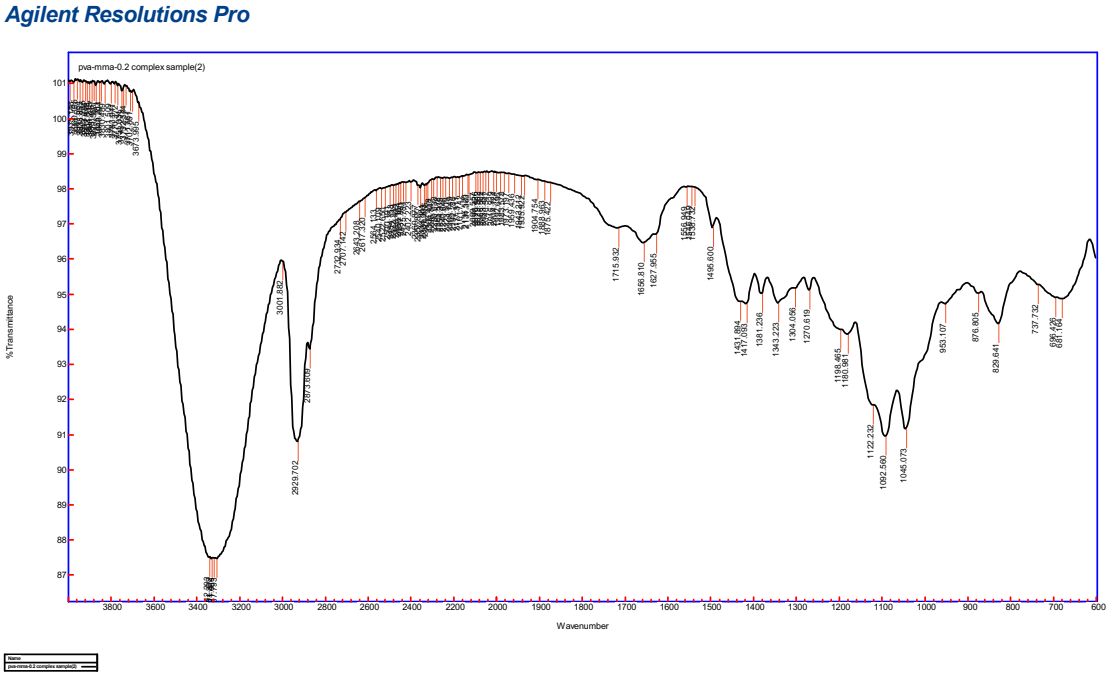

Figure A17. FTIR spectrum of Cu (II)-Acorga P50-complex-imprinted-full-IPN PVA/P(MMA-co-IA) gel.

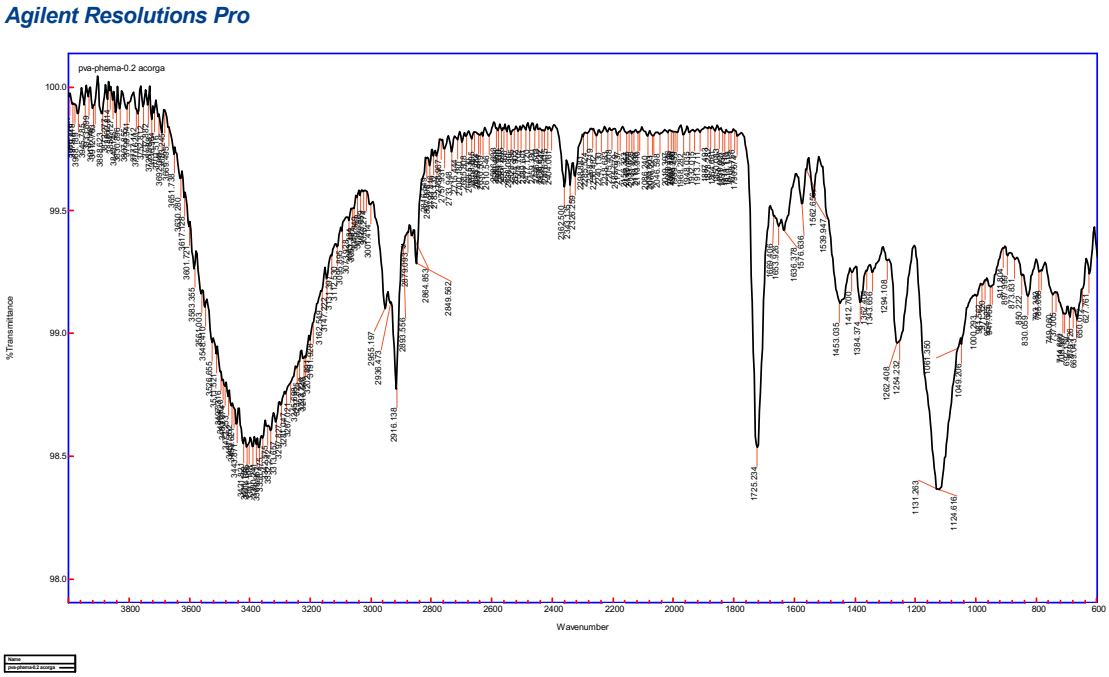

Figure A18. FTIR spectrum of Acorga P50-imprinted-full-IPN PVA/PHEMA gel.

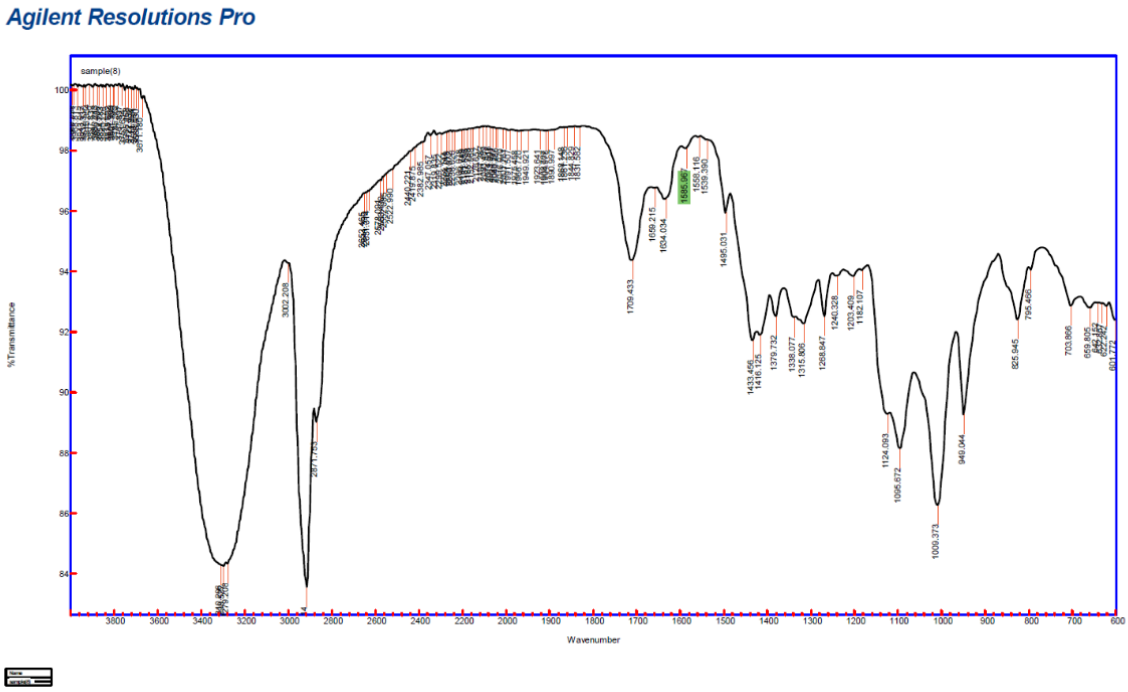

Figure A19. FTIR spectrum of Acorga P50-PVA/P(MMA-co-IA) gel.

References

1. *Wona, G.; Janik, H., . Chem Chem Technol **2010,** 4 (4), 297-304.*
2. *Peppas, N.; Bures, P.; Leobandung, W.; Ichikawa, H., Eur. J. Pharm. Biopharm **2000,** 50 (1), 27-46.*
3. *Chatterjee, S.; Hui, P. C. L., Molecules **2019,** 24 (14), 18.*
4. *Koetting, M. C.; Peters, J. T.; Steichen, S. D.; Peppas, N. A., Mater. Sci. Eng. R Rep **2015,** 93, 1-49.*
5. *Ullah, F.; Othman, M. B. H.; Javed, F.; Ahmad, Z.; Akil, H. M., Mater. Sci. Eng. R Rep **2015,** 57, 414-433.*
6. *Tomić, S. L.; Dimitrijević, S. I.; Marinković, A. D.; Najman, S.; Filipović, J. M., Polym. Bull. **2009,** 63 (6), 837.*
7. *Dobić, S. N.; Filipović, J. M.; Tomić, S. L., Chem. Eng. J. **2012,** 179, 372-380.*
8. *Lin, C.-C.; Metters, A. T., Adv. Drug. Deliv. Rev **2006,** 58 (12-13), 1379-1408.*
9. *Hu, X.; Feng, L.; Wei, W.; Xie, A.; Wang, S.; Zhang, J.; Dong, W., Carbohydr. Polym. **2014,** 105, 135-144.*
10. *Park, H.; Park, K.; Shalaby, W. S., CRC Press: 1993.*
11. *Kashyap, N.; Kumar, N.; Kumar, M. R., Crit. Rev. Ther. Drug. Carrier. Sys **2005,** 22 (2).*
12. *Khademhosseini, A.; Langer, R., Biomaterials **2007,** 28 (34), 5087-5092.*
13. *Ding, R.; Yu, X.; Wang, P.; Zhang, J.; Zhou, Y.; Cao, X.; Tang, H.; Ayres, N.; Zhang, P., RSC Advances **2016,** 6 (24), 20392-20398.*
14. *Lee, K. Y.; Mooney, D. J., Chem. Rev. **2001,** 101 (7), 1869-1880.*
15. *Pan, L.; Yu, G.; Zhai, D.; Lee, H. R.; Zhao, W.; Liu, N.; Wang, H.; Tee, B. C.-K.; Shi, Y.; Cui, Y., Natl. Acad. Sci **2012,** 109 (24), 9287-9292.*
16. *Zhai, D.; Liu, B.; Shi, Y.; Pan, L.; Wang, Y.; Li, W.; Zhang, R.; Yu, G., ACS nano **2013,** 7 (4), 3540-3546.*
17. *Li, L.; Wang, Y.; Pan, L.; Shi, Y.; Cheng, W.; Shi, Y.; Yu, G., Nano Lett. **2015,** 15 (2), 1146-1151.*
18. *El-Aassar, M.; El Fawal, G.; Kamoun, E. A.; Fouda, M. M., Int. J. Biol. Macromol. **2015,** 77, 322-329.*
19. *Dinu, M. V.; Dinu, I. A.; Lazar, M. M.; Dragan, E. S., Carbohydr. Polym. **2018,** 186, 140-149.*
20. *Jaiswal, M.; Koul, V., J. Biomater. Appl. **2013,** 27 (7), 848-861.*

21. *Al-qudah, Y. H.; Mahmoud, G. A.; Abdel Khalek, M., Radiat. Res. Appl. Sc* ***2014,*** *7 (2), 135-145.*
22. *Klouda, L., J. Pharm. Biopharm* ***2015,*** *97, 338-349.*
23. *Sun, Y.; Kaplan, J. A.; Shieh, A.; Sun, H.-L.; Croce, C. M.; Grinstaff, M. W.; Parquette, J. R., Chem. Commun.* ***2016,*** *52 (30), 5254-5257.*
24. *Kim, S. H.; Sun, Y.; Kaplan, J. A.; Grinstaff, M. W.; Parquette, J. R., New J. Chem.* ***2015,*** *39 (5), 3225-3228.*
25. *Verhulsel, M.; Vignes, M.; Descroix, S.; Malaquin, L.; Vignjevic, D. M.; Viovy, J.-L., Biomaterials* ***2014,*** *35 (6), 1816-1832.*
26. *Chai, Q.; Jiao, Y.; Yu, X., Gels* ***2017,*** *3 (1), 6.*
27. *Peppas, N.; Mikos, A. G., In Hydrogels in Med and Pharm, CRC Press Inc: 1986; pp 1-26.*
28. *Peppas, N. A.; Khare, A. R., Adv. Drug. Deliv. Re* ***1993,*** *11 (1-2), 1-35.*
29. *Niu, Y. H.; Han, X. X.; Huang, L. X.; Song, J., J. Chem. Eng. Data* ***2020,*** *65 (4), 1954-1967.*
30. *Rizwan, M.; Yahya, R.; Hassan, A.; Yar, M.; Azzahari, A.; Selvanathan, V.; Sonsudin, F.; Abouloula, C., Polymers* ***2017,*** *9 (4), 137.*
31. *Zhang, H.; Zhai, Y.; Wang, J.; Zhai, G., Mater. Sci. Eng. C* ***2016,*** *60, 560-568.*
32. *Hamidi, M.; Azadi, A.; Rafiei, P., Adv. Drug. Deliv. Re* ***2008,*** *60 (15), 1638-1649.*
33. *Aly, H. M.; Abd El-Mohdy, H. L., Arab. J. Sci. Eng* ***2016,*** *41 (6), 2199-2209.*
34. *Nasef, S.; ElNesr, E.; Hafez, F.; Badawy, N.; Slim, S., G Arab J. Nucl. Sci. Appl* ***2020,*** *53 (1), 208-221.*
35. *Sohail, K.; Khan, I. U.; Shahzad, Y.; Hussain, T.; Ranjha, N. M., Braz. J. Pharm. Sci* ***2014,*** *50 (1), 173-184.*
36. *Pal, K.; Banthia, A.; Majumdar, D., Des. Monomers. Polym* ***2009,*** *12 (3), 197-220.*
37. *Ahmed, E. M., J. Adv. Res* ***2015,*** *6 (2), 105-121.*
38. *Jagur-Grodzinski, J., Polym. Adv. Technol.* ***2010,*** *21 (1), 27-47.*
39. *Buwalda, S. J.; Boere, K. W.; Dijkstra, P. J.; Feijen, J.; Vermonden, T.; Hennink, W. E., J. Controlled Release* ***2014,*** *190, 254-273.*
40. *Baroli, B., J. Pharm. Sci.* ***2007,*** *96 (9), 2197-2223.*
41. *Zhang, L.; Zheng, G.-J.; Guo, Y.-T.; Zhou, L.; Du, J.; He, H., Asian. Pac. J. Trop. Medl* ***2014,*** *7 (2), 136-140.*

42. *Tomić, S. L.; Dimitrijević, S. I.; Marinković, A. D.; Najman, S.; Filipović, J. M., Polym. Bull.* ***2009,*** *63 (6), 837.*
43. *Coelho, E. C.; Dos Santos, D. P.; Ciuffi, K. J.; Ferrari, J. L.; Ferreira, B. A.; Schiavon, M. A., J. Pplym. Res* ***2014,*** *21 (9), 561.*
44. *Gupta, N.; Srivastava, A., Polym. Int.* ***1994,*** *35 (2), 109-118.*
45. *Myung, D.; Waters, D.; Wiseman, M.; Duhamel, P. E.; Noolandi, J.; Ta, C. N.; Frank, C. W., Polym. Adv. Technol.* ***2008,*** *19 (6), 647-657.*
46. *Şanli, O.; Asman, G., J. Appl. Polym. Sci.* ***2004,*** *91 (1), 72-77.*
47. *Simeonov, M.; Monova, A.; Kostova, B.; Vassileva, E., J. Appl. Polym. Sci.* ***2017,*** *134 (42), 45380.*
48. *Dragan, E. S., Chem. Eng. J.* ***2014,*** *243, 572-590.*
49. *Xuequan, L.; Maolin, Z.; Jiuqiang, L.; Hongfei, H., Radiat. Phys. Chem.* ***2000,*** *57 (3-6), 477-480.*
50. *Maitra, J.; Shukla, V. K., Am. J. Polym. Sci* ***2014,*** *4 (2), 25-31.*
51. *Buenger, D.; Topuz, F.; Groll, J., Prog. Polym. Sci.* ***2012,*** *37 (12), 1678-1719.*
52. *Siegel, R. A.; Firestone, B. A., Macromolecules* ***1988,*** *21 (11), 3254-3259.*
53. *Hendri, J.; Hiroki, A.; Maekawa, Y.; Yoshida, M.; Katakai, R., Radiat. Phys. Chem.* ***2001,*** *60 (6), 617-624.*
54. *Brannon-Peppas, L.; Peppas, N. A., J. Controlled Release* ***1989,*** *8 (3), 267-274.*
55. *Kou, J. H.; Amidon, G. L.; Lee, P. I., Pharm. Res.* ***1988,*** *5 (9), 592-597.*
56. *Peppas, N. A., J. Bioact. Compat. Polyml s* ***1991,*** *6 (3), 241-246.*
57. *Kodzwa, M. G.; Staben, M. E.; Rethwisch, D. G., J. Membr. Sci.* ***1999,*** *158 (1-2), 85-92.*
58. *Bae, Y. H.; Okano, T.; Kim, S. W., J. Controlled Release* ***1989,*** *9 (3), 271-279.*
59. *Freitas, R. F.; Cussler, E., Chem. Eng. Sci.* ***1987,*** *42 (1), 97-103.*
60. *Zrınyi, M.; Szabó, D.; Kilian, H.-G., Polym. Gels Networks* ***1998,*** *6 (6), 441-454.*
61. *Qiu, Y.; Park, K., Adv. Drug. Deliv. Re* ***2001,*** *53 (3), 321-339.*
62. *Gupta, P.; Vermani, K.; Garg, S., Drug Discovery Today* ***2002,*** *7 (10), 569-579.*
63. *Satish, C.; Satish, K.; Shivakumar, H., Indian. J. Pharm. Sci* ***2006,*** *68 (2).*
64. *Laftah, W. A.; Hashim, S.; Ibrahim, A. N., Polymer-Plastics Technology and Engineering* ***2011,*** *50 (14), 1475-1486.*
65. *Kikuchi, A.; Okano, T., Biorelated Polymers and Gels, Academic Press, Boston, MA* ***1998****, 1-28.*

66. *Zhang, J. T.; Cheng, S. X.; Huang, S. W.; Zhuo, R. X., Macromol. Rapid Commun.* ***2003,*** *24 (7), 447-451.*

67. *Hirotsu, S.; Hirokawa, Y.; Tanaka, T., J. Chem. Phys* ***1987,*** *87 (2), 1392-1395.*

68. *Akhtar, M. F.; Hanif, M.; Ranjha, N. M., Saudi. Pharm. J* ***2016,*** *24 (5), 554-559.*

69. *Kamoun, E. A.; Chen, X.; Eldin, M. S. M.; Kenawy, E.-R. S., Arab. J. Chem* ***2015,*** *8 (1), 1-14.*

70. *Bell, C.; Peppas, N., In Biopolymers II, Springer: 1995; pp 125-175.*

71. *Gulrez, S. K.; Al-Assaf, S.; Phillips, G. O., Progress in molecular and environmental bioengineering—from analysis and modeling to technology applications* ***2011****, 117-150.*

72. *Meng, Y.; Lu, J.; Cheng, Y.; Li, Q.; Wang, H. S., Int. J. Biol. Macromol.* ***2019,*** *135, 1006-1019.*

73. *Caló, E.; Khutoryanskiy, V. V., Eur. Polym. J.* ***2015,*** *65, 252-267.*

74. *Varaprasad, K.; Raghavendra, G. M.; Jayaramudu, T.; Yallapu, M. M.; Sadiku, R., Mater. Sci. Eng. C. Mater. Biol. Appl* ***2017,*** *79, 958-971.*

75. *Peppas, N. A.; Merrill, E. W., J. Appl. Polym. Sci.* ***1977,*** *21 (7), 1763-1770.*

76. *Young, C.-D.; Wu, J.-R.; Tsou, T.-L., J. Membr. Sci.* ***1998,*** *146 (1), 83-93.*

77. *Silliman, J. E. Network hydrogel polymers-application in hemodialysis. Ph.D Thesis, Massachusetts Institute of Technology, June 1972.*

78. *Figueiredo, K. C.; Alves, T. L.; Borges, C. P., J. Appl. Polym. Sci.* ***2009,*** *111 (6), 3074-3080.*

79. *Campos, E.; Coimbra, P.; Gil, M., Polym. Bull.* ***2013,*** *70 (2), 549-561.*

80. *Hassan, C. M.; Peppas, N. A., In Biopolymers· PVA Hydrogels, Anionic Polymerisation Nanocomposites, Springer: 2000; pp 37-65.*

81. *Halima, N. B., Rsc Advances* ***2016,*** *6 (46), 39823-39832.*

82. *Baker, M. I.; Walsh, S. P.; Schwartz, Z.; Boyan, B. D., J. Biomed. Mater. Res. B. Appl* ***2012,*** *100 (5), 1451-1457.*

83. *Holland, N. An Investigation into the Role of Morphology on the Performance of Molecularly Imprinted Polymers. Ph.D Thesis, Waterford Institute of Technology, August 2008.*

84. *More, S. M.; Kulkarni, R. V.; Sa, B.; Kayane, N. V., J. Appl. Polym. Sci.* ***2010,*** *116 (3), 1732-1738.*

85. *Nguyen, N.-T.; Liu, J.-H., Eur. Polym. J.* ***2013,*** *49 (12), 4201-4211.*

86. *Zhang, C.; Wang, J. M.; Chi, R. F.; Shi, J.; Yang, Y. Q.; Zhang, X. Y., Materials & Design* ***2019,*** *183, 13.*
87. *Sardinha, V. M.; Lima, L.; Belangero, W.; Zavaglia, C.; Bavaresco, V.; Gomes, J., Wear* ***2013,*** *301 (1-2), 218-225.*
88. *Kumar, A.; Han, S. S., Int. J. Polym. Mater. Po* ***2017,*** *66 (4), 159-182.*
89. *Jiang, S.; Liu, S.; Feng, W., J. Mech. Behav. Biomed* ***2011,*** *4 (7), 1228-1233.*
90. *Liu, J.; Wang, W.; Wang, A., Polym. Adv. Technol.* ***2011,*** *22 (5), 627-634.*
91. *Sahoo, P. K.; Rana, P. K.; Swain, S. K., Int. J. Polymer. Mater.* ***2006,*** *55 (1), 65-78.*
92. *Sekhavat Pour, Z.; Ghaemy, M., Polym. Adv. Technol.* ***2016,*** *27 (12), 1557-1568.*
93. *Kenawy, E.-R.; Kamoun, E. A.; Eldin, M. S. M.; El-Meligy, M. A., Arab. J. Chem* ***2014,*** *7 (3), 372-380.*
94. *Gupta, B.; Agarwal, R.; Alam, M. S., J. Appl. Polym. Sci.* ***2013,*** *127 (2), 1301-1308.*
95. *Karimi, A.; Wan Daud, W. M. A., Polym. Compos.* ***2017,*** *38 (6), 1086-1102.*
96. *Wang, Q.; Zhou, X.; Zeng, J.; Wang, J., Nucl. Instrum. Meth. B* ***2016,*** *368, 90-95.*
97. *Pines, E.; Prins, W., Macromolecules* ***1973,*** *6 (6), 888-895.*
98. *Takeshita, H.; Kanaya, T.; Nishida, K.; Kaji, K., Macromolecules* ***1999,*** *32 (23), 7815-7819.*
99. *Hassan, C.; Ward, J.; Peppas, N., Polymer* ***2000,*** *41 (18), 6729-6739.*
100. *Tretinnikov, O.; Sushko, N.; Zagorskaya, S., J. Appl. Spectrosc.* ***2015,*** *82 (1), 40-45.*
101. *Hajizadeh, S.; Xu, C.; Kirsebom, H.; Ye, L.; Mattiasson, B., J. Chromatogr. A* ***2013,*** *1274, 6-12.*
102. *Lozinsky, V. I.; Galaev, I. Y.; Plieva, F. M.; Savina, I. N.; Jungvid, H.; Mattiasson, B., Trends Biotechnol.* ***2003,*** *21 (10), 445-451.*
103. *Kobayashi, H.; Ikada, Y.; Moritera, T.; Ogura, Y.; Honda, Y., Journal of biomedical materials research* ***1992,*** *26 (12), 1583-1598.*
104. *Cha, W. I.; Hyon, S. H.; Graiver, D.; Ikada, Y., Sticky poly (vinyl alcohol) hydrogels. J. Appl. Polym. Sci.* ***1993,*** *47 (2), 339-343.*
105. *Hassan, C. M.; Peppas, N. A., Macromolecules* ***2000,*** *33 (7), 2472-2479.*
106. *Peppas, N.; Tennenhouse, D., S Journal of Drug Delivery Science and Technology* ***2004,*** *14 (4), 291-297.*
107. *Spiller, K. L.; Maher, S. A.; Lowman, A. M., Tissue. Eng. Part. B. Rev* ***2011,*** *17 (4), 281-299.*

108. *Fumio, U.; Hiroshi, Y.; Kumiko, N.; Sachihiko, N.; Kenji, S.; Yasunori, M., Int. J. Pharm.* ***1990,*** *58 (2), 135-142.*
109. *Gholap, S. G.; Jog, J. P.; Badiger, M. V., Polymer* ***2004,*** *45 (17), 5863-5873.*
110. *Das, S.; Subuddhi, U., J. Pharm. Anal* ***2019,*** *9 (2), 108-116.*
111. *Korytkowska-Wałach, A., Polym. Bull.* ***2013,*** *70 (5), 1647-1657.*
112. *Firestone, B. A.; Siegel, R. A., J. Biomater. Sci. Polym. Ed* ***1994,*** *5 (5), 433-450.*
113. *Gemeinhart, R. A.; Chen, J.; Park, H.; Park, K., J. Biomater. Sci. Polym. Ed* ***2000,*** *11 (12), 1371-1380.*
114. *Yılmaz, Y.; Gelir, A.; Alveroglu, E., J. Sol-Gel Sci. Technol.* ***2016,*** *80 (1), 77-86.*
115. *Cheong, W. J.; Yang, S. H.; Ali, F., J. Sep. Sci.* ***2013,*** *36 (3), 609-628.*
116. *Pamfil, D.; Schick, C.; Vasile, C., Ind. Eng. Chem. Res* ***2014,*** *53 (28), 11239-11248.*
117. *Hosseinzadeh, F.; Galehassadi, M.; Mahkam, M., J. Appl. Polym. Sci.* ***2011,*** *122 (4), 2368-2373.*
118. *Young, C.-D.; Wu, J.-R.; Tsou, T.-L., Biomaterials* ***1998,*** *19 (19), 1745-1752.*
119. *Muggli, D. S.; Burkoth, A. K.; Anseth, K. S., J. Biomed. Mater. Res* ***1999,*** *46 (2), 271-278.*
120. *Li, L.; Wang, Z.; Ma, P.; Bai, H.; Dong, W.; Chen, M., J. Polym. Res* ***2015,*** *22 (8), 150.*
121. *Kim, S. J.; Park, S. J.; Kim, S. I., React. Funct. Polym* ***2003,*** *55 (1), 61-67.*
122. *Jayaramudu, T.; Ko, H.-U.; Kim, H. C.; Kim, J. W.; Li, Y.; Kim, J., Int. J. Smart. Nano. Mater* ***2017,*** *8 (2-3), 80-94.*
123. *Khalid, I.; Ahmad, M.; Minhas, M. U.; Barkat, K., Polym. Bull.* ***2018,*** *75 (3), 1075-1099.*
124. *Mandal, B.; Ray, S. K.; Bhattacharyya, R., J. Appl. Polym. Sci.* ***2012,*** *124 (3), 2250-2268.*
125. *Milosavljević, N. B.; Kljajević, L. M.; Popović, I. G.; Filipović, J. M.; Kalagasidis Krušić, M. T., Polym. Int.* ***2010,*** *59 (5), 686-694.*
126. *Ma, G.; Ran, F.; Feng, E.; Zhang, Z.; Lei, Z., J. Compos. Mater.* ***2016,*** *50 (14), 1865-1874.*
127. *Sasaki, S.; Murakami, T.; Suzuki, A., Biosurf. Biotribol* ***2016,*** *2 (1), 11-17.*
128. *De Azevedo, W.; De Souza, J.; De Melo, J., Synth. Met.* ***1999,*** *100 (3), 241-248.*
129. *Yeom, C.-K.; Lee, K.-H., J. Membr. Sci.* ***1996,*** *109 (2), 257-265.*
130. *XIONG, D.-s., Journal of China University of Mining and Technology* ***2008,*** *18 (2), 271-274.*

131. *Wu, X. Y.; Huang, S. W.; Zhang, J. T.; Zhuo, R. X., Macromol. Biosci* ***2004,*** *4 (2), 71-75.*
132. *Jose, J.; Shehzad, F.; Al-Harthi, M. A., Polym. Bull.* ***2014,*** *71 (11), 2787-2802.*
133. *Dey, A.; Bera, R.; Chakrabarty, D., Polymer* ***2017,*** *116, 178-190.*
134. *Sohail, M.; Ahmad, M.; Minhas, M. U.; Khan, S.; Khan, S.; Kousar, M., J. Mater.Sci. Mater. Med* ***2017,*** *28 (10), 147.*
135. *Moon, Y.-E.; Jung, G.; Yun, J.; Kim, H.-I., Mater. Sci. Eng. B* ***2013,*** *178 (17), 1097-1103.*
136. *Taşdelen, B.; Kayaman-Apohan, N.; Güven, O.; Baysal, B. M., Int. J. Pharm.* ***2004,*** *278 (2), 343-351.*
137. *Tomić, S. L.; Mićić, M. M.; Dobić, S. N.; Filipović, J. M.; Suljovrujić, E. H., Radiat. Phys. Chem.* ***2010,*** *79 (5), 643-649.*
138. *Carrillo-Rodríguez, J. C.; Meléndez-Ortiz, H. I.; Puente-Urbina, B.; Padrón, G.; Ledezma, A.; Betancourt-Galindo, R., Polym. Compos.* ***2018,*** *39 (1), 171-180.*
139. *Tomic, S. L.; Micic, M. M.; Filipovic, J. M.; Suljovrujic, E. H., Radiat. Phys. Chem.* ***2007,*** *76 (5), 801-810.*
140. *El-Halah, A.; Machado, D.; González, N.; Contreras, J.; López-Carrasquero, F., J. Appl. Polym. Sci.* ***2019,*** *136 (4), 46999.*
141. *Islam, A.; Yasin, T.; Sabir, A.; Khan, S. M.; Sultan, M.; Shafiq, M.; Khan, A. U.; Jamil, T., e-Polymers* ***2015,*** *15 (4), 255-261.*
142. *Hui, B.; Ye, L., J. Ind. Eng. Chem* ***2016,*** *35, 309-317.*
143. *Minhas, M. U.; Ahmad, M.; Ali, L.; Sohail, M., DARU Sciences* ***2013,*** *21 (1), 44.*
144. *Mishra, R. K.; Majeed, A. B. A.; Banthia, A. K., J. Plast. Technol* ***2011,*** *15 (1), 21-32.*
145. *Zhang, N.; Shen, Y.; Li, X.; Cai, S.; Liu, M., Biomedical Materials* ***2012,*** *7 (3), 035014.*
146. *Bera, R.; Dey, A.; Chakrabarty, D., RSC Advances* ***2015,*** *5 (93), 75870-75880.*
147. *Zhang, J.-T.; Bhat, R.; Jandt, K. D., Acta. Biomater* ***2009,*** *5 (1), 488-497.*
148. *Tanan, W.; Saengsuwan, S., Energy Procedia* ***2014,*** *56, 386-393.*
149. *Katono, H.; Maruyama, A.; Sanui, K.; Ogata, N.; Okano, T.; Sakurai, Y., J. Controlled Release* ***1991,*** *16 (1-2), 215-227.*
150. *Peppas, N. A.; Wright, S. L., J. Pharm. Biopharm* ***1998,*** *46 (1), 15-29.*
151. *Krezović, B. D.; Dimitrijević, S. I.; Filipović, J. M.; Nikolić, R. R.; Tomić, S. L., Polym. Bull.* ***2013,*** *70 (3), 809-819.*
152. *Bai, H.; Li, Z.; Zhang, S.; Wang, W.; Dong, W., Carbohydr. Polym.* ***2018,*** *200, 468-476.*
153. *Hernández, R.; Pérez, E.; Mijangos, C.; López, D., Polymer* ***2005,*** *46 (18), 7066-7071.*

154. *Lee, Y. M.; Kim, S. H.; Cho, C. S., J. Appl. Polym. Sci.* ***1996,*** *62 (2), 301-311.*

155. *Hosseinzadeh, F.; Galehassadi, M.; Mahkam, M., J. Appl. Polym. Sci.* ***2011,*** *122 (4), 2368-2373.*

156. *Samanta, H. S.; Ray, S. K., Carbohydr. Polym.* ***2014,*** *99, 666-678.*

157. *Sullad, A. G.; Manjeshwar, L. S.; Aminabhavi, T. M., Ind. Eng. Chem. Res* ***2010,*** *49 (16), 7323-7329.*

158. *Hu, X. Y.; Feng, L. D.; Wei, W.; Xie, A. M.; Wang, S. M.; Zhang, J. F.; Dong, W., Carbohydr. Polym.* ***2014,*** *105, 135-144.*

159. *Dobić, S. N.; Filipović, J. M.; Tomić, S. L., Chem. Eng. J.* ***2012,*** *179, 372-380.*

160. *Wang, W.; Jin, X.; Zhu, Y.; Zhu, C.; Yang, J.; Wang, H.; Lin, T., Carbohydr. Polym.* ***2016,*** *140, 356-361.*

161. *Kwon, G. H.; Choi, Y. Y.; Park, J. Y.; Woo, D. H.; Lee, K. B.; Kim, J. H.; Lee, S.-H., Lab on a Chip* ***2010,*** *10 (12), 1604-1610.*

162. *Mansur, H. S.; Sadahira, C. M.; Souza, A. N.; Mansur, A. A., Mater. Sci. Eng. C* ***2008,*** *28 (4), 539-548.*

163. *Siddiqui, M. N.; Redhwi, H. H.; Tsagkalias, I.; Softas, C.; Ioannidou, M. D.; Achilias, D. S., Thermochim. Acta* ***2016,*** *643, 53-64.*

164. *González-Henríquez, C. M.; Pizarro, G. d. C.; Sarabia-Vallejos, M. A.; Terraza, C. A.; Lopez-Cabana, Z. E., Arab. J. Chem* ***2014****.*

165. *Passos, M.; Dias, D.; Bastos, G.; Jardini, A.; Benatti, A.; Dias, C.; Maciel Filho, R., J. Therm. Anal. Calorim.* ***2016,*** *125 (1), 361-368.*

166. *He, J.; Chen, J. P., Ind. Eng. Chem. Res* ***2014,*** *53 (52), 20223-20233.*

167. *Todica, M.; Stefan, R.; Pop, C.; Olar, L., Acta Phys. Pol., A* ***2015,*** *128 (1), 128-135.*

168. *Zhang, S.; Zhou, Y. F.; Nie, W. Y.; Song, L. Y., Cellulose* ***2012,*** *19 (6), 2081-2091.*

169. *Zeng, J.; Zhang, Z.; Zhou, H.; Liu, G.; Liu, Y.; Zeng, L.; Jian, J.; Yuan, Z., Polym. Adv. Technol.* ***2019****.*

170. *Dazzi, A.; Deniset-Besseau, A.; Lasch, P., Analyst* ***2013,*** *138 (14), 4191-4201.*

171. *Duan, G.; Zhang, C.; Li, A.; Yang, X.; Lu, L.; Wang, X., Nanoscale Res Lett* ***2008,*** *3 (3), 118-122.*

172. *Krusic, M. K.; Dzunuzovic, E.; Trifunovic, S.; Filipovic, J., Polym. Bull.* ***2003,*** *51 (2), 159-166.*

173. *Zeghioud, H.; Lamouri, S.; Safidine, Z.; Belbachir, M., J. Serb. Chem. Soc.* ***2015,*** *80 (7), 917-931.*

174. *Taylor, M.; Scurr, D.; Lutolf, M.; Buttery, L.; Zelzer, M.; Alexander, M., Biointerphases* ***2016,*** *11 (2), 02A301.*
175. *Bajpai, A. K.; Bhatt, R., Polymer* ***2017,*** *110, 211-217.*
176. *Wagner, M., Surf. Interface Anal.* ***2005,*** *37 (1), 62-70.*
177. *Dietrich, P. M.; Hennig, A.; Holzweber, M.; Thiele, T.; Borcherding, H.; Lippitz, A.; Schedler, U.; Resch-Genger, U.; Unger, W. E., . J. Phys. Chem. C* ***2014,*** *118 (35), 20393-20404.*
178. *Huang, H. L.; Goh, S. H.; Lai, D. M. Y.; Huan, C. H. A., Appl. Surf. Sci.* ***2004,*** *227 (1-4), 373-382.*
179. *Naderi-Gohar, S.; Huang, K. M.; Wu, Y.; Lau, W. M.; Nie, H. Y., Rapid Commun. Mass Spectrom.* ***2017,*** *31 (4), 381-388.*
180. *Rudra, R.; Kumar, V.; Kundu, P. P., RSC Advances* ***2015,*** *5 (101), 83436-83447.*
181. *Elliott, J. E.; Macdonald, M.; Nie, J.; Bowman, C. N., Polymer* ***2004,*** *45 (5), 1503-1510.*
182. *Wang, K.; Fu, Q.; Chen, X.; Gao, Y.; Dong, K., Rsc Advances* ***2012,*** *2 (20), 7772-7780.*
183. *Wiśniewska, M.; Ostolska, I.; Szewczuk-Karpisz, K.; Chibowski, S.; Terpiłowski, K.; Gun'ko, V. M.; Zarko, V. I., J. Nanopart. Res.* ***2015,*** *17 (1), 12.*
184. *Bodugöz, H.; Pekel, N.; Güven, O., Radiat. Phys. Chem.* ***1999,*** *55 (5-6), 667-671.*
185. *Tomić, S. L.; Suljovrujić, E. H.; Filipović, J. M., Polym. Bull.* ***2006,*** *57 (5), 691-702.*
186. *Gerlach, G.; Guenther, M.; Sorber, J.; Suchaneck, G.; Arndt, K.-F.; Richter, A., Sensor. Actuat. B-Chem* ***2005,*** *111, 555-561.*
187. *Wang, X.; Hou, H.; Li, Y.; Wang, Y.; Hao, C.; Ge, C., J. Ind. Eng. Chem* ***2016,*** *41, 82-90.*
188. *Nesrinne, S.; Djamel, A., Arab. J. Chem* ***2017,*** *10 (4), 539-547.*
189. *Babić, M. M.; Antić, K. M.; Vuković, J. S. J.; Božić, B. Đ.; Davidović, S. Z.; Filipović, J. M.; Tomić, S. L., J. Mater. Sci.* ***2015,*** *50 (2), 906-922.*
190. *Wang, J.; Li, Z., J. Hazard. Mater.* ***2015,*** *300, 18-28.*
191. *Jung, H. S.; Kwon, P. S.; Lee, J. W.; Kim, J. I.; Hong, C. S.; Kim, J. W.; Yan, S.; Lee, J. Y.; Lee, J. H.; Joo, T., JACS* ***2009,*** *131 (5), 2008-2012.*
192. *Denna, M. C. F. J.; Camitan, R. A. B.; Yabut, D. A. O.; Rivera, B. A., Sensor. Actuat. B-Chem* ***2018,*** *260, 445-451.*
193. *Kandile, N. G.; Nasr, A. S., Carbohydr. Polym.* ***2009,*** *78 (4), 753-759.*
194. *Zheng, Y.; Wang, A., Chem. Eng. J.* ***2010,*** *162 (1), 186-193.*
195. *Wang, J.; Li, X., Ind. Eng. Chem. Resl* ***2012,*** *52 (2), 572-577.*

196. *Trikkaliotis, D. G.; Christoforidis, A. K.; Mitropoulos, A. C.; Kyzas, G. Z., Carbohydr. Polym.* ***2020,*** *234, 115890.*
197. *Çavuş, S.; Gürdağ, G.; Sözgen, K.; Gürkaynak, M. A., Polym. Adv. Technol.* ***2009,*** *20 (3), 165-172.*
198. *Ali, A. E.-H.; Shawky, H.; El Rehim, H. A.; Hegazy, E., Eur. Polym. J.* ***2003,*** *39 (12), 2337-2344.*
199. *Toledo, P. V.; Limeira, D. P.; Siqueira, N. C.; Petri, D. F., Cellulose* ***2019,*** *26 (1), 597-615.*
200. *Wang, N.; Han, Y.; Liu, Y.; Bai, T.; Gao, H.; Zhang, P.; Wang, W.; Liu, W., J. Hazard. Mater.* ***2012,*** *213, 258-264.*
201. *Chen, L.; Xu, S.; Li, J., Chem. Soc. Rev.* ***2011,*** *40 (5), 2922-2942.*
202. *Zheng, X.; Fan, R.; Zhao, J., Sep. Sci. Technol.* ***2012,*** *47 (10), 1571-1582.*
203. *Ulbricht, M., J. Chromatogr. B* ***2004,*** *804 (1), 113-125.*
204. *Wang, J.; Ding, L.; Wei, J.; Liu, F., Appl. Surf. Sci.* ***2014,*** *305, 412-418.*
205. *Yuan, Z.; Zhu, Y.; Lan, Y.; Chen, D., Sep. Sci. Technol.* ***2015,*** *50 (10), 1480-1486.*
206. *Alguacil, F., Revista de Metalurgia* ***1999,*** *35 (1), 53-61.*
207. *Sastre, A. M.; Szymanowski, J., Solvent Extr. Ion Exch.* ***2004,*** *22 (5), 737-759.*
208. *Wang, D.; Hu, J.; Li, Y.; Fu, M.; Liu, D.; Chen, Q., J. Membr. Sci.* ***2016,*** *501, 228-235.*
209. *de Gyves, J.; Hernández-Andaluz, A. M.; de San Miguel, E. R., J. Membr. Sci.* ***2006,*** *268 (2), 142-149.*
210. *Pouramini, Z.; Moradi, A., Res. Chem. Intermed.* ***2012,*** *38 (9), 2401-2409.*
211. *Wang, D.; Hu, J.; Li, Y.; Fu, M.; Liu, D.; Chen, Q., J. Membr. Sci.* ***2016,*** *501, 228-235.*
212. *Katime, I.; Rodríguez, E., J. Macromdl. Sci. A* ***2001,*** *38 (5-6), 543-558.*
213. *Ding, B.; Wang, J.; Tao, S.; Ding, Y.; Zhang, L.; Gao, N.; Li, G.; Shi, H.; Li, W.; Ge, S., J. Colloid Interface Sci.* ***2018,*** *522, 1-9.*
214. *Maleki, L.; Edlund, U.; Albertsson, A.-C., ACS S ACS Sustain. Chem. Eng* ***2016,*** *4 (8), 4370-4377.*
215. *Fang, L.; Li, L.; Qu, Z.; Xu, H.; Xu, J.; Yan, N., J. Hazard. Mater.* ***2018,*** *342, 617-624.*
216. *Godiya, C. B.; Xiao, Y.; Lu, X., Int. J. Biol. Macromol.* ***2020,*** *144, 671-681.*
217. *Barak, A.; Goel, Y.; Kumar, R.; Shukla, S., Materials Today: Proceedings* ***2019,*** *12, 529-535.*
218. *Ehtesabi, H.; Bagheri, Z.; Yaghoubi-Avini, M., Environ. Nanotechnol. Monit. Manag* ***2019,*** *12, 100274.*

219. *Kong, Y.; Zhuang, Y.; Shi, B., J. Hazard. Mater.* ***2020,*** *382, 121060.*

220. *Ma, J.; Jiang, Z.; Cao, J.; Yu, F., Chemosphere* ***2020,*** *242, 125188.*

221. *Al-Rifai, J. H.; Gabelish, C. L.; Schäfer, A. I., Chemosphere* ***2007,*** *69 (5), 803-815.*

222. *Heberer, T.; Reddersen, K.; Mechlinski, A., Water Sci. Technol.* ***2002,*** *46 (3), 81-88.*

223. *Mohamed, A. K.; Mahmoud, M. E., Bioresour. Technol.* ***2020****, 123263.*

224. *Namazi, H.; Pooresmaeil, M.; Hasani, M., Int. J. Polym. Mater. Po****2020****, 1-10.*

225. *Pereira, N.; St John, A.; Cattrall, R. W.; Perera, J. M.; Kolev, S. D., Desalination* ***2009,*** *236 (1-3), 327-333.*

226. *Kogelnig, D.; Stojanovic, A.; Galanski, M.; Groessl, M.; Jirsa, F.; Krachler, R.; Keppler, B. K., Tetrahedron Lett.* ***2008,*** *49 (17), 2782-2785.*

227. *O'Rourke, M.; Cattrall, R. W.; Kolev, S. D.; Potter, I. D., Solvent Extr. Res. Dev. Jpn* ***2009,*** *16, 1-12.*

228. *Abdul-Halim, N.-S.; Whitten, P. G.; Nghiem, L. D., Sep. Purif. Technol.* ***2013,*** *119, 14-18.*

229. *Cui, H.; Chen, J.; Yang, H.; Wang, W.; Liu, Y.; Zou, D.; Liu, W.; Men, G., Chem. Eng. J.* ***2013,*** *232, 372-379.*

230. *Nasser, I. I.; Amor, F. I. E. H.; Donato, L.; Algieri, C.; Garofalo, A.; Drioli, E.; Ahmed, C., Chem. Eng. J.* ***2016,*** *295, 207-217.*

231. *Wei, M.; Shi, S.; Wang, J.; Li, Y.; Duan, X., J. Solid State Chem.* ***2004,*** *177 (7), 2534-2541.*

232. *Taepaiboon, P.; Rungsardthong, U.; Supaphol, P., Nanotechnology* ***2006,*** *17 (9), 2317.*

233. *Nghiem, L. D.; Mornane, P.; Potter, I. D.; Perera, J. M.; Cattrall, R. W.; Kolev, S. D., J. Membr. Sci.* ***2006,*** *281 (1-2), 7-41.*

234. *Hua, J.; Ng, P. F.; Fei, B., J. Polym. Sci., Part B: Polym. Phys.* ***2018,*** *56 (19), 1325-1335.*

235. *Johnson, B.; Beebe, D.; Crone, W., Mater. Sci. Eng. C* **2004,** *24* (4), 575-581.